UNCLASSIFIED

AD 265 514

Reproduced
by the

ARMED SERVICES TECHNICAL INFORMATION AGENCY
ARLINGTON HALL STATION
ARLINGTON 12, VIRGINIA

Reproduced From
Best Available Copy

19990921079

UNCLASSIFIED

NOTICE: When government or other drawings, specifications or other data are used for any purpose other than in connection with a definitely related government procurement operation, the U. S. Government thereby incurs no responsibility, nor any obligation whatsoever; and the fact that the Government may have formulated, furnished, or in any way supplied the said drawings, specifications, or other data is not to be regarded by implication or otherwise as in any manner licensing the holder or any other person or corporation, or conveying any rights or permission to manufacture, use or sell any patented invention that may in any way be related thereto.

265 514

ARF

ARMOUR RESEARCH FOUNDATION OF ILLINOIS INSTITUTE OF TECHNOLOGY

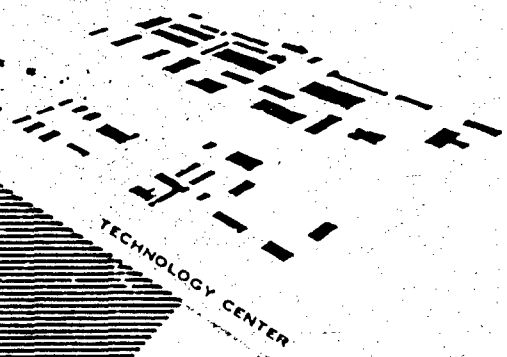

ARF Project No. 8130

LONG RANGE STUDY PROGRAM
LIGHTWEIGHT ARTILLERY WEAPON

Final Report

R. M. Brach

Completed in April, 1961

ASTIA
NOV 6 1961
TIPDR

for

Commanding Officer
Rock Island Arsenal
Rock Island, Illinois

25 years of research

XEROX

ARMOUR RESEARCH FOUNDATION
of
ILLINOIS INSTITUTE OF TECHNOLOGY
Technology Center
Chicago 16, Illinois

Final Report

LONG-RANGE STUDY PROGRAM
LIGHTWEIGHT ARTILLERY WEAPON

Completed in April, 1961

for

Commanding Officer
Rock Island Arsenal
Rock Island, Illinois

under

Contract No. DA-11-022-ORD-2543
Ordnance Project TW-201
D/A Project No. 5U17-07-021
ILS No. 1-4-1-11
ARF Project No. 8130

FOREWORD

In June 1957, Armour Research Foundation completed a feasibility study of a lightweight field artillery weapon intended for use by the Marine Corps. The study specifically explored the possibility of development of a helicopter-transportable field weapon with a high-rate-of-fire burst capability. The results of this study indicated that a lightweight field artillery weapon could be developed to use boosted rocket ammunition, be capable of helicopter transport, and fire six rounds in approximately two seconds. A project was then initiated at ARF to design and develop such a launcher.

The first phase of the program consisted of the design and fabrication of the XM70 Launcher, Prototype No. 1. This prototype displayed an exceptionally optimistic performance such that a second phase of the program was initiated. The second phase consisted of the incorporation design improvements and construction of two more prototypes, XM70E1, Prototypes 2 and 3. Subsequently, Prototypes 4 and 5, XM70E2, were designed and built.

Although the early performance of the XM70 Launcher was satisfactory, it was realized that improvements in performance were possible and necessary. In order to determine the best methods of improving performance, specifically the launcher dynamic response and its effect upon accuracy, a long-range study program was initiated. This program consisted of a concentrated effort of both experimental and analytical investigations of the launcher dynamics.

This long-range study program was begun in October of 1959 and concluded in March, 1961. Progress reports concerning this program were included in the bi-monthly reports of the design and development project. The following staff members contributed significantly to the results of this program: P. Eakins, R. A. Eubanks, L. Gardiner, C. Murray, K. Norikane, N. Pearson, R. Pratt, J. Ross, R. H. Van Beek, and C. Youngdahl.

Respectfully submitted,

ARMOUR RESEARCH FOUNDATION
of Illinois Institute of Technology

R. M. Brach

R. M. Brach
Associate Research Engineer

APPROVED:

W. D. Bobco

W. D. Bobco
Assistant Director
Mechanics Research

LONG RANGE STUDY PROGRAM
LIGHTWEIGHT ARTILLERY WEAPON

ABSTRACT

Prototype No. 3 Launcher, XM70E1, 115 mm was instrumented with strain, pressure and displacement gages; these furnished the actual loading and motion of the launcher structure. In addition to certain simple dynamic analyses, a 3-degree-of-freedom, nonlinear mathematical model of the launcher dynamics was derived and programmed for solution on Armour Research Foundation's Univac 1105. The output of the computer program was correlated with experiment and used to study the effect of physical parameter variations.

Regions of instability of the launcher motions were shown to exist for burst firings; relationships between component stiffness and damping were found which optimized the launcher response to firing loads, based upon a simple accuracy criterion. Certain design suggestions were evaluated and shown to benefit the accuracy of the launcher.

TABLE OF CONTENTS

Section		Page
FOREWORD		ii
ABSTRACT		iv
I.	INTRODUCTION	1
II.	DESCRIPTION OF THE LAUNCHER STRUCTURE	4
	A. TIPPING ASSEMBLY	4
	B. SUPPORTING STRUCTURE	4
	C. ELEVATING SYSTEM	9
	D. DAMPING	9
	E. DEFLECTIONS	10
	F. EXPERIMENTAL STRUCTURE MODIFICATIONS	11
III.	EXPERIMENTAL WORK	14
	A. PHYSICAL PARAMETER MEASUREMENTS	14
	B. LAUNCHER RESPONSE DETERMINATION	17
	C. HORIZONTAL DISPERSION	23
IV.	THEORETICAL ANALYSES	31
	A. PLANAR, LINEAR, 3-DEGREE-OF-FREEDOM MODEL	31
	B. SUPPLEMENTARY ANALYSES	66
	1. THIRD-ORDER SYSTEM	
	2. RESPONSE DECAY OF SECOND-ORDER SYSTEMS	
	3. LINEAR, 2-DEGREE-OF-FREEDOM SYSTEM	
	C. 3-DIMENSIONAL, n-DEGREE-OF-FREEDOM MODEL	69
	D. ACCURACY CRITERION	71
V.	CONCLUSIONS	75
APPENDIX A:	STUDY OF THE RELATIVE EFFECTIVENESS OF VARIOUS DAMPER LOCATIONS	A-1
APPENDIX B:	OPTIMUM RESPONSE DECAY OF A SECOND-ORDER SYSTEM	B-1
APPENDIX C:	EQUATIONS OF MOTION OF THE LAUNCHER WITH THREE DEGREES OF FREEDOM	C-1
APPENDIX D:	COMPUTER PROGRAM, 3-DEGREE-OF-FREEDOM MODEL	D-1

TABLE OF CONTENTS (Continued)

Section		Page
APPENDIX E:	OPTIMUM ELEVATING SYSTEM PARAMETERS	E-1
APPENDIX F:	GENERAL EQUATIONS OF MOTION OF LAUNCHER DYNAMICS	F-1
APPENDIX G:	FIXTURE DESIGNS	G-1
APPENDIX H:	STRUCTURAL STIFFNESS MEASUREMENTS	H-1
APPENDIX I:	FIRING PROGRAM	I-1
APPENDIX J:	EXPERIMENTAL LAUNCHER RESPONSE CURVES	J-1

LIST OF ILLUSTRATIONS

Figure		Page
1	PHOTOGRAPH OF LAUNCHER	5
2	PHOTOGRAPH OF LAUNCHER	6
3	SKETCH OF RECOILING ASSEMBLY	7
4	EXPLODED VIEW OF THE SUPPORTING STRUCTURE	8
5	EXPERIMENTAL LAUNCHER EMPLACEMENT	12
6	SCHEMATIC OF RECOILING ASSEMBLY	25
7	FRAMEWORK REACTIONS	26
8	BARREL STRAIN	28
9	TARGET PATTERNS	29
10	TYPICAL COMPUTER SOLUTION -- POWDER GAS FORCE	35
11	TYPICAL COMPUTER SOLUTION -- RECOIL FORCE	36
12	TYPICAL COMPUTER SOLUTION -- RECOIL DISPLACEMENT	37
13	TYPICAL COMPUTER SOLUTION -- CARRIAGE ROTATION	38
14	TYPICAL COMPUTER SOLUTION -- CARRIAGE ROTATIONAL VELOCITY	39
15	TYPICAL COMPUTER SOLUTION -- CRADLE ROTATION	40
16	TYPICAL COMPUTER SOLUTION -- CRADLE - CARRIAGE RELATIVE ROTATION	41
17	TYPICAL COMPUTER SOLUTION -- CRADLE - CARRIAGE RELATIVE ROTATIONAL VELOCITY	42
18	TYPICAL COMPUTER SOLUTION -- ELEVATING SYSTEM SPRING FORCE	43
19	TYPICAL COMPUTER SOLUTION -- ELEVATING SYSTEM DAMPER FORCE	44
20	TYPICAL COMPUTER SOLUTION -- RECOILING ASSEMBLY - CRADLE MOMENT REACTION	45
21	TYPICAL COMPUTER SOLUTION -- AXIAL CAM FORCE	46
22	TYPICAL COMPUTER SOLUTION -- CRADLE ROTATION, 6-RD BURST	47
23	COMPARISON OF COMPUTED AND EXPERIMENTAL RESPONSE CURVES	48

LIST OF ILLUSTRATIONS (Continued)

Figure		Page
24	THEORETICAL RESPONSE WITH REDUCED STRUCTURAL STIFFNESS	49
25	THEORETICAL RESPONSE WITH A BILINEAR STIFFNESS	51
26	EXPERIMENTAL ELEVATING ROD STRAIN	52
27	EXPERIMENTAL ELEVATING SYSTEM DAMPER SUPPORT STRAIN	53
28	CRADLE RESPONSE AT 20° ELEVATION	54
29	CRADLE RESPONSE AT 60° ELEVATION	55
30	GEOMETRY OF ELEVATION CHANGES	56
31	CRADLE RESPONSE, LOW ZONE BOOST	58
32	CRADLE RESPONSE WITH A VERY STIFF ELEVATING SYSTEM	59
33	CRADLE RESPONSE WITH A VERY STIFF ELEVATING SYSTEM NEGLECTING THE CORIOLIS ACCELERATION	60
34	CRADLE RESPONSE FOR DELAYED RECOIL ROD CUT-BACK 11-1/2 IN.	62
35	CRADLE RESPONSE FOR DELAYED RECOIL, NOTCHED ROD	64
36	CRADLE RESPONSE FOR DELAYED RECOIL ROD CUT-BACK 11-1/2 IN.	65
A-1	TWO-DEGREE-OF-FREEDOM REPRESENTATION OF AN XM70 LAUNCHER	
A-2	MOMENT PRODUCED BY THE RECOIL FORCE	
A-3	CALCULATED UNDAMPED RESPONSE OF AN XM70-TYPE LAUNCHER	
A-4	CALCULATED RESPONSE OF AN XM70-TYPE LAUNCHER WITH c_1-DAMPING ONLY	
A-5	CALCULATED RESPONSE OF AN XM70-TYPE LAUNCHER WITH c_2-DAMPING ONLY	
A-6	CALCULATED RESPONSE OF AN XM70-TYPE LAUNCHER WITH c_3-DAMPING ONLY	
A-7	CALCULATED RESPONSE OF AN XM70-TYPE LAUNCHER WITH c_1-AND c_2-DAMPING COMBINED	

LIST OF ILLUSTRATIONS (Continued)

Figure	
A-8	CALCULATED RESPONSE OF AN XM70-TYPE LAUNCHER WITH c_1- AND c_2- DAMPING COMBINED AND WITH REDUCED CARRIAGE STIFFNESS
B-1	MATHEMATICAL MODEL
B-2	FORCING FUNCTION
B-3	TYPICAL TIME DISPLACEMENT CURVE OF THE XM70 LAUNCHER
B-4	TYPICAL GRAPH OF DIMENSIONLESS TIME VERSUS FREQUENCY FOR VARIOUS DAMPING RATIOS
B-5	MINIMUM WEIGHT REQUIRED TO SATISFY ACCURACY CRITERION
C-1	SCHEMATIC REPRESENTATION OF THE LAUNCHER
C-2	GEOMETRIC REPRESENTATION OF AN XM70-TYPE LAUNCHER
C-3	VECTOR COMPONENT TRANSFORMATION
C-4	FREE BODY DIAGRAM OF THE RECOILING MASS
C-5	FREE BODY DIAGRAM OF THE CRADLE
C-6	FREE BODY DIAGRAM OF THE EQUIVALENT FIRING SUPPORT
D-1	COMPUTER PROGRAM FLOW CHART
D-2	POWDER-GAS FORCE SELECTION FLOW DIAGRAM
D-3	COMPUTER PROGRAM
D-4	TYPICAL OUTPUT DATA
D-5	LAUNCHER RESPONSE FROM EARLY COMPUTER PROGRAM
D-6	LAUNCHER RESPONSE FROM PRESENT COMPUTER PROGRAM
D-7	EXPERIMENTAL LAUNCHER RESPONSE
D-8	LAUNCHER RESPONSE FROM PRESENT COMPUTER PROGRAM CORRESPONDING TO EXPERIMENTAL RESPONSE
E-1	MODEL OF THIRD-ORDER SYSTEM
E-2	CRADLE ROTATION FROM THIRD-ORDER SYSTEM ANALYSIS
E-3	EFFECTS OF DAMPING ON CRADLE ROTATION WITH LOW ELEVATING SYSTEM STIFFNESS

LIST OF ILLUSTRATION (Continued)

Figure	
E-4	OPTIMUM RESPONSES
E-5	CRADLE ROTATION FOR A 6-RD. BURST WITH OPTIMUM ELEVATING SYSTEM
E-6	RESPONSES FOR VARIOUS ELEVATING SYSTEM DAMPING COEFFICIENTS
E-7	COMPARISON OF CRADLE ROTATION FOR A LOW ELEVATING STIFFNESS TO AN OPTIMUM SYSTEM
E-8	CRADLE ROTATION FOR A 4-RD. BURST WITH LOW ELEVATING SYSTEM STIFFNESS
E-9	EFFECT OF CARRIAGE STIFFNESS ON CRADLE ROTATION
F-1	DIAGRAM OF COORDINATE SYSTEMS DESCRIBING LAUNCHER MOTION
F-2	COORDINATE SYSTEM
G-1	DAMPER ASSEMBLY
G-2	DAMPER-PISTON
G-3	SPRING ASSEMBLY
G-4	SPRING DATA
G-5	SPRING-DAMPER COMBINATION
H-1	TEST SETUP FOR MEASURING CARRIAGE STIFFNESS AT TRUNNIONS
H-2	LAUNCHER COMPONENTS UNDERGOING TESTS
H-2a	STIFFNESS OF ELEVATING SCREW SUPPORT
H-2b	STIFFNESS OF TRAILS
H-2c	NATURAL FREQUENCY OF CARRIAGE
H-3	STIFFNESS OF CARRIAGE AT TRUNNIONS WITHOUT STIFFNESS
H-4	STIFFNESS OF CARRIAGE AT TRUNNIONS WITH WEDGES AND TIES
H-5	STIFFNESS OF CARRIAGE AT TRUNNIONS WITH WEDGES TIES AND LINKS BETWEEN TRUNNIONS AND TRAILS
H-6	STIFFNESS OF CARRIAGE AT FULL TRAVERSE, 20° RIGHT
H-7	STIFFNESS OF CARRIAGE AT FULL TRAVERSE, 20° LEFT
H-8	STIFFNESS OF ELEVATING SCREW SUPPORTS
H-9	STIFFNESS OF PROTOTYPE NO. 3 TRAILS

LIST OF ILLUSTRATIONS (Continued)

Figure	
H-10	STIFFNESS OF PROTOTYPE NO. 1 TRAILS
H-11	NATURAL FREQUENCY OF LAUNCHER CARRIAGE
H-12	STIFFNESS OF ELEVATING SCREWS AND UPPER BRACKETS
J-1	CRADLE MOTION, BURST B-2
J-2	CRADLE MOTION, BURST B-2
J-3	TRAIL STRAIN, BURST B-2
J-4	TRAIL STRAIN, BURST B-2
J-5	CRADLE MOTION, BURST B-5
J-6	TRAIL STRAIN, BURST B-5
J-7	CRADLE MOTION, BURST B-6
J-8	TRAIL STRAIN, BURST B-6
J-9	CRADLE MOTION, BURST B-7
J-10	TRAIL STRAIN, BURST B-7
J-11	CRADLE MOTION, BURST B-8
J-12	TRAIL STRAIN, BURST B-8
J-13	CRADLE ROTATION, BURST B-9
J-14	TRAIL STRAIN, BURST B-9
J-15	TRAIL STRAIN, BURST B-10
J-16	CRADLE MOTION, BURST B-10

LIST OF TABLES

Table		Page
1	MODIFICATIONS TO LAUNCHER	18
[illegible]	COMPARISON OF MODELS AND LAUNCHER PARAMETERS	D-3
D-2	INPUT DATA TO COMPUTER PROGRAM	D-3
I-1	FIRING SCHEDULE	I-2

DISTRIBUTION LIST

Copies of this report are being distributed as follows

Copy No.	Recipient	Copy No.	Recipient
1	Chief of Ordnance Department of the Army Washington 25, D. C. Attn: ORDTB	26	Commanding Officer Frankford Arsenal Philadelphia 37, Pennsylvania Attn: [illegible]
2	Chief of Ordnance Department of the Army Washington 25, D. C. Attn: ORDTB-AB	27	Commanding Officer Watervliet Arsenal Watervliet, New York Attn: [illegible]
3	Chief of Ordnance Department of the Army Washington 25, D. C. Attn: ORDTB, Ships Parking, [illegible]	28	Commander Naval Ordnance Test Station China Lake, California Attn: Code [illegible]
4	Commander Army Rocket and Guided Missile Agency U. S. Army Ordnance Missile Command Redstone Arsenal, Alabama Attn: ORDGU-SM-P	29	Commanding Officer Diamond Ordnance Fuze Labs Connecticut Avenue and Van Ness Street Washington 25, D. C. Attn: [illegible] Div, Bldg. [illegible], Room [illegible]
5	Commander Army Rocket and Guided Missile Agency U. S. Army Ordnance Missile Command Redstone Arsenal, Alabama Attn: ORDGU-SMJ,	30	Director, Ordnance Corporation 52.1 Small Arms Depot Hialeah, Florida Attn: Mr. F. A. Fisher
6	Commander Army Rocket and Guided Missile Agency U. S. Army Ordnance Missile Command Redstone Arsenal, Alabama Attn: ORDGU-SMJ	31	Commanding General Ordnance Tank Automotive Command 2501 Grand Island Detroit 9, Michigan Attn: [illegible]
7	Commanding Officer Picatinny Arsenal Dover, New Jersey Attn: ORDBB-TK7	32	Director Detroit Arsenal Tank Automotive Center Detroit Arsenal Warren, Michigan Attn: [illegible]
8	Commanding Officer Picatinny Arsenal Dover, New Jersey Attn: ORDBB-TK7	33	Director Ordnance Tank Automotive Command The Office of the Chief of Ordnance Washington 25, D. C. Attn: [illegible]
9	Commanding Officer Picatinny Arsenal Dover, New Jersey Attn: ORDBB-TK6	34	Commanding Officer Frankford Arsenal Philadelphia 37, Pennsylvania Attn: [illegible]
10	Commanding Officer Picatinny Arsenal Dover, New Jersey Attn: ORDBB-TK5	35	Commanding Officer Redstone Arsenal, Ordnance Huntsville, Alabama Attn: [illegible]
11	Commanding Officer Picatinny Arsenal Dover, New Jersey Attn: ORDBB-TK3	36	Commanding General Ordnance Ammunition Command U. S. Army Joliet, Illinois Attn: [illegible]
12	Commanding Officer Rock Island Arsenal Rock Island, Illinois Attn: [illegible]	37	Commanding Officer Springfield Armory Springfield 1, Massachusetts Attn: [illegible]
13	Commanding General Aberdeen Proving Ground Aberdeen, Maryland Attn: Ballistics Research Laboratories Market Division	38-40	Director of Supply Staff Detroit Tank Arsenal Division 1500 G Street, N. W. Washington 6, D. C. Attn: [illegible]
14	Commanding General Aberdeen Proving Ground Aberdeen, Maryland Attn: Market Division, [illegible]	41-43	Canadian Army Staff, Washington [illegible] Washington 6, D. C. Attn: [illegible]
15	Office, Chief of Army Field Forces Research Division Research and Development Branch Fort Monroe, Virginia Attn: Executive Chief of Staff for Developments and Test	44	Commanding General [illegible] Army Chemical Center Maryland Attn: [illegible]
16	District Chief Chicago Ordnance District 209 West Jackson Boulevard Chicago 6, Illinois Attn: Research and Development Branch	45	Commanding Officer Picatinny Arsenal Dover, New Jersey Attn: [illegible]
17	Commandant U. S. Army Artillery and Guided Missile Fort Sill, Oklahoma Attn: Combat Developments Branch	46	Commanding General Aberdeen Proving Ground, Maryland Attn: Ballistic Research Laboratories, Computation Laboratory
18	Commandant Command and General Staff Fort Leavenworth, Kansas Attn: Archives	47	Commanding General Aberdeen Proving Ground, Maryland Attn: Ballistic Research Laboratories, Terminal Ballistics Laboratory
19	North Carolina State College of Agriculture and Engineering University of North Carolina Raleigh, North Carolina Attn: Dr. Daniel [illegible]	48	Commanding Officer Rock Island Arsenal Rock Island, Illinois Attn: [illegible] U. S. Navy
20	Arthur D. Little, Inc. 30 Memorial Drive Cambridge 42, Massachusetts Attn: Mr. R. A. Brown	49	Commander Army Rocket and Guided Missile Agency U. S. Army Ordnance Missile Command Redstone Arsenal, Alabama Attn: ORDGU-SMJ, Mr. Audin,
21	Firestone Marine and Propulsion Controls 1200 South Kolmar Avenue Chicago 5, Illinois Attn: Mr. F. Rosenberg	50	Commander Army Rocket and Guided Missile Agency U. S. Army Ordnance Missile Command Redstone Arsenal, Alabama Attn: [illegible]
22	Chesapeake Research Office The Johns Hopkins University Chevy Chase, Maryland Attn: Mr. Thomas Piper		
23	Commanding General U. S. Continental Army Command Fort Monroe, Virginia Attn: ATDEV-1	51	Naval Files
		52	Project Library
24	President Board No. 1 Office, Chief of Army Field Forces Fort Sill, Oklahoma	53-54	[illegible]
		55-60	[illegible]
25	Commanding General Headquarters Chicago Ordnance District Rock Island, Illinois Attn: ORDCH-TB	61	[illegible]
26	Commanding Officer Frankford Arsenal Philadelphia 37, Pennsylvania Attn: ORDBA-[illegible]		

ARMOUR RESEARCH FOUNDATION OF ILLINOIS INSTITUTE OF TECHNOLOGY

LONG-RANGE STUDY PROGRAM
LIGHTWEIGHT ARTILLERY WEAPON

I. INTRODUCTION

A unique automatic rocket launcher in the field artillery weapon class has been designed and developed by Armour Research Foundation under the technical supervision of Rock Island Arsenal. This weapon is a 115mm launcher capable of firing single shots or bursts of up to six rounds. Boost charge variations combined with rocket thrust increments and variable elevation provide an exceptionally wide range capability. The launcher can be traversed $\pm 20^{\circ}$ without disturbing its original emplacement. Based upon early feasibility studies and also upon the performance of the first prototype, this lightweight, automatic launcher concept showed itself to be unusually capable as an effective weapon. It was realized, however, that production schedule requirements for succeeding prototypes might hinder the development of the concept, because of the tendency to freeze important design features. As a result, this long-range study program was initiated to investigate the dynamic behavior of the launcher during burst firing, relate this behavior to accuracy, and determine the important physical parameter values which will insure good accuracy.

The program was comprised of theoretical and experimental studies of the dynamics of the launcher. These consisted of finding the effects of certain parameter variations upon the launcher motion; accuracy was related to the motion by simple criteria. Some of the important launcher parameters which were considered are: structural rigidity, damping, recoil system characteristics, launcher geometry, and ground restraints.

The majority of the work accomplished, both theoretical and experimental, is presented in the appendices. A description of the work and results as well as the important conclusions are presented in the following sections. Section II is an introductory portion of the report containing a description of the launcher structure and its relationship to its dynamic response. Some of the operational characteristics of the launcher system, as they affect the response, are also discussed.

Section III presents the results of the experimental work, and is broken into three parts. These respectively describe stiffness measurements of the structural components and two separate firing programs. Stiffness measurements were made, both statically, of all the major structural components, and dynamically of the entire supporting structure assembly (carriages and trails). The second experimental effort was a firing program wherein approximately 75 proof slugs were fired. During these firings the launcher was instrumented with pressure gages, displacement transducers, and strain gages to provide information on the force input, the response of the launcher, and accuracy in the vertical plane. Finally, horizontal dispersion was significantly reduced, as shown by targets, with the use of two fixtures -- one restraining the trails from horizontal motion while the second stiffened the recoiling assembly framework.

In Section IV, the theoretical analyses are described; they consist of the following mathematical models:

1. A planar, nonlinear 3-degree-of-freedom model (called Mathematical Model V in progress reports),
2. A third-order, linear model,
3. A linear, 2-degree-of-freedom model,
4. A three-dimensional, nonlinear, n-degree-of-freedom system,
5. A second-order, linear system.

The first of these was implemented with a computer program and was widely applied to study launcher motion. It contained representations of the hydro-pneumatic recoil system, the indexing cams, and flexibilities and damping of both the supporting structure and elevating system. Information about the response of linear, third-order systems led to a structural optimization of the elevating system. The 2-degree-of-freedom system was an approximation of the launcher used to determine the best location for auxiliary dampers. The fourth model is a relatively complex representation of the launcher; its significant contribution was the inclusion of structural flexibilities of both the recoiling assembly framework and firing tube and also consideration of motion out of the vertical plane. Unfortunately, this model could only be developed to the point where it was programmed for the Univac but not run. The final system was a single-degree-of-freedom system used

to investigate the important parameter values which can cause the response to decay by a desired amount between rounds of a burst.

The 3-degree-of-freedom model was used to correlate theoretical response curves with the experimental response obtained with various structural changes. The correlation was very good for certain parameter combinations, but the theoretical response curves lacked certain characteristics as some parameters were varied. The reason for this is postulated; allowing conclusions to be drawn which indicate the desirability of certain combinations of structural parameters which correspond to improved accuracy.

A theoretical investigation was made of a specific design recommendation -- delayed recoil rods. Because the 3-degree-of-freedom model had an explicit representation of the recoil system, the behavior resulting from increasing the orifice area during the time the rocket is in the launcher could be studied. This cutback on the recoil rods resulted in near free recoil for a short time.

The final item studied was done as a matter of interest; the terms representing the Coriolis acceleration of the recoiling assembly were neglected during one computer run. Comparison was then made with a normal response to determine the effect.

Although the launcher has a $\pm 20^{\circ}$ traverse capability, all of the studies considered only zero traverse accuracy because of its order of importance. Ground restraints and soil considerations were included in the n-degree-of-freedom model and could not be studied because of the status of the model. One method of auxiliary ground restraint, horizontal trail ties, was tried and is discussed with horizontal dispersion reduction.

II. DESCRIPTION OF THE LAUNCHER STRUCTURE

The complete launcher is shown in two firing positions, in Fig. 1 and 2. It consists of two main assemblies: the tipping assembly and the supporting structure. The total weight of the launcher, 3150 lb, is almost equally divided between these two assemblies. The tipping assembly rotates relative to the supporting structure at the trunnion; the elevating system separates them at any fixed position from -6° to 65°.

A. Tipping Assembly

The tipping assembly is composed of a cradle and recoiling assembly; the former is simply the containment for the latter. The firing tube is fixed to the front of the structural framework of the recoiling assembly (see Fig. 3); it also supports two, contrarotating breech clusters of three rounds each and holds the recuperator and recoil system. The framework consists essentially of the front plate, rear plate, two side tie bars, the recuperator cylinder and a lower tie bar; the recoil cylinders are not load bearing members of this framework. Two indexing cams extend into the hubs of the breech clusters and cause them to alternately rotate into firing position during counterrecoil. These cams are fixed to the front of the cradle.

B. Supporting Structure

The supporting structure is the name given to the portion of the launcher below the trunnions; this structure is made up of what are commonly called the upper carriage, lower carriage and trails. An exploded view of the supporting structure in Fig. 4 shows its essential components. This entire structure is composed of hollow, sheet steel construction with various necessary non-structural components accounting for 20% of its total weight. These components are the traverse and elevating mechanisms, wheels, firing base, lunnette and a jack for raising and lowering the firing base. In firing position, the trails are separated by an included angle of 40° which permits $\pm 20^{\circ}$ traverse firing; the upper box, trunnion sides and tipping assembly rotate relative to the remaining structure to attain the desired traverse positions.

MAXIMUM ELEVATION 65°
ZERO TRAVERSE

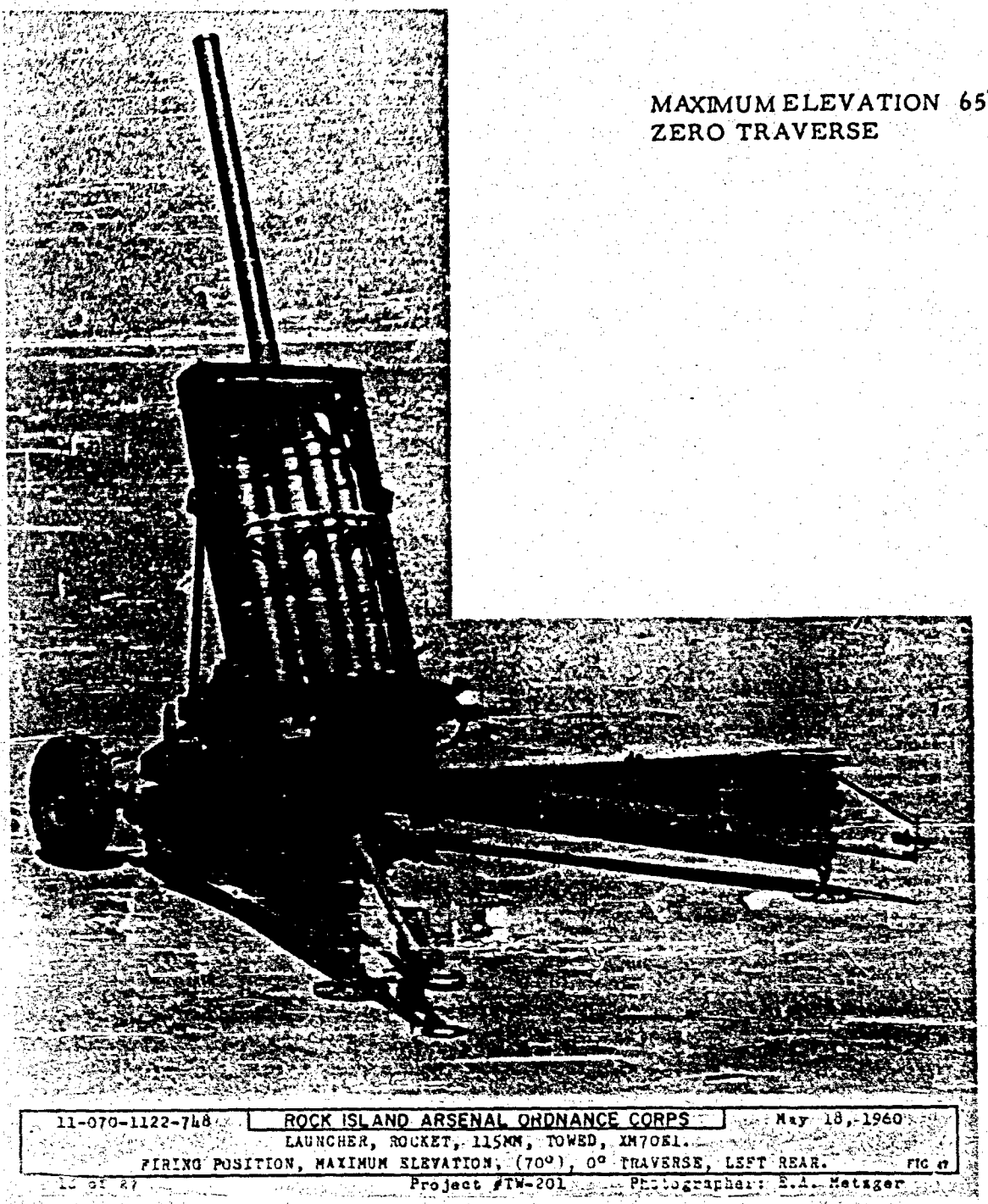

Fig. 1 PHOTOGRAPH OF LAUNCHER

MINIMUM ELEVATION, -6°
ZERO TRAVERSE

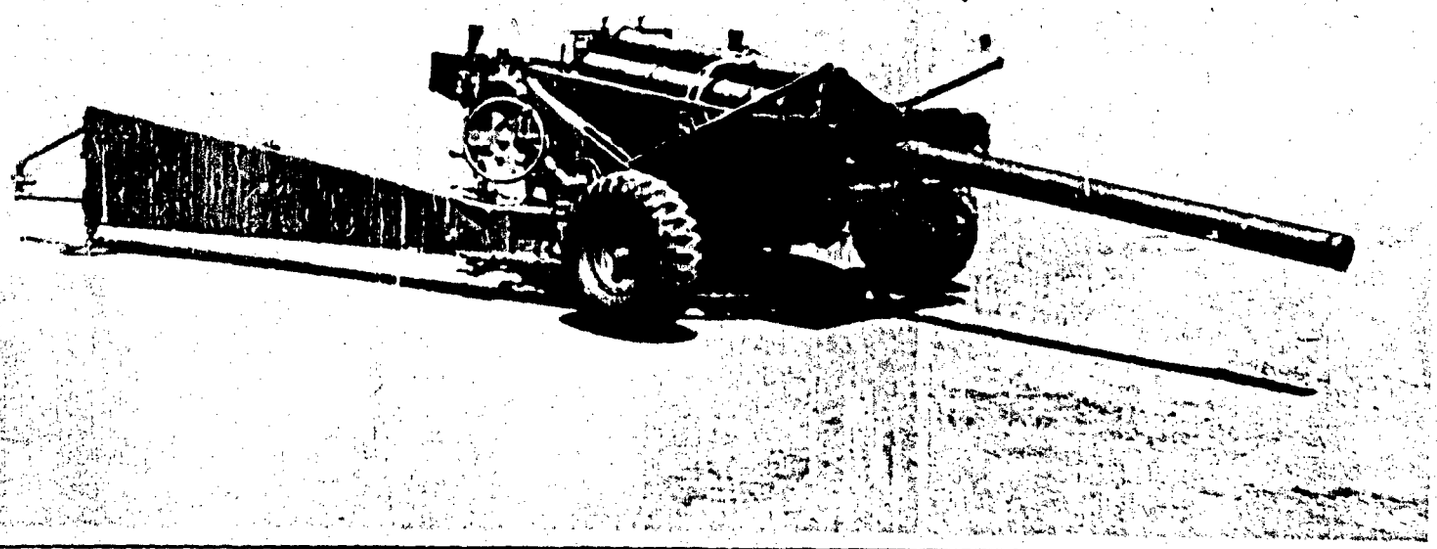

11-070-1122-746	ROCK ISLAND ARSENAL ORDNANCE CORPS	May 18, 1960

LAUNCHER, ROCKET, 115MM, TOWED, XM70E1.
FIRING POSITION, MINIMUM ELEVATION, (-6°), 0° TRAVERSE, RIGHT FRONT. FIG 48

16 of 27 Project #TW-201 Photographer: E.A. Metzger

Fig. 2 PHOTOGRAPH OF LAUNCHER

ARMOUR RESEARCH FOUNDATION OF ILLINOIS INSTITUTE OF TECHNOLOGY

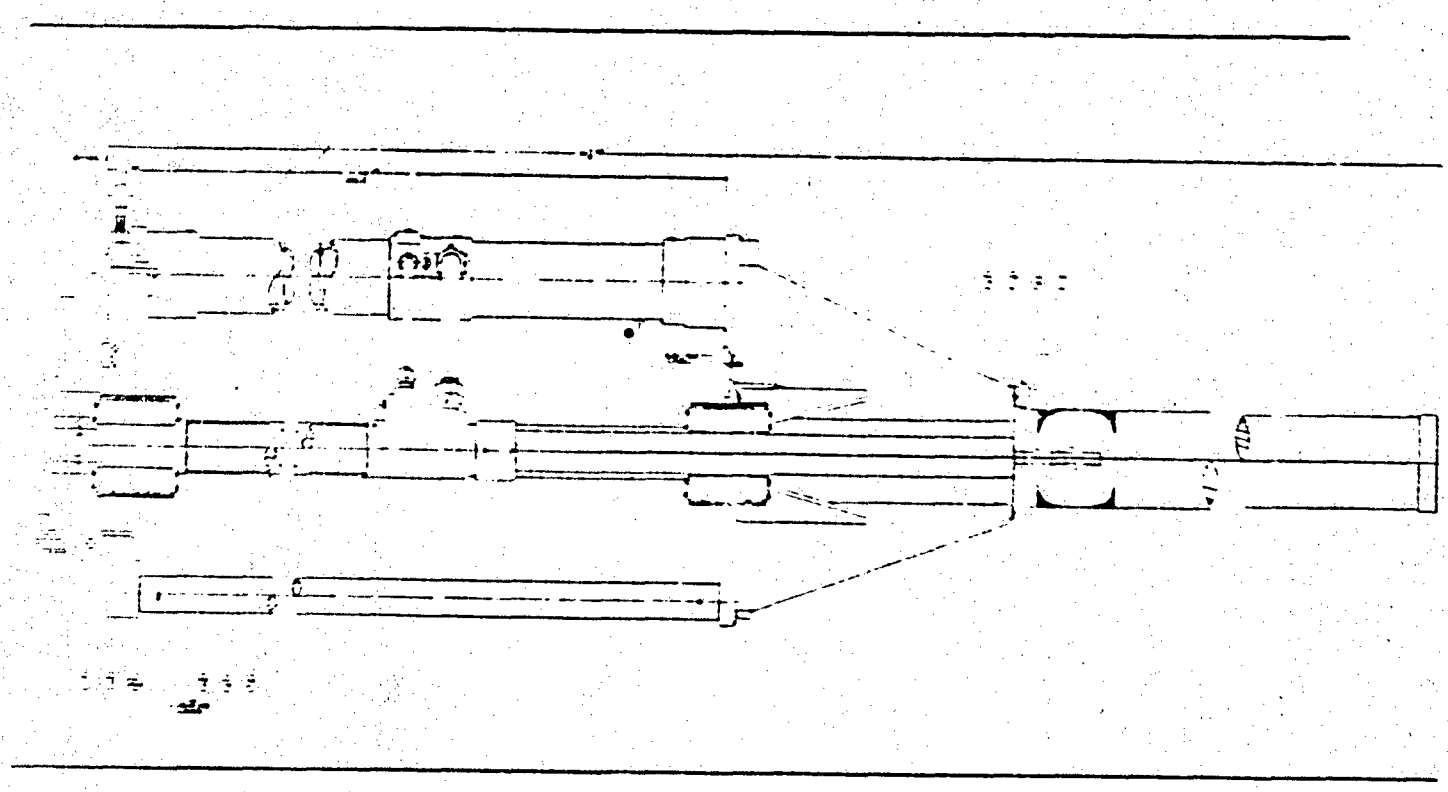

Fig. 3 SKETCH OF RECOILING ASSEMBLY

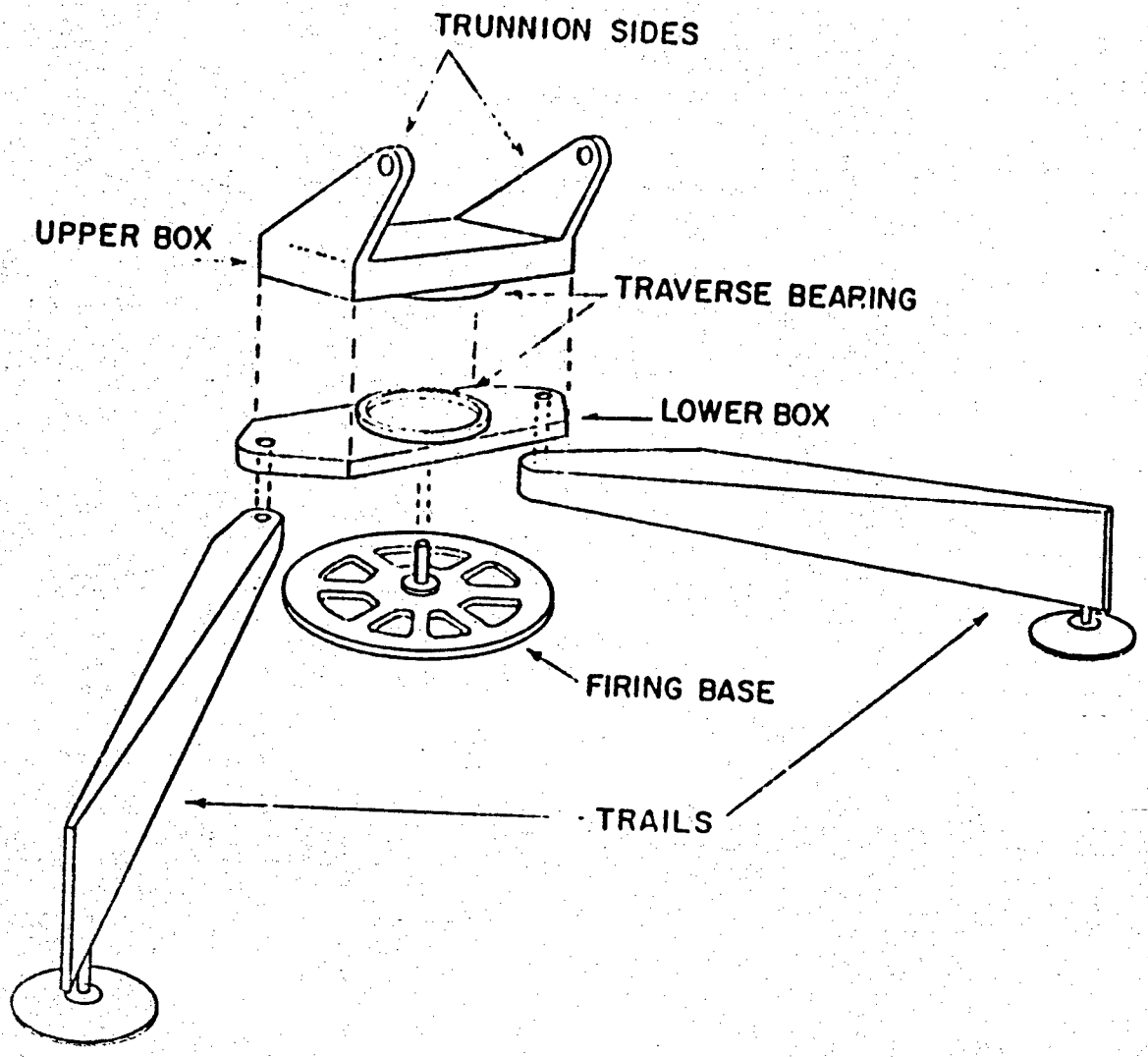

Fig. 4 EXPLODED VIEW OF THE SUPPORTING STRUCTURE

C. Elevating System

The elevating system plays an important role in the dynamic response of the launcher and deserves some discussion. This system is composed of hollow threaded rods passing through ball bearing nut assemblies held in brackets on each side of the cradle. The lower ends of these rods are inserted into the trunnion sides where they are supported by a thrust bearing in a gear box. The rods themselves are relatively stiff in tension and compression; certain other components of this system, however, comprise a significant flexibility. The brackets at the cradle are cantilevered and are inherently flexible; torsion of the cradle sides also contributes to effective relative motion of the tipping assembly and supporting structure. The ball bearings in the screw-nut mechanism, due to unavoidable clearances also add to the system flexibility in the form of nonlinearities. Likewise, the lower connections, through local deflections of the sheet metal box and trunnion sides, are relatively flexible. Thus, significant rotation of the tipping assembly mass center can occur about the trunnions (in the vertical plane) during firing, due to the flexibility of the elevating system.

D. Damping

As designed, damping of the launcher motions can occur from four sources:

1. Structural material damping,
2. Interaction with the soil,
3. The hydraulic recoil system,
4. The support buffers.

The first damping source is negligible in the presence of the others. The second source varies with the type of soil and can be either negligible or significant. The third source of damping is important because relative motion between the cradle and recoiling assembly can cause relatively large amounts of energy to be damped out by forcing oil through the orifice in each recoil cylinder. The support buffers consist of two cylinder and piston assemblies attached to the front of the lower carriage; the cylinders are fixed to the carriage and the piston rods rest against the firing base. When the supporting structure rotates forward, about the ball joint connection to the base, the

pistons force oil through orifices and damp out this forward motion. Small springs in parallel with the pistons restore the position of the supporting structure. These buffers are mainly to prevent the launcher from tipping over following the final shot of a burst when the recoiling assembly returns to battery. These buffers operate during bursts, however, when any forward rotation of the supporting structure occurs.

E. Deflection

Before discussing the dynamic response of the launcher structure to firing loads, it is necessary to first examine the supporting structure to see how it deflects to a load at the trunnions. We will consider zero traverse, a completely symmetric structure and loads in the vertical plane only. Let us assume that the tipping assembly and elevating system are removed; a force at the trunnions (for example, at 45° with respect to the ground) causes the trunnion sides to deflect relative to the upper box. Since these members are essentially short, stubby beams, both bending and shear are of equal significance. We now have a shear force and moment at the sides of the upper box; this causes bending and shear of both sides of this member relative to the bearing. However, this loading also causes torsion of the upper box section, and is the most significant deflection of this member compared to shear and bending deflections. The shear load is further transferred through the bearing down to the ground at the firing base. The moment reaction, however, is transferred through the bearing and causes torsion of the lower box, which eventually places a bending moment on the front of each trail. With respect to trunnion deflection in the vertical plane we then see that the following values of stiffness of the structure components are important:

1. Bending and shear of the trunnion sides,
2. Torsion of the upper and lower box,
3. Separation of the traverse bearing,
4. Bending of the trails.

Significant deflections occur both from the supporting structure and from the elevating system and cause a nonlinear relationship between the various deflections, due to the geometry.

F. Experimental Structure Modifications

During the experimental firings conducted on this program, various modifications to the structure were made. These took essentially two forms, changes in stiffness and changes in damping. Modifications of the structure which essentially affect only the response in the vertical plane are discussed first. The stiffening fixtures are:

1. Variable stiffness elevating rods,
2. Upper and lower box end-clamps,
3. Trunnion-to-trail struts.

The utility of the first fixture is self explanatory. The second and third sets of fixtures were designed to permit a temporary increase in the stiffness of the supporting structure by decreasing the torsion of the upper and lower boxes. The clamps were 1/2 in. thick steel brackets which joined each of the four corners of the boxes and transferred the moment reaction from the base of the trunnion sides directly to the trails. The trunnion-to-trail struts caused most of the trunnion reaction to be directly transferred to the trails. For these struts, the trails had to be rotated inward until they were set directly beneath the trunnions. Having the trails straight back caused an additional stiffness increase in this configuration.

Damping was added to the elevating system in either of two ways. Auxiliary, hydraulic dampers were placed between the cradle front and trunnion sides in parallel to the elevating screws. Figure 5 shows these dampers on the launcher. Provisions were made to change the damping source by the use of frictional ring springs in the variable flexibility elevating rods. A more complete description of these fixtures is presented in Appendix G.

The above fixtures were intended to cause a direct change of the launcher response in the vertical plane (neglecting coupling of vertical and horizontal motions). Another temporary change to the launcher structure was made, this time for the purpose of affecting the horizontal motion of the launcher. This change was the addition of a thin, sheet metal shell which surrounded the recoiling assembly and was attached to the side tie bars. This shell stiffened the framework in a manner such that the front plate and rear plate would be more securely restrained from rotating with respect to

Fig. 5 EXPERIMENTAL LAUNCHER EMPLACEMENT

each other about a vertical axis. This type of rotation was experienced in the launcher and caused a significant horizontal dispersion. For the same purpose, reduction of horizontal dispersion, the trail ends were fastened by cables to small stakes at the side of each trail. This prevented the trails from rotating (in the plane of the ground) and caused a decrease in horizontal dispersion.

III. EXPERIMENTAL WORK

The experimental effort was composed of three separate ventures:

1. The determination of the structural component flexibilities,
2. Determination of the dynamic response of the launcher in the vertical plane,
3. Testing of fixtures which were to decrease horizontal dispersion.

The values of stiffness of the structural components were needed for two reasons: first, as input to the theoretical studies and second, to determine if the particular structural designs yielded the desired stiffness, as required by earlier analyses. The stiffness was found experimentally because of the complexity of the structure; it was more efficient than corresponding calculations. In cases where calculations were made, the measurements afforded a method of checking.

The dynamic response in the vertical plane was determined for correlation with theory and thereby used to validate the corresponding mathematical model, and/or point out its deficiencies.

A. Physical Parameter Measurements

Static stiffness measurements of the following components or assemblies were made:

1. The entire supporting structure,
2. The entire supporting structure with the upper and lower boxes clamped,
3. The entire supporting structure with the box clamps and with the trunnion-to-trail struts.
4. The entire supporting structure in traverse position,
   a. 20° right
   b. 20° left
5. The lower elevating screw support,
6. Trails,
7. Elevating screw - upper bracket combination.

Since rotational motion is the sole significant contributor to dispersion, the moment of the recoil force per unit rotation of a line through the ball joint and the trunnions (in the vertical plane), is used as an indication of supporting structure stiffness. The static stiffness of the

supporting structure is therefore given in units of in.-lb/radian. For the entire supporting structure at zero traverse, this was measured to be 32×10^6 in.-lb/radian. When the box clamps were added, this stiffness became 38.5×10^6, approximately 20% greater. A much larger increase occurred when the trunnion-to-trail struts were added; the stiffness rose to 55.5×10^6, a 73% increase. This was due not only to the direct load transfer from the trunnion to the trails but is also because the trails were straight back; in this position they contributed more rigidity to moments in the vertical plane. During traverse (20° left or right) the stiffness of the supporting structure dropped to 25×10^6 in.-lb/radian for the "as-designed" structure. This decrease is expected since the stiffness of one trail is almost completely lost in this configuration.

The trail stiffness (total, for both trails straight back) for a bending moment applied at the forward end resulted in 145×10^6 in.-lb/radian. In this case, the stiffness was lower than predicted by calculation, and is believed due to local deflections in the area of the trail hinge pins.

Measurement of the stiffness of the lower elevating screw supports illustrated an unanticipated result. The left support was nonlinear up to a load of 800 lb; at this load it assumed a relatively linear, load-deflection curve shape, with a slope of 3.5×10^5 lb/in. The right support had a linear stiffness of 3.5×10^5 lb/in. from zero load. This would indicate that unsymmetrical elevating system deflections would occur. This actually happened and can be seen in the experimental records in Appendix J.

The elevating rods with their upper brackets attached exhibited nonlinear load-deflection curves as assemblies. In this situation, the nonlinearities are due to either or both of the following reasons:

1. Clearances between the ball-nut and the ball bearings.
2. Nonlinear local deflections of the balls and ball-nut.

The clearances can cause nonlinearities because as more balls come into contact at higher loads, the stiffness increases until all the balls are in contact. The resulting stiffness curves are shown in Fig. H-12.

In addition to the static stiffness measurements, dynamic measurements were made of the supporting structure. As opposed to the

static measurements where the deflection is measured under a very slowly varying load, the dynamic stiffness is a measurement of the rms value of a sinusoidally varying force and the rms value of the displacement. (Maximum values also could have been used.) This, of course, varies with frequency.

A standard 600 lb electrodynamic vibration shaker was used to excite the launcher structure for the dynamic stiffness measurements. Figure H-2c shows the physical arrangement. The tipping assembly and elevating rods were removed and a relatively stiff bar was placed across the trunnions. The shaker was coupled to the bar with a dynamic force transducer which yielded the input force. Accelerometers were placed on the trunnions to yield the motion output; the dymamic stiffness, k_D, is simply,

$$k_D = \frac{F\omega^2}{a}$$

where

F = Measured, input force, rms (or peak),

ω = Input force frequency,

a = Measured, linear trunnion acceleration, rms (or peak).

Although the repeatability of the magnitude of the measurements was not good, the shape of the stiffness-frequency curve was the same for each of the two runs. The relative minimum values of this curve (Fig. H-11) correspond to resonance frequencies of the structure. The first mode frequency (the frequency at the first resonant point) of the entire supporting structure is near 70 cps. Since the firing frequency of a burst is slightly less than 3 rounds per second, we can be confident that an undesirable structural resonance will not occur. The recoil force itself could possibly contain variations at a frequency near 70 cps, however, previous experimental and calculated curves show that the magnitude of the recoil force does not have these high frequency variations. The result is that for this launcher, calculation of the first mode response should be sufficient to predict the response accurately.

A rough check of the magnitude of this frequency can be made, combining the measured, static stiffness with the result of a calculation of an equivalent structure inertia. The equivalent structure inertia was found by assuming that the structure and its equivalent both respond harmonically

in the static deflection shape of the actual structure. Imposing the conditions that the maximum deflection and kinetic energy of both systems are identical yields an equivalent inertia; for this structure it is 115 in.-lb-sec^2. The first mode frequency is found by treating the equivalent system as a 1-degree-of-freedom system. This frequency is:

$$f = \frac{1}{2\pi} \cdot \sqrt{\frac{k_s}{I_e}} = \frac{1}{2\pi} \cdot \sqrt{\frac{32 \times 10^6}{115}}$$

$$f = 84$$

where

k_s = measured static stiffness,

I_e = calculated equivalent inertia about the ball joint.

These two frequencies correspond sufficiently close when experimental errors and simplified calculations are considered. (The methods of determination of the values of stiffness of the launcher structural components are described more fully in Appendix H.)

B. Launcher Response Determination

The dynamic response (both displacement and velocity) of the launcher in the vertical plane to firing loads was obtained directly by instrumenting the launcher during a controlled firing program. The general procedure was to fire a two or three round burst for each structural condition, followed by two single shots. The reason six-round bursts were not necessary for each condition is that the response to rounds 3, 4, 5, and 6 do not differ appreciably from the second. The short test bursts, therefore, illustrated full burst conditions and the single shots provided a reasonable check on repeatability of the type of response. The firing program with the instrumentation and structural configurations listed for each test is shown in Table I-1. A list of the type and use of recorded data is as follows:

1. Strain adjacent to the firing pin (on the rear plate of the recoiling assembly), for a firing signal proportional to the boost charge,
2. Strain of the upper trail flanges near the forward pin connections, to indicate the supporting structure rotation.

3. Cradle displacement, in the vertical plane, at the tip of the cradle. (Combined with similar trunnion motion, this furnishes cradle rotation).
4. Elevating rod strain to furnish the force in the rods,
5. Displacement of the trunnion, parallel and perpendicular to the cradle (some firings only),
6. Damper-support strain to furnish the damper force,
7. Recoil system pressure to indicate the recoil force.

The rotational response of the cradle and the trail strain (structure rotation) comprised the response data of primary significance. The cradle rotation was used as the primary indication of the effectiveness of a particular structural change in reducing dispersion. The trail strain formed an important quantity in correlating theory and experiment. The forcing functions in the form of rear plate strain and recoil system pressure were also necessary quantitites. (It should be mentioned that the trail strain measured is linearly proportional to the trail rotation only during positive rotation, the initial direction of deflection. This is because during negative rotation, the supporting structure rotates forward, the trail ends leave the ground and the strain is then a measurement of the trail inertial loads.)

Table 1 summarizes the launcher conditions during the various bursts which are discussed here. Except for the modifications listed, the launcher was as designed.

Table 1

Burst No.	Modifications to Launcher
B-2	None
B-5	Elevating system -- coil springs (total rate of 14,000 lb/in.) and little damping.
B-6	Elevating system -- coil springs and much damping.
B-7	Elevating system -- same as B-6, stiffened supporting structure.
B-8	Elevating system -- stiff rods and much damping, stiffened supporting structure.
B-9	Elevating system -- ring springs (self damping).
B-10	Elevating system -- coil spring (low boost charge, 720 fps muzzle velocity).

All the burst response curves are shown in Appendix J for each of the significant structural configurations. These response curves indicate that the structure, although theoretically symmetric about the vertical plane, has an unsymmetric response. The difference in stiffness between right and left elevating systems (as determined by measurements) is probably the major cause of this unsymmetrical response. Unsymmetrical supporting structure deflections were noted during the measurements also, but these were much smaller. These differences in response from one side of the launcher to the other increases the difficulty in analyzing these curves especially when comparing them to theoretical, planar response curves. Although these unsymmetrical deflections can increase dispersion, we will discuss the response curves as though they were identical.

In order to judge relative accuracy of these experimental response curves let us use a simple criterion. Since the recoiling assembly is relatively rigid in the plane of motion we are considering, its motion relative to the cradle due to its own flexibilities will be at a higher frequency and should damp out more quickly than the launcher response. Therefore, prior to each subsequent shot of a burst the only residual motion of significant magnitude is the gross launcher motion. The amount of residual gross launcher motion should then indicate the amount of dispersion, since if each round fires with identical initial conditions, the response of the launcher should be the same, neglecting recoil force variations due to weight changes.

Fig. J-5 shows the cradle rotation for burst B-5, fired with a softened and lightly damped elevating system. This burst had the greatest nonsymmetrical response in comparison to all the other firings. This could be due to additional nonsymmetry from the dampers. In discussing the general response, we will still neglect the difference in the curves. The cradle oscillation for this burst is a well damped response; the maximum slope of the response prior to the second shot is near 0.2 radians/sec. The time of shot ejection was not recorded; however, for maximum boost rounds (muzzle velocity of 1000 fps), this time is about 20 msec following ignition. The ignition time is marked, and we see that the slope or velocity is near zero. The trail strain, or supporting structure response in Fig. J-6 indicates some trail hop by the relatively high frequency oscillations about zero, immediately

following the large initial response. This response is also well damped. Fig. J-7 shows the cradle rotation for burst B-6 which had approximately 15 times more damping in the elevating system. As expected, the cradle response decays more rapidly, but not as much as was expected. The trail strain, Fig. J-8, still shows evidence of rebound of the structure. The maximum cradle velocity of the last oscillation prior to the second shot was reduced to 0.08 radians/sec. At the estimated time of shot ejection the cradle response is very unsymmetrical where one side has a positive velocity near 0.5 radians/sec and the other has a negative velocity near 0.08 radians/sec. Theoretically, the actual rotational velocity in the vertical plane is the average, however, since motion existed out of the plane, this number may be meaningless. The important fact is that the overall response damped out more quickly.

When the supporting structure was stiffened with the box clamps and trunnion to trail struts, burst B-7, the launcher response changed significantly. Fig. J-9 shows the cradle response and Fig. J-10 the corresponding trail strain. The cradle rotation essentially remained positive at all times as did the trail strain. In addition, the magnitude of the cradle rotation was significantly lower; the peak trail strain was slightly lower. The most important change, however, is the shape of the cradle response just prior to the second shot; the slope remains close to zero with only small variations. This indicates small cradle velocity and improved accuracy.

Another modification was made to the launcher by replacing the soft coil springs in the elevating rods by relatively rigid members in burst B-8. The dampers and supporting structure stiffeners were retained. The response of this system (Fig. J-11) was very similar to that of the previous one with possibly a small increase in the residual cradle oscillations. This would seem to indicate that elevating rod flexibility is not a significant parameter. Another possibility exists, however, and is more likely the situation. As indicated in the section describing the launcher, significant elevating system flexibilities occur from sources other than the rods themselves. For this reason, when the rods were stiffened, the system flexibility was not significantly changed. This is due to the fact that for a series system of flexibilities, the overall flexibility is always less than the smallest of the

component flexibilities. An interesting cradle response occurred during this burst (three rounds). The cradle rotation had a larger mean residual value between each of the succeeding rounds; in other words, the response had a tendency to climb. Although the cradle velocity was insignificant prior to each shot, the displacement was increasing. This leads to an undesirable effect upon accuracy.

Burst B-9, Fig. J-13 and J-14, shows the result of using ring springs in the elevating system; ring springs have inherent damping since their deflection is accompanied by sliding upon each other. These were designed to furnish near the maximum possible damping for the stiffness equivalent to the coil springs. Apparently, this amount is insufficient to furnish a good response.

The final firing of a modified launcher, burst B-10, consisted of a two-round burst with a zone 7 boost charge (muzzle velocity of 720 fps). The only change in the launcher structure was the addition of coil springs into the elevating system; a lower zone of boost ammunition was necessary to prevent bottoming of the springs. The cradle response (Fig. J-15) is very similar in shape to the response of burst B-5. The newer response has a generally lower magnitude because of the lower projectile boost. It is very interesting to note that the response is still very well damped even though no damping was added. This is pointed out again and discussed when the response of the unmodified launcher is discussed.

A very important characteristic of this launcher is illustrated in burst B-10, i.e., the variation in rate independent of the response. The second round fired at approximately 0.7 seconds after the first, compared to less than 0.6 seconds in the other bursts. Although the variation in this burst was later discovered to be caused by mechanical interference in the indexing cams, other changes can produce the same effect. For example, changing the bypass valve in the counterrecoil flow can vary the duration of counterrecoil and therefore the firing rate. Also, variations in recuperator preload (which is sensitive to ambient temperature) can also cause rate changes. The point is that a negative cradle velocity prior to ignition of the rounds such as in burst B-5, cannot be depended upon to decrease the value of the initial positive response following ignition. This is because firing time, relative to the cradle

oscillation, would be very difficult to control. The proposed alternative, sought here, is to reduce the cradle oscillations to a minimum and rely on consistency. This was implicit in the simple criterion previously stated.

One last point to be mentioned about the response of burst B-10 is the very slow initial rise time of the cradle on both shots. This is in comparison to all the other bursts. It is due mainly to the slower rise time of the recoil force for the smaller boost. The type of recoil system used has this characteristic feature.

We will now discuss how these response curves differ from those of the launcher in its as-designed condition. Fig. J-1 shows the cradle response during a 6-round burst, B-2. In comparison to the launcher with a more flexible elevating system, the response is similar in that the negative cradle rotation has appreciable magnitude; the residual oscillation, however, has a very small magnitude as well as negligible variation. (Because of the perfectly flat, residual response, the consideration of instrument error must be made. However, two other 6-round bursts yielded the same result.) It appears that the as-designed structural configuration, by the simple criterion set up, should produce the best burst accuracy. To a limited extent this is true, but there are two important considerations which must be mentioned. The first consideration is the reason why the as-designed structure responded the way it did. If we look at the corresponding trail strain curves (Fig. J-2 and J-3) we can see that because of the high frequency oscillation about zero, the rear of the trails must have lifted from the ground. This is due simply to the elastic rebound, or overshoot, of the structure caused by the recoil force characteristics. This means that the supporting structure rotated forward about the ball joint and compressed the two support buffers between the lower box and the firing base. The amount of trail hop is dependent upon the following quantities:

1. Shape and magnitude of the recoil force,
2. Drop off time of the recoil force relative to the natural period of the system.

Variations in the structural stiffness or the inertia of the launcher can alter the occurrence of hop. This was shown when the supporting structure was stiffened -- the hop was absent.

The second consideration is that while the supporting structure is tipped forward, the launcher can turn about a vertical axis through the ball joint. This allows the launcher to lose its aimed orientation and cause horizontal dispersion. Since a method exists to eliminate this rotation during hop (discussed in the next section), choice can be made to either eliminate the hop, by a stiffer carriage for example, or eliminate the rotation during hop. Either is an acceptable method to insure good horizontal dispersion. Other considerations may enter into a choice of whether or not trail hop should be eliminated, such as the safety of the crew.

C. Horizontal Dispersion

Early tests of the XM70E1 tipping parts indicated that horizontal dispersion was larger than vertical and followed a left-right-left sequence of impact points in burst firings. No analytical attack was made on the dispersion problem when it was first recognized because at that time no logical theory of the behavior could be constructed. In particular, the powder couple did not offer a logical explanation because it does not change direction after each shot.

A test program was planned to investigate the sequential horizontal dispersion. The weapon was prepared and the tests were conducted with the extensive cooperation of the Rock Island Arsenal. It was possible to conduct the tests on the force mount at Rock Island Arsenal because the dispersion evidenced itself with a high degree of repeatability during the proof tests of both Prototype No. 2 and Prototype No. 3.

The first group of tests showed that any round fired from a breech tube in the left cluster would fall 5 in. or more to the left of the vertical boresight line and that any round fired from the right would fall 5 in. or more to the right, at an 85-yd range, for all conditions tried. The boresight spot on the target coincided before and after each firing.

Instrumentation changes were made, and the weapon was prepared for a second series of tests. The tests showed no substantial improvement with slugs more accurately centered in the breech tubes or with disconnected igniter tubes, but some improvement was obtained with the clusters shimmed tight between the front and back plates. The instrumentation indicated that

the hub of the cluster being fired was not being properly loaded with the inertia force of the cluster.

Instrumentation changes were made, and the weapon was prepared for a third series of tests. These tests showed that a round could be fired accurately from either cluster if that cluster were drawn back tight against the back plate when the round was in the firing position. This was accomplished by preloading the cluster thrust bearing located in the back plate of the recoiling assembly framework. Indexing during firing was then impossible and was prevented by removing the indexing cam followers.

At this time, it was realized that the breech tube being fired was being driven back against the back plate and was carrying the connected cluster rearward with it. This resulted in the application of a large moment to the rear plate since the inertia force of the non-firing cluster was being applied at its thrust bearing.

A final series of tests was conducted with the breech tubes permitted a few thousandths of an inch axial movement in the retaining spiders. This allowed the tube being fired to move rearward without carrying its cluster with it. The horizontal dispersion was very substantially reduced. Several 6-rd bursts at zone 10 (1000 fps muzzle velocity) were fired through targets at 85-yd range. The target pattern was nearly rectangular with overall dimensions of approximately 5 in. vertical by 10 in. horizontal.

The remaining horizontal dispersion is still sequential. Calculations show that because the breech tube being fired is driven rearward primarily by the powder-gas pressure acting on a belled portion at the front of the tube, its mass is lost from the cluster assembly and the loss of that mass then produces the sequential horizontal dispersion. Figure 6 and 7 show schematically how the cluster inertia forces are distributed throughout the recoiling framework.

A series of firing tests[1/] was conducted with Prototype No. 3 during September and October, 1960 at Redstone Arsenal to determine the effect of increased rigidity between the front and rear plates (i.e. rigidity

---

[1/] Armour Research Foundation Report 8130-20, P. II-4.

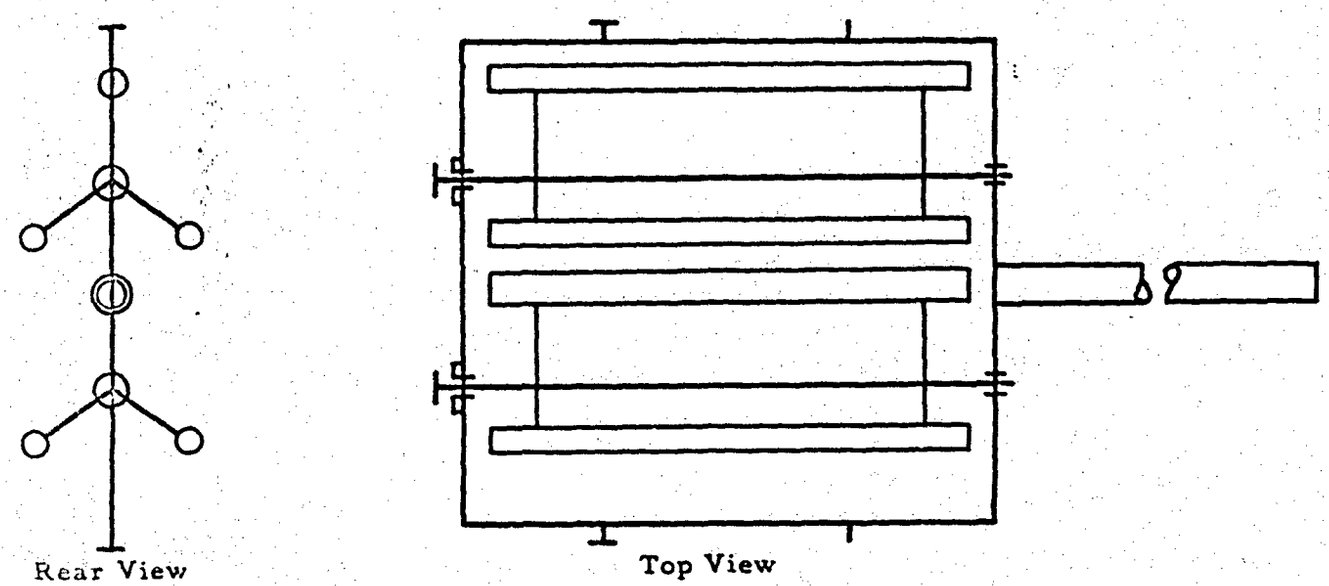

Fig. 5 SCHEMATIC OF RECOILING ASSEMBLY

ARMOUR RESEARCH FOUNDATION OF ILLINOIS INSTITUTE OF TECHNOLOGY

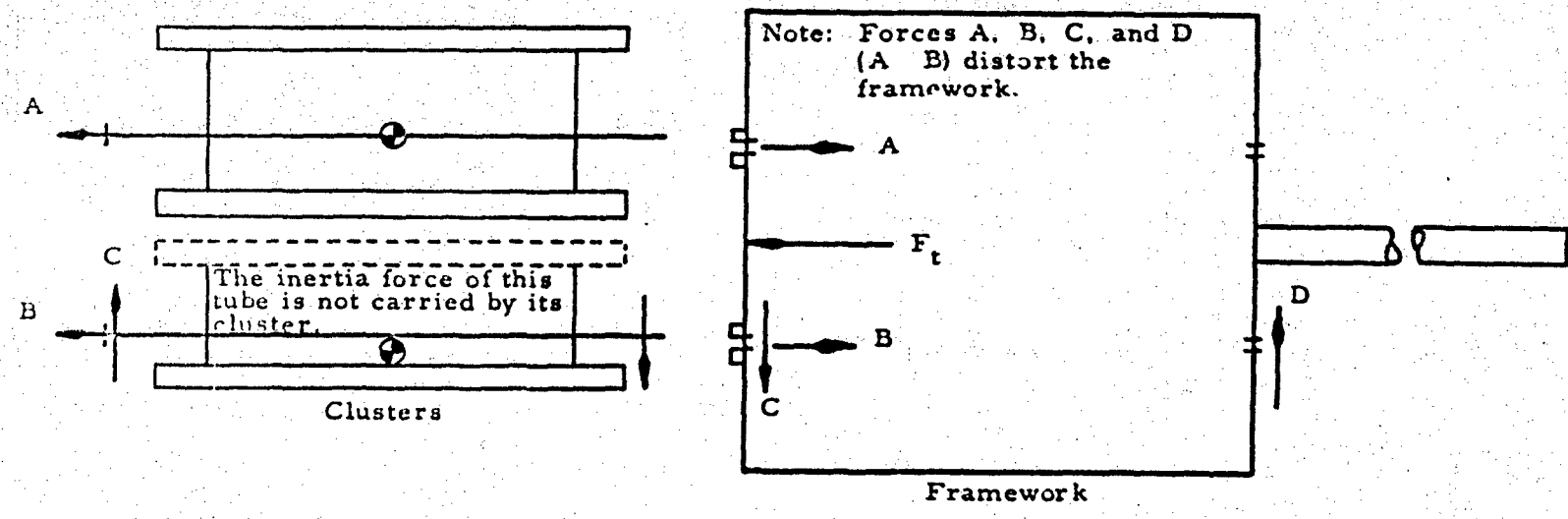

Fig. 7 REACTIONS BETWEEN CLUSTERS AND FRAMEWORK

ARMOUR RESEARCH FOUNDATION OF ILLINOIS INSTITUTE OF TECHNOLOGY

of the recoiling assembly framework) on the sequential horizontal dispersion.

A calculation showed that sequential horizontal dispersion would be very small if the recoiling assembly framework was very rigid. The problem then was to find a lightweight structure that would greatly increase the stiffness of the framework. It was decided that the most efficient structure would be a thin metal skin or shell enclosing the entire framework.

The firing program was set up to fire 6-round bursts with and without the shell. To measure shell effectiveness, two quantities were recorded: (1) the bending strain of the firing tube near its base in the horizontal plane, and (2) the target patterns. Six bursts were fired, three with and three without the shell. (The launcher also contained additional stiffening fixtures used in the previous Fort Sheridan firings, consisting of carriage clamps at the front and rear corners of the box sections, trunnion-to-trail struts.)

The records of bending strain in the firing tube without the shell exhibited the alternating direction of initial bending moment. With the shell, the initial direction of the bending moment was consistently in one direction, which can be logically explained by the rifling torque; see Fig. 8. The target patterns, however, did not show any reduction in horizontal dispersion. It was decided that the rigid body rotation of the launcher, due to the trail pads shifting along the ground, was hindering the effectiveness of the shell.

A portion of the test was thus repeated in an attempt to obtain less horizontal dispersion. This time the trails were restrained from rotating about the ball joint in the plane of the ground by placing a pinned connection between a stake and a trail on each side of the launcher. This permitted small rearward and upward trail motions. In this condition, four 6-round bursts were fired, two with and two without the shell. The resulting target patterns are shown in Fig. 9. The two bursts with the shell are rounds No. 93 - 98 and 99 - 104; the two bursts without the shell are No. 106 - 111 and 112 - 117. The firings with the shell had a total horizontal dispersion of approximately 1.5 and 1.9 mils, while the two without the shell had a total horizontal dispersion of 3.7 and 2.9 mils. Because of the single-hole targets, it is impossible to calculate the standard deviation, but it can be inferred

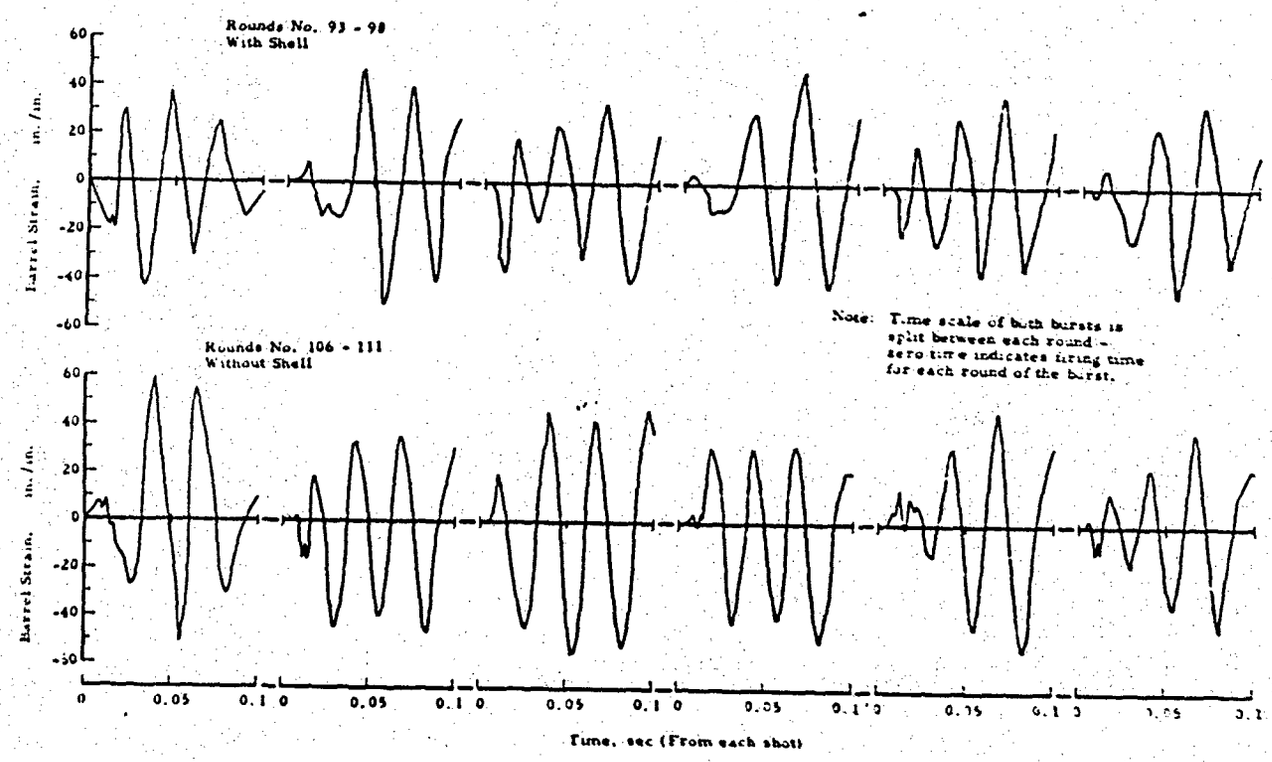

Fig. 8 BARREL STRAIN

ARMOUR RESEARCH FOUNDATION OF ILLINOIS INSTITUTE OF TECHNOLOGY

Fig. 9 TARGET PATTERNS

that, for the two bursts with the shell, the standard deviation is less than 1 mil.

The results of these tests indicate that the shell offers a reduction of horizontal dispersion of nearly 100%. (The trial ties showed a reduction of 200 to 300%.) The reliability or consistency is fairly satisfactory since these targets represent four consecutive bursts fired from Prototype No. 3 under identical conditions. But in order to obtain these results, it must be emphasized that the trails were restrained from rotating about a vertical axis through the ball joint.

IV. THEORETICAL ANALYSES

The theoretical analyses of the launcher dynamics consist of two specific mathematical models to determine launcher motion, and three supplemental studies which used very simple dynamic models in order to directly study the effects of certain parameter variations. The two models which were developed to calculate the launcher motion are:

1. A planar, nonlinear, 3-degree-of-freedom system,
2. A three-dimensional, nonlinear, n-degree-of-freedom system.

The three supplemental studies include:

1. A linear, 2-degree-of-freedom analysis to study the effectiveness of various locations for auxiliary damper locations,
2. A third-order, linear single-degree-of-freedom model to determine optimum elevating system structural parameters,
3. A linear, second-order system to determine the parameters which bring about an optimum response decay.

The derivation, assumptions, and some results of these models and studies are presented in the appendices; a discussion of their development, applications and results are presented in this section.

The derivation and discussion of a mathematical accuracy criterion is also included in this section. This criterion is based upon the sensitivity of the rocket to the different launcher motions studied in the mathematical models.

A. Planar, Nonlinear, 3-Degree-of-Freedom Model

Prior to the initiation of this Long-Range Study Program, some dynamic studies were conducted which aided the formulation of this model. One study, in particular, was a similar, planar, 3-degree-of-freedom model with the following degrees of freedom:

1. Rigid body rotation of the launcher about the trail ends; base hop,
2. Recoil motion,
3. Elastically restrained rotation about the ball joint.

The last type of motion was assumed to the first mode response of the relatively flexible supporting structure, with a rigid tipping mass and rigid elevating system.

Subsequent experience, both from the use of the above model and from actual launcher firings, provided valuable information for making assumptions for the new model. For example, instrumented firings and the output of the above model both showed that rotation about the trail ends was very small. It was therefore neglected in the new model. Recoil motion calculated in the above model agreed fairly well with experiment except during counterrecoil. The difference was traced to seal friction and indexing forces. The former results in longer counterrecoil durations, while the latter brings about two changes. Indexing forces cause small changes in the recoil motion but more important, they significantly affect the cradle response. Consequently, they were both included in the new model. Inability to obtain a good correlation of the experimental response with the output of the prior model led to the conclusion that the elevating system was flexible. Again, this flexibility was therefore included. The assumption of the first mode response of the supporting structure was supported by previous experimental firings, and was reconfirmed with the dynamic analysis described earlier; this assumption was retained. The three degrees of freedom of the model developed on this program correspond to:

1. Elastically restrained rotation of the supporting structure about the ball joint, φ_1.
2. Recoil motion relative to the cradle, u,
3. Rotation of the tipping parts about the trunnion relative to the supporting structure, φ_2.

The last motion is a consequence of the flexible elevating system. Although no auxiliary damping in the elevating system was included in the as-designed launcher, linear damping terms were placed in the equations for dampers in parallel with the elevating rods and also a damper between the lower box and the ground.

The frictional forces were added in the form of a constant frictional force due to the preload plus a term proportional to the recoil pressure. This corresponds to the type of seals employed. The equation of motion of the recoiling mass in the u direction also includes terms representing the constant-force, constant-stopping distance recoil system used in the launcher.

The final equations of motion consisted of three, second-order, nonlinear differential equations. In order to solve these without making any restrictive, simplifying assumptions, they were programmed for ARF's Univac 1105 in the Univac Scientific Exchange (USE) language. This program is described in Appendix D. Solution of the three, second-order differential equations was effected by using the Runge-Kutta numerical integration technique. Launcher parameters such as damping, stiffness, recoil rod shape, initial boost charge force, etc. were all included as input data; a sample output sheet is shown in Fig. D-2.

The purpose of the computer solutions of launcher motion can be grouped into three divisions by considering their purpose. The first group of solutions was aimed at matching the experimental launcher response. The second was to verify the existence of an optimum response and determine the optimum parameters. (This is described later when the optimum system is discussed.) The final group of computer runs was to show the results of various changes, e.g., low zone response, efforts of elevation changes, and delayed recoil.

1. Correlation of Theory with Experiment

The success of correlation between computed and experimental response curves varied and depended upon launcher parameters; in general the agreement was better when less negative carriage rotation occurred. The difficulty was due to the fact that the original model did not represent the nonlinear stiffness and damping displayed by the launcher supporting structure. This was subsequently corrected and closer correlation obtained, though not entirely satisfactory.

Figures 10 through 21 show typical information obtained from the computer program. Figure 18 shows a full burst response. The numerical input corresponded to either measured or calculated values of physical parameters of Prototype No. 3 Launcher. Certain parameters were varied, however, to obtain the correlation. All of the parameters not designated on the curves are listed on the computer program in Appendix D.

The two curves shown superimposed in Fig. 23 are the cradle response from Fig. 15 and the experimental cradle response from firing

R-38, listed in Table I-1. This experimental response was from a single shot with identical launcher conditions to burst B-8, Fig. J-11. The supporting structure stiffness measured for this condition was 5.5×10^7 in.-lb/radian. The numerical value of carriage stiffness used in the computer program was 4.5×10^7 in.-lb/radian and is significantly lower. The fact that this lower value was necessary to match the experimental response is probably due to the flexibility added to the system by the soil in the actual firing. (The structural stiffness measurements were made on concrete.) The measured elevating system stiffness for shot R-38 was approximately 4.5×10^5 compared to 1.4×10^4 used in the computer. The difference, though very large, is probably due to the unmeasured elevating system flexibilities discussed earlier. (Burst B-7 had an elevating system stiffness of 1.4×10^4 lb/in. but had a very similar response to burst B-8, even though the latter supposedly had a much stiffer elevating system. This further supports the conclusion that the high, measured stiffness value is not correct.)

A further comparison can be made between the computed carriage rotation (Fig. 13) and the trail strain from burst B-8, Fig. J-11. These curves agree in less detail, but their main characteristics are the same. The computed curve is generally smoother since it does not contain any higher mode response characteristics.

Figures 26 and 27 show experimentally obtained strain from the elevating screw and damper supports. These curves are tensile and compressive strain in circular, pinned rods and are directly proportional to the forces. They compare reasonably well with the spring force and damper force shown in Fig. 18 and 19 respectively.

Because of the similarity of the response of burst B-7 and B-8, we see that the computed response also agrees reasonably well with B-7. In this case the actual launcher had an elevating stiffness of 1.4×10^4. Burst B-6, Fig. J-7, reveals a large negative dip after the initial positive displacement, which did not occur in burst B-7 or B-8. The only difference is that B-6 did not have a stiffened supporting structure. Reduction of only the supporting structure stiffness in the computer model produced the response in Fig. 24. The expected correspondence does not occur; the cradle response remains essentially positive. The negative supporting structure response, however, doubled compared to the previous theoretical response which indi-

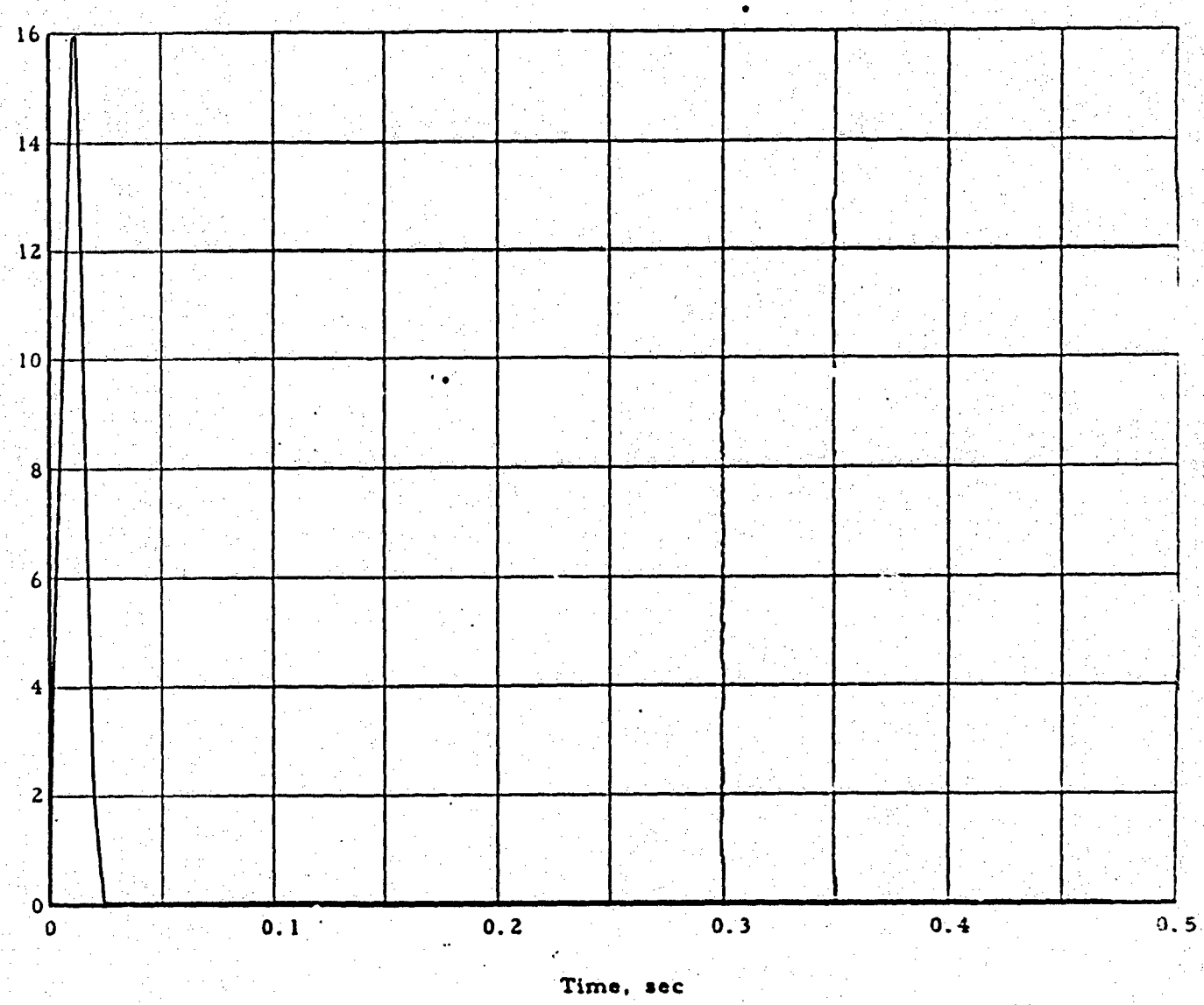

Fig. 10 TYPICAL COMPUTER SOLUTION -- POWDER GAS FORCE

ARMOUR RESEARCH FOUNDATION OF ILLINOIS INSTITUTE OF TECHNOLOGY

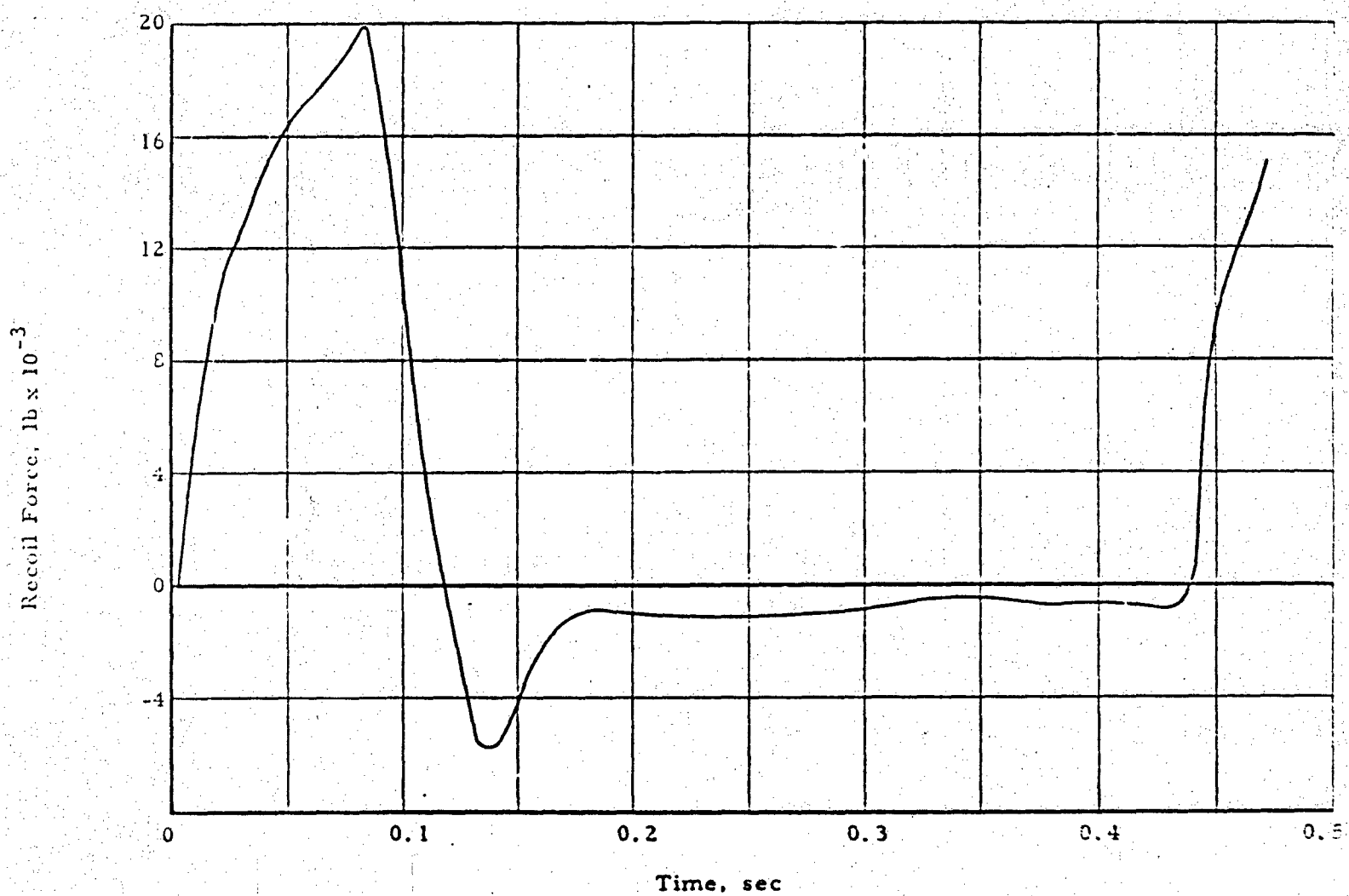

Fig. 11 TYPICAL COMPUTER SOLUTION -- RECOIL FORCE

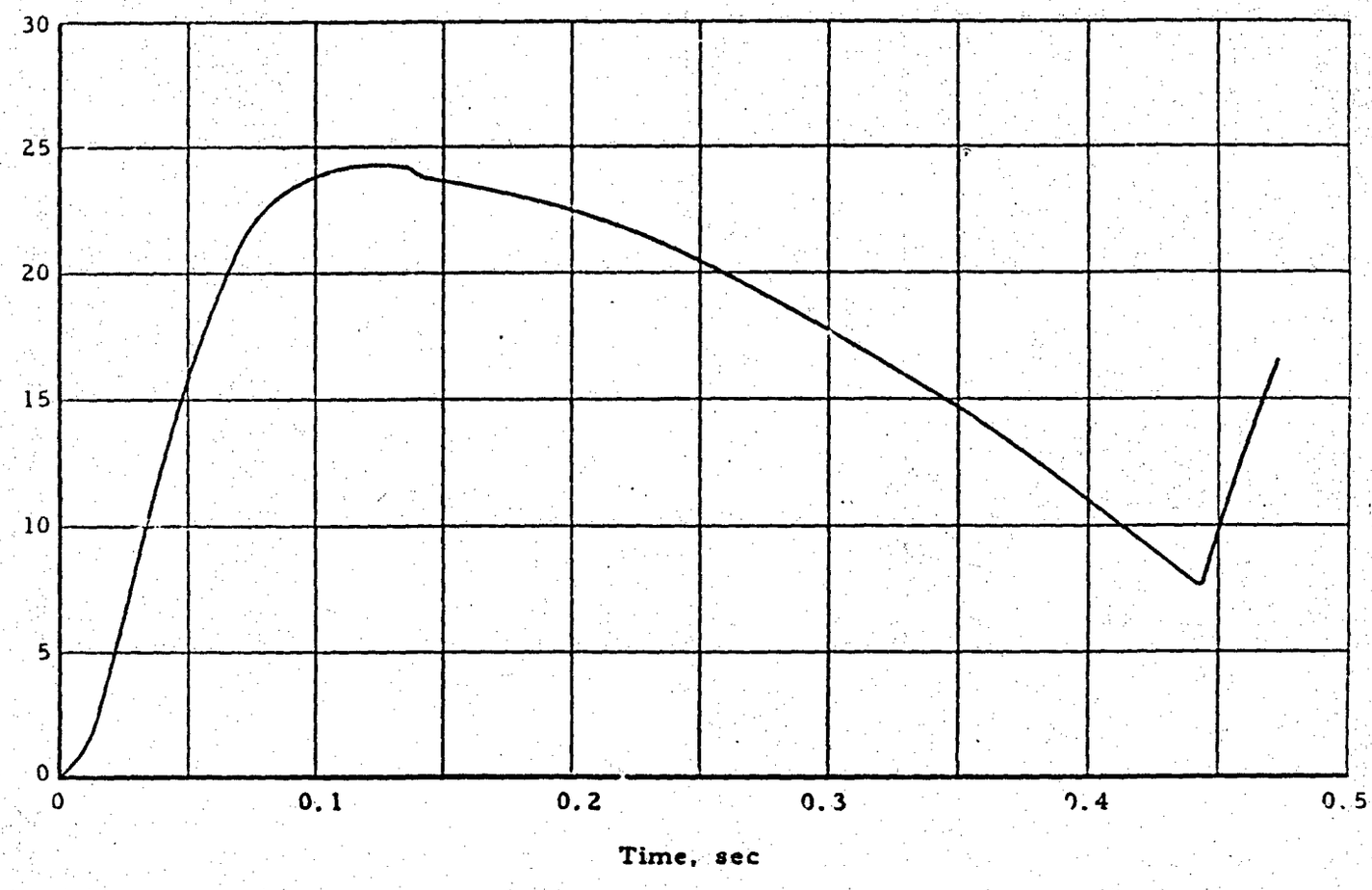

Fig. 12 TYPICAL COMPUTER SOLUTION -- RECOIL DISPLACEMENT

ARMOUR RESEARCH FOUNDATION OF ILLINOIS INSTITUTE OF TECHNOLOGY

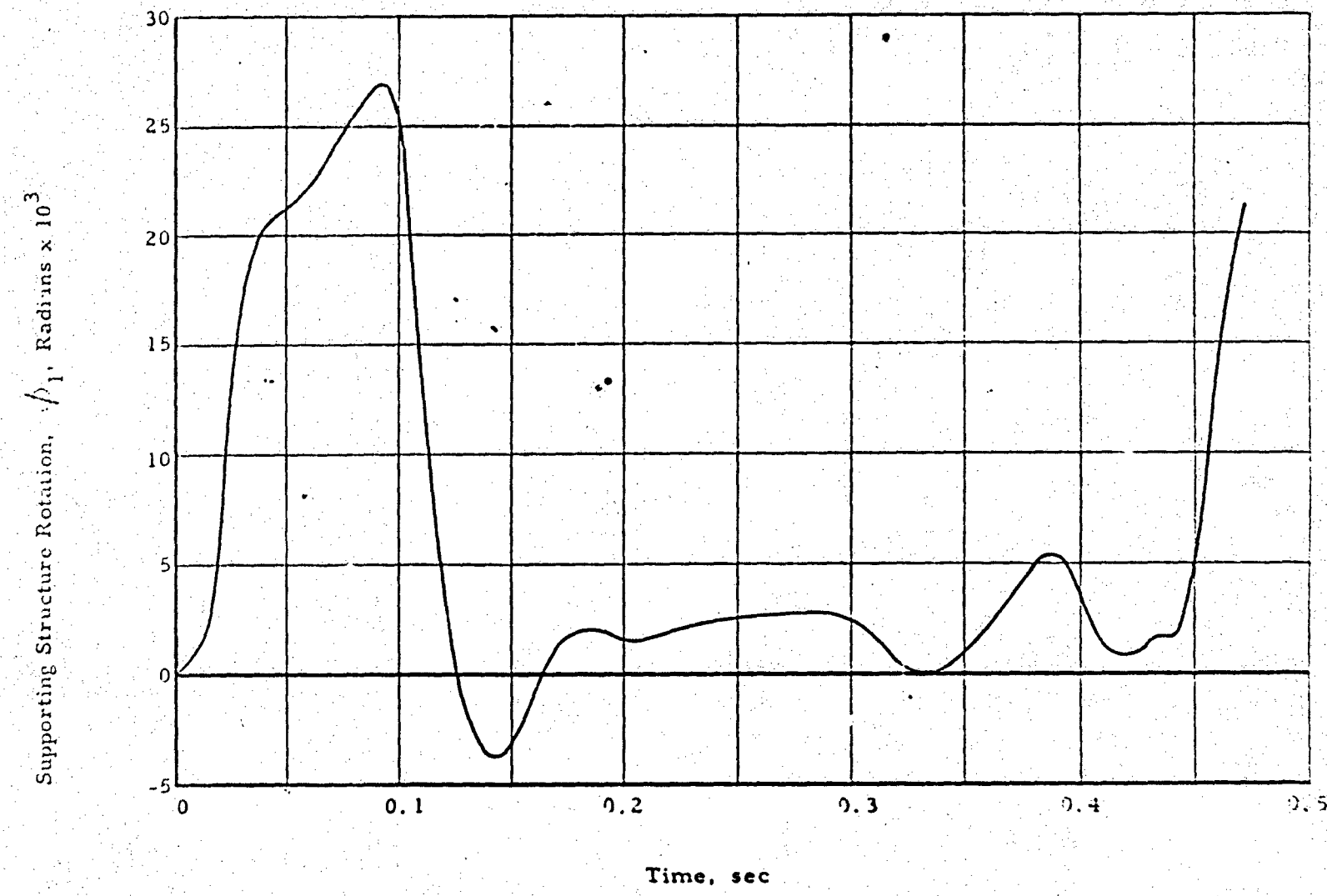

Fig. 13 TYPICAL COMPUTER SOLUTION -- CARRIAGE ROTATION

ARMOUR RESEARCH FOUNDATION OF ILLINOIS INSTITUTE OF TECHNOLOGY

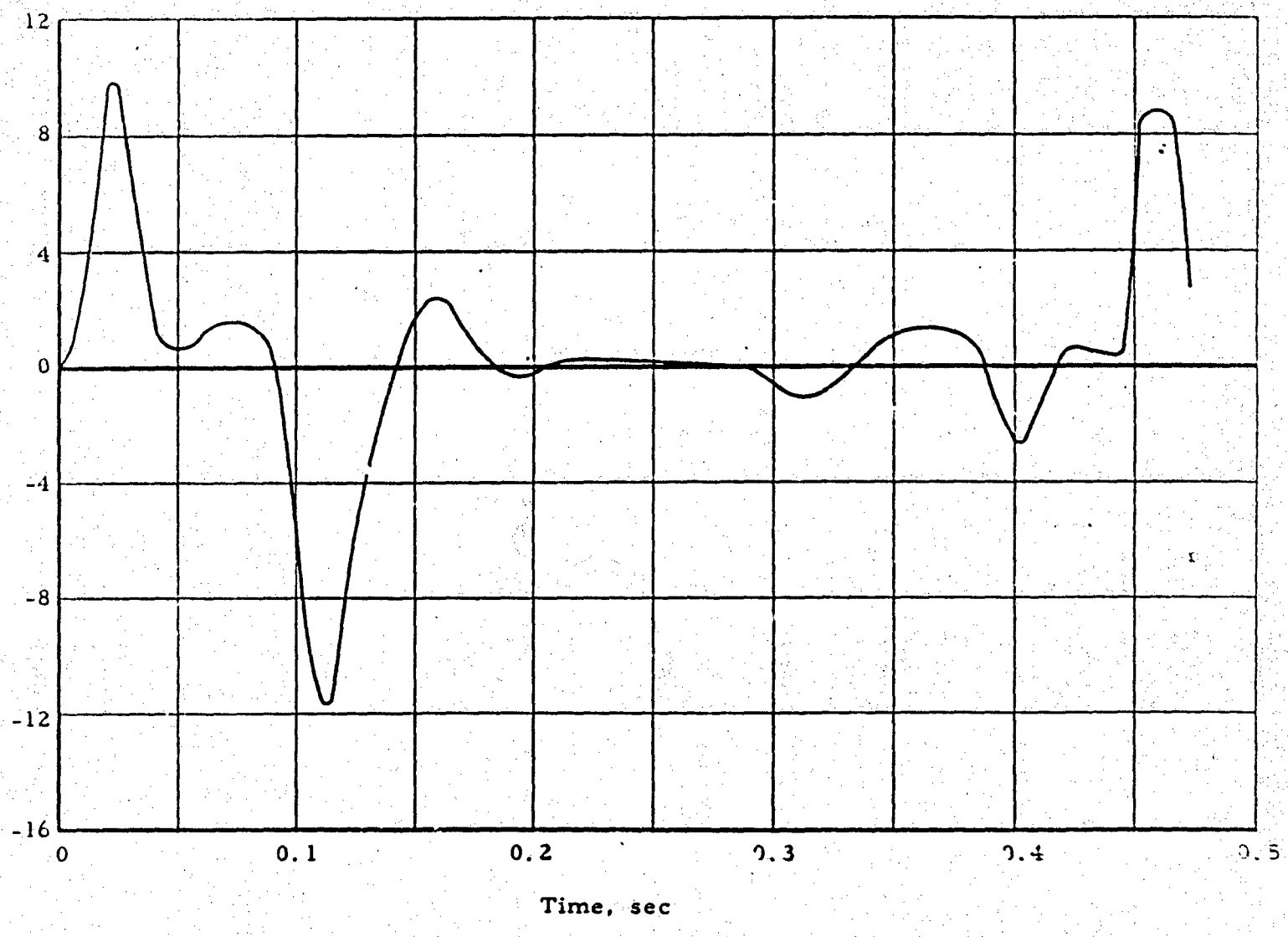

Fig. 14 TYPICAL COMPUTER SOLUTION -- CARRIAGE ROTATIONAL VELOCITY

ARMOUR RESEARCH FOUNDATION OF ILLINOIS INSTITUTE OF TECHNOLOGY

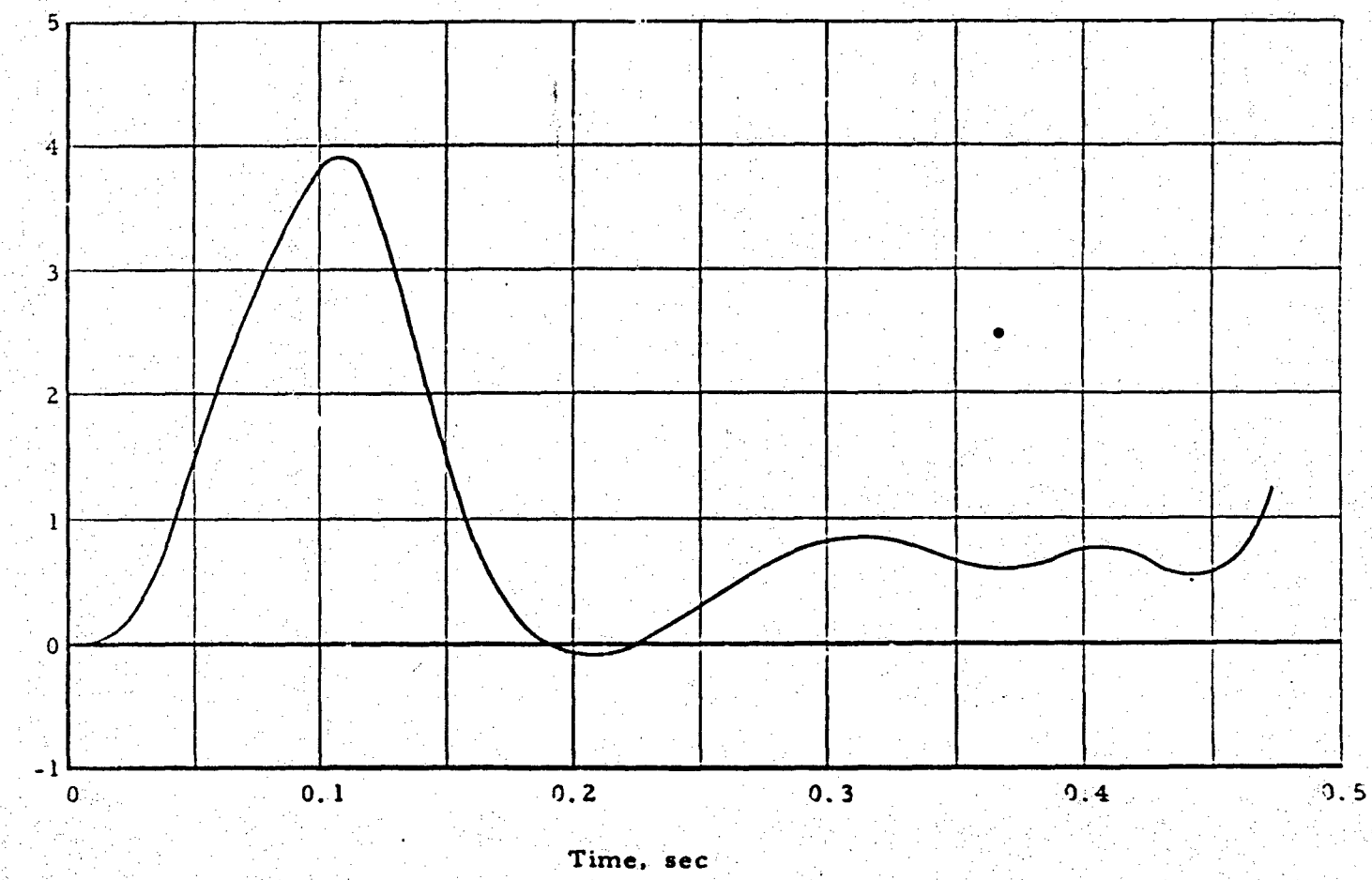

Fig. 15 TYPICAL COMPUTER SOLUTION -- CRADLE ROTATION

ARMOUR RESEARCH FOUNDATION OF ILLINOIS INSTITUTE OF TECHNOLOGY

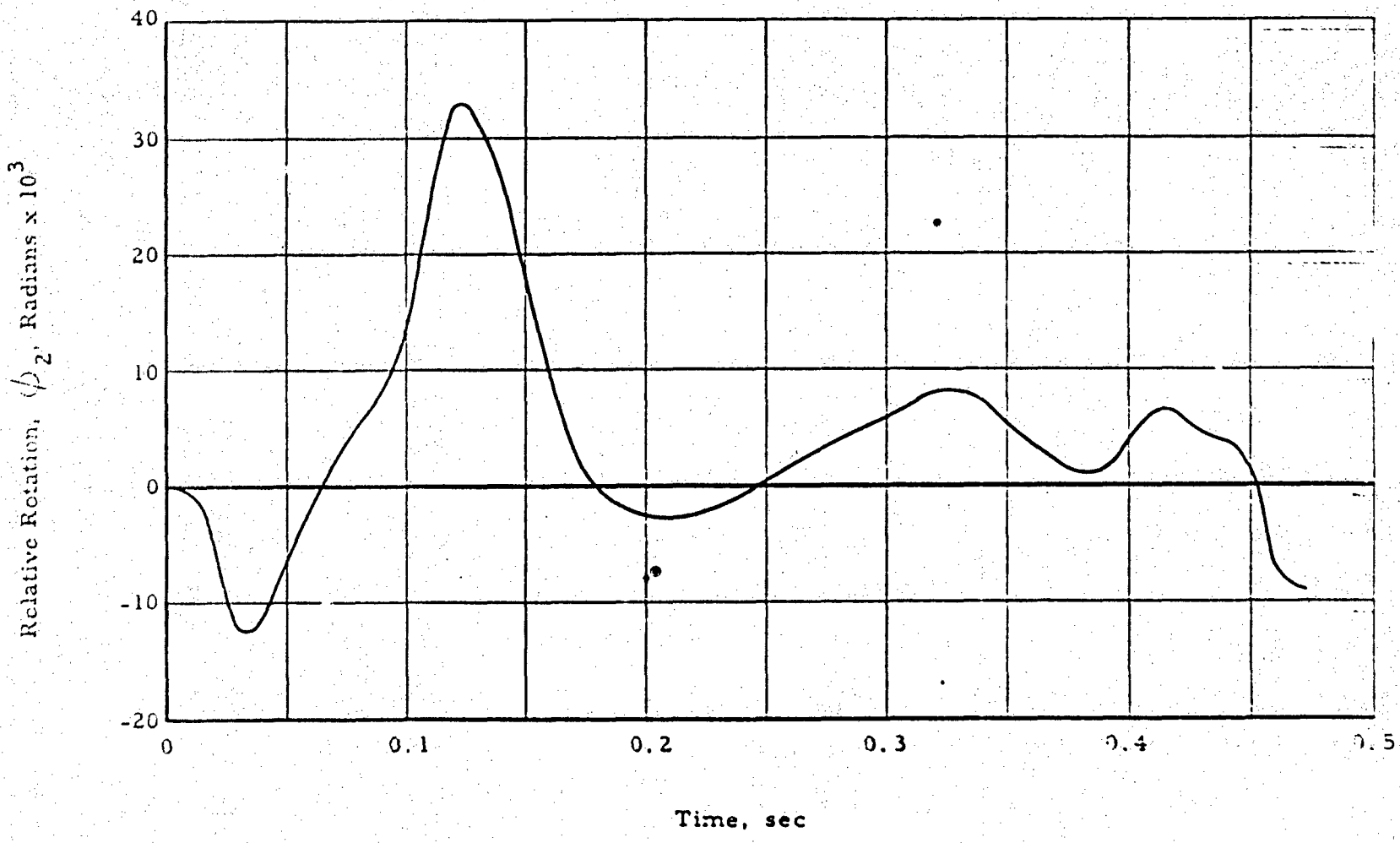

Fig. 16 TYPICAL COMPUTER SOLUTION -- CRADLE-CARRIAGE RELATIVE ROTATION

ARMOUR RESEARCH FOUNDATION OF ILLINOIS INSTITUTE OF TECHNOLOGY

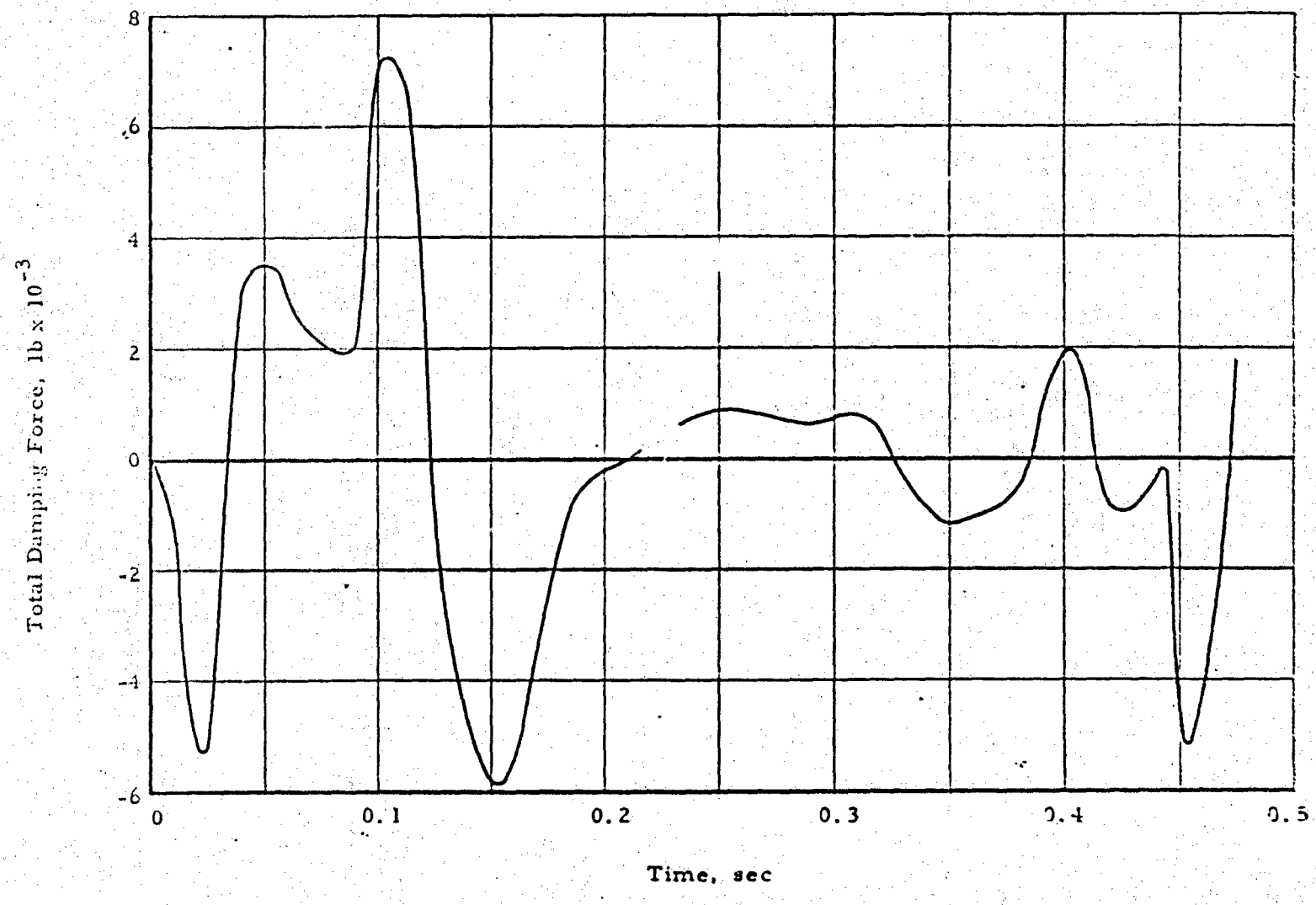

Fig. 17 TYPICAL COMPUTER SOLUTION -- CRADLE-CARRIAGE RELATIVE ROTATIONAL VELOCITY

ARMOUR RESEARCH FOUNDATION OF ILLINOIS INSTITUTE OF TECHNOLOGY

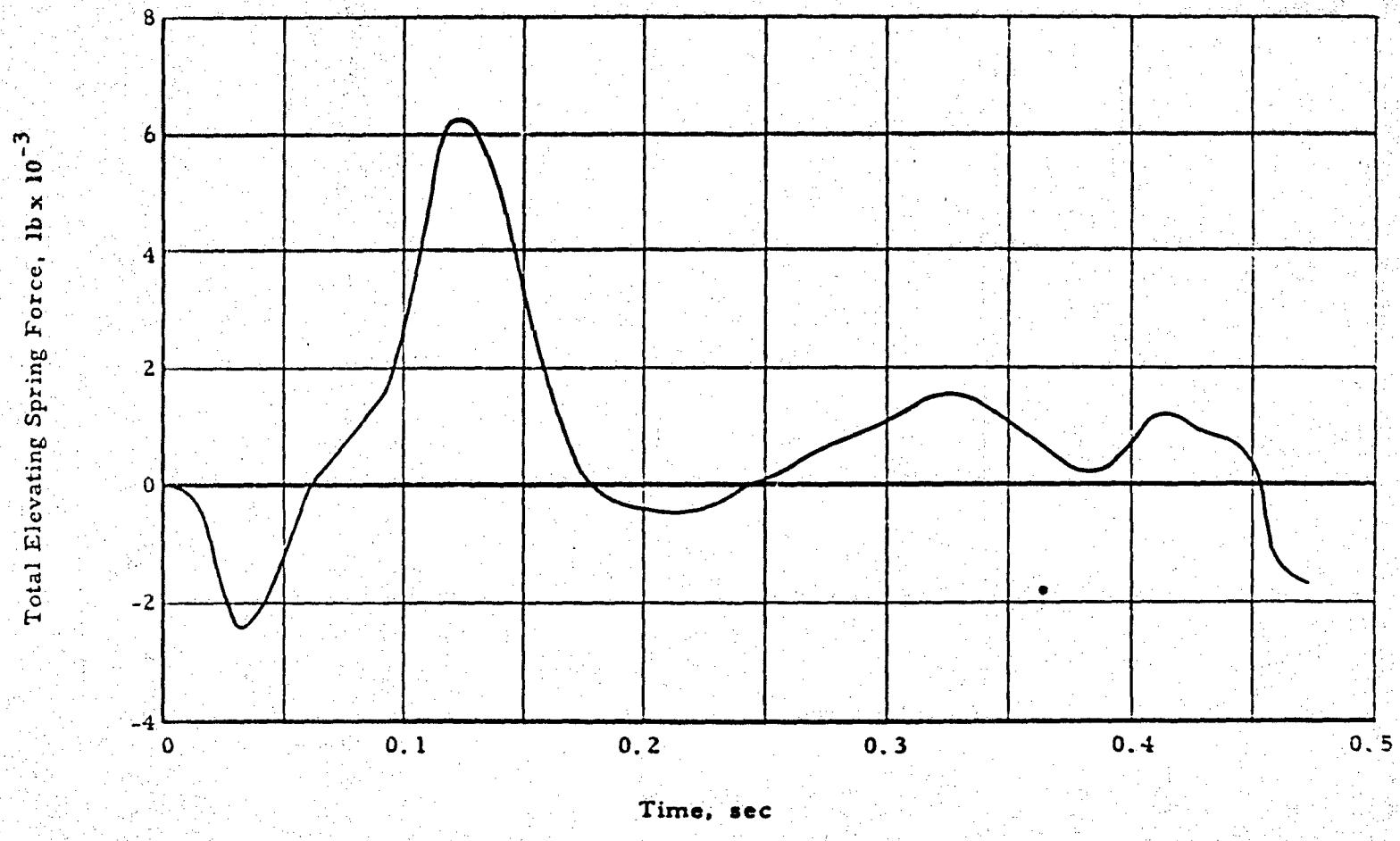

Fig. 18 TYPICAL COMPUTER SOLUTION -- ELEVATING SYSTEM SPRING FORCE

ARMOUR RESEARCH FOUNDATION OF ILLINOIS INSTITUTE OF TECHNOLOGY

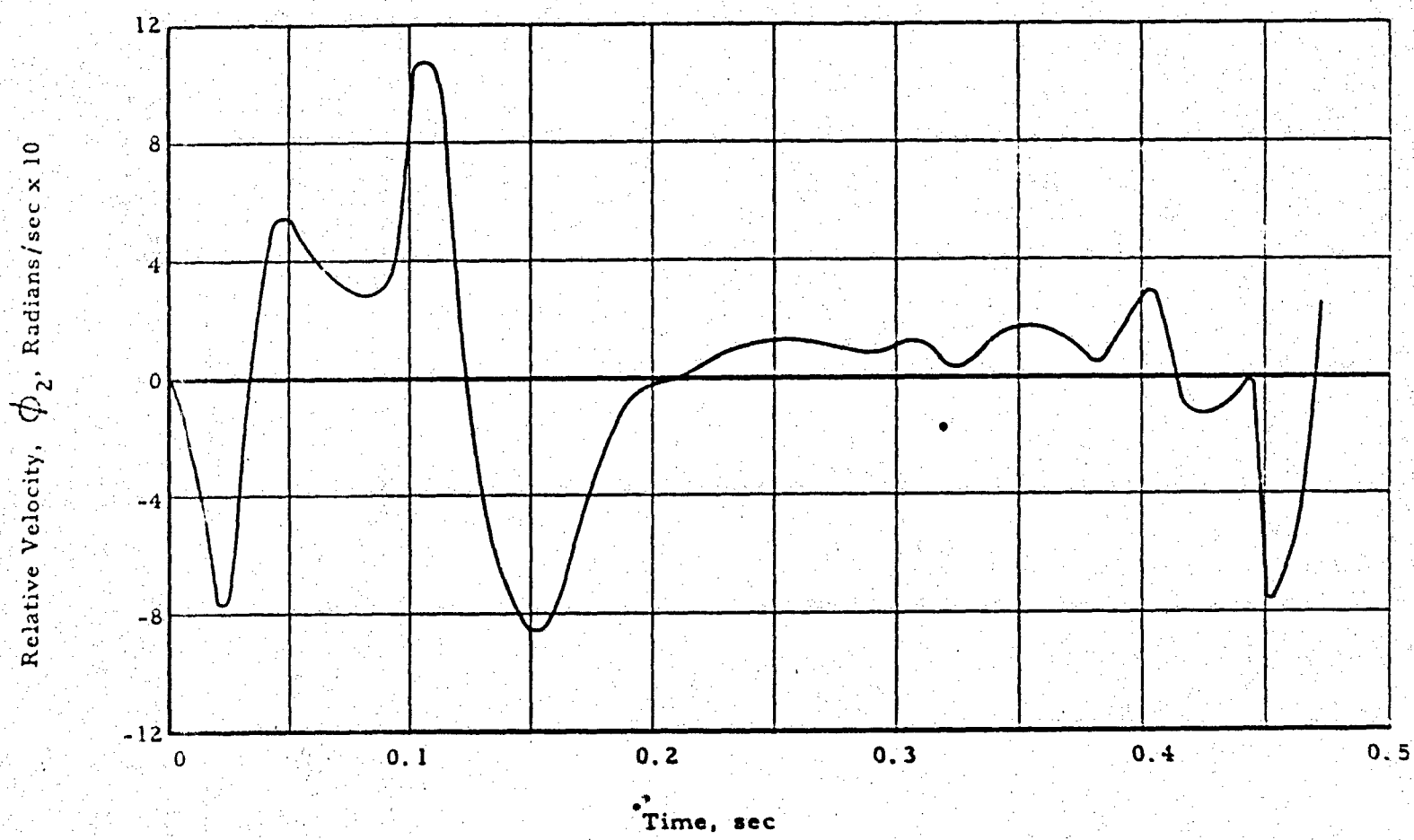

Fig. 19 TYPICAL COMPUTER SOLUTION -- ELEVATING SYSTEM DAMPER FORCE

ARMOUR RESEARCH FOUNDATION OF ILLINOIS INSTITUTE OF TECHNOLOGY

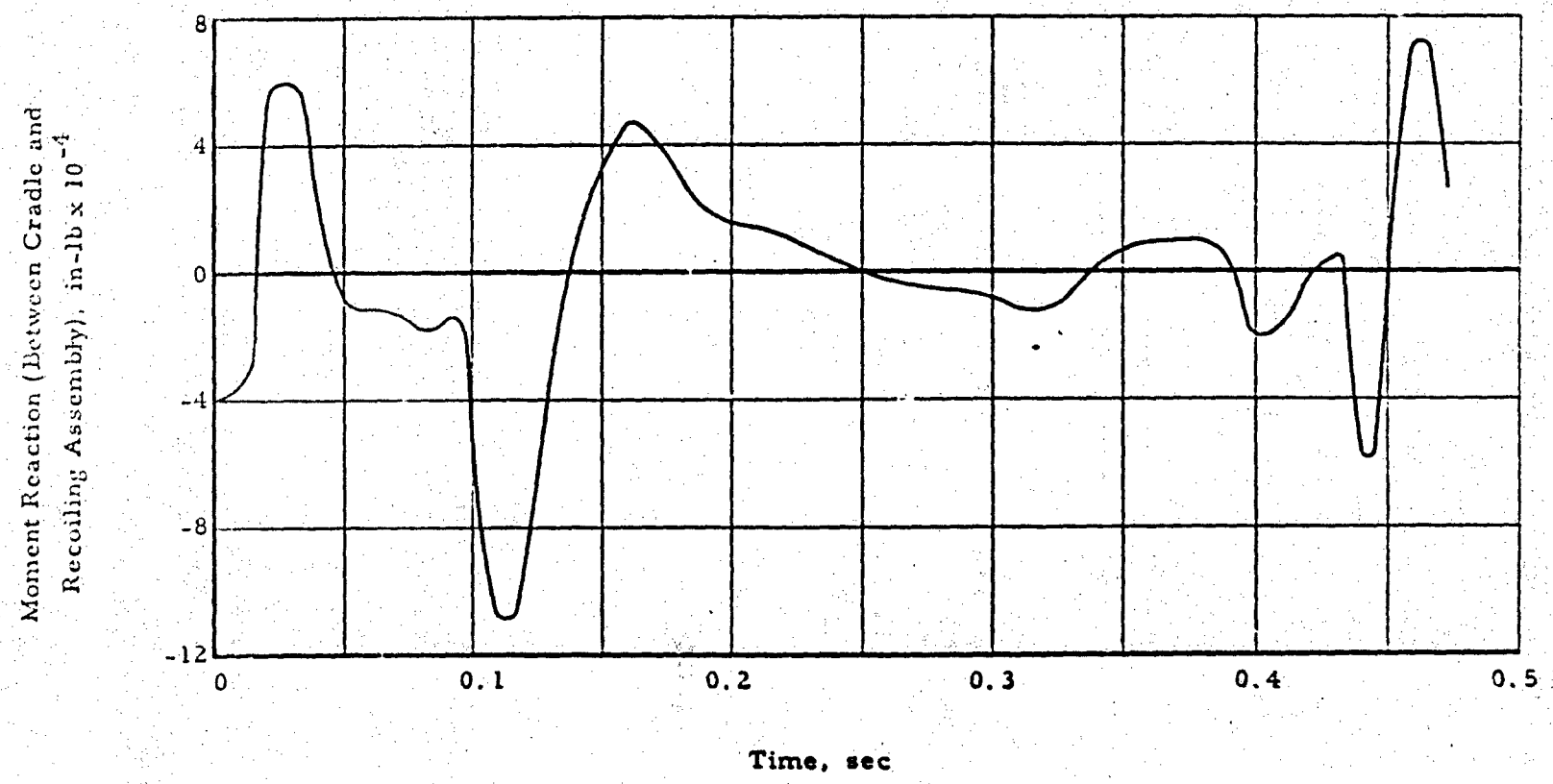

Fig. 20 TYPICAL COMPUTER SOLUTION -- RECOILING ASSEMBLY - CRADLE MOMENT REACTION

ARMOUR RESEARCH FOUNDATION OF ILLINOIS INSTITUTE OF TECHNOLOGY

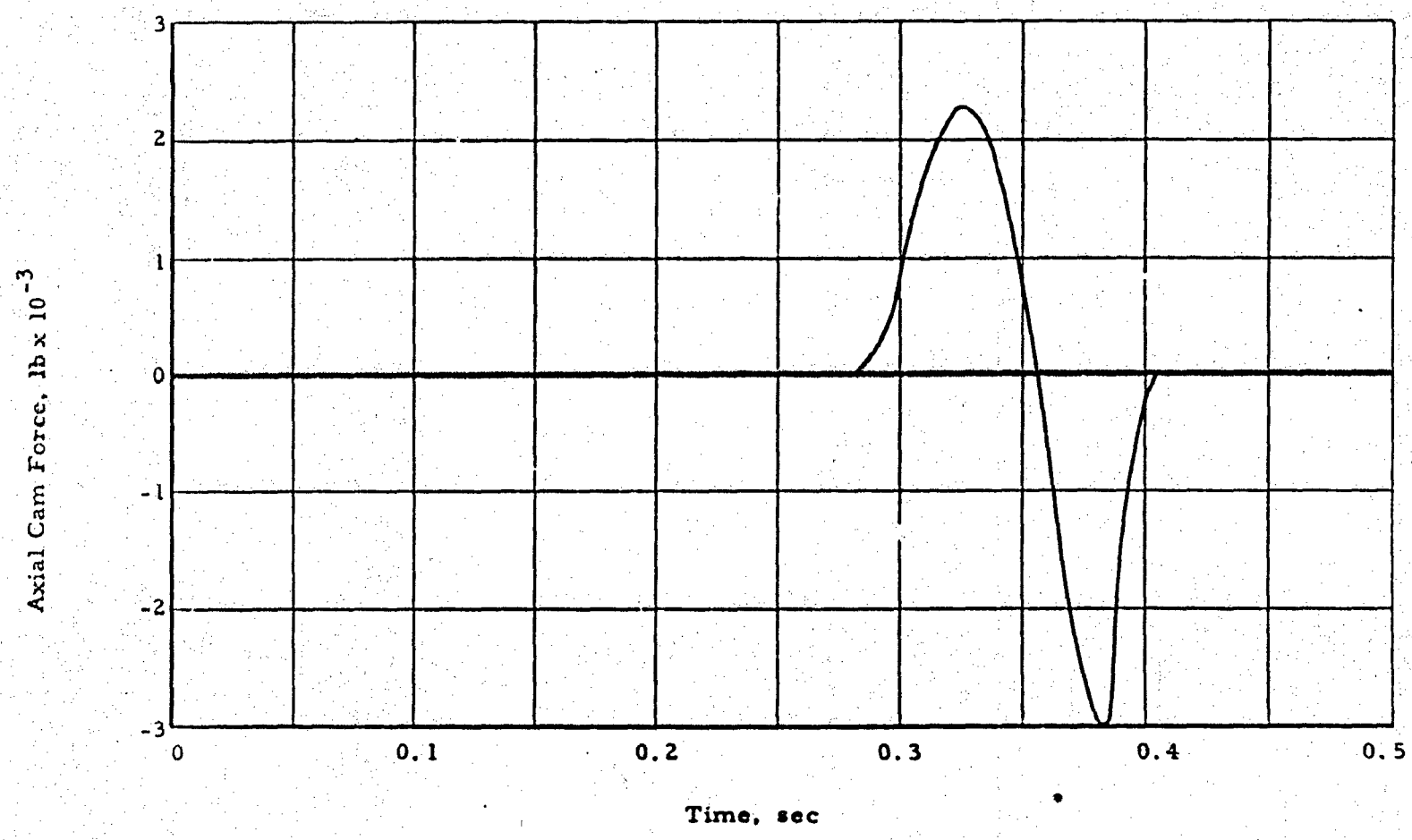

Fig. 21 TYPICAL COMPUTER SOLUTION -- AXIAL CAM FORCE

ARMOUR RESEARCH FOUNDATION OF ILLINOIS INSTITUTE OF TECHNOLOGY

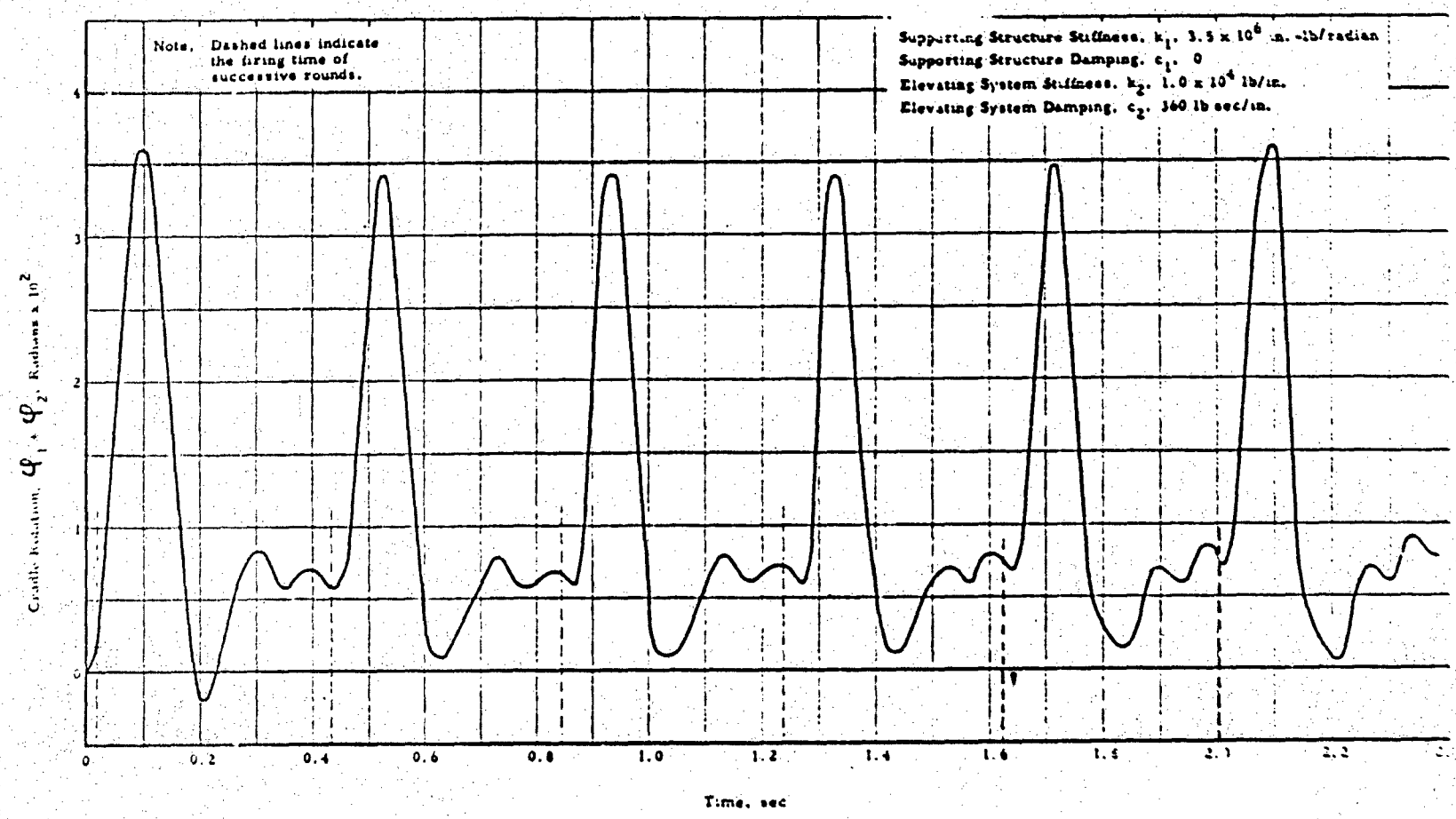

Fig. 22 TYPICAL COMPUTER SOLUTION -- CRADLE ROTATION, 6-RD BURST

ARMOUR RESEARCH FOUNDATION OF ILLINOIS INSTITUTE OF TECHNOLOGY

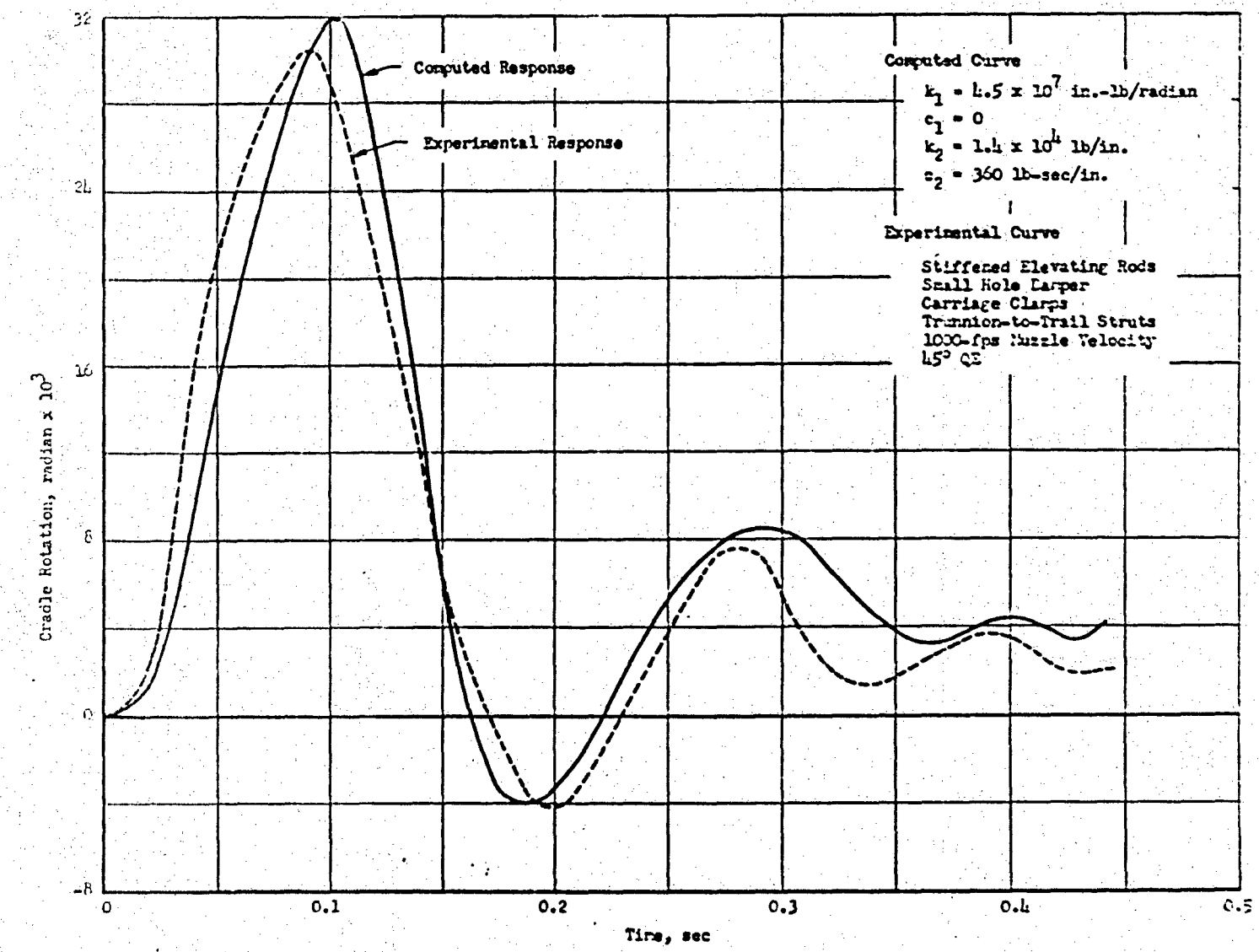

Fig. 23 COMPARISON OF COMPUTED AND EXPERIMENTAL RESPONSE CURVES

ARMOUR RESEARCH FOUNDATION OF ILLINOIS INSTITUTE OF TECHNOLOGY

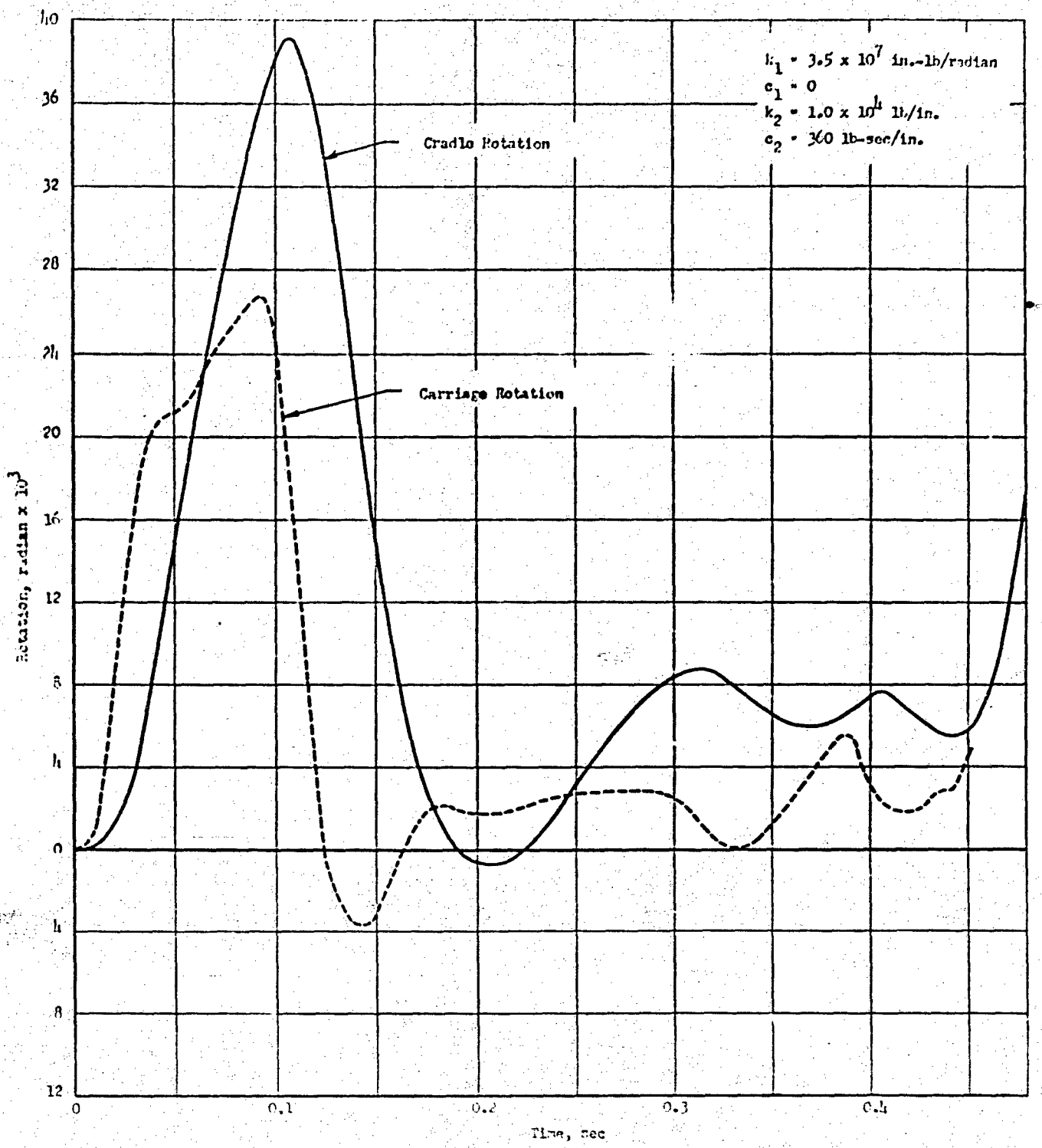

Fig. 24 THEORETICAL RESPONSE WITH REDUCED STRUCTURAL STIFFNESS

cates that the nonlinear negative supporting structure characteristics are very significant here. To investigate the effects of a bilinear stiffness the computer program was modified. Figure 25 shows the cradle response using a bilinear supporting structure stiffness. Although the agreement is much better, it could probably be improved with slightly different values of stiffness and also the additional simulation of a bilinear damping coefficient. The effect of these nonlinearities has been demonstrated, however, even though perfect correlation was not obtained.

2. Effects of Elevation Changes

It was important to investigate the effects of elevation changes upon the response of the launcher. This was done easily, because the elevation was an input to the computer program. Figures 28 and 29 show the cradle response of the launcher with structural parameters identical to those in the previously computed curves. These responses are at 20° and 60° elevation, respectively. (The previous ones were at (45°). There are some definite changes in the details of the response, especially at the time immediately following the ignition of the rounds. At 20° elevation, the initial rise time (velocity at shot ejection) is significantly higher than at 45°, and at 45° the initial response is higher than that corresponding to 60°. There is a very simple reason for this. The geometry change brings about a change in the inertial moment of the tipping assembly. To demonstrate this, Fig. 30 illustrates that as the supporting structure deflects due to the application of the recoil force, the trunnion moves in a direction perpendicular to a line through the trunnion and ball joint. At 20° elevation, this motion causes the tipping assembly to react with an initial counterclockwise rotation which adds to the normal response. At 60°, however, the initial tendency of the tipping assembly is to rotate clockwise which opposes the normal counterclockwise rotation. The result here is a delay in the cradle response, which occurs at every round of the burst. The response at 45° elevation is similar to 60°, but the delay is smaller in magnitude. We now have a situation where increases in elevation bring about greater accuracy -- an inherent characteristic of this launcher. This characteristic has less importance when delayed recoil is used and is apparent when delayed recoil is discussed in Section IV-E.

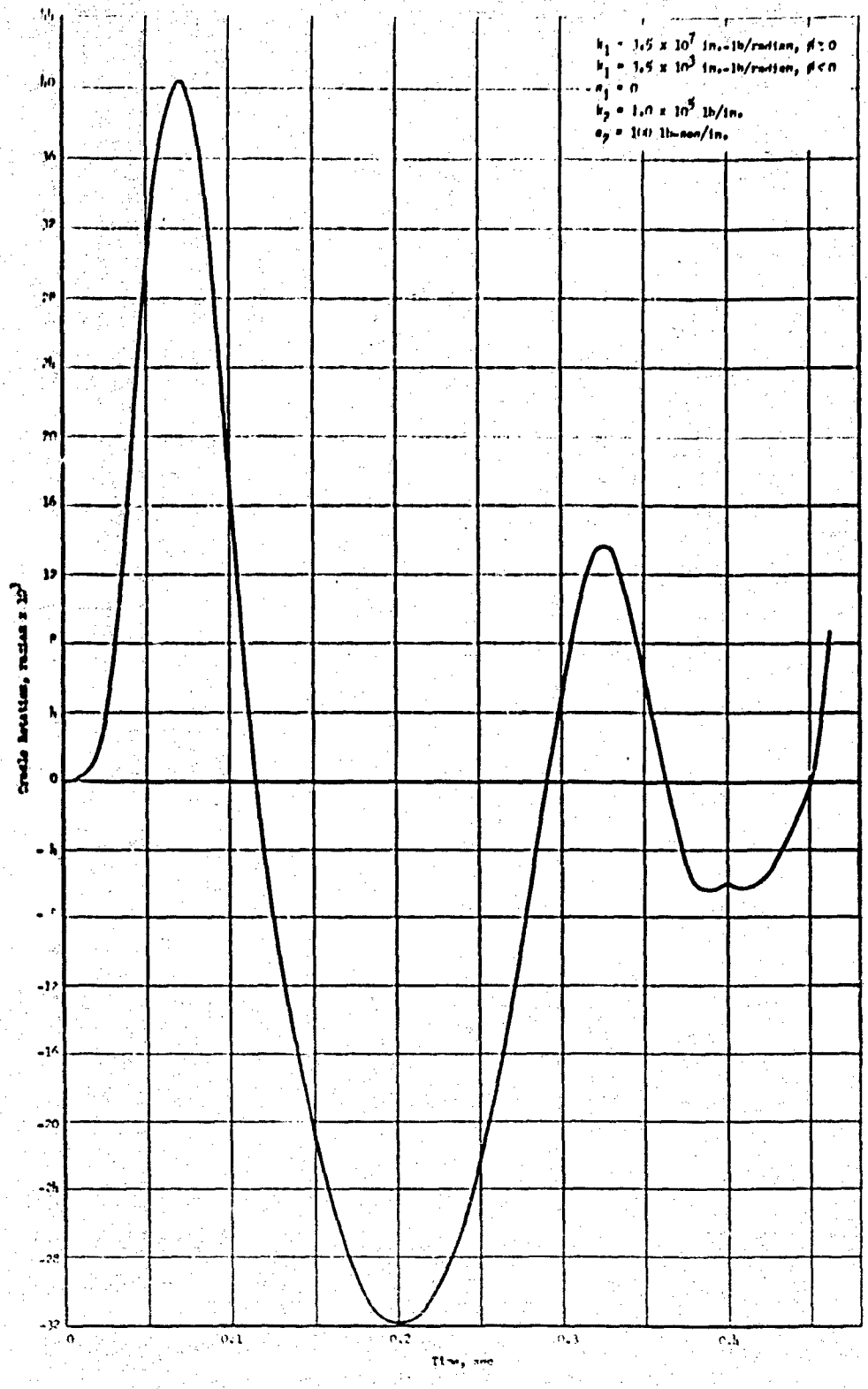

Fig. 25 THEORETICAL RESPONSE WITH A BILINEAR STIFFNESS

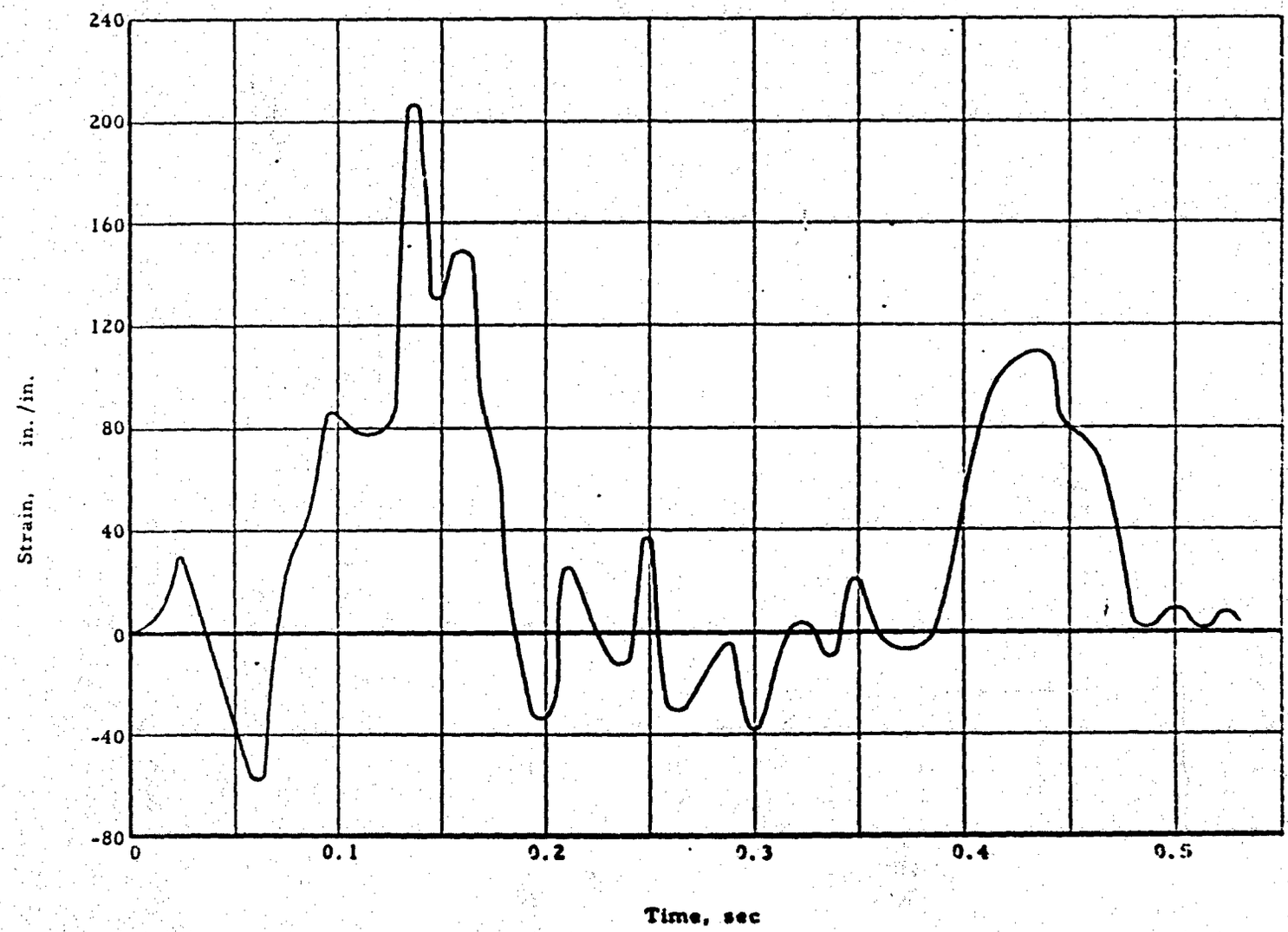

Fig. 26 EXPERIMENTAL ELEVATING ROD STRAIN

ARMOUR RESEARCH FOUNDATION OF ILLINOIS INSTITUTE OF TECHNOLOGY

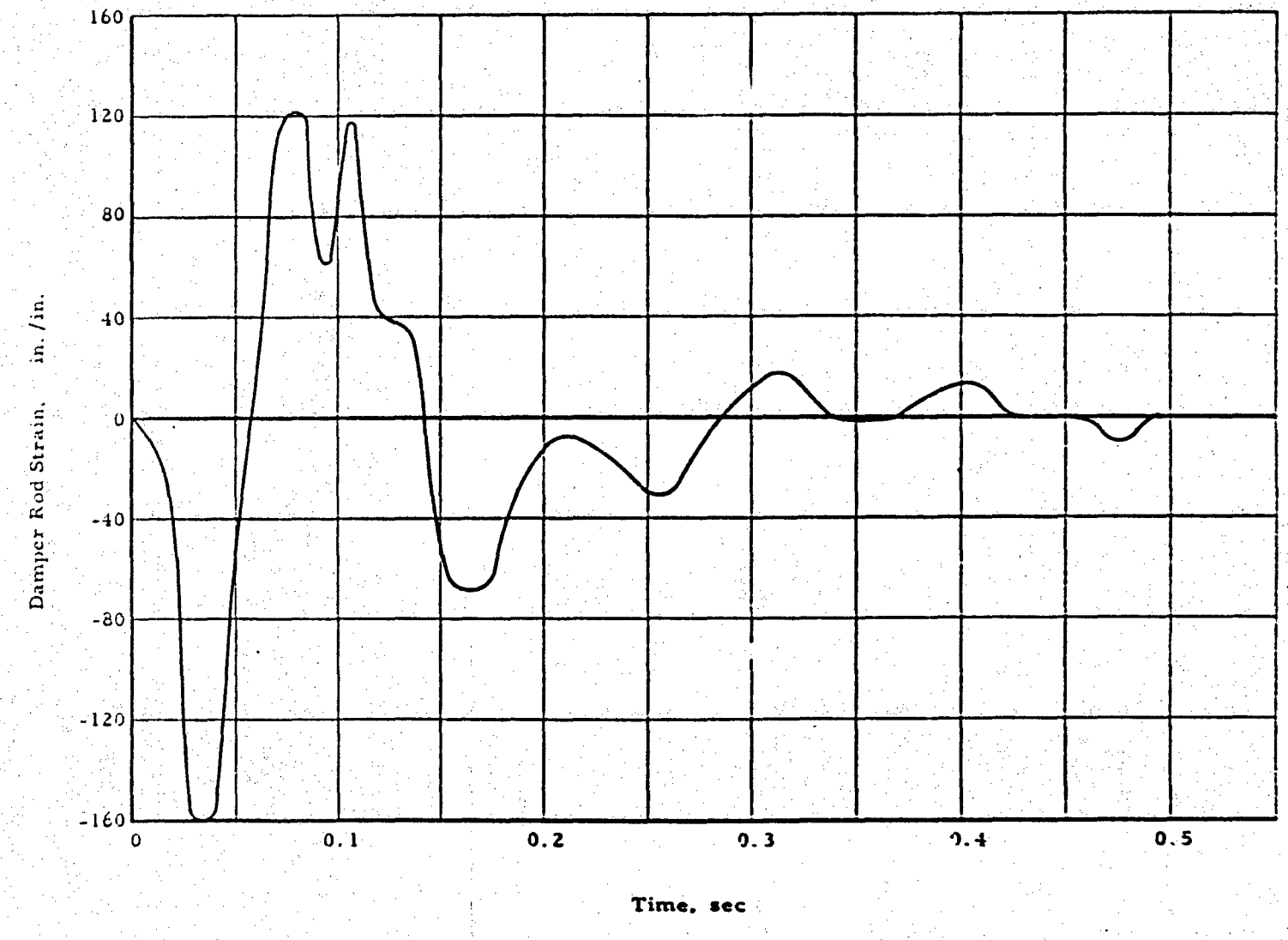

Fig. 27 EXPERIMENTAL ELEVATING SYSTEM DAMPER SUPPORT STRAIN

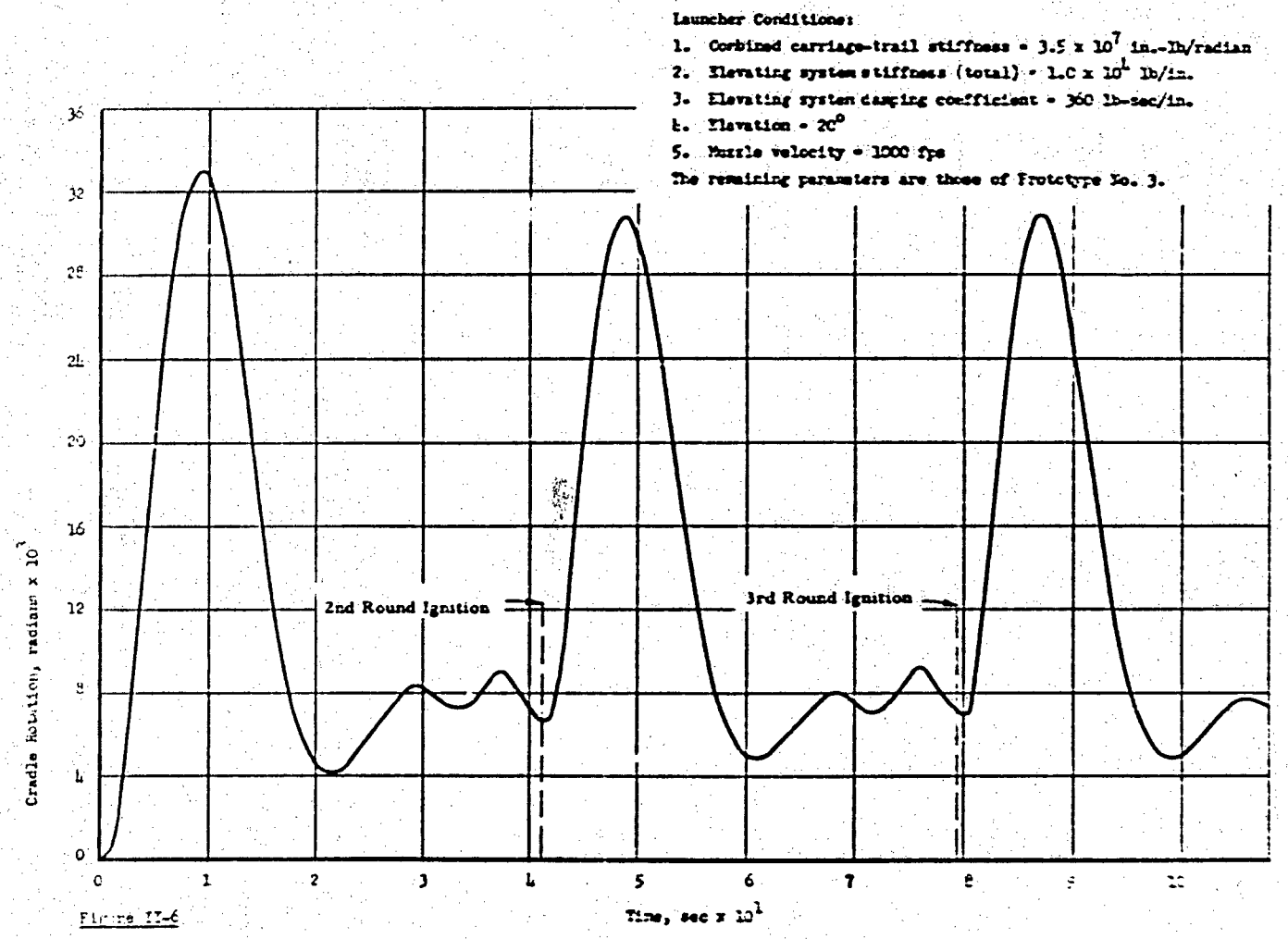

Figure II-6

Fig. 28 CRADLE RESPONSE AT 20° ELEVATION

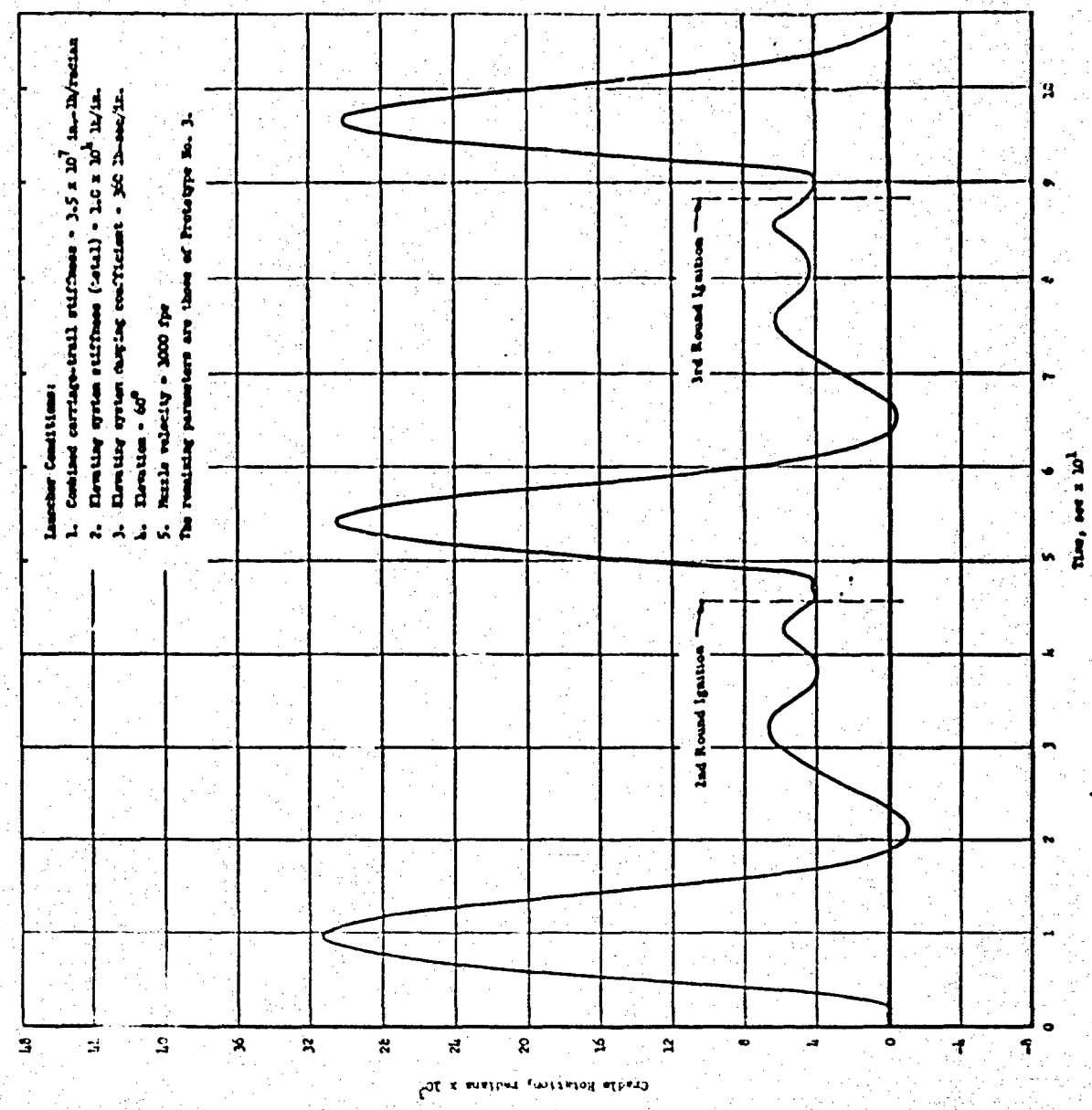

Fig. 29 CRADLE RESPONSE AT 60° ELEVATION

ARMOUR RESEARCH FOUNDATION OF ILLINOIS INSTITUTE OF TECHNOLOGY

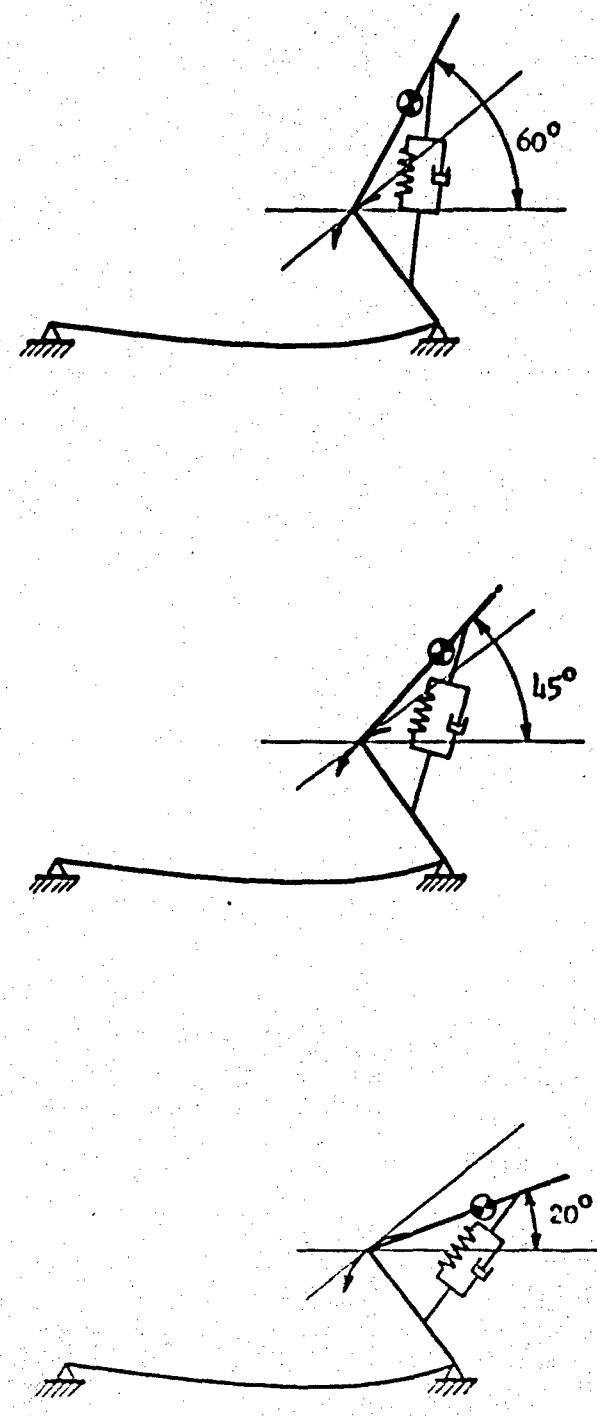

Fig. 30 GEOMETRY OF ELEVATION CHANGES

3. Low Boost Firings

This launcher has the capability of firing rockets with various muzzle velocities (zones of ammunition) simply by varying the amount of gunpowder. The powder-gas force curve corresponding to a muzzle velocity of 380 fps was used in the computer program. Figure 31 shows the cradle response for 60° elevation at this low boost. (The high value of elevation was necessary to insure a large enough recoil distance to cause automatic indexing.) As would be expected, the rise time of the initial cradle response is much smaller than for the high boost rounds and was due to the slower rise time in the recoil force. The amplitude of the residual motion prior to successive shots is also less, but it is still significant. The variation in the residual motion, however, is very similar to the high zone bursts since the counterrecoil forces developed are a function of the recuperator force and the indexing forces. These are both relatively independent of the boost, because of the constant stopping distance recoil system. The maximum recoil distance for this burst was near 20 inches compared to 24 at higher zones. As a result of the slower rise times of the recoil force, we see that it is much more possible to have a negative cradle velocity at shot ejection. In addition, delayed recoil will have less of an effect in changing the response.

4. Importance of Coriolis Acceleration

Because of the high recoil velocity (400 in./sec) combined with the rotational velocity of the tipping assembly, a question arose concerning the importance of the Coriolis acceleration. This acceleration is proportional to the product of these two velocities. For this mathematical model, because of computer solution, there was no particular reason to neglect this term; in other situations, this might lead to a convenient simplification in the equations of motion. For this reason, Coriolis' effect upon the cradle response was investigated. Because the term is proportional to the product of the velocities $\dot{u}$ and $(\dot{\varphi}_1 + \dot{\varphi}_2)$, a set of parameters was selected where these velocities were high. The recoil velocity $\dot{u}$ is almost independent of the structural parameters, so the selection was reduced to finding parameters which increased $(\dot{\varphi}_1 + \dot{\varphi}_2)$. This is done by increasing the stiffness of the elevating system. Figures 32 and 33 show the cradle response with and without the Coriolis terms. The overall response shape has not changed

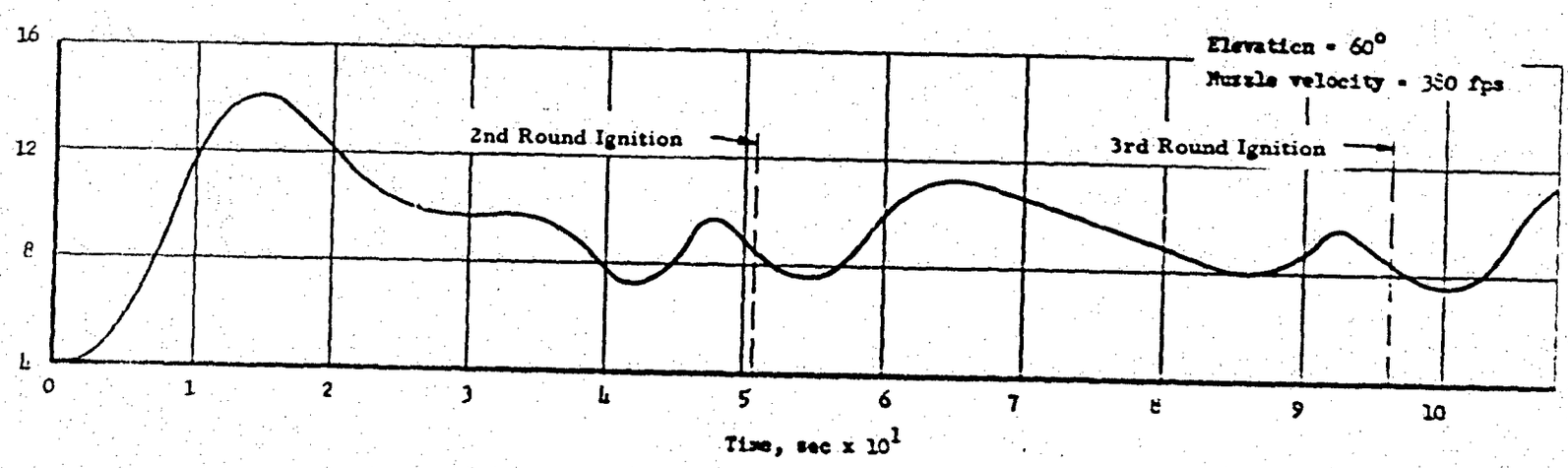

Fig. 31 CRADLE RESPONSE, LOW ZONE BOOST

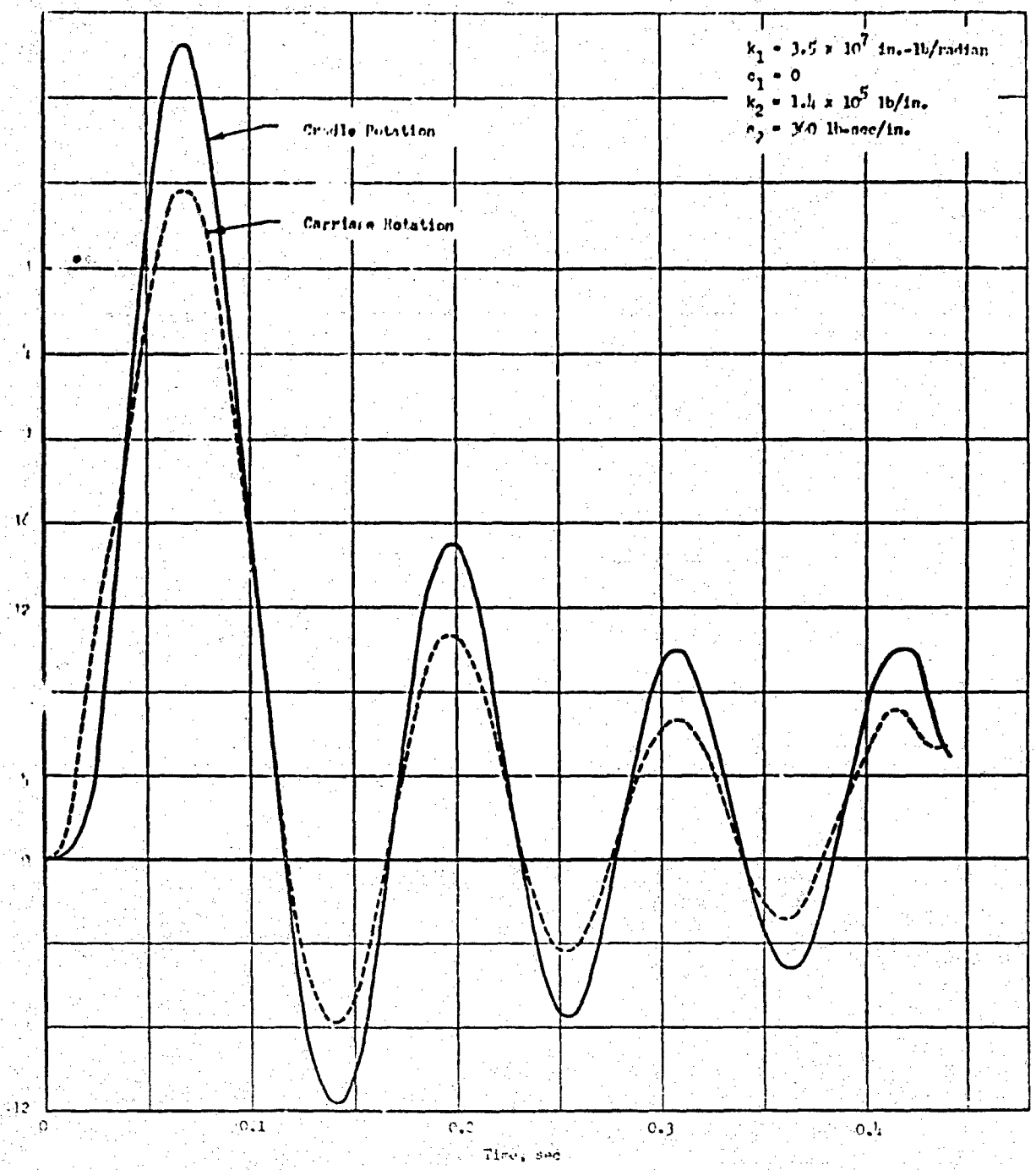

Fig. 32 CRADLE RESPONSE WITH A VERY STIFF ELEVATING SYSTEM

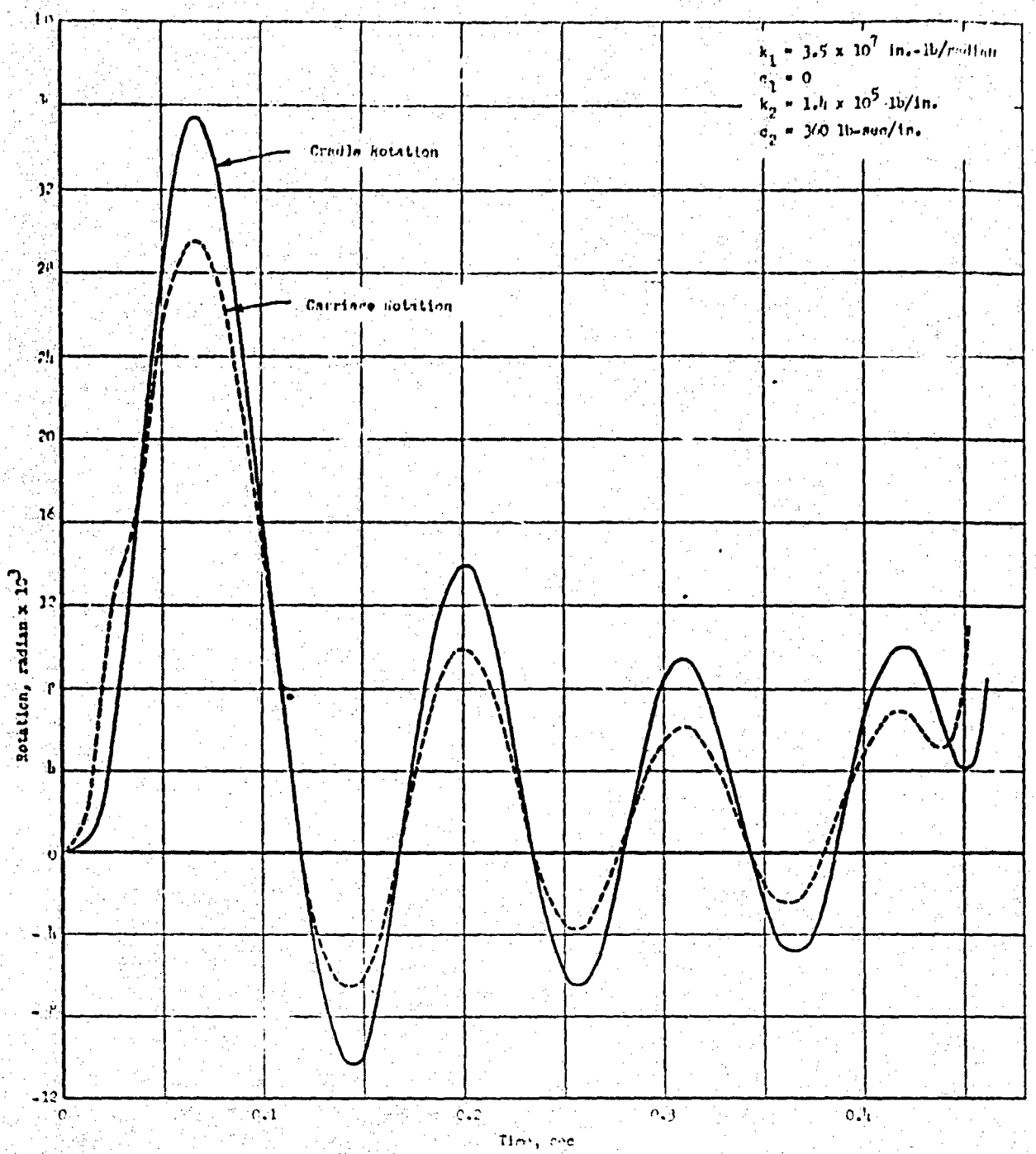

Fig. 33 CRADLE RESPONSE WITH A VERY STIFF ELEVATING SYSTEM NEGLECTING THE CORIOLIS ACCELERATION

while the peak response has a difference of 7%. This indicates that the Coriolis acceleration is of second order importance with respect to the shape of the cradle response, though the change in magnitude may be significant. This serves to indicate that some of the simplified models used in the supplementary analyses may be a reasonable representation of the launcher for predicting large scale changes in the response.

5. Delayed Recoil

The recoil system on the XM70 Launcher makes use of a variable area orifice which was designed to stop the recoiling assembly in a constant distance with a constant force. The orifice area varies as a function of the recoil distance; this was effected by pulling variable diameter rods through a fixed area orifice plate. A design suggestion was made to modify the recoil system in such a way that the recoil force is zero (or of negligible magnitude) until the rocket has left the firing tube. In this way the carriage deflections will be zero (for the first shot of a burst), the velocity will be small, and the launcher accuracy will be near perfect. Certain problems arise with delayed recoil; the magnitude of the recoil force increases due to the shorter distance over which the recoil force acts, because of the constant stopping distance system. A question also arose about the effect of the delay on shots following the first.

The 3-degree-of-freedom mathematical model was used to study the effect of delayed recoil since the recoil rod shape is entered into the model as a tabular function of the recoil displacement. Inserting a rod shape into this mathematical model corresponds identically to inserting new recoil rods into an actual launcher.

The first rod shape tried was a standard rod with a decreased diameter (increase in orifice area) for the first 11-1/2 in. of recoil motion. The first rocket leaves the launcher at about 3 to 4 in. of recoil; subsequent shots are fired by an adjustable cam, 9 in. out of battery. Because of the residual counterrecoil velocity during all shot ignitions except the first, these rockets leave the launcher at a recoil distance near 11-1/2 in. Figure 34 shows the cradle rotation and the recoil force much larger than obtained for the standard rod. Figure 5 shows a peak force near 20,000 lb compared with the new force

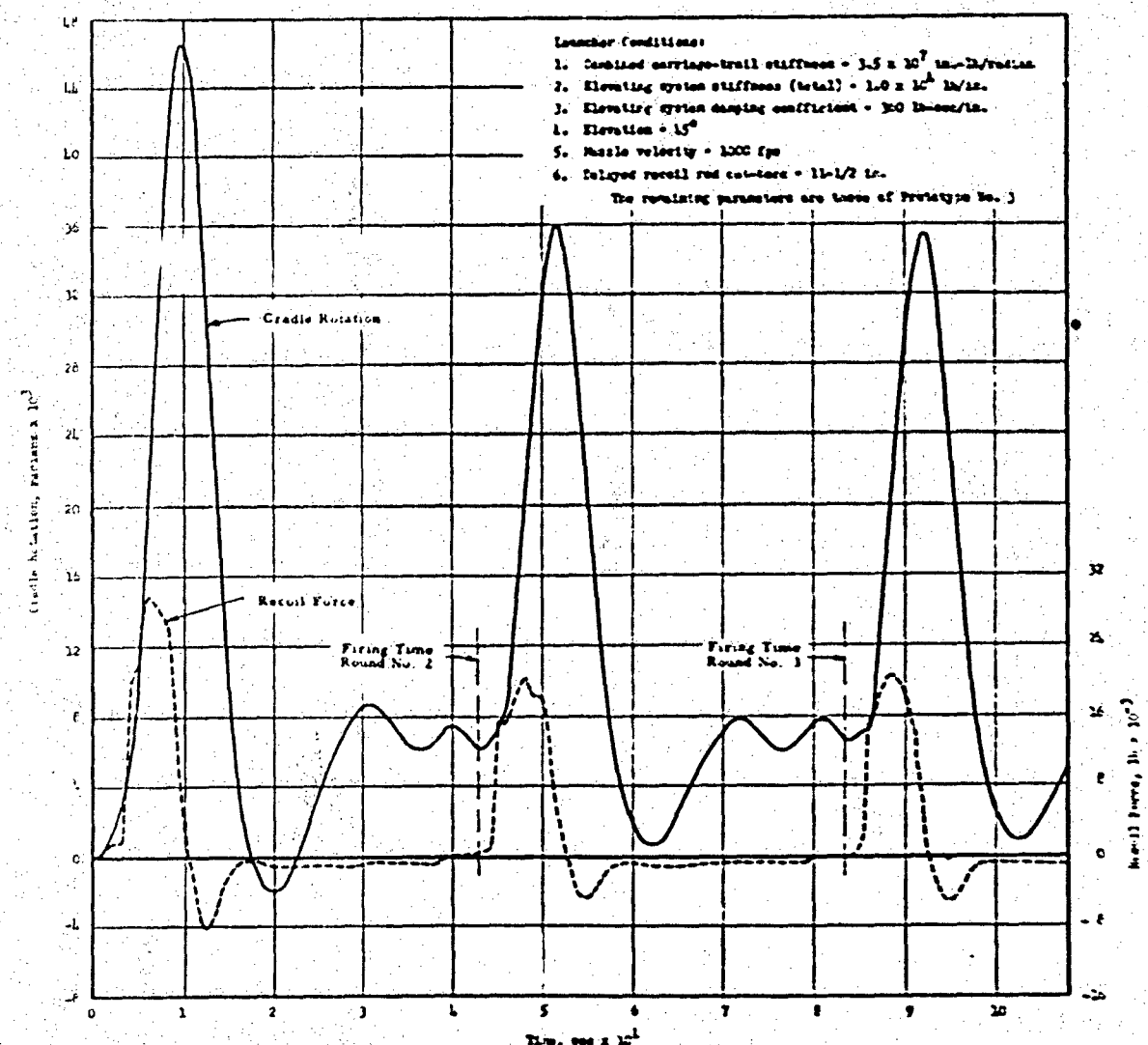

Fig. 34 CRADLE RESPONSE FOR DELAYED RECOIL ROD CUTBACK 11-1/2 IN.

ARMOUR RESEARCH FOUNDATION OF ILLINOIS INSTITUTE OF TECHNOLOGY

near 30,000 lb. The later shots, however, are near the 20,000 lb peak reflecting the fact that of the 11-1/2 in. cutback, only about 2-1/2 in. of it affect the later shots, compared to the entire 11-1/2 for the first shot. Comparison of the response to that shown in Fig. 20 (optimum elevating system parameters) shows that delayed recoil cut the cradle rotation by about 50% at shot ejection (approximately 20 msec after t = 0) and lowered the velocity by approximately 30%. The displacement effect for later shots is almost negligible because it is fairly large to begin with. Close inspection of the curves shows that the velocity reduction is significant for the second shot. The third rocket, however, left the launcher when the cradle had a negative velocity (for the regular control rod). The use of the cutback rods changed the burst characteristics such that the third shot fired prior to a region of positive cradle velocity. We then realize the situation that delayed recoil does not aid the accuracy if the cradle would normally have a negative velocity at the time a round is ignited. The normal launcher response tends to lessen this negative velocity with a desirable result. This leads us to the conclusion that in order to gain the benefits of delayed recoil, the residual cradle motion should be as small as possible. In this situation, delayed recoil is definitely useful.

In order to decrease the high, first-round recoil force a rod was tried with two diameter cutbacks, the first from 0 to 3 in. and the second from 8 to 11-1/2 in. It was expected that the extra raised portion between 3 and 8 in. would help decrease the first force level. Figure 35 shows the result; the peak force is reduced from 30,000 to 26,000 lb. The peak cradle rotation was also reduced. The later rounds were unaffected because the section of the rod over which they operate was unchanged.

We saw earlier that firings at 60° elevation have less initial cradle rotation due to the geometry of the elevating system and tipping assembly mass center. A computed response for a 60° firing using a cutback recoil rods is shown in Fig. 36. In this situation, the cradle velocity is nowhere near that of the cradle for the ordinary launcher. In the same respect, the response for 20° elevation (with a cutback rod) is probably near the ordinary response.

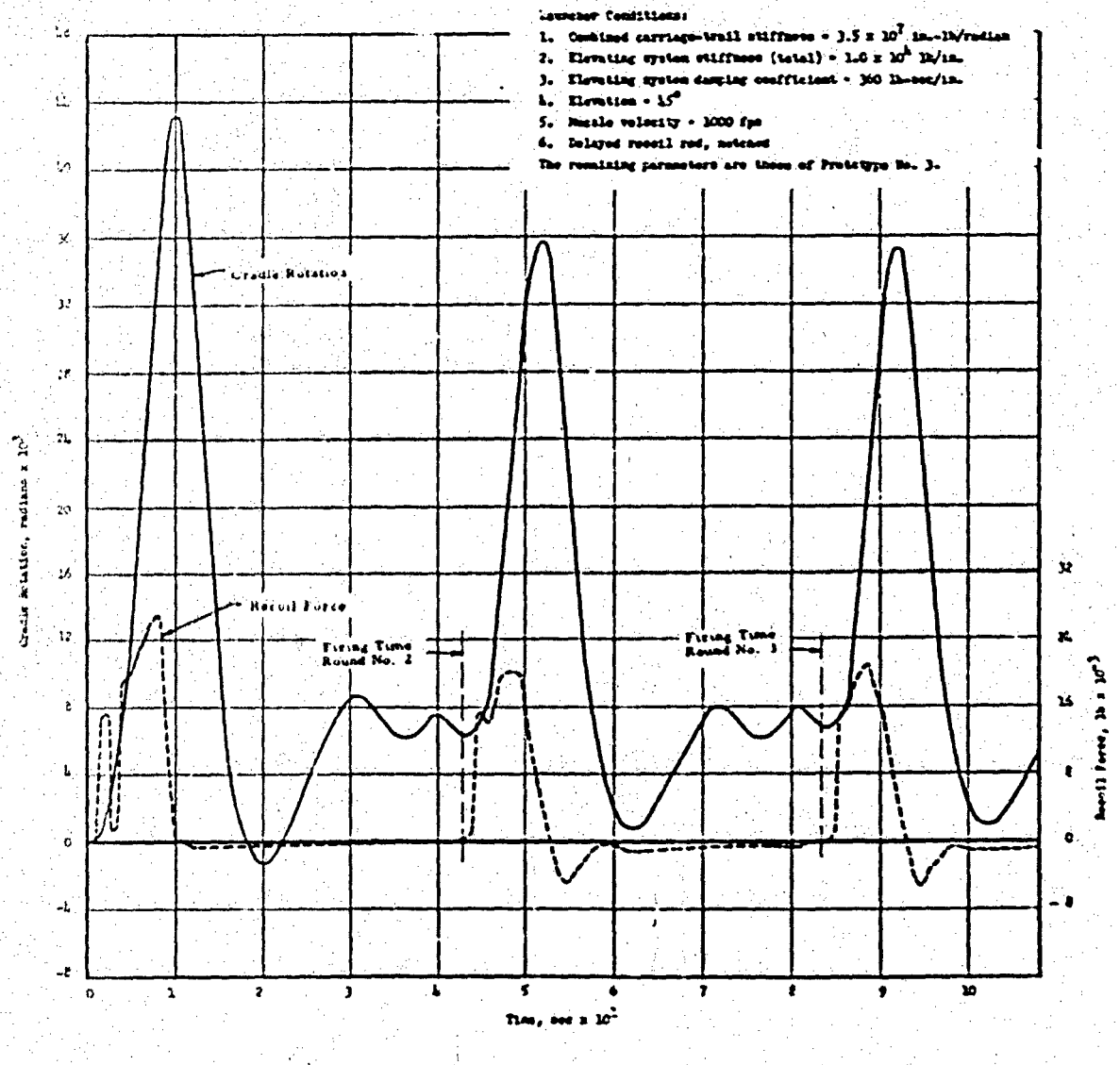

Fig. 35 CRADLE RESPONSE FOR DELAYED RECOIL, NOTCHED ROD

ARMOUR RESEARCH FOUNDATION OF ILLINOIS INSTITUTE OF TECHNOLOGY

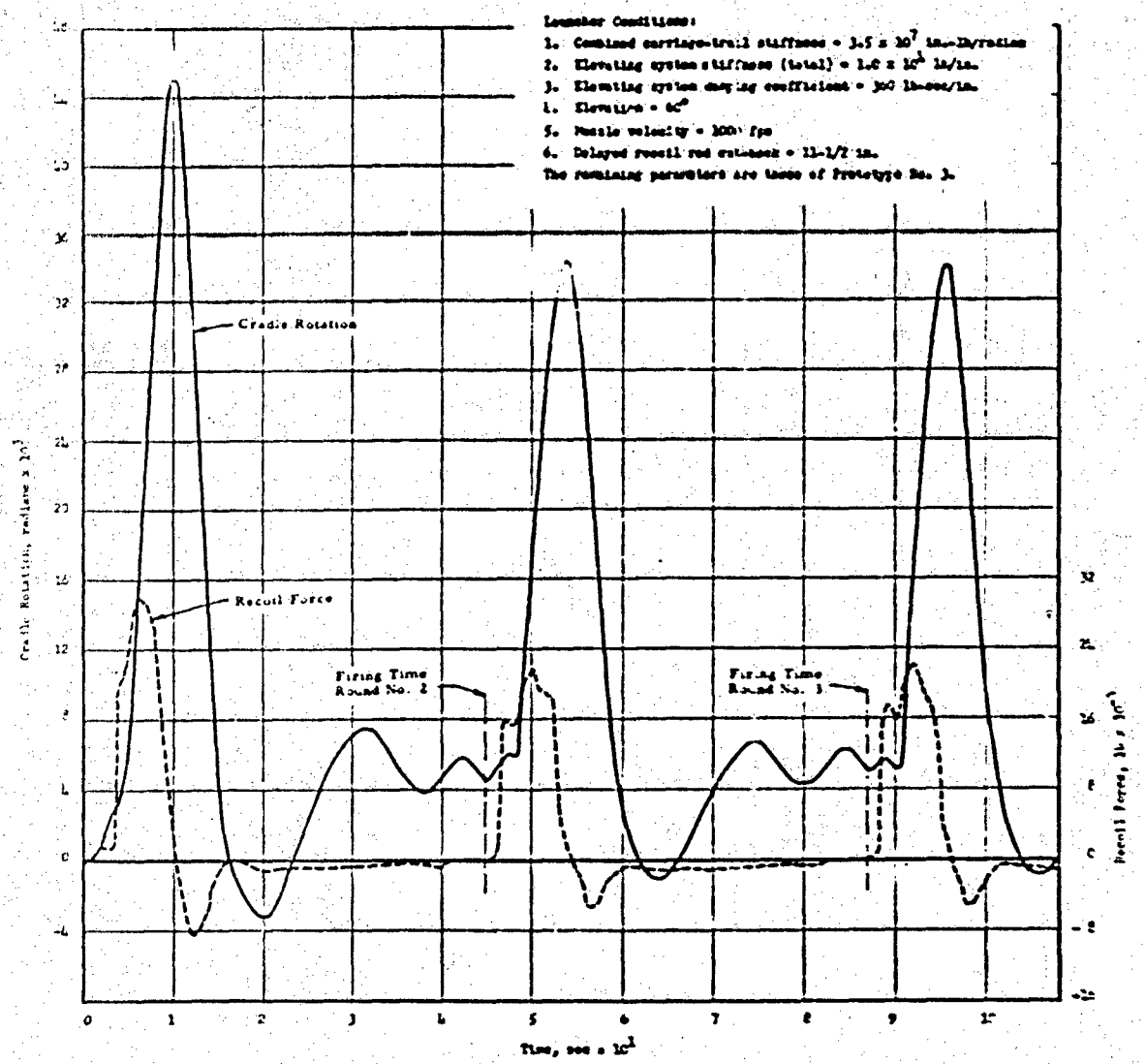

Fig. 36 CRADLE RESPONSE FOR DELAYED RECOIL ROD CUTBACK 11-1/2 IN.

ARMOUR RESEARCH FOUNDATION OF ILLINOIS INSTITUTE OF TECHNOLOGY

B. Supplementary Analyses

1. Third-Order System

A third-order linear system was developed as a mathematical model and used to find the stiffness and damping which should be incorporated into the elevating system of the launcher. This model was obtained by simplification of the launcher representation shown in Fig. C-1. The simplifications were:

1. The inertia of the carriage and trails, I_o, was assumed negligible compared to the moment of inertia of the tipping assembly -- a ratio of approximately 115:8000.
2. Nonlinear coupling terms between the motion of tipping assembly and supporting structure were neglected.
3. The recoiling motion was neglected.
4. The recoil force was treated as the primary disturbance and was approximated by an impulse.

These assumptions are considered valid because the resulting solution is not intended to represent the actual launcher motion, but rather to indicate the variation of the response behavior for a wide range of parameter variations. The linear analog of the resulting model is shown in Fig. E-1.

The responses of this third-order system were determined by using the response plots contained in "Dynamic Response Plots and Design Charts for Third-Order Linear Systems" 1/. This report contains the solution of such systems in the form of dimensionless response plots for forty-eight different combinations of parameters. These plots were obtained from evaluation of Equation E-5, as a function of time, on a digital computer.

The design charts in the report 1/ show areas of three types of responses.

1. Parameter combinations which produce a normal damped response.
2. Parameter combinations which produce an unstable response.
3. Parameters which result in three real roots to Eq. E-3.

In order to establish the undesirability of the third type of response, a set of

---

1/ Meyfarth, P., Dynamic Response Plots and Design Charts for Third-Order Linear Systems, Research Memo No. R. M. 7401-3, Massachusetts Institute of Technology, 1958.

parameters which produce this was used in the computer solution for the 3-degree-of-freedom system. The resulting cradle response was continuously increasing (non-oscillating), as shown in Fig. E-3, for 150 lb-sec/in. damping and 100 lb/in. stiffness.

Despite the various assumptions, the response curves obtained were a fair representation of the actual launcher motion for a single shot. (Compare Figures E-2 and E-4.) The optimum response for this system was defined as one with both a low first peak displcaement and a low ratio of second peak to first peak displacement. Three response plots which satisfy this definition are shown in Figure E-2. The corresponding optimum elevating system parameters are a stiffness of 1.0×10^4 to 1.4×10^4 lb/in. and damping of 360 to 540 lb-sec/in.

2. An Approximate Dynamic Analysis of the Minimum Weapon Weight Required for a Specified Accuracy

A relatively simple mathematical model of the XM70 and a simple dynamic performance requirement for accuracy was formulated in order to evaluate several basic design parameters including the minimum total weight of the weapon. Mathematically, the procedure was one of finding a second order system which had a specified response decay. The details of the analysis are contained in Appendix B of this report.

For the purposes of this analysis, the complete weapon was represented by a linear, forced, damped, single-degree-of-freedom oscillator. The displacement of the oscillator represented angular rotation of the firing tube in a vertical plane. This representation was shown to be useful[1/] when the stiffness is taken to be the total stiffness of the weapon structure and the mass is a computed dynamic equivalent. Values of the damping coefficient were chosen to be consistent with experimental data of the weapon's response to firing loads. The force applied to the oscillator to simulate firing was a rectangular pulse whose amplitude and duration were chosen to represent the recoil force of the actual weapon.

As a criterion for adequate dynamic performance, it was assumed

---

[1/] See ARF Project K130, Bimonthly Report No. 11, Appendix A.

that the amplitude of firing tube oscillations (in a vertical plane) must be less than some small value, which is considered to produce negligible error at the target, prior to firing of each round of a burst.

Under the assumptions of the analysis, a closed form solution can be obtained to the equation of motion of the weapon. The solutions consists of the displacement of the firing tube as a function of time and the stiffness, damping and mass of the weapon but what is ultimately desired from the analysis is the time required for adquate damping of the response as a function of the weapon weight.

The weight of the weapon was explicity introduced into the solution by writing expressions for the stiffness, damping coefficient, and equivalent mass of the weapon as functions of the weight of the major subassemblies of the XM70. These expressions were obtained by assuming linear relationships and using the XM70 Prototype Model No. 1 weights for reference. Using the solution containing these expressions, it was possible to obtain a time-displacement curve, and hence the time required for adequate damping, for a particular total weapon weight. Several solutions must be obtained in order to obtain a plot of required damping time versus total weight from which the minimum weight can be obtained. The analysis procedure is facilitated by using the envelope of the response curves rather than the curves themselves.

This analysis formed the basis for the computation of the optimum recoiling assembly weight for the XM70 which is reported upon in ARF Project K130 Bimonthly Report No. 8 Appendix B. In addition, this analysis was used to estimate the minimum weight of a weapon having a small recoiling assembly weight (500 lb) and a delayed recoil force. The minimum weight of such a weapon was found to be only 1340 lb., but the resulting ground reaction was too large and the calculated carriage weight was inadequate from a strength standpoint. These calculations led to the development of an auxiliary strength criterion for the carriage and hence to the procedure referred to above for calculating optimum recoiling assembly weight.

3. Linear, 2-Degree-of-Freedom Model

A classical, 2-degree-of-freedom system was another system studied

to obtain information about the best location for auxiliary damping of the cradle motion. Because only qualitative information was desired, the lack of representation of system nonlinearities is not considered important. Fig. A-1 shows the system which was studied where m_2 represented the tipping assembly, and m_1, the supporting structure. The three damper locations which were considered correspond to the following:

1. c_1; damping between the supporting structure and the ground (the ground was assumed to be capable of furnishing a tensile load).
2. c_2; damping between the supporting structure and tipping assembly.
3. c_3; damping between the tipping assembly and the ground.

The equations of motion were solved by digital computation where the input disturbance, F_1, was a tabular representation of an actual recoil force. All three damper locations are physically attainable, though the second is certainly the most convenient location. Equivalent damping between the three locations was determined by estimating the amount of forcible damping for the same weight contribution to the launcher from the respective dampers.

As expected, damping directly between the cradle and ground was most effective, of the three locations. However, damping between the tipping assembly and supporting structure was relatively effective, especially compared to damping between the supporting structure and ground. Combinations of the latter two, c_1 and c_2, was better, but on the estimated weight basis, the improvement was not significant. Since c_3-damping is the most difficult to attain, the most promising damper location was concluded to be relative to the supporting structure and tipping assembly.

C. Three-Dimensional, n-Degree-of-Freedom Model

This mathematical model (called Mathematical Model VI in progress reports) was developed with a view toward the incorporation of several of the modes of motion which were not included in earlier models. It contains all of the freedom of the previous models and, in addition, permits the investigation of the following types of behavior.

1. Ground Flexibility

Results of some of the experiments showed that an elastic and plastic deformation of the earth underneath the ball joint and the trail paths can

sizably affect the burst accuracy of the weapon. The new model, consequently, will allow the introduction of an arbitrary force-displacement relationship at the support points.

2. Sidewise Rotation at the Ball Joint

Incorporation of this freedom necessitated that a full three-dimensional representation be utilized. This representation should permit simulation of a portion of the lateral dispersive action associated with the weapon.

3. Left-Right Sequencing

This is also a three-dimensional effect; it arises because the inertial unbalance in the recoiling assembly cannot be eliminated. Left-right sequencing is discussed in detail in another portion of this report. Its incorporation into this model was somewhat simplified through the interpretation of the recoiling assembly framework flexibility in the form of a single torsional spring.

4. Flexible Barrel

The barrel flexibility was considered to be very important to the overall burst dispersion of this weapon. In particular, it would appear that phasing between the barrel vibration and the time of firing of the various rounds is quite significant. This barrel vibration is even more important because it is evidently coupled with the rotation of the weapon about the ball joint to Coriolis force terms and gyroscopic moments which arise due to the moving projectile.

5. Moving Projectile

The flexible barrel is excited by the traveling load induced through a projectile as well as through the gross forces which arise through firing. This operation motivated the inclusion in the model of a representation for the coupled motion of a traveling mass and the barrel proper. This representation is so organized that an experimentally determined time-displacement relationship can be introduced to describe the axial projectile behavior. It is thus possible to determine the instantaneous muzzle position orientation and velocity at the time of projectile exit. It is felt that this

information should be of aid in the development of more complete accuracy criteria for rocket launchers of this type.

This 3-dimensional mathematical model was not completed until near the close of the present project. The equations were programmed for the UNIVAC 1105 digital computer at Armour Research Foundation, but the program was not run on the machine because it was felt that the time and efforts which remained on the project could be more efficiently applied to other facets of launcher behavior. The equations for this model are presented in Appendix F of the present report. These equations are quite complex; their full solution should prove to be time consuming. Conversely, specific items of interest to future rocket launcher programs can certainly be obtained through specilization of these very general equations.

D. Accuracy Criterion

The main direction of effort on this program has been to study the response of the XM70 Launcher structure in the vertical plane due to burst firing loads. The intention was to find that combination of launcher parameters, e.g., weight, stiffness, moment of inertia, mass distribution, recoil force, etc., which would optimize or at least improve the response. In order to evaluate the effects of parameter changes, a simple accuracy criterion was used. This criterion was: the most accurate burst has the smallest residual angular cradle displacement and velocity prior to each succeeding round. This was not expressed mathematically, but was applied simply by examining graphs of both computer and experimental responses. A mathematical accuracy criterion is presented here that permits a more accurate basis for judgment. This criterion is a relationship between the launcher response and the points of projectile impact. General application of this criterion is limited only by the fact that it employs the motion characteristics of a short-burning-time, ballistic rocket. Because the development of this criterion came late in this program, its application was not completed. It is presented here, however, because of its generality.

The significant sources of rocket dispersion (of a rocket with a relatively short burning time) are:

1. Initial cross spin, i.e., angular yaw (pitch) velocity when the rocket leaves the launcher,

2. Launch mal-point, i.e., initial yaw (pitch) when the rocket leaves the launcher,
3. Dynamic unbalance of rocket,
4. Cross winds during burning,
5. Total rocket impulse variations,
6. Rocket spin at burnout,
7. Thrust malalignment.

Only the first three of these are influenced by the launcher. The particular launcher motion that can contribute significantly to dispersion by influencing these three quantities is the cradle motion in combination with the firing tube motion relative to the cradle. The cradle angular displacement and angular velocity in the vertical plane are considered here. At present, we are limited to consider only these because all completed mathematical models assume a rigid firing tube and plane motion only. Because of these two limitations, dynamic unbalance must also be neglected. In addition, during the transition period when the rocket is partially out of the firing tube, the rocket is assumed to have the orientation of the tip of the tube.

The purpose of this criterion is to permit a comparison of launcher responses to burst firings (or a group of single shot firings with the same launcher) and a subsequent selection of the best response; with this in mind, the following characteristics can be imposed upon the criterion:

1. Only relative changes in dispersion or accuracy between burst responses need be indicated by the criterion.
2. In the case of computed responses, an indication of accuracy improvement by the mathematical output of the criterion must correspond to an actual accuracy improvement. (This can be checked experimentally or with a complete, bailistics mathematical model). This correspondence will not be required to be linear, however.
3. The criterion will yield a numerical answer for each burst and will be zero for a perfect burst. (A perfect burst is attained when all rounds impact at the same point.)
4. The criterion must allow for the different contributions to dispersion from unit deviations in initial yaw and initial cross spin.
5. Each round of a burst is to be considered separately, and its sequential position will be neglected.

These are the criterion characteristics that are inferred prior to the development of the criterion simply by considering its purpose and application. The implications of each of these are: Item 1 states that the criterion output for a single burst will not indicate anything about the accuracy of that burst, when compared to the criterion output of another burst; however, it will indicate which of the two is better, i.e., more accurate. Item 2 states that the indication of which of two bursts was more accurate must correspond to the indication of relative accuracy of an actual launcher firing of two bursts under the same conditions: the criterion must agree with reality. In order that the criterion contain the characteristics implied by Item 3, the deviations of both displacement and velocity of the cradle will be measured with respect to their mean. Item 4 states that the criterion must account for the fact that a unit deviation in angular cradle displacement does not necessarily produce the same dispersion as a unit deviation in angular cradle velocity; this is accomplished by using what are known as "unit effects", coefficients determined by the magnitude of dispersion due to a unit deviation in each quantity. The last item, No. 5 merely states that no priority is given to any of the six rounds of a burst.

The combination of the above characteristics narrows the choice of mathematical expressions describing this accuracy criterion to a point where an expression can be deduced:

$$L = U_y \sum_{k=1}^{6} \left|\Delta_y\right|_k + U_s \sum_{k=1}^{6} \left|\Delta_s\right|_k ,$$

where

L	=	the numerical output from the above expression indicating relative burst accuracy,
U_y	=	unit effect for mal-point or initial yaw,
U_s	=	unit effect for initial cross spin,
Δ_y	=	deviation from the mean in initial yaw,
Δ_s	=	deviation from the mean in initial cross spin,
k	=	index.

The two deviations are written as:

$$\left|\Delta_{y'|k}\right| = \left|\phi_k - \phi_m\right| \qquad \left|\Delta_s\right|_k = \dot{\phi}_k - \dot{\phi}_m ,$$

where ϕ_k and ϕ_m are the initial yaw and cross spin, respectively. In this criterion, the smaller the value of L, the better the burst. Other criteria may be deduced that conform to the given conditions, but for small deviations they will reduce to the above expression.

This criterion was to be incorporated directly into the computer program of the 3-degree-of-freedom mathematical model. A 6-rd burst computation would then automatically give the quantity, L. The unit effects are obtained from solutions of the equations of motion of the rocket; the unit effects for the XM54 rocket were tabulated in previous progress reports of this project. [1/]

[1/] For more information of the unit effects of rocket dispersion, see: Bi-Monthly Report No. 18, ARF Project D124, January 22, 1960.

V. CONCLUSIONS

All the results derived from this study are based upon considerations of cradle motion near the time of shot ejection of each round of a burst. There was no intention of neglecting the effects of firing tube flexibilities, but this effort represents a first step to increase the weapon accuracy. There was no reason to suspect that flexible firing tube motions may be simply additive to cradle motion because of the coupling which exists. However, the correlation obtained between theory and experiment, despite neglecting this coupling theoretically, indicates that the effects upon gross cradle rotation are small. This points to the conclusion that the accuracy criterion based upon cradle motion was valid, i.e., a reduction in the residual cradle motion prior to the successive rounds of a burst will improve accuracy.

The residual cradle oscillations of the as-designed launcher (Prototype No. 3) were seen experimentally to be small. The only disturbing factor was that the as designed structure was subjected to elastic rebond, or trail hop; this permitted serious, gross horizontal dispersion to occur. This horizontal dispersion was eliminated by simple ties restraining the trails from moving in a horizontal plane. An alternative was shown to exist where trail hop was eliminated -- this was shown to be accomplished by stiffening the supporting structure. With this stiffened structure, the ties at the trails are unnecessary.

When trail hop does not occur, an optimum combination of elevating system structural parameters was found. This was based upon a study which showed that the best location (based upon effectiveness per weight) at which auxiliary damping should be added to the launcher is between the tipping assembly and the supporting structure. The optimum elevating system had the following structural parameters:

k_2 (total stiffness) = 1.4×10^4 lb/in.

c_2 (Damping coefficient) = 400 lb-sec/in.

This combination caused a minimum of residual cradle oscillation between shots of a burst, and is independent of the stiffness of the supporting

structure. The possibility of an unstable response during a burst was demonstrated for very low elevating system stiffness. It should be mentioned that due to the damping of the hydraulic recoil system and possibly soil interaction, the launcher, as designed, displayed much inherent damping.

Elevation changes were shown theoretically to influence the accuracy because of the corresponding geometry changes. The overall effect was to increase accuracy with elevation. Changes in accuracy were also observed due to difference in ammunition boost charge. The difference, however, was much less than might be expected because of the large reduction in the recoil force at the lower zones. This was because the forces developed during counterrecoil, from the recuperator and indexing system, are of the same order of magnitude as during the high boost bursts.

Delayed recoil is effective in reducing the velocity and displacement of the cradle response for single shots. For bursts, the effectiveness is questionable since it will improve accuracy when the ignition of the round occurs simultaneously with positive cradle velocity, but it does not help when ignition occurs during a duration of a negative cradle velocity. Rods cut back to delay the recoil force for the first shot only will probably yield the best overall accuracy improvement. This improves single shot accuracy while it eliminates the possibility of detracting during later shots.

When considering horizontal dispersion, the shell which stiffens the recoiling assembly framework reduces the dispersion by more than 100%. In addition, when trail hop is present, horizontal ties between the trails and the ground are necessary to achieve good accuracy. They may also improve dispersion in the absence of hop if a tendency exists for the trail pads to slide.

Finally, inclusion of Coriolis acceleration was shown to be significant in the calculation of peak response magnitude, but neglecting it did not alter the overall response shape.

In order to completely investigate launcher contributions to dispersion, two additional efforts are recommended. These are a completion of the development of the three-dimensional mathematical model begun in this

project, and a comprehensive experimental program utilizing the stiffening fixtures developed. This experimental program should include firing tube motion instrumentation as well as rocket instrumentation. It is felt that this combined effort can produce a weapon whose accuracy in burst fire exceeds that of present single shot artillery.

APPENDIX A

A STUDY OF THE RELATIVE EFFECTIVENESS OF VARIOUS DAMPER LOCATIONS

N. P. Pearson, R. M. Brach, and R. H. Van Beek

I. INTRODUCTION

This appendix concerns the theoretical possibility of damping the motions of the supporting structure and tipping parts of an XM70-type launcher between consecutive shots of a burst. Ideal viscous dampers are considered to be located between the ground and supporting structure, and/or between the supporting structure and the tipping parts, and/or between the ground and the tipping parts.

II. THE MATHEMATICAL MODEL

Figure A-1 is a schematic drawing of an XM70-type launcher simplified and idealized to the point where it has only two degrees-of freedom. The general procedure for forming such a discrete system from an elastic system consists of lumping equivalent masses at points where the stiffness is known and/or loads are applied and determining the values of the equivalent masses in such a way that the actual and reduced systems have the same kinetic and potential energy during their first-mode oscillation.[1/] The accuracy of the technique depends upon the nature of the forcing function and upon the location where the motion is desired. Deflection magnitudes at any given instant are not expected to be accurate because important features, such as the indexing forces, are not considered. However, the relative effectiveness of the three damper locations is expected to be correctly represented. Clearly, in this particular case, if the calculations showed the motions to be thoroughly damped after some relatively long time, say t_o, and if the actual weapon were equipped with analogous dampers, the motion of the actual carriage or cradle would be thoroughly damped after t_o also.

---

1. Jacobsen, L. S., Ayre, R. S., Engineering Vibrations, McGraw Hill Book Co., Inc., New York, 1958.

The equations of motion of the system shown in Fig. A-1 are;

$$I_2 \ddot{\phi}_2 = -k_2(\phi_2 - \phi_1) - c_2(\dot{\phi}_2 - \dot{\phi}_1) - c_3 \dot{\phi}_2 \qquad \text{A-1}$$

and

$$(I_e + m_r \ell^2)\ddot{\phi}_1 = k_2(\phi_2 - \phi_1) + \ell F(t) - k_1 \phi_1 - c_1 \dot{\phi}_1 + c_2(\dot{\phi}_2 - \dot{\phi}_1) \qquad \text{A-2}$$

or, letting

$$I_e + m_r \ell^2 = I_1$$

and

$$\ell F(t) = M(t)$$

then

$$I_1 \ddot{\phi}_1 - k_2(\phi_2 - \phi_1) + k_1 \phi_1 + c_1 \dot{\phi}_1 + c_2(\dot{\phi}_2 - \dot{\phi}_1) = M(t) \qquad \text{A-3}$$

$$I_2 \ddot{\phi}_2 + k_2(\phi_2 - \phi_1) + c_2(\dot{\phi}_2 - \dot{\phi}_1) + 3\dot{\phi}_2 \qquad \text{A-4}$$

Equations A-3 and A-4 have been solved with a forcing function, M (t), derived from an experimental record of recoil pressure. Figure A-2 shows the forcing function used for all the solutions given in this appendix. The value of the function is just the recoil pressure multiplied by the appropriate area and moment arm. Figures A-3 through A-8 show the calculated response for various choices of the parameters. The stiffness values, k_1 and k_2, represent the values either measured or calculated for the existing weapons. In addition to the values of damping and stiffness, each of the graphs is labeled with the maximum value of the quantity $c_2(\dot{\phi}_1 - \dot{\phi}_2)$ which is the maximum force developed in the damper between the supporting structure and the tipping parts.

III. DISCUSSION AND CONCLUSIONS

Figure A-3 describes the undamped response of the system, which is not representative of the actual weapon response, primarily because the actual weapon contains inherent damping. The figure does show, however, that significantly larger amplitudes may be obtained on shots after the first. This phenomenon was observed experimentally for Prototype No. 1. It is worthwhile noting that, in all of these response plots, the negative values of ϕ_1 may be taken as a rough indication of the system's tendency to produce trail hop.

The parameters used in the calculation represented by Fig. A-4, A-5, and A-6 are identical except for the values of damping, with c_1, c_2, and c_3 alternately taking on the value 1.25×10^5 lb-sec^2/in., the other two being zero in each case. Note from Fig. A-6 that damping between the ground and the tipping parts, c_3-damping, gives the best results. The relative effectiveness of c_2-damping, as shown by Fig. A-5, and the relative ineffectiveness of c_1-damping, as shown by Fig. A-4, constitute the most important result of this study.

Damping between the tipping parts and the ground, c_3-damping, is the most difficult type to obtain practically. Figure A-7 shows an attempt to obtain the effectiveness of c_3-damping using only c_1- and c_2-damping. The results are seen to be not as good as c_3-damping alone. This is particularly discouraging when the weight added by the two dampers is considered. Figure A-8 shows the results of attempts to compensate for the weight of the two dampers by reducing the supporting structure stiffness and, hence, its weight. This performance is seen to be slightly less satisfactory, but further conclusions are unwarranted because of the simplicity of the model which does not include indexing forces and elevating system geometry. Because these factors affect the optimum stiffness-damping relationship, this relationship will be studied by means of a more elaborate mathematical model.

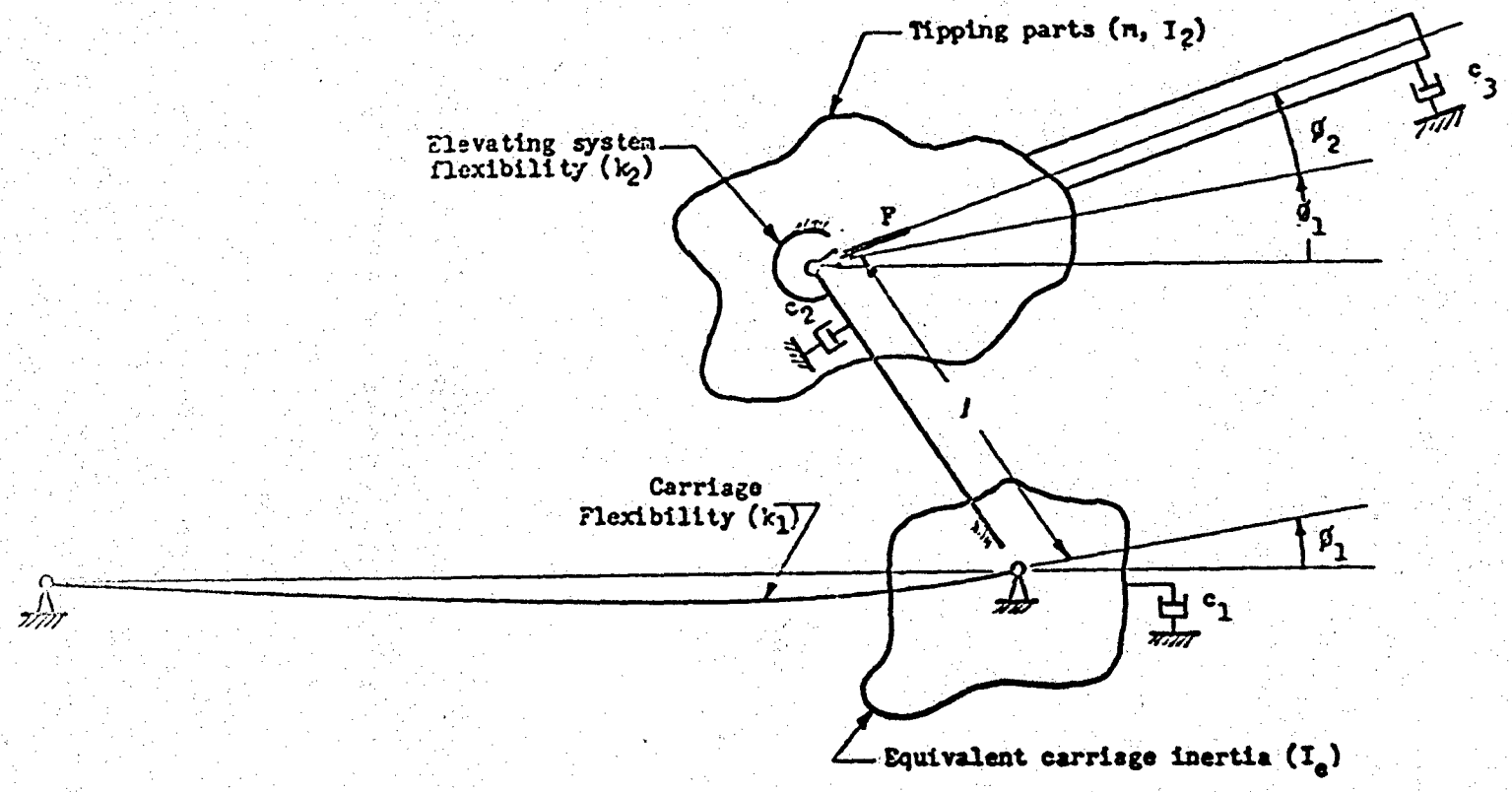

Fig. A-1 TWO-DEGREE-OF-FREEDOM REPRESENTATION OF A XM70 LAUNCHER

ARMOUR RESEARCH FOUNDATION OF ILLINOIS INSTITUTE OF TECHNOLOGY

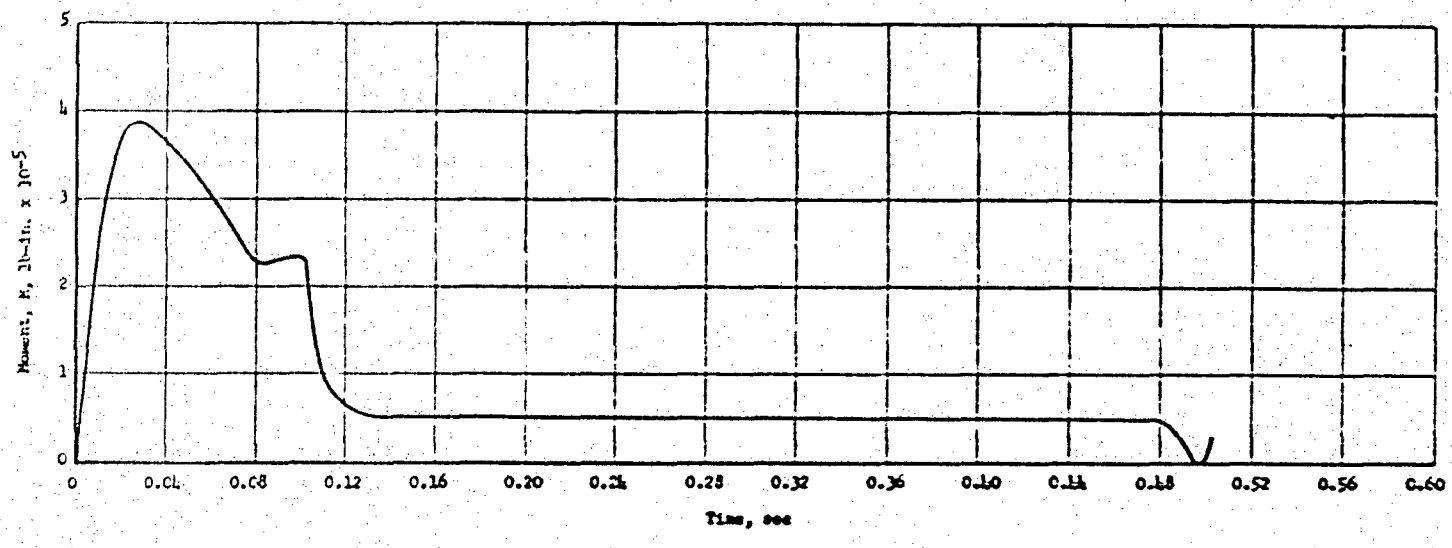

Fig. A-2 MOMENT PRODUCED BY THE RECOIL FORCE

ARMOUR RESEARCH FOUNDATION OF ILLINOIS INSTITUTE OF TECHNOLOGY

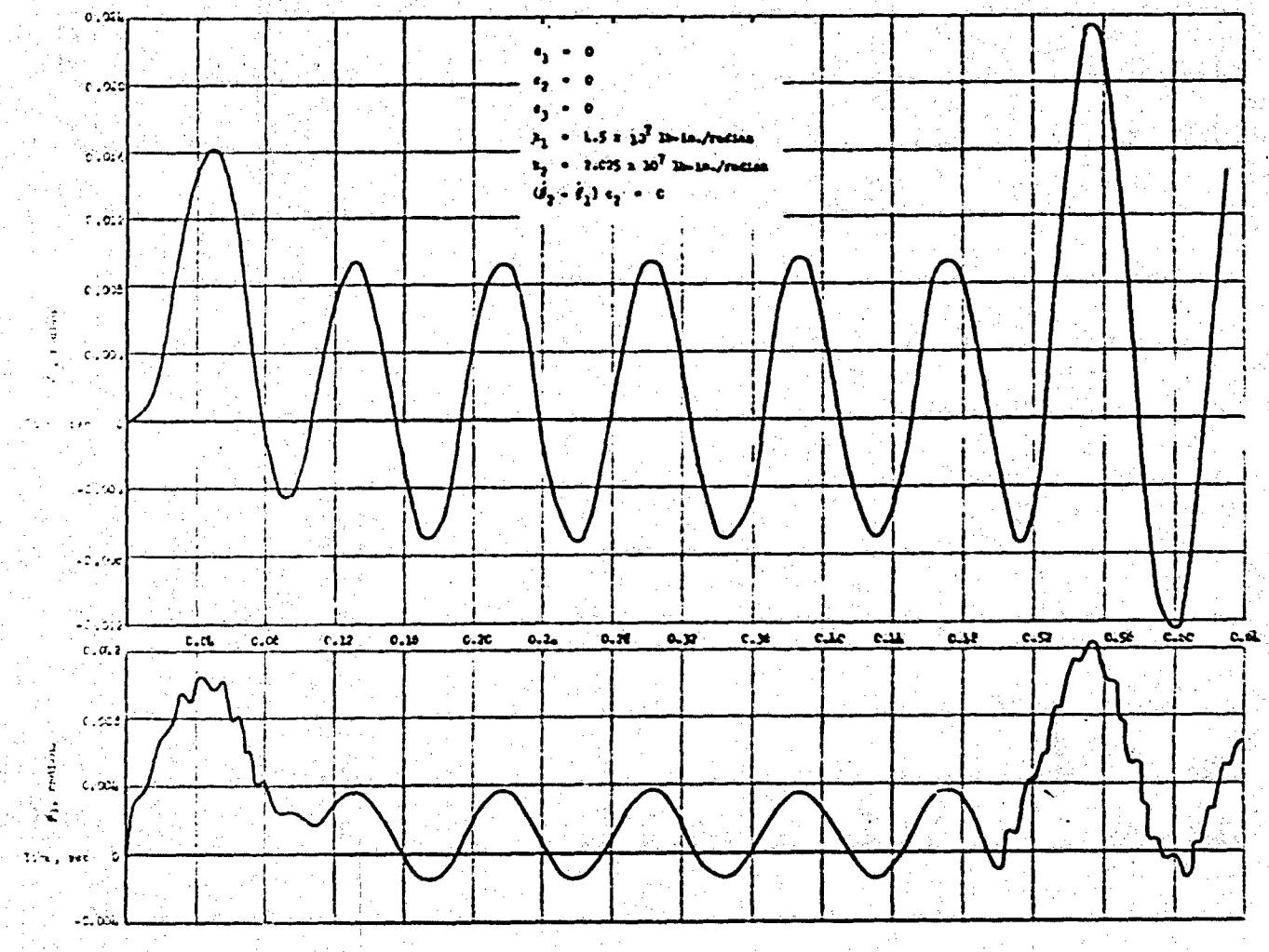

Fig. A-3 CALCULATED UNDAMPED RESPONSE OF AN XM70-TYPE LAUNCHER

ARMOUR RESEARCH FOUNDATION OF ILLINOIS INSTITUTE OF TECHNOLOGY

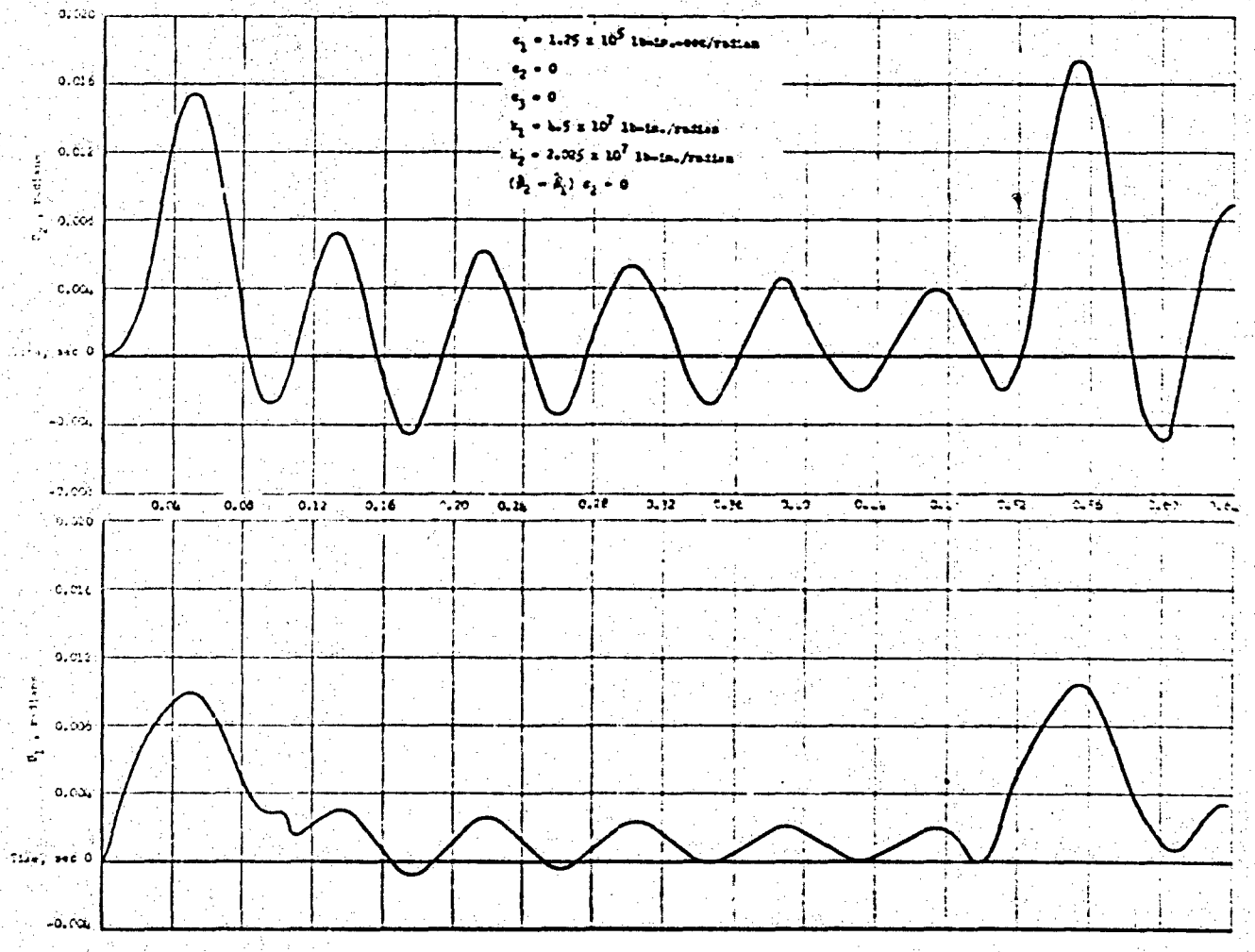

Fig. A-4 **CALCULATED RESPONSE OF AN XM70-TYPE LAUNCHER WITH c_1-DAMPING ONLY**

ARMOUR RESEARCH FOUNDATION OF ILLINOIS INSTITUTE OF TECHNOLOGY

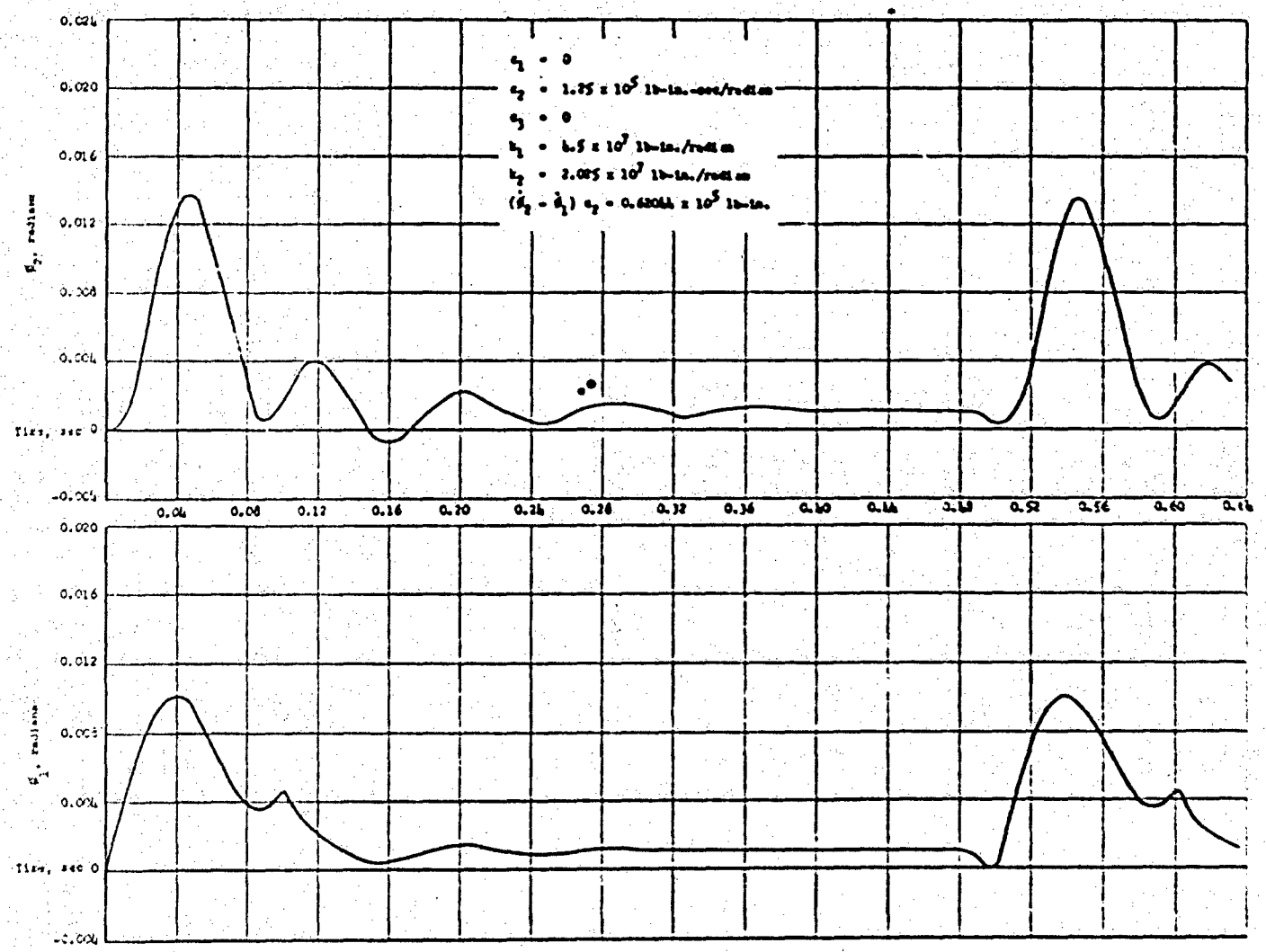

Fig. A-5 CALCULATED RESPONSE OF AN XM70-TYPE LAUNCHER WITH c_2-DAMPING ONLY

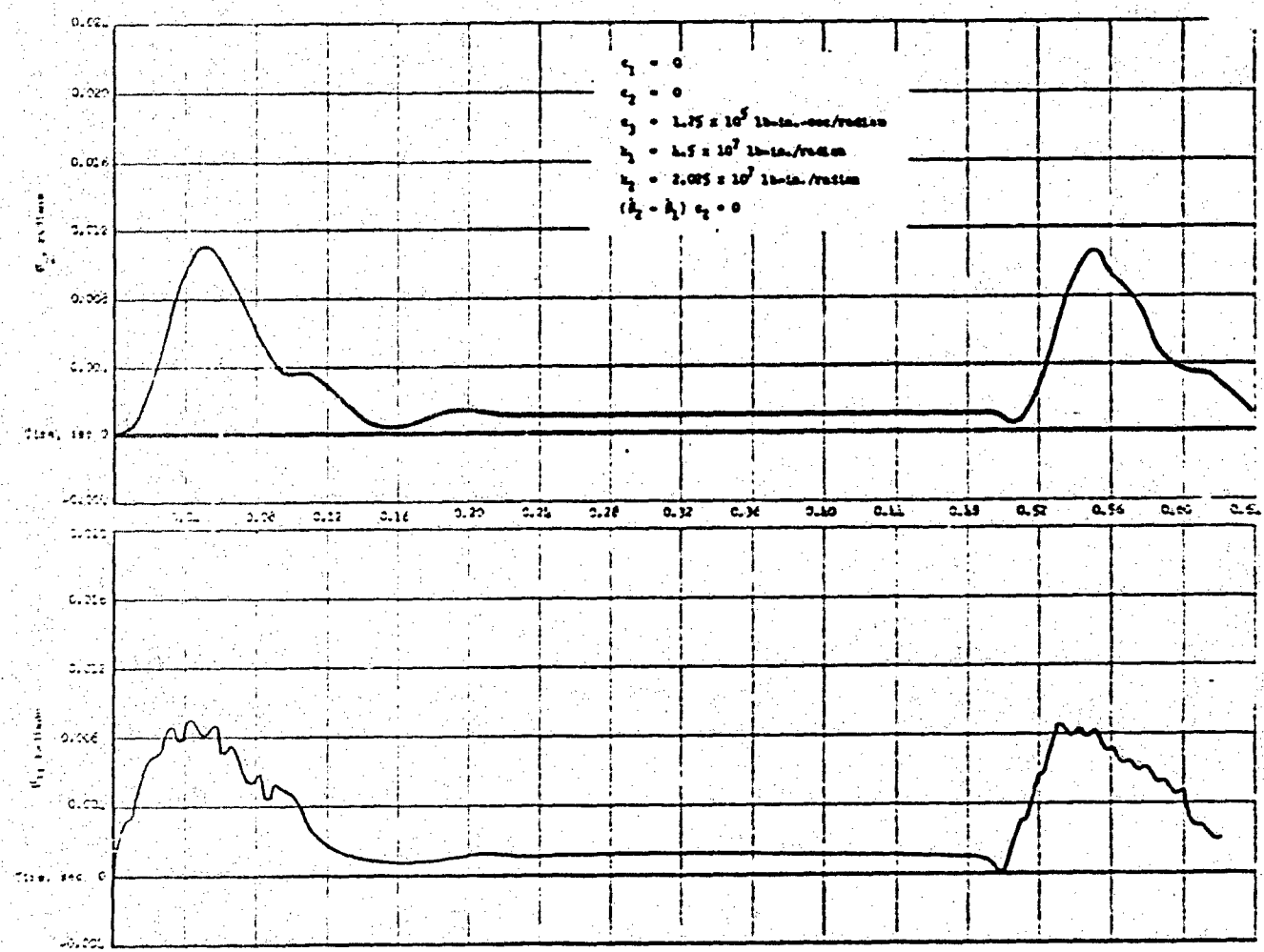

Fig. A-6 CALCULATED RESPONSE OF AN XM70-TYPE LAUNCHER WITH c_3 - DAMPING ONLY

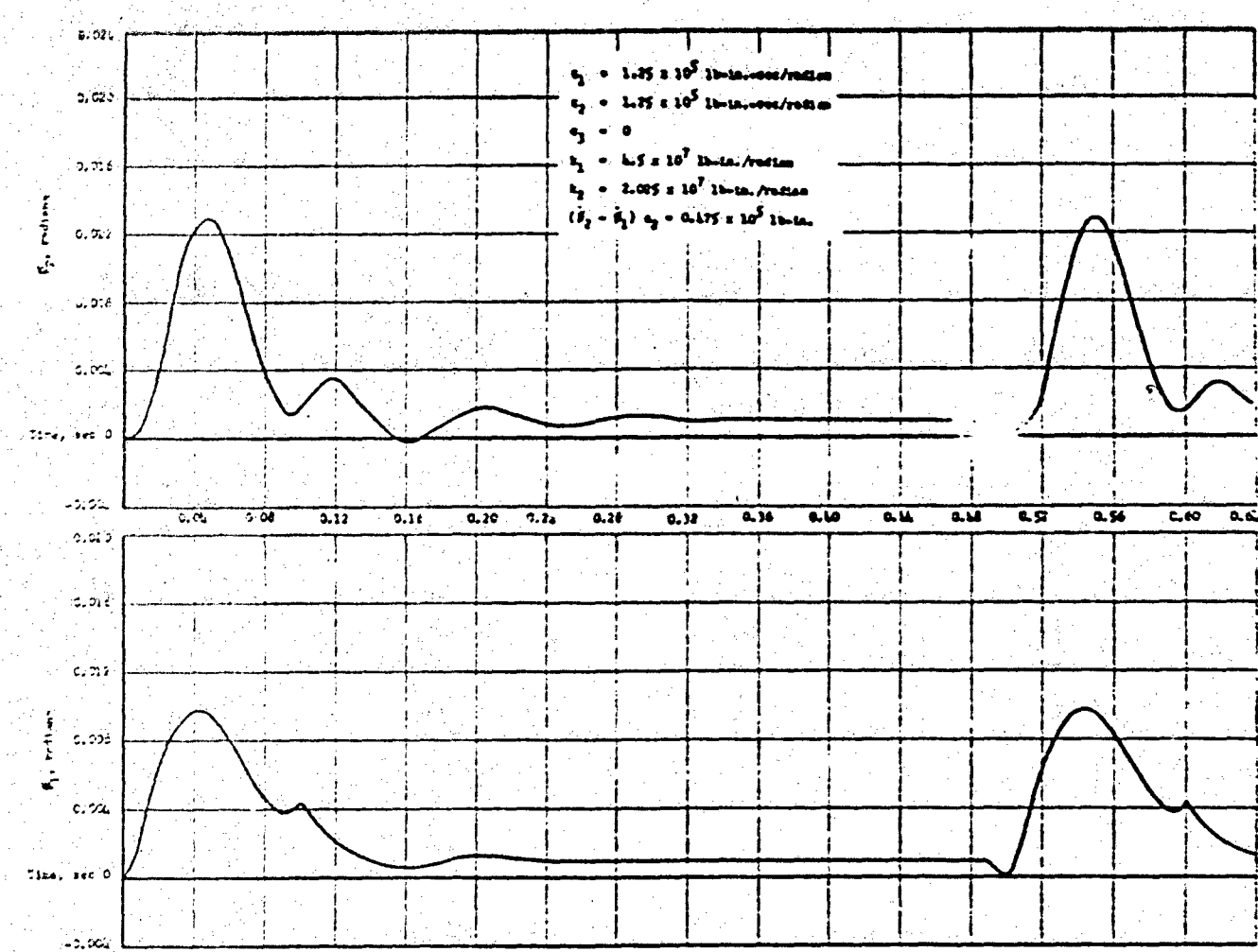

Fig. A-7 CALCULATED RESPONSE OF AN XM70-TYPE LAUNCHER WITH c_1- AND c_2 - DAMPING COMBINED

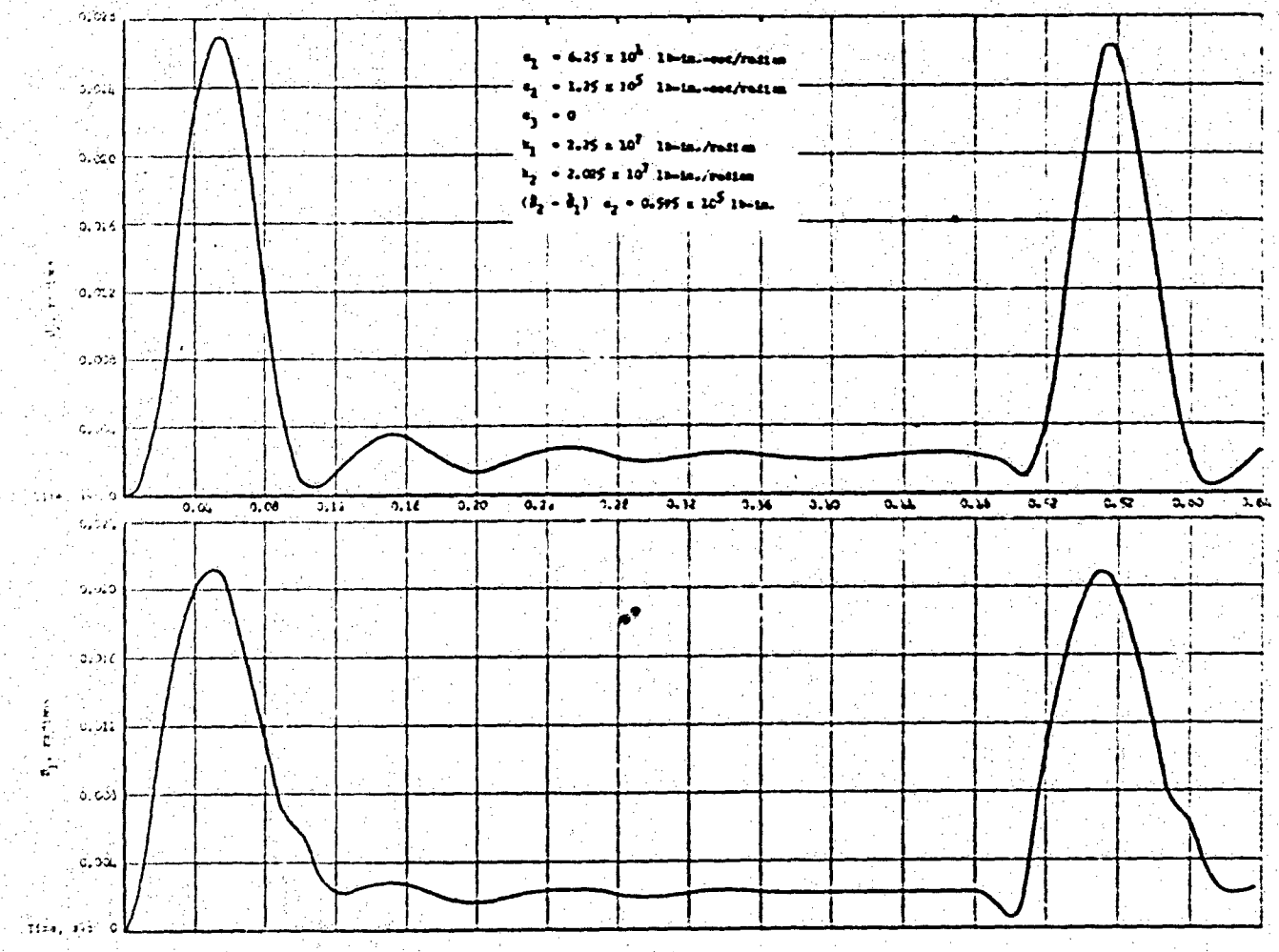

Fig. A-8 CALCULATED RESPONSE OF AN XM70-TYPE LAUNCHER WITH c_1- AND c_2-DAMPING COMBINED AND WITH REDUCED CARRIAGE STIFFNESS

ARMOUR RESEARCH FOUNDATION OF ILLINOIS INSTITUTE OF TECHNOLOGY

APPENDIX B

A DYNAMIC ANALYSIS OF SOME BASIC DESIGN PARAMETERS

By R. H. Van Beek

I. INTRODUCTION

This appendix contains a dynamic analysis which was intended to aid in determinimg some of the basic design parameters, such as weight and stiffnesses, of weapons of the XM70 type. This analysis uses a relatively simple mathematical model of a weapon together with semiempirical data from the XM70 Prototype Model No. 1. A nomenclature list is at the end of this Appendix.

II. ANALYSIS

It has been shown that the weapon can be represented by a single-degree-of-freedom dynamic model with the recoil force (rod pull) as a forcing function. The assumed model and forcing function are shown in figures B-1 and B-2.

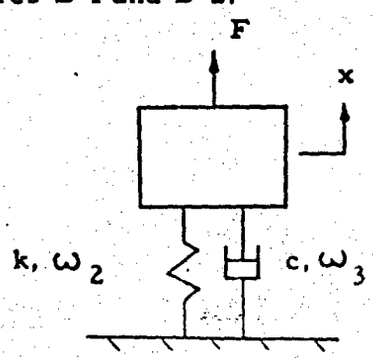

Fig. B-1 MATHEMATICAL MODEL

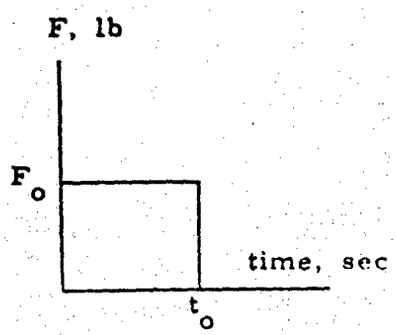

Fig. B-2 FORCING FUNCTION

The differential equation for the system of figure B-1 is

$$M = \ddot{x} + c\dot{x} + kx = F \qquad \text{Eq. (B-1)}$$

$$\text{Let } \eta \equiv \sqrt{\frac{K}{M}}\, t_o, \quad \mu \equiv \frac{c}{2\sqrt{KM}}, \quad \tau \equiv \frac{t}{t_o}, \quad \mathcal{X} \equiv \frac{XM}{F_o t_o^2} \qquad \text{Eq. (B-2)}$$

The solution to differential equation (B-1) in terms of these quantities is

$$x(\tau) = \frac{1}{\eta^2}\left[1 - e^{-\eta\mu\tau}\left(\frac{\mu}{\sqrt{1-\mu^2}} \sin \eta\sqrt{1-\mu^2}\,\tau + \cos \eta\sqrt{1-\mu^2}\,\tau\right)\right] \quad \text{for } 0 \leq \tau \leq 1 \qquad \text{Eq. (B-3)}$$

$$x(\tau) = e^{-\eta\mu\tau}\left[L_1 \sin \eta\sqrt{1-\mu^2}\,\tau + L_2 \cos \eta\sqrt{1-\mu^2}\,\tau\right]$$

$$\text{for } \tau \geq 1 \qquad \text{Eq. (B-4)}$$

$$\text{where } L_1 = \frac{1}{\eta^2}\left[\frac{-\mu}{\sqrt{1-\mu^2}} + e^{\mu\eta}\left(\frac{\mu}{\sqrt{1-\mu^2}} \cos \eta\sqrt{1-\mu^2} + \sin \eta\sqrt{1-\mu^2}\right)\right] \qquad \text{Eq. (B-5)}$$

$$\text{and } L_2 = -\frac{1}{\eta^2}\left[1 + e^{\mu\eta}\left(\frac{\mu}{\sqrt{1-\mu^2}} \sin \eta\sqrt{1-\mu^2} - \cos \eta\sqrt{1-\mu^2}\right)\right] \qquad \text{Eq. (B-6)}$$

For a single degree-of-freedom torsional system, the same solution holds with the dimensionless variables given by

$$x = \frac{\theta I}{T_o t_o^2}, \quad \eta = \sqrt{\frac{k}{I}}\, t_o, \quad \mu = \frac{c}{2\sqrt{kI}}, \quad \tau = \frac{t}{t_o} \qquad \text{Eq. (B-7)}$$

A typical displacement time plot is shown in figure B-3.

Adequate dynamic performance, i.e. acceptable accuracy, results when t_c is less than the time to a subsequent firing and θ_c is a displacement which produces negligible error at the target. Several primary design parameters can be logically determined by finding the minimum weight weapon which will give the required performance.

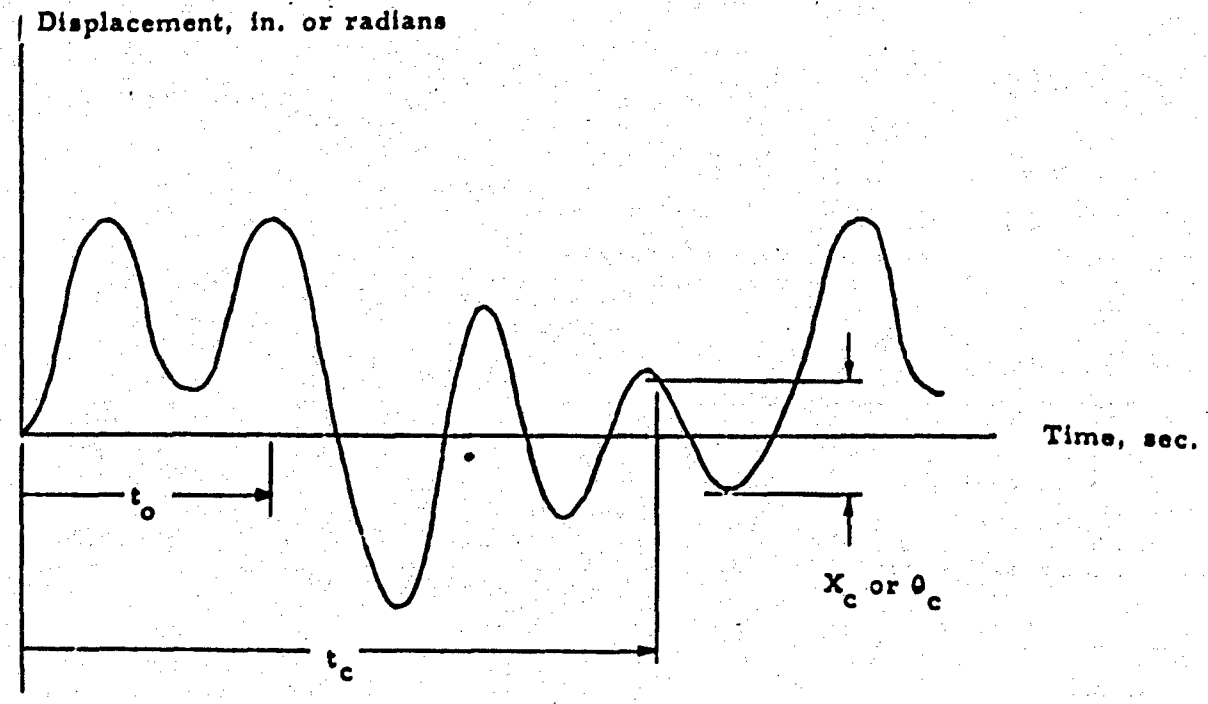

FIG. B-3 TYPICAL TIME DISPLACEMENT CURVE OF THE XM70 LAUNCHER

For given μ and η the graph of $\varkappa$ versus τ can be drawn. The last intersection of the curve with $\theta = \pm \theta_c$ determines τ_c. Repeating this procedure for a number of combinations of μ and η gives data for a plot of τ_c versus η for various values of μ. For a given τ_c, a plot of η versus μ can then be drawn. All points on this curve are such that the corresponding η and μ produce a displacement of θ_c at $\tau = \tau_c$ and $\theta < \theta_c$ for $\tau > \tau_c$. All points give values of μ and η for which τ_c is less than the value of τ_c for which the curve is drawn. Figure B-4 shows a typical graph of τ versus η.

As an approximation, the envelope of equation (B-4) can be used. It is given by

$$\theta_e = L_1^2 + L_2^2 \quad e^{-\eta\mu\tau} \qquad \text{Eq. (B-8)}$$

$$L_1^2 + L_2^2 = \frac{\sqrt{1 - 2e^{\mu\eta} \cos\eta \sqrt{1-\mu^2} + e^{2\mu\eta}}}{\eta^2 \sqrt{1-\mu^2}} \qquad \text{Eq. (B-9)}$$

Then

$$(\theta_e)_c = L_1^2 + L_2^2 \quad e^{-\eta\mu\tau_c} \qquad \text{Eq. (B-10)}$$

This eliminates the necessity of drawing the first two of the above mentioned graphs, since, given τ_c and θ_c, for each μ the corresponding η can be found numerically by trial and error. In all cases where the graphs of μ versus η were found by both methods the difference between the graphs was negligible.

Let the total weight of the weapon be given by

$$W_t = W_1 + W_2 + W_3 + W_{NS} \qquad \text{Eq. (B-11)}$$

Assume that the weight of the carriage is related to its rotational stiffness by the linear relation

$$W = \alpha k \qquad \text{Eq. (B-12)}$$

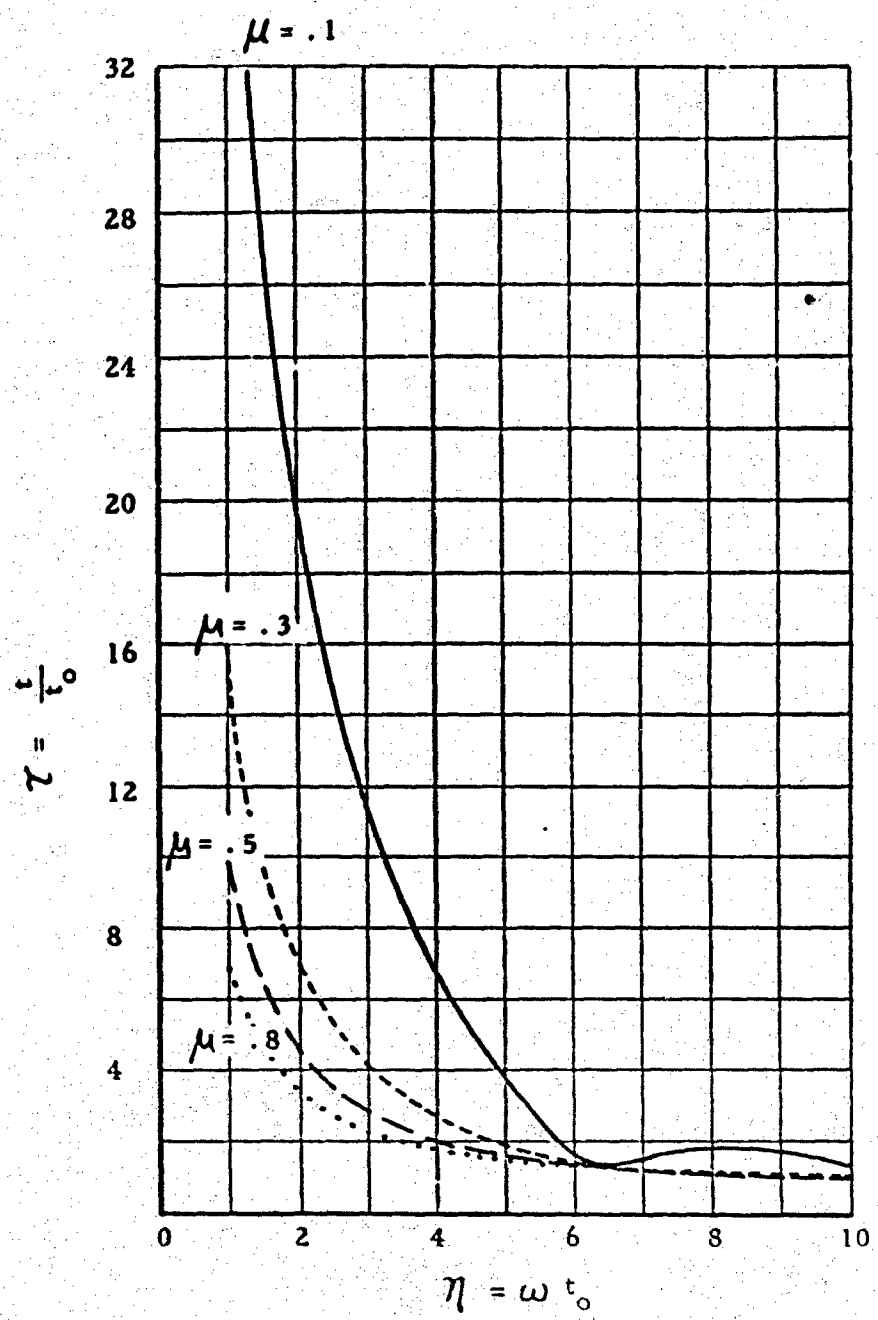

FIG. B-4 TYPICAL GRAPH OF DIMENSIONLESS TIME VERSUS FREQUENCY FOR VARIOUS DAMPING RATIOS

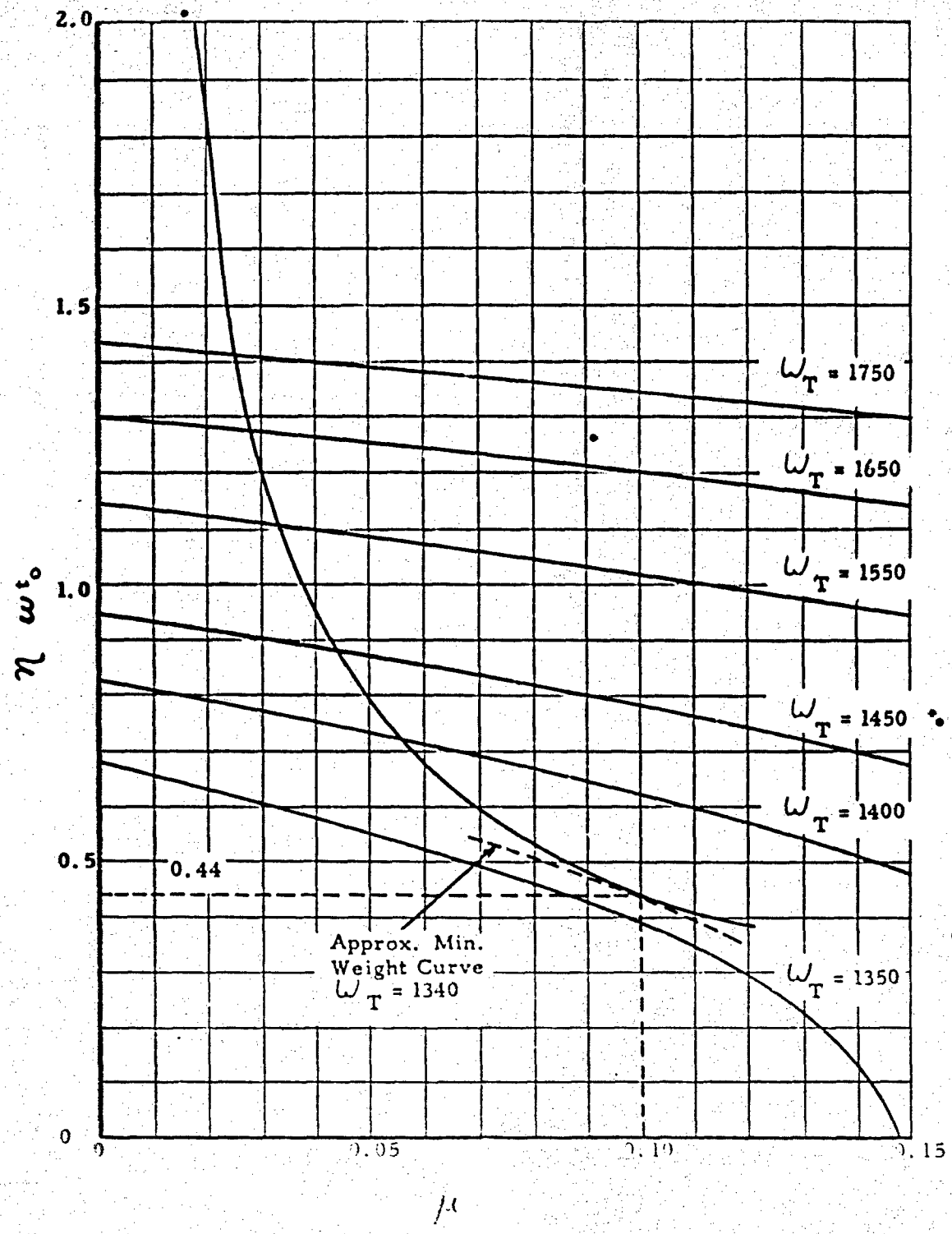

FIG. B-5 MINIMUM WEIGHT REQUIRED TO SATISFY ACCURACY CRITERION

In addition, assume that the weight of the damper is related to the damping ratio by the linear relation

$$W_3 = \beta\mu \qquad \text{Eq. (B-13)}$$

By (B-1), (B-2), and (B-3)

$$W_T - W_H - W_1 = \alpha k + \beta\mu \qquad \text{Eq. (B-14)}$$

By definition

$$\eta = \omega t_o = \frac{k}{I} t_o \qquad \text{Eq. (B-15)}$$

Assuming that one-third of the moment of inertia of the carriage should be added to the moment of inertia of the recording assembly given

$$I = I_1 + 1/3\, I_2$$

$$I = \frac{W_1}{g} r_1^2 + \frac{W_2}{3g} r_2^2$$

$$I = \frac{W_1}{g} r_1^2 + \frac{2k}{3g} r_2^2 \qquad \text{Eq. (B-16)}$$

By eliminating k and I between Eq. (B-4), (B-5), and (B-6), the relation between η and μ for constant W_T is obtained, assuming W_1 and W_H are constants.

$$\eta^2 = \frac{3 g t_o^2}{2 r_2^2} \left[\frac{\gamma}{3 \frac{r_1^2}{r_2^2} + \gamma} \right] \qquad \text{Eq. (B-17)}$$

where $$\gamma \equiv \frac{W_T - W_H - W_1 - \beta\mu}{W_1} \qquad \text{Eq. (B-18)}$$

III. RESULTS

From this relationship, curves of η versus μ for various values of W_T can be plotted. If a curve of η versus μ for the desired value of τ is plotted on the same graph, the lowest possible weight giving acceptable accuracy can be determined. The situation is illustrated in Fig. 5. The constant τ curve can be thought of as representing acceptable performance and the other curves are the constant weight curves. Then the lowest weight curve which just intersects the performance curve gives the minimum total weight and the point of intersection determines the desired damping ratio and η. Then by the use of equations (B-11), (B-12), and (B-13), the carriage stiffness and weight and the damper weight can be calculated. Fig. 5 also shows the results of applying this analysis with the following input data:

Projectile weight*	50 lb.
Muzzle velocity*	1000 ft/sec.
Firing rate	20 rnds/min.
Maximum Amplitude of Vibration at triggering (θ_c)	0.0005 rad.
Maximum Recoil Displacement (Free Recoil until shot ejection is assumed and requires 12 in. of recoil)	24 in.
Recoiling Assembly Weight	500 lb.

The inertia-weight relationships and the carriage stiffness- weight relationship, (α), of the XM 70 were assumed. It will be noted that the hypothetical weapon has a very low firing rate and small recoiling assembly weight and hence has a small mimimum weight. From the graph, the minimum total weight which gives the desired accuracy is 1340 lb. Included in this is a total accessory or non-structural weight which is assumed to be 750 lb. This is the same as the XM70 and includes everything except the recoiling assembly and the carriage structure. Using the values of μ and η from the graph, the damper weight is found to be 67.5 lb. and the carriage weight

* these quantities determine the forcing function

22.5 lb. The carriage stiffness required is 1.12×10^6 lb. in./rad.

This example design, although it theoretically satisfies the accuracy criterion, is impossible because a carriage weighing 22.5 lb. could not carry the rod pull. This result led to the development of strenghth criterion and a method of optimizing recoiling assembly weight. This latter method was used for the XM70 Prototype Model No. 2 and is presented in ARF Project K130 Bi-monthly Report No. 8, Appendix B.

IV. NOMENCLATURE

W_T total weight of gun

W_{NS} weight of gun hardware

W_1 weight of recoiling assembly

W_2 weight of carriage

W_3 weight of damper

k torsional stiffness of carriage

K spring stiffness for linear vibration system

c damping stiffness for linear vibration system

M mass stiffness for linear vibration system

$b = \frac{c}{2M}$

$\omega = \sqrt{\frac{K}{M}} = \sqrt{\frac{k}{I}}$, natural frequency of undamped system

I effective moment of inertia of torsional vibration system

μ ratio of damping to critical damping

$\eta = \omega t_o$, non-dimensional frequency

x displacement for linear vibration system

θ displacement for torsional vibration system

t time

$\chi = \frac{Mx}{F_o t_o^2} = \frac{I_\theta}{T_o t_o^2}$ non-dimensional displacement

t_o length of pulse

F_o amplitude of pulse-linear vibration system

T_o amplitude of pulse-torsional vibration system

$\tau = t/t_o$ non-dimensional time

I_1 moment of inertia of recoiling assembly about the base

I_2 moment of inertia of carriage about the base

APPENDIX C

EQUATIONS OF MOTION OF THE LAUNCHER WITH THREE DEGREES OF FREEDOM

R. M. Brach

I. INTRODUCTION

The following equations apply to launchers with a structural geometry corresponding to that of the XM70 automatic rocket launcher. It is a three-degree-of-freedom analysis of gross launcher motion in the vertical plane. These equations are to be used to investigate the stability of the system and the influence on stability of changes in: (1) elevating system stiffness and damping, (2) carriage and trail stiffness, (3) mass distribution, (4) recoil force, and (5) indexing cam length. They can also furnish an indication of the effects due to variations in the muzzle momentum of the projectile. However, because the analysis considers a rigid firing tube, it cannot predict the precise projectile motion at the time of muzzle ejection.

The three degrees of freedom (see Fig. C-1) are the following: (1) the linear displacement of the recoiling mass relative to the cradle, u, (2) the angular motion of the tipping parts relative to the carriage, ϕ_2, and (3) the absolute angular motion of the supporting structure, ϕ_1. The supporting structure in this analysis is taken to be the entire structure that supports the tipping parts; i.e., the supporting structure includes a rigid, massless, trunnion side, an inertia, and a massless, flexible trail. The inertia is an equivalent inertia found by letting the above support contain kinetic and potential energy equal to that of the actual launcher vibrating in its static deflection shape. The supporting structure is assumed to rotate about the ball joint, point 0 in Fig. C-1; a provision for damping the rotation is included. The elevating system is assumed to be a massless spring and damper. The cradle and recoiling mass are both assumed to be rigid bodies.

The equations of motion of the recoiling mass include those describing the constant-force, constant-stopping-distance recoil system,

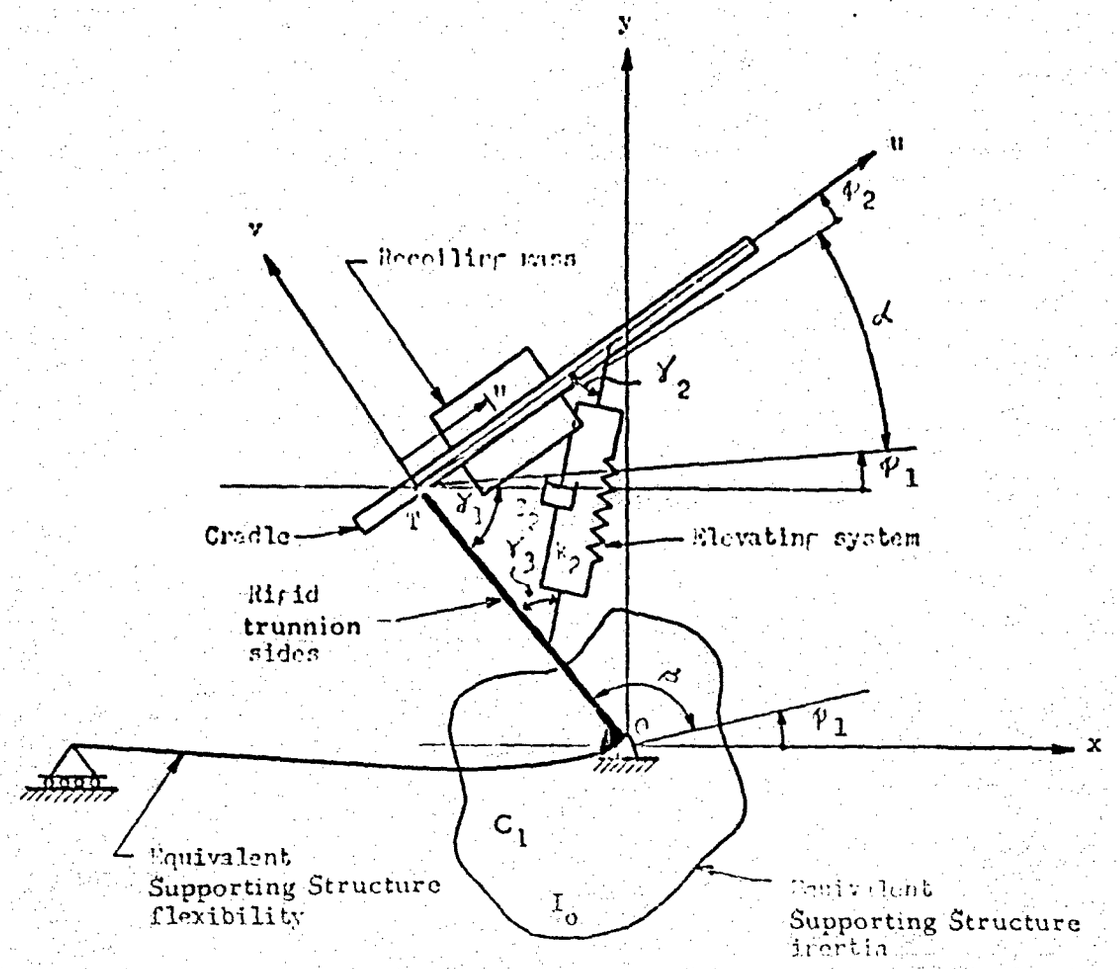

Fig. C-1 SCHEMATIC REPRESENTATION OF THE LAUNCHER

used in the XM70, and also the axial reactions of the indexing cam since these have been found to be significant from past experience.

II. ANALYSIS

A. Kinematics

If the motion of the recoiling mass is described by x_r and y_r with respect to the ground and by u with respect to the cradle, we see from Fig. C-2 that

$$x_r = \ell \cos(\beta + \phi_1) + u \cos(\alpha + \phi_1 + \phi_2)$$

and C-1

$$y_r = \ell \sin(\beta + \phi_1) + u \sin(\alpha + \phi_1 + \phi_2)$$

In these equations, ℓ is the distance from the point 0 to the trunnion, point T, β is the fixed obtuse angle made with ground and the trunnion sides, α is the angle of elevation, ϕ_1 is the angular motion of the supporting structure and ϕ_2 is the angular motion of the tipping parts with respect to the supporting structure. The velocities, $\dot{x}_r$ and $\dot{y}_r$, and the accelerations, $\ddot{x}_r$ and $\ddot{y}_r$, are found by differentiation to be

$$\dot{x}_r = -\ell\dot{\phi}_1 \sin(\beta + \phi_1) + \dot{u} \cos(\alpha + \phi_1 + \phi_2) - u(\dot{\phi}_1 + \dot{\phi}_2) \sin(\alpha + \phi_1 + \phi_2)$$

$$\dot{y}_r = \ell\dot{\phi}_1 \cos(\beta + \phi_1) + \dot{u} \sin(\alpha + \phi_1 + \phi_2) + u(\dot{\phi}_1 + \dot{\phi}_2) \cos(\alpha + \phi_1 + \phi_2) \qquad \text{C-2}$$

and

$$\ddot{x}_r = -\ell\ddot{\phi}_1 \sin(\beta + \phi_1) - \ell\dot{\phi}_1^2 \cos(\beta + \phi_1) + \ddot{u} \cos(\alpha + \phi_1 + \phi_2) - \dot{u}(\dot{\phi}_1 + \dot{\phi}_2) \sin(\alpha + \phi_1 + \phi_2) - u(\ddot{\phi}_1 + \ddot{\phi}_2) \sin(\alpha + \phi_1 + \phi_2) - \dot{u}(\dot{\phi}_1 + \dot{\phi}_2) \sin(\alpha + \phi_1 + \phi_2) - u(\dot{\phi}_1 + \dot{\phi}_2)^2 \cos(\alpha + \phi_1 + \phi_2) \qquad \text{C-3}$$

$$\ddot{y}_r = \ell\ddot{\phi}_1 \cos(\beta+\phi_1) - \ell\dot{\phi}_1^2 \sin(\beta+\phi_1) + \ddot{u} \sin (\alpha+\phi_1+\phi_2) + \dot{u}(\dot{\phi}_1+\dot{\phi}_2) \cos(\alpha+\phi_1+\phi_2) + u(\ddot{\phi}_1+\ddot{\phi}_2) \cos(\alpha+\phi_1+\phi_2) + \dot{u}(\dot{\phi}_1+\dot{\phi}_2) \cos(\alpha+\phi_1+\phi_2) - u(\dot{\phi}_1+\dot{\phi}_2)^2 \sin(\alpha+\phi_1+\phi_2) \qquad \text{C-4}$$

The vector sum of the component $\ddot{x}_r$ and $\ddot{y}_r$ may be resolved into components in the u- and v- directions. These components are denoted as η and ξ, respectively. From Fig. C-3, these are:

$$\ddot{\eta} = \ddot{x}_r \cos \omega_1 + \ddot{y}_r \sin \omega_1 \qquad \text{C-5}$$

$$\ddot{\xi} = \ddot{y}_r \cos \omega_1 - \ddot{x}_r \sin \omega_1 , \qquad \text{C-6}$$

where

$$\omega_1 = \alpha + \phi_1 + \phi_2 . \qquad \text{C-7}$$

Substituting Eq. C-3 and 4 into Eq. C-5 and 6 gives the following expression,

$$\ddot{\eta} = -\ell\ddot{\phi}_1 \sin \omega_2 - \ell\dot{\phi}_1^2 \cos \omega_2 + \ddot{u} - u(\dot{\phi}_1+\dot{\phi}_2)^2 \qquad \text{C-8}$$

$$\ddot{\xi} = \ell\ddot{\phi}_1 \cos \omega_2 - \ell\dot{\phi}_1^2 \sin \omega_2 + 2\dot{u}(\dot{\phi}_1+\dot{\phi}_2) + u(\ddot{\phi}_1+\ddot{\phi}_2) . \qquad \text{C-9}$$

where

$$\omega_2 = \beta - \alpha - \phi_2 . \qquad \text{C-10}$$

B. Equations of Motion

Equations C-8 and C-9 are the components of the absolute acceleration of the recoiling mass. The free body diagram of the recoiling mass is shown in Fig. C-4. Summing forces acting through the mass center, we obtain

$$m_r \ddot{\eta} = -F(t) + \Phi(t) + e\mu |N| - m_r g \sin \omega_1 . \qquad \text{C-11}$$

$$m_r \ddot{\xi} = N - m_r g \cos \omega_1 . \qquad \text{C-12}$$

In these equations the following nomenclature is used:

F (t) applied force

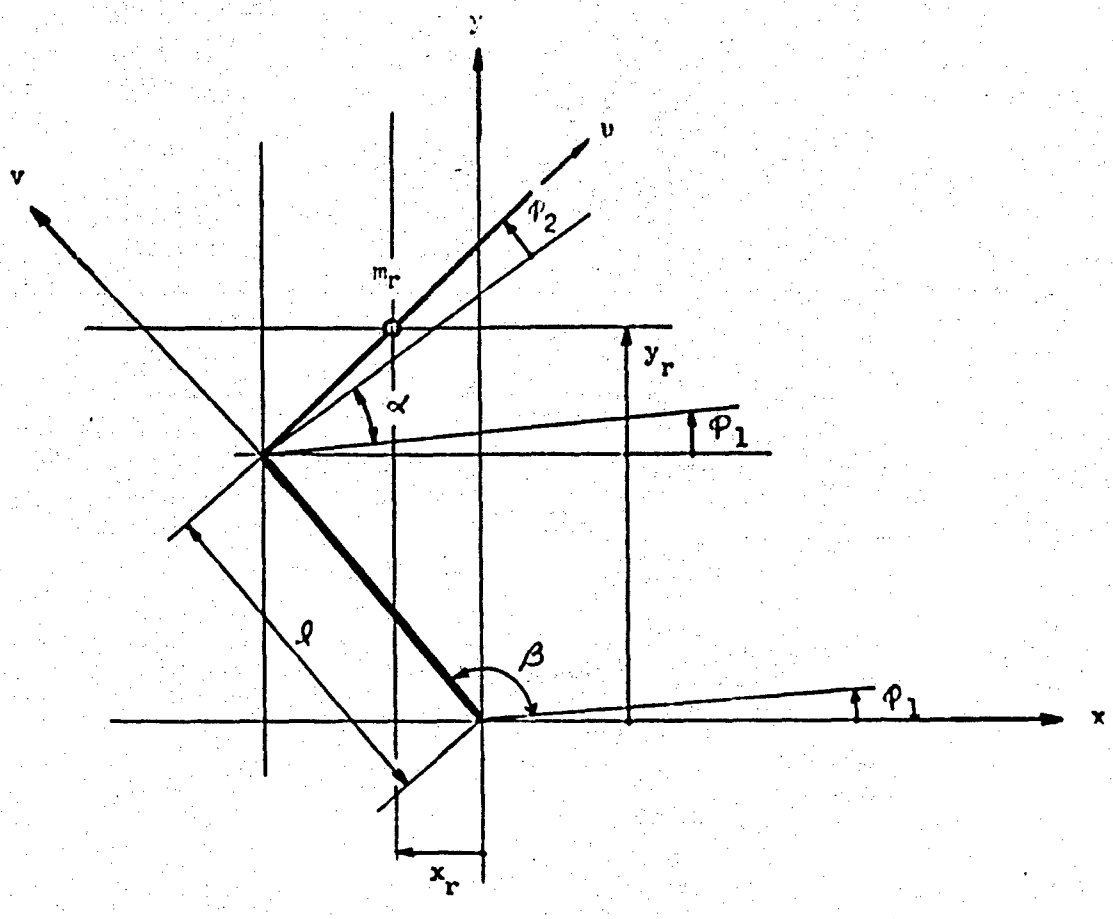

Fig. C-2 GEOMETRIC REPRESENTATION OF AN XM70-TYPE LAUNCHER

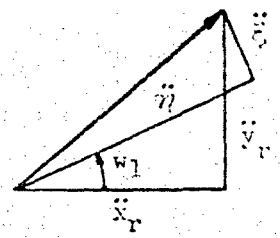

Fig. C-3 VECTOR COMPONENT TRANSFORMATION

$T'(t)$	applied moment (powder couple equal to $\epsilon F(t)$ where ϵ is the moment arm from the bore center to the recoiling mass cg.
$\Phi(t)$	reactions of the recoil system and cam
N	normal reaction force between the cradle and recoiling mass
T	moment reaction between the cradle and recoiling mass
μ	coefficient of Coulomb friction between the cradle and recoiling mass
e	$e = 1,\ \dot{u}<0;\ e = -1,\ \dot{u}>0;\ e = 0,\ \dot{u} = 0$

The XM70 launchers have very low friction ball bearings between the cradle and recoiling parts; the force $\mu|N|$ is therefore negligible compared to the seal friction. Because the absolute value sign, the term becomes unwieldy in later expressions and is neglected at this point.

If I_r is the moment of inertia of the recoiling mass about an axis through the mass center, we may write

$$I_r(\ddot{\phi}_1 + \ddot{\phi}_2) = T + T' \qquad \text{C-13}$$

In order to evaluate the retarding force, $\Phi(t)$, we must know what type of resistance is furnished by the recoil system. The system used in the XM70 launchers contains a preloaded recuperator or air spring to hold the mass in battery position at angles of elevation. Sufficient accuracy will be obtained if a linear spring rate is used to represent the recuperator. The recoil force is furnished by forcing oil through a variable-area orifice. The total retarding force is then made up of the following terms:*

$$K,\ k(u_o - u),\ R(\dot{u}^2, u),\ H_1,\ H_3(\dot{u}^2, u) \quad . \qquad \text{C-14}$$

The nomenclature used is

K	recuperator preload
k	recuperator spring rate
R	hydraulic resistance
H_1	constant friction force
H_3	hydraulic system seal frictional force
u_o	in-battery position of the recoiling mass

* For a more complete description of the recoil system, see Bimonthly Report No. 7 of this Project (8130)

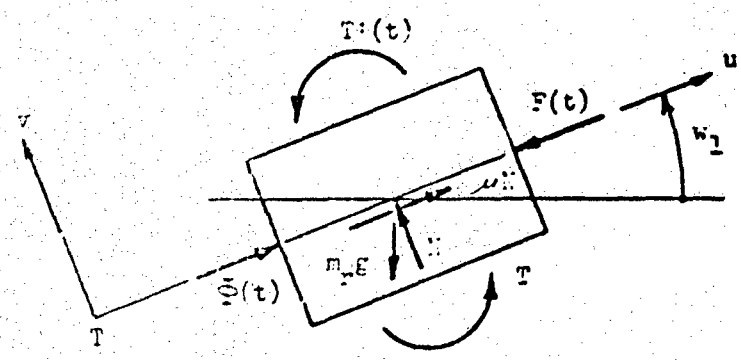

Fig. C-4 FREE BODY DIAGRAM OF THE RECOILING MASS

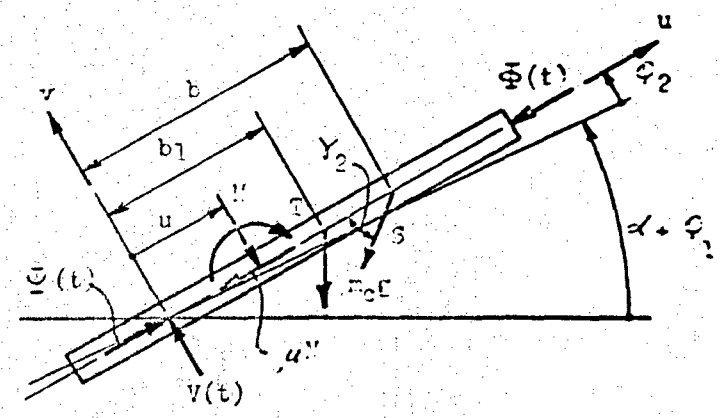

Fig. C-5 FREE BODY DIAGRAM OF THE CRADLE

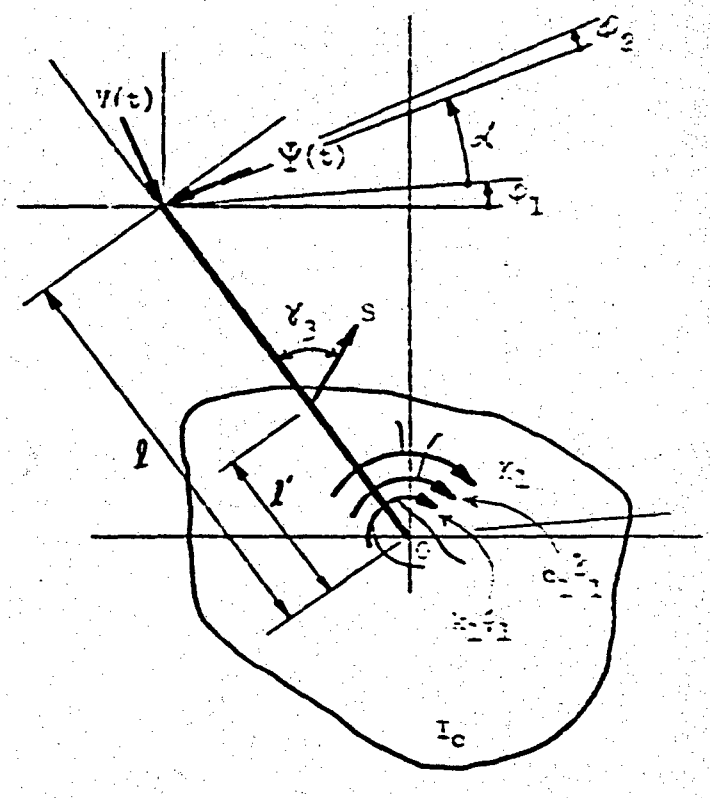

Fig. C-6 FREE BODY DIAGRAM OF THE EQUIVALENT FIRING SUPPORT

The cam reaction force in the direction of recoil may be represented by $C(\ddot{u}, \dot{u}, u)$; the actual functions will be introduced later, in order to keep the lengths of the expressions to a minimum. The total retarding force is, then,

$$\Phi(t) = K + k(u_o - u) + eR(\dot{u}^2, u) + eH_1 + eH_3(\dot{u}^2, u) + efC(\ddot{u}, \dot{u}, u). \qquad \text{C-15}$$

In this expression, $f = 0$, except when $u_1 < u < u_2$ and $u < 0$, that is when the recoiling mass is counterrecoiling through the cam, beginning at u_1 and ending at u_2, otherwise $f = +1$.

We will now consider a rigid cradle with a free body diagram as shown in Fig. C-5. It is assumed that there is no relative angular motion between the cradle and recoiling mass; because of this, the coordinates of the mass center of the cradle may be immediately written from Eq. C-1. This is done by substituting the constant length b_1 for u. These equations are

$$x_c = \ell \cos(\beta + \phi_1) + b_1 \cos \omega_1$$

and

$$y_c = \ell \sin(\beta + \phi_1) + b_1 \sin \omega_1 \qquad \text{C-16}$$

The length b_1 is the distance along the u-axis from the trunnion to the cradle mass center, and x_c and y_c are the absolute coordinates of the mass center of the cradle. The corresponding velocity and acceleration components may be found by differentiation of Eq. C-16 or by similar substitution of b_1 for u in Eq. C-2, 3, and 4. The components of acceleration of the cradle mass center are:

$$\ddot{x}_c = -\ell\ddot{\phi}_1 \sin(\beta + \phi_1) - \ell\dot{\phi}_1^2 \cos(\beta + \phi_1) - b_1(\ddot{\phi}_1 + \ddot{\phi}_2)\sin\omega_1 - b_1(\dot{\phi}_1 + \dot{\phi}_2)^2 \cos\omega_1 \qquad \text{C-17}$$

$$\ddot{y}_c = \ell\ddot{\phi}_1 \cos(\beta + \phi_1) - \ell\dot{\phi}_1^2 \sin(\beta + \phi_1) + b_1(\ddot{\phi}_1 + \ddot{\phi}_2)\cos\omega_1 - b_1(\dot{\phi}_1 + \dot{\phi}_2)^2 \sin\omega_1 \qquad \text{C-18}$$

If we let the vector sum of the components of x_c and y_c be resolved into components ζ and λ, respectively, in the u-, v-coordinate system using Fig. C-3, we have

$$\ddot{\zeta} = -\ell\ddot{\phi}_1 \sin\omega_2 - \ell\dot{\phi}_1^2 \cos\omega_2 - b_1(\dot{\phi}_1 + \dot{\phi}_2) \qquad \text{C-19}$$

and

$$\ddot{\lambda} = \ell \ddot{\phi}_1 \cos \omega_2 - \ell \dot{\phi}_1^2 \sin \omega_2 - b_1 (\ddot{\phi}_1 + \ddot{\phi}_2) \qquad \text{C-20}$$

The equations of motion of the cradle mass center may now be found by summing forces in the u- and v-directions. These are:

$$m_c \ddot{\zeta} = \Psi(t) - \Phi(t) - S \cos \gamma_2 - m_c g \sin \omega_1 \qquad \text{C-21}$$

$$m_c \ddot{\lambda} = V(t) - N - m_c g \cos \omega_1 - S \sin \gamma_2 \ , \qquad \text{C-22}$$

where the following nomenclature is used:

$\Psi(t)$	trunnion reaction in the u-direction
$V(t)$	trunnion reaction in the v-direction
S	force in the elevating system.

The displacement of one end of the elevating system relative to the other is given by $b\phi_2 \sin \gamma_2$. The force developed, assuming a linear spring and damping proportional to the first derivative of the displacement, is

$$S = K_2 + k_2 b(\sin \gamma_2)\phi_2 + c_2 b(\sin \gamma_2)\dot{\phi}_2 \qquad \text{C-23}$$

The preload is given by K_2, the rate by k, and the damping coefficient by c_2. In this expression, the angle γ_2 is assumed constant. The angular equation of motion of the cradle is found by summing moments about the mass center. From this we get

$$I_c (\ddot{\phi}_1 + \ddot{\phi}_2) = - b_1 V(t) - T + N(b_1 - u) - S(b - b_1) \sin \gamma_2 \qquad \text{C-24}$$

In Eq. C-24, I_c is the moment of inertia of the cradle about the mass center. The preload K_2 is the preload necessary to balance the component of force due to the weight of the recoiling mass and the cradle itself.

The final equation of motion may now be found by summing moments on the firing support about the fixed point 0 (see Fig. C-6):

$$I_o \ddot{\phi}_1 = \Psi(t)\, \ell \sin \omega_2 - V(t)\, \ell \cos \omega_2 - S \ell' \sin \gamma_3 - K_1 - k_1 \phi_1 - c_1 \dot{\phi}_1 \qquad \text{C-25}$$

For any angle of elevation, it will be assumed that γ_3 is a constant; also the following relationship will be used:

$$\gamma_3 \approx \gamma_3 \Big|_{\alpha = 0} - \alpha \equiv \gamma_o - \alpha \qquad \text{C-26}$$

We must now express the recoil and cam forces in terms of the variables of this analysis. The recoil force is given as

$$eR(\dot{u}^2, u) = \frac{e\,\gamma A_p^{\,3}}{2\,g\,C_o^{\,2}\alpha_o^{\,2}}\,\dot{u}^2 , \qquad \text{C-27}$$

where the following nomenclature is used:

γ	density of the oil
A_p	piston area
C_o	orifice coefficient
α_o	orifice area (function of u)

For this analysis, it is assumed that the seal friction is directly proportional to the recoil pressure (or force) and may be expressed as

$$H_3 = \delta R , \qquad \text{C-28}$$

where δ is a constant.

A cycloidal indexing cam shape is used in this analysis (as on the XM70 launcher). The axial component of force is

$$C = \frac{I_B}{R_1^2}\left[\frac{h^2}{(u_2 - u_1)^2}\right]\left[\frac{2\pi}{u_2 - u_1}\sin 2\pi\frac{u - u_1}{u_2 - u_1}\left(1 - \cos 2\pi\frac{u - u_1}{u_2 - u_1}\right)\dot{u}^2 + \left(1 - \cos 2\pi\frac{u - u_1}{u_2 - u_1}\right)^2 \ddot{u}\right] \qquad \text{C-29}$$

The launcher has two breech clusters containing three rounds each. For this analysis, it is assumed that only one cluster exists containing six rounds; however, the proper moment of inertia, I_B, corresponding to the combined, double cluster will be used. In Eq. C-29, h is the height of the cam path development and R_1 is the pitch radius.

Substituting the last three relationships into Eq. C-11, 12, 13, 21, 22, 24, and 25, and eliminating the four unknown reactions, T, V, N, and Ψ, leaves three equations. These three equations are second order, non-linear, differential equations, with the variables ϕ_1, ϕ_2, and u.

They are:

$$m_r\,(\ell \sin \omega_2 + u)\,\ddot{\phi}_1 + \left[ef\,\frac{I_B}{R_1^2}\,\frac{h^2}{(u_2 - u_1)^2}\,\left(1 - \cos 2\pi \frac{u - u_1}{u_2 - u_1}\right)^2 - m_r\right]\ddot{u}$$

$$= -m_r u\,(\dot{\phi}_1 + \dot{\phi}_2)^2 + F(t) - K - k\,(u_o - u) + m_r \ell \cos \omega_2\,\dot{\phi}_1^2$$

$$- e\left[(1+\delta)\left(\frac{\gamma A_p^3}{2g\,C_o^2 \alpha_o^2}\right) + f\,\frac{I_B}{R_1^2}\left(\frac{2\pi h^2}{(u_2 - u_1)^3}\,\sin 2\pi \frac{u - u_1}{u_2 - u_1}\right)\cdot\right.$$

$$\left.\cdot\left(1 - \cos 2\pi\,\frac{u - u_1}{u_2 - u_1}\right)\right]\dot{u}^2 \quad - eH_1 + m_r g \sin \omega_1 \qquad \text{C-30}$$

and

$$\ddot{\phi}_1\left[I_o + m_c \ell^2 + (\ell \cos \omega_2 + u)\,m_r \ell \cos \omega_2 + m_c\,b_1 \ell \cos \omega_2\right] +$$

$$+ \ddot{\phi}_2\left[m_r\,u \ell \cos \omega_2 + m_c\,b_1 \ell \cos \omega_2\right] + \ddot{u}\left[-ef\ell \sin \omega_2 \cdot\right.$$

$$\left.\cdot\,\frac{I_B\,h^2}{R_1^2\,(u_2 - u_1)^2}\left(1 - \cos 2\pi\,\frac{u - u_1}{u_2 - u_1}\right)^2\right] = \ell \sin \omega_2\left[-\,b_1\,m_c\cdot\right.$$

$$\left.\cdot\,(\dot{\phi}_1 + \dot{\phi}_2)^2 + m_r \ell \cos \omega_2 + K + k\,(u_o - u) + m_c g \sin \omega_1\right] +$$

$$\ell \cos \omega_2\left[-2\,m_r \dot{u}\,(\dot{\phi}_1 + \dot{\phi}_2) - g \cos \omega_1\,(m_r + m_c)\right] +$$

$$+ e\,\ell \sin \omega_2\left[(1+\delta)\,\frac{A_p^2}{2g\,C_o^2 \alpha_o^2}\,\dot{u}^2 + H_1 + f\,\frac{I_B\,2\pi h^2}{R_1^2\,(u_2 - u_1)^3}\right.$$

$$\left.\sin 2\pi\,\frac{u - u_1}{u_2 - u_1}\left(1 - \cos 2\pi\,\frac{u - u_1}{u_2 - u_1}\right)\dot{u}^2\right] \quad - C_1\,\dot{\phi}_1 +$$

$$- k_1\,\phi_1 - K_1 + \left[K_2 + k_2 b(\sin \gamma_2)\,\phi_2 + C_2\,b(\sin \gamma_2)\,\dot{\phi}_2\right]\cdot$$

$$\cdot\left[\ell \sin(\omega_2 - \gamma_2) - \ell' \sin(\gamma_o - \alpha)\right] \qquad \text{C-31}$$

and

$$\ddot{\phi}_1\left[I_c + I_r + m_r\,u\,(\ell \cos \omega_2 + u) + b_1\,m_c\,(\ell \cos \omega_2 + b_1)\right]$$

$$+ \ddot{\phi}_2\left[I_c + I_r + m_r\,u^2 + m_c\,b_1^2\right] = \dot{\phi}_1^2\,\ell \sin \omega_2\,(m_r\,u + m_c\,b_1) +$$

$$- 2 m_r u \dot{u} (\dot{\phi}_1 + \dot{\phi}_2) - g \cos \omega_1 (m_r u + m_c b_1) + \epsilon F(t)$$

$$- b \sin \gamma_2 \left[K_2 + b \sin \gamma_2 \; (k_2 \phi_2 + c_2 \dot{\phi}_2) \right] . \qquad \text{C-32}$$

III. DISCUSSION

Based upon the assumption made, the solution to the three differential equations of motion just derived will furnish the first mode response of the launcher in the vertical plane. The reaction forces and moments may also be found when the equations of motion are solved. Because of the complexity of these expressions, their solution is obtained on the Technology Center Univac 1105 digital computer. The programming of these equations and the results obtained is presented in other appendices.

APPENDIX D

DIGITAL COMPUTER PROGRAM, THREE-DEGREE-OF-FREEDOM MATHEMATICAL MODEL

R. M. Brach

I. INTRODUCTION

The equations of motion of a three-degree-of-freedom system representing an XM70-type launcher are presented in Appendix C. Because of the complexity of these equations, they are being solved numerically on Armour Research Foundation's Univac 1105 digital computer. In this appendix, the computer program is described and some results are compared with previous work.

II. COMPUTER PROGRAM

Basically, the computer program constitutes the numerical solution of a set of three, second-order, non-linear differential equations. The solution was programmed in a non-algebraic, symbolic language called USE (Univac Scientific Exchange). A side-by-side listing of the program, as written, and its octal representation are shown in Fig. D-3. Program output format is illustrated in Fig. D-4, which is the first page of output of a typical run.

A subroutine was written for general use by Robert Floyd of Armour Research Foundation based on the numerical technique of Runge and Kutta for the solution of up to 50, first-order, simultaneous differential equations. It is applied here to solve the three, second-order equations after a reduction of their order by three trivial substitutions, such as $\dot{u} = s$. The subroutine is shown listed after the main program with the call address, RWF999. One other special subroutine was written, RWF998, to allow the use of two tabular functions: in this case, an experimental powder-gas forcing function and a table of recoil-system orifice areas. This subroutine employs linear interpolation between points. It is also listed after the main program. All other subroutines used are from the standard ARF library.

Fig. D-1 shows a general program flow diagram. A detailed flow diagram showing how the time of application of the powder gas force is derived from the position and velocity of the recoiling parts is shown in Fig. D-2.

III. RESULTS

Two comparisons of the output of this program will be made in this appendix: (1) a comparison with a previous computer program of the parent project and (2) a comparison with experimental curves obtained from firings of the Prototype No. 1 launcher.

The physical launcher parameters used for the first comparison are taken from Prototype No. 1. The response curve from an early computer program is shown in Fig. D-5; the corresponding response curve from the present computer program is shown in Fig. D-6. Table D-1 points out the significant similarities of and differences between the two sets of equations of motion and launcher parameters.

The two curves are seen to differ slightly in amplitude and frequency. The amplitude differences may be accounted for by the difference in recoil forces between the two: the recoil force in the current program peaks significantly near the end of recoil as does the recoil force of the actual launcher, whereas in the early program, the recoil force remains nearly constant. The frequency differences probably are due to the inclusion of the elevating system flexibility in the current program, even though that system is very stiff.

The second comparison utilizes the experimental record of the first shot of Burst No. L68-L73, which was fired at Redstone Arsenal on February 22, 1959 (presented in Appendix II-A of Report No. 11 of the parent project). Figure D-7 shows the trail strain, cradle motion, and recoil force measured during that burst. The response as given by the current computer program is shown in Fig. D-8. The input data to the computer program to be compared are shown in Table D-2. The chosen elevating system stiffness value is seen to be relatively low; it may be recalled that the elevating screw brackets on the Prototype No. 1 were found to be relatively flexible.

Table D-1

COMPARISON OF MODELS AND LAUNCHER PARAMETERS

Item	Old Program	New Program
Degrees of freedom	Recoil motion, carraige rotation, hop of firing base	Recoil motion, carraige rotation, cradle rotation relative to the carriage
Launcher Geometry	Pilot No. 1 at 15° elevation	Pilot No. 1 at 15° elevation
Values of Mass	Pilot No. 1	Pilot No. 1
Elevating System Stiffness	Rigid	1×10^{6} lb/in.
Equivalent Carriage Stiffness	100×10^{6} in.-lb/radian	100×10^{6} in.-lb/radian
Recoil System	Computed from equations of a theoretical recoil system	Computed from equations of a theoretical recoil system using actual orifice areas from Pilot No. 3 rods.
Auxiliary damping	None	None

Table D-2

INPUT DATA TO COMPUTER PROGRAM

Item	Value in Program
Launcher Geometry	Pilot No. 3 at 45° elevation
Values of Mass	Pilot No. 3 (See parameter list in Program, Fig. D-3)
Elevating System Stiffness	1.405×10^{4} lb/in.
Elevating System Damping Coefficient	90 lb-sec/in.
Equivalent Carriage Stiffness	45×10^{6} in.-lb/radian

The similarity between the experimental and computed curves is striking, even down to details such as the influence of indexing forces between times 0.26 and 0.4. Especially important is the reproduction of the computed curve of cradle motion in the experimental curve just prior to the time of firing of the second round. This cradle motion, the most undesirable part of the gross response of the Prototype No. 1 launcher, was subsequently reduced by designing a stiffer elevating system. By means of an accurate computer program, however, the optimum combination of parameters can easily be found for a desired response.

IV. CONCLUSIONS

The examples presented in this appendix indicate: (1) that the current computer program corresponds closely to previous theoretical work, which means that errors do not exist either in the equations that were programmed or in the program itself; and (2) that the data derived from the current computer program represent gross experimental launcher response very accurately, which means that the program may be used to improve that response.

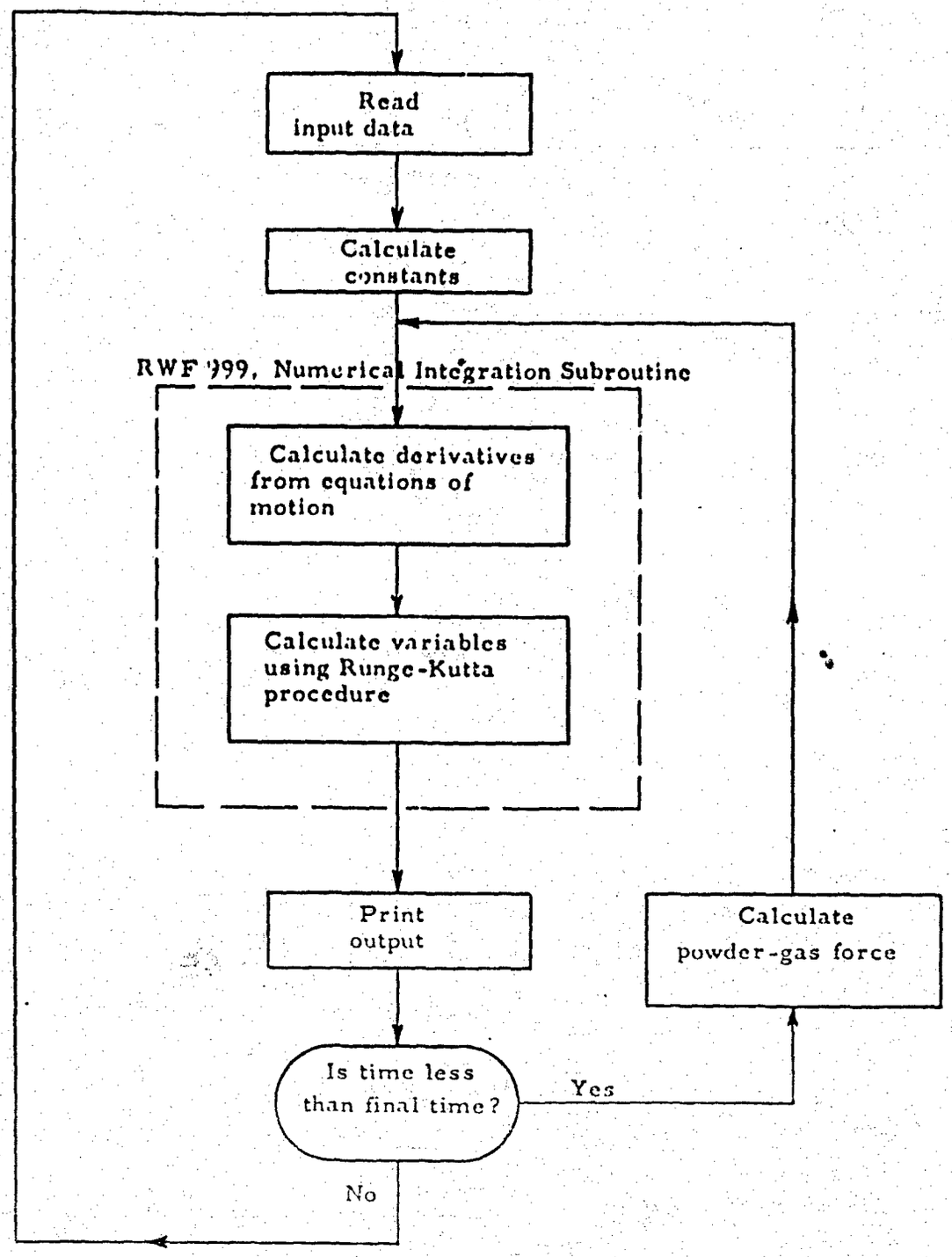

Fig. D-1 COMPUTER PROGRAM FLOW CHART

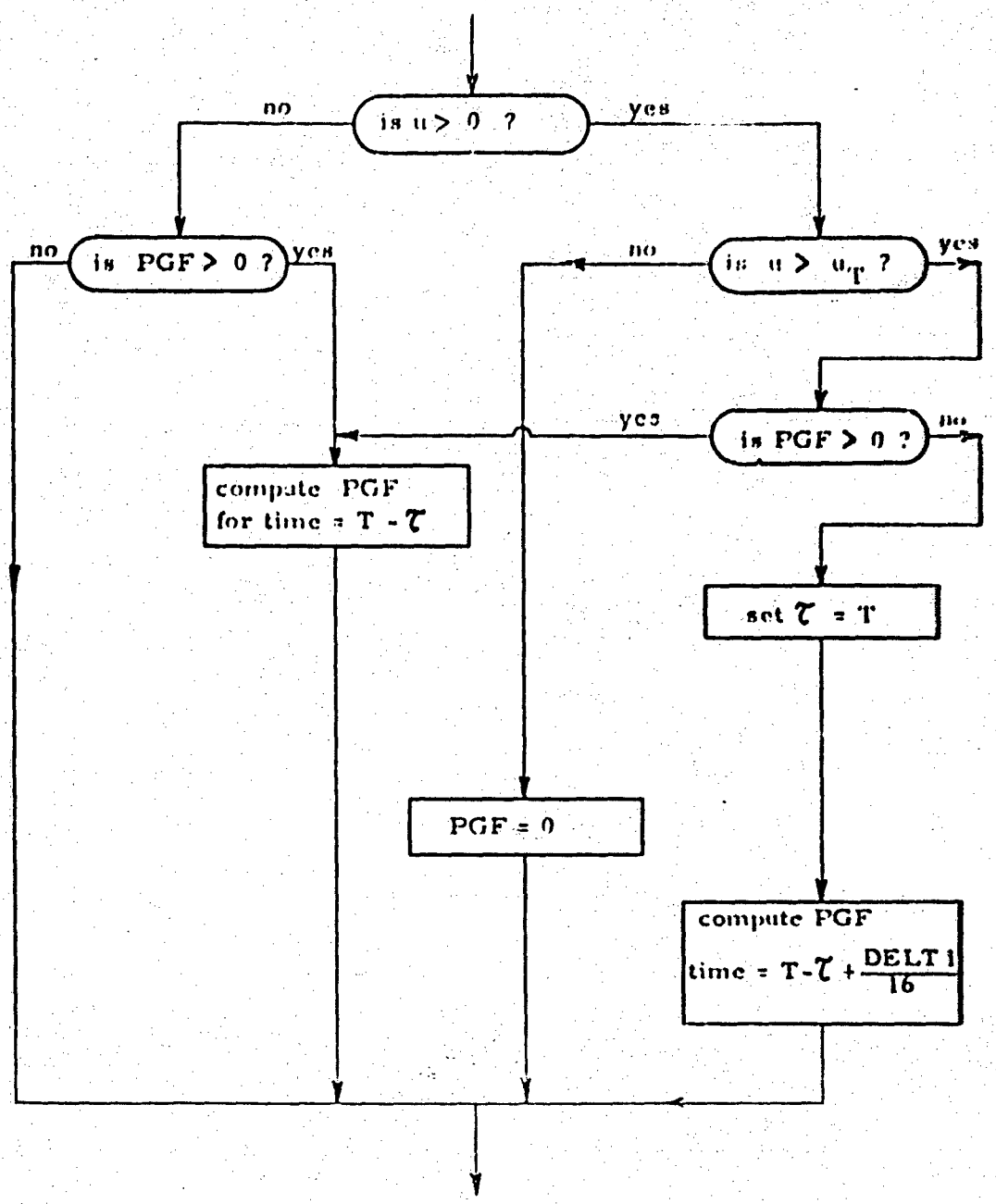

PGF . . . . . Powder-gas force

T . . . . . Time

UT . . . . . Trigger Position

τ . . . . . Time between shots of a burst

DELT 1 . . . . . Increment of tabular powder-gas force function

Fig. D-2 POWDER-GAS FORCE SELECTION FLOW DIAGRAM

```
                                    1100.   .DELT   . EQUAL* .300     .300     .TABLEN TIME INTERVAL LOCATIONS
                                    1110.   .       . EQUAL* .4      .4       .S
                                    1120.   .M      . EQUAL* .5      .5       .S
                                    1130.   .I      . EQUAL* .6      .6       .S
                                    1140.   .PT41   . EQUAL* .9      .9       .S

                                    1150.   .PT42   . EQUAL* .10     .10      .S
                                    1160.   .       . EQUAL* .11     .11      .S
                                    1170.   .M11    . EQUAL* .12     .12      .S
                                    1180.   .M12    . EQUAL* .13     .13      .S
                                    1190.   .       . EQUAL* .18     .18      .S
                                    1200.   .JPT41  . EQUAL* .59     .59      .S
                                    1210.   .JPT42  . EQUAL* .60     .60      .S
                                    1220.   .J      . EQUAL* .61     .61      .S
                                    1230.   .JM11   . EQUAL* .62     .62      .S
                                    1240.   .JM12   . EQUAL* .63     .63      .S
                                    1250.   .       . EQUAL* .64     .64      .S
                                    1260.   .       . SETLOC .310    .310     .S

00485   00486   30 00030 00030     1270.   .TBL1    . F      .0      .        .TABLE OF REPCF.PGES
                                    1280.   .       . SETLOC .310    .310     .S
00632   00632   30 00030 00030     1290.   .TBL2    . F      .0      .        .TABLE OF 1 REP.CYL. OVFICF AREAS
                                    1300.   .       . SETLOC .510    .510     .S
                                    1310.   .RS1    . RESERV .2      .2       .S
                                    1320.   .RS2    . RESERV .2      .2       .S
                                    1330.   .RS3    . RESERV .2      .2       .S
01004   01004   30 15435 37310     1340.   .VC      . F      .1.3664  .        .VESS.CHAIRES
01005   01005   30 24431 37441     1350.   .VM      . F      .3.2749  .        .VESS.MECHALIKS ASSEMBLYS
01006   01006   30 54441 36132     1360.   .IM      . F      .51.429  .        .VVV.OF INFR..REFECM CLUSTERSS
01007   01007   31 54455 14432     1370.   .IC      . F      .117.4   .        .VVV.OF INFR..CRACKES
01010   01010   31 04770 00030     1380.   .IM      . F      .2552.0  .        .VVV.OF INFR..REC.ASSEMBLYS
```

FIG. D-3 COMPUTER PROGRAM

FIG. D-3 COMPUTER PROGRAM (Continued)

```
01011  01011  31 35275 00000   139.   * AK     * F   *1975.0    *   *PRELOAD.RECIPROCATORS
01012  01012  30 75540 00000   140.   * A      * F   *91.0      *   *GATE.RECIPROCATORS
01013  01013  30 00000 00000   141.   * KK1    * F   *0         *   *PRELOAD.COMPLIANCE FLEXIBILITYS
01014  01014  30 00000 00000   142.   * KK2    * F   *0         *   *PRELOAD.ELEVATING SYSTEMS
01015  01015  30 44530 00000   143.   * L      * F   *30.       *   *LENGTH.TRUNNION TO ELEVATING SYS.S
01016  01016  30 56514 65144   144.   * L1     * F   *24.6      *   *LENGTH. TRUNNION TO CRADLE C. OEM.S
01017  01017  30 44130 00000   146.   * LT     * F   *36.       *   *LENGTH.BALL JOINT TO TRUNNIONS
01020  01020  30 17030 00000   147.   * M1     * F   *1.75      *   *CAMPAIN PITCH RADIUS$
01021  01021  30 17317 73717   148.   * M      * F   *1.832     *   *WEIGHT OF PROJECTILE CAN OFMEL.S
01022  01022  31 16723 00000   149.   * G      * F   *386.      *   *ACCELERATION OF GRAVITYS
01023  01023  17 94033 61755   150.   * GAMA   * F   *0.0313    *   *OIL DENSITYS
01024  01024  30 24554 57411   151.   * AP     * F   *2.35017   *   *AREA OF 1 REC.SYS.PISTONS

01025  01025  30 05115 34453   152.   * CD     * F   *0.65      *   *ORIFICE COEFFICIENTS
01026  01026  30 77530 00000   153.   * DELTA  * F   *173.5     *   *ANGLE OF TRUNNION SIDE PAT GRO.DEG.S
01027  01027  17 75775 34132   154.   * DELTA  * F   *0.31      *   *COEFFICIENT OF SEAL FRICTIONS
01030  01030  17 45775 34132   155.   * DD     * F   *0.08      *   *COEFFICIENT OF CRADLE BEA.FRICTIONS
01031  01031  30 05747 61115   156.   * DMS    * F   *0.533     *   *PRADZM CRADLE MOMENT ARMS
01032  01032  30 75237 16771   157.   *        * F   *0.694     *   *SAMES
01033  01033  17 77429 40203   158.   *        * F   *0.497     *   *SAMES
01034  01034  17 74441 62710   159.   *        * F   *0.321     *   *SAMES
01035  01035  17 75724 30741   160.   *        * F   *0.315     *   *SAMES
01036  01036  30 04151 30152   161.   *        * F   *0.557     *   *SAMES
01037  01037  16 76111 50457   162.   * DELT1  * F   *0.0215    *   *INTERVAL OF TMLIS
01040  01040  17 74030 00000   163.   * DELT2  * F   *0.25      *   *INTERVAL OF TMLZS

01041  01041  30 04030 00000   164.   * SINGA2 * F   *0.5       *   *SIN(GAMMA2).ELEVATING SYS.S
01042  01042  30 04733 17204   165.   * COSGA2 * F   *0.866025  *   *COS(GAMMA2).ELEVATING SYS.S
01043  01043  30 07431 00000   166.   * SINGA  * F   *0.4999999 *   *SIN(GAMMA)AT ALPHA EQUAL ZERO$
01044  01044  30 34534 41217   167.   * LT2    * F   *9.42      *   *LENGTH.BALL JOINT TO ELEVATING BRACKETS
01045  01045  30 00000 00000   168.   * I      * X   *0         *   *PRINTOUT CONSTANTS$
01046  01046  30 00000 00000   169.   * II     * X   *4         *   *NO. OF TIME INTERVALS BETW. PRINTOUTS$
01047  01047  30 26320 77325   170.   * PI     * F   *3.141592654 *   *$
01050  01050  30 00000 00000   171.   * ZERO   * F   *0         *   *$
01051  01051  30 14030 00000   172.   * ONE    * F   *1         *   *$
01052  01052  37 53777 77777   173.   * MONE   * F   *-1.0      *   *$
01053  01053  30 24030 00000   174.   * TWO    * F   *2.        *   *$
01054  01054  30 16735 17307   175.   * SQ3    * F   *1.732051  *   *$

01055  01055  30 14715 00213   176.   * IP     * F   *1.220     *   *NO. OF INTER..PROJECTILE IN ROLLS
01056  01056  17 54150 31156   177.   * MP     * F   *.13180    *   *MASS.PROJECTILES
01057  01057  30 15130 00000   178.   * KP     * F   *5.5       *   *CLUSTER RATIOS
01060  01060  30 57420 30447   179.   * IPP    * F   *7.532     *   *NO.OF INTER..PROJECTILE IN PITCHS
01061  01061  30 00000 00000   180.   * TAU    * F   *0         *   *FIRING INTERVAL(COMPUTED IN PROG.)$
01062  01062  30 00000 00000   181.   * NP     * I   *5         *   *NUMBER OF EQUATIONS$
01063  01063  16 74031 11555   182.   * DELTAT * F   *1.00-3    *   *TIME INTERVAL(INTEGRATION)$
01064  01064  30 00000 00000   183.   *        * F   *0         *   *ALWAYS ZERO$
01065  01065  30 00000 00000   184.   *        * F   *0         *   *ALWAYS ZERO$
01066  01066  30 00000 00000   185.   * TO     * F   *0         *   *INITIAL TIMES$
01067  01067  30 00000 00000   186.   * TETA10 * F   *0         *   *INITIAL CONDITIONS
01070  01070  30 00000 00000   187.   * TETA20 * F   *0         *   *$
```

```
01071  01071  30 00000 00000   183.   . 30    . F     .0      .       .SAMES
01072  01072  30 00000 00000   184.   . MI10  . F     .0      .       .SAMES
01073  01073  30 00000 00000   185.   . MI20  . F     .0      .       .SAMES
01074  01074  30 57359 14932   191.   . 30    . F     .29.9   .       .INITIAL POSITIONS
01075  01075  30 00000 00000   192.   . 1A    . 300   .00001  .00000  .TOTAL COUNTAYS
01075  01076  30 14000 00000   193.   . 1P    . F     .1.0    .       .NO. OF ROWING FINGS
01077  01077  30 77140 00000   194.   . 1C    . F     .115.   .       .NO.OF INFOTI.CARRIAGE EQUIVALENTS
01100  01100  30 00000 00000   195.   . 52    . F     .0      .       .RATE.ELEVATING SYS.S
01101  01101  30 00000 00000   196.   . 53    . F     .0      .       .DAMPING COEFF..ELEVATING SYS.S
01102  01102  30 00000 00000   197.   . 51    . F     .0      .       .RATE.CARRIAGE ELEVIBILITY
01103  01103  30 00000 00000   198.   . 61    . F     .0      .       .DAMPING COEFF..CARRIAGES
01104  01104  30 54759 14932   199.   . 62    . F     .19.9   .       .END OF CAMBERS

01105  01105  30 14745 31443   200.   . 61    . F     .9.9    .       .BEGINNING OF CAMBERS
01106  01106  30 76300 00000   201.   . 61    . F     .100.   .       .CONSTANT RECOIL FRICTION FORCES
01107  01107  30 55530 00000   202.   . ALPHA . F     .85.    .       .ANGLE OF ELEVATION..DEGREES
01110  01110  30 55353 14932   203.   . 6T    . F     .21.9   .       .TRIGGER POSITIONS
01111  01111  17 76519 03146   204.   . 1S    . F     .0.0    .       .PROGRAM STOP AT THIS TIME
01112  01112  11 01115 17700   205.   . START . TP    .PAR    .1770013 .$
01113  01113  37 17759 17753   206.   .       . RU    .1775519 .1775319 .$
01114  01114  45 00000 01115   207.   .       . RU    .       .L.2    .$
01115  01115  00 31000 00012   208.   . PAR   . 30    .0      .10     .$
01116  01116  11 01124 16000   209.   .       . ARF031 .21    .       .$
01117  01117  37 15777 15775
01120  01120  45 00000 01155   210.   .       . RU    .       .WEAT1  .$

01121  01121  75 30000 01123   211.   .       . ARF039 .      .AL     .$
01122  01122  11 00000 16510
01123  01123  37 16515 16513
01124  01124  00 01751 01125   212.   . 21    . 30    .1001   .L.1    .$
01125  01125  00 01131 27940   213.   .       . 30    .41     .12000  .$
01126  01126  00 00000 16513   214.   .       . 30    .       .AL     .$
01127  01127  00 00000 00000   215.   .       . 30    .       .       .$
01130  01130  00 00000 00000   216.   .       . 30    .       .       .$
01131  01131  54 30750 33446   217.   . 41    . X53-5 .NECOIL.MASS...CARRIAGE.INERTS
01132  01132  01 47315 56531
01133  01133  71 02010 24074
01134  01134  54 54342 43230

01135  01135  01 54533 05446
01136  01136  34 24310 15434   218.   .       . X53-5 .IARC.NATIRC.CAMPI.NG.COEFF.........
01137  01137  46 30210 12734
01140  01140  47 52315 03231
01141  01141  26 03533 13122
01142  01142  31 01010 16131
01143  01143  32 01023 04030   219.   .       . X53-5 .--.ELEVATING.SY.STEM.RELUACE.PS
01144  01144  70 24543 45032
01145  01145  31 55734 56030
01146  01146  47 01525 43046
01147  01147  03 24272 16154
01150  01150  34 46302 16127   220.   .       . X53-5 .ATE.C.MAMPING.CO.EFF.............
```

FIG D-3 COMPUTER PROGRAM (Continued)

```
01151  01151  34 47523 45032
01152  01152  31 26333 05131
01153  01153  33 01310 16131
01154  01154  31 01310 16131
01155  01155  11 01130 16070      221.   .  .XT1  . AMF031 .43      .        .$
01156  01156  37 15777 15775
01157  01157  45 00330 01211      222.   .       . 4W     .        .MEAT2   .$
01158  01158  30 01731 01151      223.   . 42    . 30     .1031    .L.1     .$
01159  01159  30 01155 27450      224.   .       . 30     .43      .13000   .$
01160  01160  30 00330 16913      225.   .       . 30     .        .$L      .$
01161  01161  30 00330 05070      226.   .       . 30     .        .        .$
01162  01162  30 00330 05070      227.   .       . 30     .        .        .$

01163  01163  35 24172 12530      228.   . 42    . X53-3  .C.MBCMEGINNINA.BC.CAMBC.E.MO--.CO\$
01164  01164  32 34535 05450
01165  01165  32 01312 02417
01166  01166  31 01330 02732
01167  01167  31 02330 35045
01168  01168  56 22013 45035      229.   .       . 453-3  .T.MEL3I_MFRICT.IMV--.ELEVATI^M$
01169  01169  35 34130 13154
01170  01170  34 26453 40353
01171  01171  32 01323 04453
01172  01172  30 24553 40353
01173  01173  32 01323 53024      230.   .       . 453-3  .--.SEAL_MFRICT.--.-.TMS..MFRICT.^C.$
01174  01174  45 01315 43435

01175  01175  56 22720 12425
01176  01176  34 32320 13154
01177  01177  34 26452 20134
01178  01178  03 30313 16272      231.   .       . 453-3  .OFEF.--.IEC.MMR.EL3A3--.T^16^9.$
01179  01179  31 02543 02432
01180  01180  31 02543 04433
01181  01181  34 27720 12445
01182  01182  34 34123 23054
01183  01183  11 01217 16070      232.   . .XT2  . AMF031 .43      .        .$
01184  01184  37 16777 15775
01185  01185  45 00330 01210      233.   .       . 4W     .        .MEAT3   .$
01186  01186  75 30032 01215      234.   .       . AMF038 .        .$L      .$

01187  01187  11 00330 16918
01188  01188  37 16319 16913
01189  01189  30 01731 01270      235.   . 43    . 30     .1031    .L.1     .$
01190  01190  30 01330 02434      236.   .       . 30     .40      .1302    .$
01191  01191  30 00330 16943      237.   .       . 30     .        .$L      .$
01192  01192  30 01077 02435      238.   .       . 30     .10      .1302    .$
01193  01193  30 00330 16943      239.   .       . 30     .        .$L      .$
01194  01194  30 01132 02436      240.   .       . 30     .41      .1302    .$
01195  01195  30 00330 16943      241.   .       . 30     .        .$L      .$
01196  01196  30 01133 02435      242.   .       . 30     .C1      .1302    .$
01197  01197  30 00330 16913      243.   .       . 30     .        .$L      .$
01198  01198  30 01314 02435      244.   .       . 30     .4.2     .1302    .$
```

FIG. D-3 COMPUTER PROGRAM (Continued)

```
01231  01231  30 00030 16513     249.   .        . 30    .       .FL      .S
01232  01232  30 01130 02426     250.   .        . 30    .C2     .1302    .S
01233  01233  30 00030 16513     251.   .        . 30    .       .FL      .S
01234  01234  30 01131 02426     252.   .        . 30    .C2     .1302    .S
01235  01235  30 00030 16513     253.   .        . 30    .       .FL      .S
01236  01236  30 00030 00000     254.   .        . 30    .       .        .S
01237  01237  30 00030 00000     255.   .        . 30    .       .        .S
01238  01238  11 01245 16000     256.   . .EXT3  . .*FO31 .Z4     .        .S
01241  01241  37 15777 15775
01242  01242  45 00030 01246     257.   .        . 00    .       .*EXT4   .S
01243  01243  30 01731 01219     258.   . Z4     . 30    .1031   .L+1     .S
01244  01244  30 01130 02426     259.   .        . 30    .U1     .1302    .S

01245  01245  30 00030 16513     260.   .        . 30    .       .FL      .S
01246  01246  30 01134 02426     261.   .        . 30    .U2     .1302    .S
01247  01247  30 00030 16513     262.   .        . 30    .       .FL      .S
01250  01250  30 01135 02426     263.   .        . 30    .M1     .1302    .S
01251  01251  30 00030 16513     264.   .        . 30    .       .FL      .S
01252  01252  30 01137 02426     265.   .        . 30    .ALPHA  .1302    .S
01253  01253  30 00030 16513     266.   .        . 30    .       .FL      .S
01254  01254  30 01127 02426     267.   .        . 30    .DELTA  .1302    .S
01255  01255  30 00030 16513     268.   .        . 30    .       .FL      .S
01256  01256  30 01130 02426     269.   .        . 30    .M1     .1302    .S
01257  01257  30 00030 16513     270.   .        . 30    .       .FL      .S
01260  01260  30 01131 02426     271.   .        . 30    .A4     .1302    .S

01261  01261  30 00030 16513     272.   .        . 30    .       .FL      .S
01262  01262  30 01110 02426     273.   .        . 30    .UT     .1302    .S
01263  01263  30 00030 16513     274.   .        . 30    .       .FL      .S
01264  01264  30 00030 00000     275.   .        . 30    .       .        .S
01265  01265  31 00030 00000     276.   .        . 31    .       .        .S
01266  01266  11 01271 16000     277.   . .EXT4  . .*FO31 .Z4     .        .S
01267  01267  37 15777 15775
01270  01270  45 00030 01327     278.   .        . 00    .       .*EXT5   .S
01271  01271  30 01731 01272     279.   . Z5     . 30    .1031   .L+1     .S
01272  01272  30 01514 01141     280.   .        . 30    .A9     .6009    .S
01273  01273  30 00030 16513     281.   .        . 30    .       .AL      .S
01274  01274  30 01315 01141     282.   .        . 00    .A8     .6009    .S

01275  01275  30 00030 16513     283.   .        . 00    .       .AL      .S
01276  01276  30 01314 01141     284.   .        . 30    .A9     .6009    .S
01277  01277  30 00030 16513     285.   .        . 30    .       .AL      .S
01300  01300  30 01317 01141     286.   .        . 30    .A4     .6009    .S
01301  01301  30 00030 16513     287.   .        . 30    .       .AL      .S
01302  01302  30 01320 02263     288.   .        . 30    .A7     .1203    .S
01303  01303  30 00030 16513     289.   .        . 30    .       .AL      .S
01304  01304  30 01322 02263     290.   .        . 30    .A8     .1203    .S
01305  01305  30 00030 16513     291.   .        . 30    .       .AL      .S
01306  01306  30 01324 01141     292.   .        . 30    .A9     .6009    .S
01307  01307  30 00030 16513     293.   .        . 30    .       .AL      .S
01310  01310  30 01325 02263     294.   .        . 30    .A10    .1203    .S
```

FIG. D-3 COMPUTER PROGRAM (Continued)

```
01311  01311  30 00030 16713   291.   .      . 30    .        .AL      .$
01312  01312  30 00030 00000   292.   .      . 30    .        .        .$
01313  01313  30 00030 00000   293.   .      . 30    .        .        .$
01314  01314  55 94475 00131   294.   . .03   . X53   .TIME..  .        .$
01315  01315  32 33140 20931   295.   . .04   . X53   .PHI-1.  .        .$
01316  01316  32 33140 20931   296.   . .05   . X53   .PHI-2.  .        .$
01317  01317  57 01010 16131   297.   . .06   . X53   .U.....  .        .$
01320  01320  32 33140 20932   298.   . .07   . X53-4 .PHI-1-DOT....    .$
01321  01321  57 03550 16131
01322  01322  52 33140 20932   299.   . .08   . X53-2 .PHI-2-DOT....    .$
01323  01323  57 03550 16131
01324  01324  57 02270 20931   300.   . .09   . X53   .U-DOT.  .$

01325  01325  54 30250 33115   301.   . .10   . X53-4 .RECIL.FORCE.     .$
01326  01326  31 31735 42933
01327  01327  11 01332 16070   302.   . .EXTD . A9F731 .ZA      .        .$
01330  01330  37 15777 15775
01331  01331  45 00030 01375   303.   .      . 30    .        .VEX19   .$
01332  01332  30 01731 01333   304.   . .09   . 30    .1701    .L+1     .$
01333  01333  30 01335 02253   305.   .      . 30    .N11     .1703    .$
01334  01334  30 00030 16713   306.   .      . 30    .        .AL      .$
01335  01335  30 01337 02253   307.   .      . 30    .N12     .1703    .$
01336  01336  30 00030 16713   308.   .      . 30    .        .AL      .$
01337  01337  30 01351 02253   309.   .      . 30    .N13     .1703    .$
01340  01340  30 00030 16713   310.   .      . 30    .        .AL      .$

01341  01341  30 01353 02253   311.   .      . 30    .N14     .1703    .$
01342  01342  30 00030 16713   312.   .      . 30    .        .AL      .$
01343  01343  30 01355 02253   313.   .      . 30    .N15     .1703    .$
01344  01344  30 00030 16713   314.   .      . 30    .        .AL      .$
01345  01345  30 01357 02253   315.   .      . 30    .N16     .1703    .$
01346  01346  30 00030 16713   316.   .      . 30    .        .AL      .$
01347  01347  30 01371 02253   317.   .      . 30    .N17     .1703    .$
01350  01350  30 00030 16713   318.   .      . 30    .        .AL      .$
01351  01351  30 01373 02253   319.   .      . 30    .N18     .1703    .$
01352  01352  30 00030 16713   320.   .      . 30    .        .AL      .$
01353  01353  30 00030 00000   321.   .      . 30    .        .        .$
01354  01354  30 00030 00000   322.   .      . 30    .        .        .$

01355  01355  37 30365 02431   323.   . .11   . X53-4 .DELTA.T.....    .$
01356  01356  45 01010 16131
01357  01357  34 72417 44031   324.   . .12   . X53-2 .AXIAL.FA.....   .$
01360  01360  36 24470 16131
01361  01361  55 24533 23033   325.   . .13   . X53-2 .TANGENT..CAN.   .$
01362  01362  46 32717 02447
01363  01363  37 03173 00056   326.   . .14   . X53-2 .NORMAL.REACT.   .$
01364  01364  31 54332 42055
01365  01365  50 03544 72416   327.   . .15   . X53-2 .NORMAL.REACT.   .$
01366  01366  31 54332 42055
01367  01367  55 52343 40032   328.   . .16   . X53-2 .SPRING.FORCE.   .$
01370  01370  31 31735 42033
```

FIG. D-3 COMPUTER PROGRAM (Continued)

FIG. D-3 COMPUTER PROGRAM (Continued)

```
01371  01371  37 24475 46291   320.   .17   .553-2  .DAW.,.FDIFE..   .$
01372  01372  41 03562 03031
01373  01373  32 03712 73094   330.   .19   .553-2  .P0102V.F)102F.  .$
01374  01374  31 01035 46290
01375  01375  11 01120 10020   331.   .XXT9  .4HF031  .Z9      .      .$
01376  01376  37 15777 15775
01377  01377  15 00720 01432   332.         .U      .      .MEX15   .$
01400  01400  00 01731 02431   333.   .4V   .YS      .1031  .L01    .$
01401  01401  30 01417 02111   334.         .YS     .113   .5YS    .$
01402  01402  30 00720 10713   335.         .YS     .      .9L     .$
01403  01403  30 01120 02253   336.         .YS     .193   .1303   .$
01404  01404  30 00720 10713   337.         .YS     .      .4L     .$

01405  01405  30 01429 02253   338.         .YS     .191   .1303   .$
01406  01406  30 00720 10713   339.         .YS     .      .4L     .$
01407  01407  30 01429 02253   340.         .YS     .192   .1303   .$
01410  01410  30 00720 10713   341.         .YS     .      .4L     .$
01411  01411  30 01429 02253   342.         .YS     .193   .1303   .$
01412  01412  30 00720 10713   343.         .YS     .      .4L     .$
01413  01413  30 01430 02253   344.         .YS     .194   .1303   .$
01414  01414  30 00720 10713   345.         .YS     .      .4L     .$
01415  01415  30 00720 02020   346.         .YS     .      .       .$
01416  01416  31 00720 02020   347.         .01     .      .       .$
01417  01417  31 01312 10131   348.   .1V   .553   .******  .       .$
01420  01420  34 03675 02731   349.   .20   .553-2  .P0U )0U1459.   .$

01421  01421  30 47472 53054
01422  01422  34 00720 33445   350.   .21   .553-2  .P.COIL.DIST..   .$
01423  01423  31 27345 50722
01424  01424  36 54122 74930   351.   .22   .553-2  .C0IDL.R)T...   .$
01425  01425  31 50735 06031
01426  01426  34 00720 33415   352.   .23   .553-2  .P.COIL.F)IST.   .$
01427  01427  31 01543 46456
01430  01430  32 71375 40125   353.   .24   .553-2  .P0)0.C0L.4B4.   .$
01431  01431  32 46712 40417
01432  01432  75 40713 01434   354.   .XXT6  .4P9    .11    .L02    .$
01433  01433  11 01702 00034   355.         .T0     .YS    .4      .$
01434  01434  47 01747 10745   356.         .F0     .P1    .L(F190.) .$

01435  01435  11 01720 10540   357.         .T0     .3     .CONV   .$
01436  01436  66 01137 10540   358.         .F4     .ALPHA .CONV   .$
01437  01437  11 01720 01137   359.         .T0     .3     .ALPHA  .$
01440  01440  55 01724 10540   360.         .F4     .BETA  .CONV   .$
01441  01441  11 01720 02035   361.         .T0     .3     .BETA   .$
01442  01442  11 01137 00775   362.         .T0     .ALPHA .MEG1   .$
01443  01443  11 01731 00777   363.         .T0     .3E    .MEG1+1  .$
01444  01444  75 00707 04446   364.         .4F078  .MEG1  .LOC1   .$
01445  01445  11 00774 17057
01446  01446  37 17755 17053
01447  01447  11 17734 10541   365.         .T0     .LOC1+3 .CONSALF .CONSALF$
01450  01450  66 01174 02035   366.         .F4     .U0    .99     .$
```

```
01451  01451  32 01714 01034   367.   .        . FI     .31      .WC      .$
01452  01452  47 01030 01015   368.   .        . FD     .0       .$       .$
01453  01453  55 01030 15941   369.   .        . FM     .0       .COSALF  .$
01454  01454  55 01030 01032   370.   .        . FM     .0       .$       .$
01455  01455  55 01030 01053   371.   .        . FM     .0       .TTC     .$
01456  01456  15 01030 01014   372.   .        . TN     .0       .KK2     .<<2S
01457  01457  55 01324 01197   373.   .        . FS     .BETA    .ALPHA   .$
01460  01460  11 01030 15952   374.   .        . TP     .0       .SMA     .$
01461  01461  11 15552 00775   375.   .        . TP     .SMA     .WFG1    .$
01462  01462  11 01137 01037   376.   .        . TP     .ALPHA   .WFG2    .$
01463  01463  11 01030 00777   377.   .        . TP     .ZFG0    .WFG1+1  .$
01464  01464  11 01030 01031   378.   .        . TP     .ZFG0    .WFG2+1  .$

01465  01465  75 00032 01447   379.   .        . ARFOTA .WFG1    .LOC1    .$
01466  01466  11 00774 17057
01467  01467  37 17039 17053
01470  01470  11 17039 15943   380.   .        . TP     .LOC1+3  .SIAMMA  .SIAMMAS
01471  01471  75 00032 01473   381.   .        . ARFOTA .WFG2    .LOC1    .$
01472  01472  11 01030 17057
01473  01473  37 17039 17053
01474  01474  11 17039 15944   382.   .        . TP     .LOC1+3  .SIAALF  .SIAALFS
01475  01475  11 15552 00775   383.   .        . TP     .SMA     .WFG1    .$
01476  01476  11 01131 00777   384.   .        . TP     .DMS     .WFG1+1  .$
01477  01477  75 00032 01471   385.   .        . ARFOTA .WFG1    .LOC1    .$
01500  01500  11 00774 17057

01501  01501  37 17039 17053
01502  01502  11 17039 15945   386.   .        . TP     .LOC1+3  .COSGMA  .COSGMAS
01503  01503  46 01322 15948   387.   .        . FM     .0       .SIAALF  .$
01504  01504  46 01030 01034   388.   .        . FM     .0       .WC      .$
01505  01505  32 01714 01032   389.   .        . FI     .K*2     .COSG2   .$
01506  01506  46 01030 15943   390.   .        . FM     .0       .SIAMMA  .$
01507  01507  46 01030 01017   391.   .        . FM     .0       .LT      .$
01510  01510  11 01030 15955   392.   .        . TP     .0       .S1      .S1S
01511  01511  44 01034 01035   393.   .        . FA     .WC      .WP      .$
01512  01512  46 01030 15951   394.   .        . FM     .0       .COSALF  .$
01513  01513  46 01030 01022   395.   .        . FM     .0       .S       .$
01514  01514  32 01714 01011   396.   .        . FI     .K*2     .SIAG2   .$

01515  01515  46 01030 15955   397.   .        . FM     .0       .COSMMA  .$
01516  01516  46 01030 01017   398.   .        . FM     .0       .LT      .$
01517  01517  15 01030 15957   399.   .        . TN     .0       .S2      .S2S
01520  01520  46 01714 01013   400.   .        . FM     .K*2     .SIAMA   .$
01521  01521  46 01030 01044   401.   .        . FM     .0       .LTP     .$
01522  01522  15 01030 31030   402.   .        . TN     .0       .0       .$
01523  01523  54 01030 15957   403.   .        . FA     .0       .S2      .$
01524  01524  54 01030 15946   404.   .        . FA     .0       .S1      .$
01525  01525  11 01030 01013   405.   .        . TP     .0       .KK1     .<<1S
01526  01526  11 01711 15970   406.   .        . TP     .K*      .BKFS
01527  01527  11 01532 00775   407.   .        . TP     .ALG     .A       .$
01530  01530  37 17173 17171   408.   . 3U3    . 38F030 .        .        .$
```

FIG. D-3 COMPUTER PROGRAM (Continued)

```
01531  01531  45 00000 01791   420.   .      . SJ     .        .FORCE   .$
01532  01532  45 00000 02533   410.   . .L5   . SJ     .        .L.1     .$
01533  01533  11 00010 15071   411.   .      . TP     .T       .TT      .$
01534  01534  54 01137 00014   412.   .      . FA     .ALPHA   .RW11    .$
01535  01535  54 01000 00015   413.   .      . FA     .0       .RW12    .$
01536  01536  11 01000 00070   414.   .      . TP     .0       .WEG1    .$
01537  01537  45 01024 01107   415.   .      . FS     .DELTA   .ALPHA   .$
01540  01540  55 01000 00015   416.   .      . FS     .0       .RW12    .$
01541  01541  11 01000 00000   417.   .      . TP     .0       .WEG2    .$
01542  01542  11 15770 00077   418.   .      . TP     .LIFO1   .WEG1+1  .$
01543  01543  75 00000 02545   419.   .      . ARFOTH .WEG1    .LOC1    .$
01544  01544  11 00770 17057
01545  01545  37 17035 17053
01546  01546  11 17035 15072   420.   .      . TP     .LOC1+3  .SIN1    .$
01547  01547  11 15770 00001   421.   .      . TP     .LIFO1   .WEG2+1  .$
01550  01550  75 00000 02552   422.   .      . ARFOTH .WEG2    .LOC1    .$
01551  01551  11 01000 17057
01552  01552  37 17035 17053
01553  01553  11 17035 15073   423.   .      . TP     .LOC1+3  .SIN2    .$
01554  01554  11 15767 00077   424.   .      . TP     .LIFO.1  .WEG1+1  .$
01555  01555  11 15767 01001   425.   .      . TP     .LIFO.1  .WEG2+1  .$
01556  01556  75 00000 02557   426.   .      . ARFOTH .WEG1    .LOC1    .$
01557  01557  11 00770 17057
01560  01560  37 17035 17053
01561  01561  11 17035 15074   427.   .      . TP     .LOC1+3  .COS1    .$
01562  01562  75 00000 01544   428.   .      . ARFOTH .WEG2    .LOC1    .$
01563  01563  11 01000 17057
01564  01564  37 17035 17053
01565  01565  11 17035 15075   429.   .      . TP     .LOC1+3  .COS2    .$
01566  01566  55 01017 15072   430.   .      . FM     .LT      .SIN1    .$
01567  01567  11 01000 15075   431.   .      . TP     .0       .LSIM1   .$
01570  01570  55 01017 15074   432.   .      . FM     .LT      .COS1    .$
01571  01571  11 01000 15077   433.   .      . TP     .0       .LCOS1   .$
01572  01572  55 01017 15073   434.   .      . FM     .LT      .SIN2    .$
01573  01573  11 01000 15070   435.   .      . TP     .0       .LSIM2   .$
01574  01574  55 01017 15075   436.   .      . FM     .LT      .COS2    .$
01575  01575  11 01000 15071   437.   .      . TP     .0       .LCOS2   .$
01576  01576  11 00010 32000   438.   .      . TP     .5       .A       .SET E AND F9
01577  01577  17 01504 01500   439.   .      . ZJ     .L+4     .L+1     .$
01600  01600  11 01000 15072   440.   .      . TP     .ZERO    .T       .$
01601  01601  11 01000 15073   441.   .      . TP     .ZERO    .F       .$
01602  01602  45 00000 01016   442.   .      . SJ     .        .JUMPX   .$
01603  01603  45 01604 00007   443.   .      . SJ     .L+1     .L+4     .$
01604  01604  11 01001 15072   444.   .      . TP     .ONE     .E       .$
01605  01605  11 01000 15073   445.   .      . TP     .ZERO    .F       .$
01606  01606  45 00000 01016   446.   .      . SJ     .        .JUMPX   .$
01607  01607  11 01002 15072   447.   .      . TP     .ONE     .E       .$
01610  01610  11 00014 32000   448.   .      . TP     .U       .A       .$
```

FIG. D-3 COMPUTER PROGRAM (Continued)

FIG. D-3 COMPUTER PROGRAM (Continued)

```
01411  01411  12 01139 01015   .649.   .        .  TJ    .01     .L02    .$
01412  01412  42 01139 01015   .650.   .        .  TJ    .02     .L03    .$
01413  01413  11 01139 15/03   .651.   .        .  TB    .ZERO   .F      .$
01414  01414  45 00039 01015   .652.   .        .  TJ    .       .L04    .$
01415  01415  11 01139 15/03   .653.   .        .  TB    .J4E    .F      .$
01416  01416  55 15739 01033   .654.   . JUMPA  .  FM    .E      .MJ     .$
01417  01417  11 01139 15/04   .655.   .        .  TB    .0      .EMU    .$
01420  01420  55 15739 15/01   .656.   .        .  FM    .EMJ    .L0092  .$
01421  01421  42 15739 00015   .657.   .        .  FI    .EMU    .M      .$
01422  01422  55 01139 01033   .658.   .        .  FM    .0      .MB     .$
01423  01423  42 01139 15/03   .659.   .        .  FI    .FM     .L01^2  .$
01424  01424  11 01139 15/05   .660.   .        .  TB    .0      .B12    .A11$
01425  01425  55 15739 01033   .661.   .        .  FM    .EMJ    .MB     .$
01426  01426  55 01139 00015   .662.   .        .  FM    .0      .M      .$
01427  01427  11 01139 15/05   .663.   .        .  TB    .0      .B12    .A12$
01430  01430  11 15739 32000   .664.   .        .  TB    .F      .1      .$
01431  01431  47 01139 01032   .665.   .        .  FJ    .L03    .L01    .$
01432  01432  11 01139 15/07   .666.   .        .  TB    .MB     .B13    .$
01433  01433  45 00139 01075   .667.   .        .  FJ    .       .M1531  .$
01434  01434  55 01139 01033   .668.   .        .  FM    .01     .B1     .$
01435  01435  47 01139 31033   .669.   .        .  FO    .IM     .0      .$
01436  01436  11 01139 15/10   .670.   .        .  TB    .0      .B1     .B1 IS IS [illegible]
01437  01437  55 01139 01021   .671.   .        .  FM    .M      .M      .$
01440  01440  11 01139 15/11   .672.   .        .  TB    .0      .M5.    .$
01441  01441  55 01139 01175   .673.   .        .  FS    .02     .M1     .$
01442  01442  11 01139 15/12   .674.   .        .  TB    .0      .M2M1   .$
01443  01443  55 01139 15/12   .675.   .        .  FM    .0      .M2M1   .$
01444  01444  47 15711 31000   .676.   .        .  FO    .M3     .M      .$
01445  01445  11 01139 15/13   .677.   .        .  TB    .0      .B2     .B2 IS [illegible]
01446  01446  55 00015 01175   .678.   .        .  FS    .0      .M1     .$
01447  01447  57 01139 15/14   .679.   .        .  FO    .0      .M2M1   .$
01450  01450  55 01139 01053   .680.   .        .  FM    .0      .B3.    .$
01451  01451  55 01139 01017   .681.   .        .  FM    .0      .B1     .$
01452  01452  11 01139 01032   .682.   .        .  TB    .0      .B4     .$
01453  01453  11 01139 01033   .683.   .        .  TB    .ZERO   .M3M1   .$
01454  01454  75 00039 01065   .684.   .        .  ABFD/B .CA4   .L0C1   .$
01455  01455  11 01139 17057
01456  01456  37 17739 17053
01457  01457  11 17739 15/14   .685.   .        .  TB    .L0C1+3 .B1XC4  .$
01460  01460  11 01131 01033   .686.   .        .  TB    .0^E    .M3M1   .$
01461  01461  75 00039 01065   .687.   .        .  ABFD/B .CA4   .L0C1   .$
01462  01462  11 01139 17057
01463  01463  37 17739 17053
01464  01464  11 17739 15/15   .688.   .        .  TB    .L0C1+3 .M0XC4  .$
01465  01465  55 01131 15/15   .689.   .        .  FM    .0^E    .M0XC4  .$
01466  01466  11 01139 15/15   .690.   .        .  TB    .0      .B5     .B5+11-C1+C2+C3
01467  01467  55 01139 15/15   .691.   .        .  FM    .0      .B5     .$
01470  01470  11 01139 15/17   .692.   .        .  TB    .0      .B3     .B3+11-C0+C1+C2+C3
```

```
01671  01671  56 31030 15734   493.   .        . FM    .Q      .E      .$
01672  01672  56 31030 15719   494.   .        . FM    .Q      .T1     .$
01673  01673  56 31030 15713   495.   .        . FM    .Q      .T2     .$
01674  01674  55 31030 01035   496.   .        . FS    .Q      .MM     .$
01675  01675  11 31030 15737   497.   .        . TP    .G      .A13    .A13. OUT*MS
01676  01676  54 00711 00012   498.   . PASS1  . FA    .TETA1  .TETA2  .$
01677  01677  11 31030 15720   499.   .        . TP    .Q      .T8     .T8+THETA1+THETA2B
01700  01700  55 31030 15720   500.   .        . FM    .Q      .T8     .$
01701  01701  56 31030 01035   501.   .        . FM    .Q      .MM     .$
01702  01702  56 31030 00015   502.   .        . FM    .Q      .U      .$
01703  01703  13 31030 15755   503.   .        . TM    .Q      .S1     .FIRST TERM OF AA15
01704  01704  56 15720 00013   504.   .        . FM    .T8     .S      .$

01705  01705  55 31030 15734   505.   .        . FM    .Q      .FMU    .$
01706  01706  56 31030 01035   506.   .        . FM    .Q      .MM     .$
01707  01707  55 31030 01055   507.   .        . FM    .Q      .TMU    .$
01710  01710  13 31030 15757   508.   .        . TM    .Q      .S2     .SECOND TERM OF AA15
01711  01711  56 15720 01035   509.   .        . FM    .EMU    .MM     .$
01712  01712  55 31030 15773   510.   .        . FM    .Q      .SIA2   .$
01713  01713  32 01030 15675   511.   .        . FI    .MM     .COS2   .$
01714  01714  56 31030 00011   512.   .        . FM    .G      .TETA1  .$
01715  01715  56 31030 00011   513.   .        . FM    .G      .TETA1  .$
01716  01716  56 31030 01017   514.   .        . FM    .Q      .LT     .$
01717  01717  11 31030 15731   515.   .        . TP    .Q      .S3     .3RDTERM OF AA15
01720  01720  45 00030 01775   516.   .        . MJ    .       .SKIP   .$

01721  01721  11 01037 00465   517.   . FORCE  . TP    .DELT1  .DELT   .$
01722  01722  11 00010 15671   518.   .        . TP    .T      .TT     .$
01723  01723  11 00010 32030   519.   .        . TP    .T      .A      .$
01724  01724  47 01727 01735   520.   .        . ZJ    .L+3    .L+1    .$
01725  01725  11 01011 15670   521.   .        . TP    .KF     .PSF    .$
01726  01726  45 00030 01773   522.   .        . MJ    .       .TAG1   .$
01727  01727  11 00010 32030   523.   .        . TP    .S      .A      .$
01730  01730  46 01732 01731   524.   .        . SJ    .TAG3   .L+1    .$
01731  01731  11 01110 32030   525.   .        . TP    .UT     .A      .$
01732  01732  42 00010 01735   526.   .        . TJ    .U      .TAG4   .$
01733  01733  11 01350 15670   527.   .        . TP    .ZERO   .PSF    .$
01734  01734  45 00030 01773   528.   .        . MJ    .       .TAG1   .$

01735  01735  11 01030 32030   529.   . TAG4   . TP    .ZERO   .A      .$
01736  01736  42 15470 01755   530.   .        . TJ    .PSF    .TAG5   .$
01737  01737  11 00010 01041   531.   .        . TP    .T      .TAU    .$
01740  01740  47 01737 15770   532.   .        . FD    .DELT1  .L(F16+1  .$
01741  01741  11 31030 00015   533.   .        . TP    .Q      .T      .$
01742  01742  75 30031 01774   534.   .        . 10F9M .L(X1)  .LOC2   .$
01743  01743  11 15771 17337
01744  01744  37 17335 17333
01745  01745  11 17334 15670   535.   .        . TP    .LOC2+3 .PSF    .$
01746  01746  55 01035 01055   536.   .        . FS    .MM     .MM     .$
01747  01747  11 31030 01035   537.   .        . TP    .Q      .MM     .$
01750  01750  55 01034 01055   538.   .        . FS    .TP     .TP     .$
```

FIG. D-3 COMPUTER PROGRAM (Continued)

```
01751  01751  11 31330 02030   539.   .        . TP    .0      .19     .$
01752  01752  55 01319 02050   540.   .        . FS    .14     .IPP    .$
01753  01753  11 31330 02010   541.   .        . TP    .0      .12     .$
01754  01754  11 01735 32030   542.   .        . TP    .FRI    .4      .$
01755  01755  35 01079 01755   543.   .        . JT    .14     .FRI    .$
01756  01756  11 01331 01031   544.   . FMI    . TP    .EMS    .EPS    .$
01757  01757  54 01331 02076   545.   .        . FA    .$0%E   .12     .$
01760  01760  11 31330 02076   546.   .        . TP    .0      .12     .$
01761  01761  15 00330 02773   547.   .        . TJ    .       .T4G1   .$
01762  01762  11 01330 32030   548.   . I433   . TP    .ZERO   .4      .$
01763  01763  42 15570 02755   549.   .        . TJ    .PGF    .L+2    .$
01764  01764  15 00330 02773   550.   .        . TJ    .       .T4G1   .$

01765  01765  55 00319 02051   551.   . I435   . FS    .T      .T4U    .$
01766  01766  11 31330 00010   552.   .        . TP    .0      .T      .$
01767  01767  75 30301 01781   553.   .        . ZOFVM .LIX11  .LOC2   .$
01770  01770  11 15771 17337
01771  01771  37 17335 17333
01772  01772  11 17335 15070   554.   .        . TP    .LOC2+9 .TSF    .$
01773  01773  11 15571 00010   555.   . I451   . TP    .TT     .T      .$
01774  01774  15 00330 02437   556.   .        . TJ    .       .LOOP   .$
01775  01775  55 01079 00016   557.   . SKIP   . FS    .U0     .11     .$
01776  01776  01 01312 01011   558.   .        . FP    .K      .KK     .$
01777  01777  55 31330 15679   559.   .        . FS    .0      .PSF    .$
02000  02000  13 31330 15732   560.   .        . TN    .0      .SS     .$

02001  02001  56 01324 01053   561.   . I432   . FM    .AP     .TRO    .$
02002  02002  11 31330 01024   562.   .        . TP    .0      .AP     .$
02003  02003  11 02334 02031   563.   .        . TP    .L+1    .T4G2   .$
02004  02004  15 00330 02035   564.   .        . TJ    .       .L+1    .$
02005  02005  56 01324 01024   565.   .        . FM    .AP     .AP     .$
02006  02006  56 31330 01024   566.   .        . FM    .0      .AP     .$
02007  02007  56 31330 01023   567.   .        . FM    .0      .SAMA   .$
02010  02010  57 31330 01053   568.   .        . FD    .0      .TRO    .$
02011  02011  57 31330 01022   569.   .        . FD    .0      .$      .$
02012  02012  57 31330 01025   570.   .        . FD    .0      .CO     .$
02013  02013  57 31330 01025   571.   .        . FD    .0      .CO     .$
02014  02014  11 31330 15723   572.   .        . TP    .0      .CONST  .$

02015  02015  55 01079 00016   573.   .        . FS    .U0     .11     .$
02016  02016  11 31330 15724   574.   .        . TP    .0      .UOFU   .$
02017  02017  11 31330 00010   575.   .        . TP    .0      .T      .$
02020  02020  11 31330 32030   576.   .        . TP    .0      .4      .$
02021  02021  42 15772 02023   577.   .        . TJ    .LIF2+1 .L+2    .$
02022  02022  11 15772 00010   578.   .        . TP    .LIF2+1 .T      .$
02023  02023  11 01369 00445   579.   .        . TP    .DELT2  .DELT   .$
02024  02024  75 30301 02025   580.   .        . ZOFVM .LIX21  .LOC2   .$
02025  02025  11 15773 17337
02026  02026  37 17335 17333
02027  02027  56 17335 01053   581.   .        . FM    .LOC2+9 .TRO    .$
02030  02030  11 31330 15735   582.   .        . TP    .0      .ALFAO  .$
```

FIG. D-3 COMPUTER PROGRAM (Continued)

```
02031  02031  66 15729 15735   583.   .      . FM   .ALFAO   .ALFAO   .$
02032  02032  67 15729 36030   584.   .      . FD   .CONST   .0       .$
02033  02033  11 51030 15726   585.   .      . TP   .0       .$5      .$
02034  02034  66 00019 00019   586.   .      . FM   .5       .6       .$
02035  02035  11 51030 15737   587.   .      . TP   .0       .$5G     .$
02036  02036  66 51030 15732   588.   .      . FM   .0       .E       .$
02037  02037  66 51030 15726   589.   .      . FM   .0       .$5      .$
02040  02040  11 51030 15730   590.   .      . TP   .0       .RF      .RECOIL FORCES
02041  02041  64 01031 01037   591.   .      . FA   .ONE     .DELTA   .$
02042  02042  66 51030 15726   592.   .      . FM   .0       .$5      .$
02043  02043  66 51030 15732   593.   .      . FM   .0       .E       .$
02044  02044  66 51030 15727   594.   .      . FM   .0       .$5G     .$

02045  02045  13 51030 15735   595.   .      . TN   .0       .$5      .5TH TERM  . F.DS
02046  02046  11 15729 36030   596.   .      . TP   .F       .A       .$
02047  02047  17 02030 02053   597.   .      . ZJ   .L+1     .PASS2   .$
02050  02050  66 15719 15713   598.   .      . FM   .T1      .T2      .$
02051  02051  67 51030 15712   599.   .      . FD   .0       .U2XU1   .$
02052  02052  66 51030 01053   600.   .      . FM   .0       .T30     .$
02053  02053  66 51030 01047   601.   .      . FM   .0       .RI      .$
02054  02054  66 51030 15714   602.   .      . FM   .0       .SIACAR  .$
02055  02055  66 51030 15716   603.   .      . FM   .0       .ARG     .$
02056  02056  66 51030 15732   604.   .      . FM   .0       .E       .$
02057  02057  66 51030 15737   605.   .      . FM   .0       .$5G     .$
02060  02060  13 51030 31030   606.   .      . TN   .0       .0       .$

02061  02061  64 51030 15726   607.   .      . FA   .0       .$5      .$
02062  02062  11 51030 15735   608.   .      . TP   .0       .$5      .5TH TERM =(N3T).DS
02063  02063  66 15732 01136   609.   . PASS2 . FM   .E       .H1      .$
02064  02064  13 51030 15731   610.   .      . TN   .0       .$6      .6TH TERM OF A215
02065  02065  66 15734 15734   611.   .      . FM   .EMU     .CONS1   .$
02066  02066  63 51030 15732   612.   .      . FS   .0       .SIN1    .$
02067  02067  66 51030 01022   613.   .      . FM   .0       .5       .$
02070  02070  66 51030 01035   614.   .      . FM   .0       .WR      .7TH TERM OF A215
02071  02071  13 51030 31030   615.   .      . TN   .0       .0       .$
02072  02072  64 51030 15645   616.   .      . FA   .0       .$1      .$
02073  02073  64 51030 15667   617.   .      . FA   .0       .$3      .$
02074  02074  64 51030 15721   618.   .      . FA   .0       .$3      .$

02075  02075  64 51030 15722   619.   .      . FA   .0       .$4      .$
02076  02076  64 51030 15725   620.   .      . FA   .0       .$5      .$
02077  02077  64 51030 15731   621.   .      . FA   .0       .$6      .$
02100  02100  11 51030 15732   622.   .      . TP   .0       .AA1     .FINISH FIRST EQUATION.S
02101  02101  66 01034 01017   623.   .      . FM   .MC      .LT      .$
02102  02102  71 01017 01077   624.   .      . FW   .LT      .IO      .$
02103  02103  11 51030 15645   625.   .      . TP   .0       .$1      .1ST 2 TERMS OF A215
02104  02104  66 15734 01092   626.   .      . FM   .EMU     .MOVE    .$
02105  02105  66 51030 01035   627.   .      . FM   .0       .WR      .$
02106  02106  66 51030 15730   628.   .      . FM   .0       .LSIMQ   .$
02107  02107  02 01035 15731   629.   .      . FI   .WW      .LCOS2   .$
02110  02110  11 51030 15667   630.   .      . TP   .0       .$2      .$
```

FIG. D-3 COMPUTER PROGRAM (Continued)

```
02111  02111  54 00015 15731   531.   .   . FA   .0     .LCOS2   .$
02112  02112  46 01030 15067   532.   .   . FM   .0     .S2      .$
02113  02113  11 01030 15067   533.   .   . TP   .0     .S2      .3RD TERM OF A21S
02114  02114  46 01015 15731   534.   .   . FM   .B1    .LCOS2   .$
02115  02115  46 01030 01074   535.   .   . FM   .0     .MC      .$
02116  02116  54 01030 15056   537.   .   . FA   .0     .S1      .$
02117  02117  54 01030 15067   538.   .   . FA   .0     .S2      .$
02120  02120  11 01030 15733   539.   .   . TP   .0     .A21     .A21S
02121  02121  46 15734 01052   540.   .   . FM   .EMU   .MMAR    .$
02122  02122  31 15730 15731   541.   .   . FP   .LSIN2  .LCOS2   .$
02123  02123  46 01030 00015   542.   .   . FM   .0     .U       .$
02124  02124  46 01030 01075   543.   .   . FM   .0     .MR      .$

02125  02125  11 01030 15056   544.   .   . TP   .0     .S1      .1ST TERM OF A22S
02126  02126  46 01015 01015   545.   .   . FM   .MC    .B1      .$
02127  02127  31 15731 15045   546.   .   . FP   .LCOS2  .S1      .$
02130  02130  11 01030 15734   547.   .   . TP   .0     .A22     .A22S
02131  02131  54 01030 15737   548.   .   . FA   .MW    .B13     .$
02132  02132  46 01030 15733   549.   .   . FM   .0     .LSIN2   .$
02133  02133  13 01030 15735   550.   .   . TN   .0     .A23     .A23S
02134  02134  46 15720 15730   551.   .   . FM   .TM    .TM      .$
02135  02135  46 01030 01015   552.   .   . FM   .0     .B1      .$
02136  02136  46 01030 01074   553.   .   . FM   .0     .MC      .$
02137  02137  13 01030 15045   554.   .   . TN   .0     .S1      .1ST TERMS
02140  02140  46 00011 00011   555.   .   . FM   .TETA1  .TETA1   .$

02141  02141  46 01030 01075   556.   .   . FM   .0     .MR      .$
02142  02142  46 01030 15731   557.   .   . FM   .0     .LCOS2   .$
02143  02143  11 01030 15067   558.   .   . TP   .0     .S2      .2ND TERMS
02144  02144  11 15722 32070   559.   .   . TP   .SM    .$       .$
02145  02145  47 02150 02145   560.   .   . ZJ   .L+3   .L+1     .$
02146  02146  11 01030 15721   561.   .   . TP   .ZERO  .S3      .< + KUS
02147  02147  45 00030 02152   562.   .   . TU   .      .L+3     .$
02150  02150  45 15722 15070   563.   .   . FS   .SM    .MGF     .$
02151  02151  13 01030 15721   564.   .   . TN   .0     .S3      .< + KUS
02152  02152  46 01030 01022   565.   .   . FM   .MC    .0       .$
02153  02153  31 15672 15721   566.   .   . FP   .SIN1  .S3      .$
02154  02154  54 01030 15067   567.   .   . FA   .0     .S2      .$

02155  02155  54 01030 15046   568.   .   . FA   .0     .S1      .$
02156  02156  46 01030 15730   569.   .   . FM   .0     .LSIN2   .$
02157  02157  11 01030 15045   570.   .   . TP   .0     .S1      .1ST  TERM OF A42S
02160  02160  46 15720 02013   571.   .   . FM   .TM    .$       .$
02161  02161  46 01030 01075   572.   .   . FM   .0     .MR      .$
02162  02162  46 01030 01053   573.   .   . FM   .0     .TMU     .$
02163  02163  13 01030 15067   574.   .   . TN   .0     .S2      .FIRST TERMS
02164  02164  54 01030 01074   575.   .   . FA   .MW    .MC      .$
02165  02165  46 01030 01022   576.   .   . FM   .0     .$       .$
02166  02166  45 01030 15074   577.   .   . FM   .0     .COS1    .$
02167  02167  13 01030 15721   578.   .   . TN   .0     .S3      .$
02170  02170  54 15657 15721   579.   .   . FA   .S2    .S3      .$
```

FIG. D-3 COMPUTER PROGRAM (Continued)

```
02171  02171  55  01030  15731   580.   .      . FM   .3     .LC352   .1
02172  02172  11  01030  15547   581.   .      . TP   .4     .57      .3HD TERM OF A*25
02173  02173  55  15720  01013   582.   .      . FM   .TM    .5       .5
02174  02174  55  01030  01035   583.   .      . FM   .3     .49      .5
02175  02175  55  01030  01033   584.   .      . FM   .3     .41      .5
02176  02176  55  01030  01053   585.   .      . FM   .3     .T*3     .5
02177  02177  11  01030  15721   586.   .      . TP   .3     .55      .1ST TERMS
02200  02200  55  00311  00011   587.   .      . FM   .TPTA1 .TPTA1   .5
02201  02201  55  01030  15723   588.   .      . FM   .3     .LSIN2   .5
02202  02202  55  01030  01035   589.   .      . FM   .3     .49      .5
02203  02203  55  01030  01033   590.   .      . FM   .3     .41      .5
02204  02204  13  01030  15732   591.   .      . TM   .3     .56      .3HD TERMS

02205  02205  55  01031  00027   592.   .      . FA   .DME   .DELTA   .5
02206  02206  11  01030  15735   593.   .      . TP   .3     .55      .5
02207  02207  12  15730  31000   594.   .      . TM   .56    .3       .5
02210  02210  55  01030  15735   595.   .      . FM   .3     .55      .5
02211  02211  11  01030  15735   596.   .      . TP   .3     .55      .3HD TERMS
02212  02212  11  01030  15731   597.   .      . TP   .T1    .54      .4TH TERMS
02213  02213  11  15730  31000   598.   .      . TP   .493   .5       .5
02214  02214  47  02217  02215   599.   .      . XD   .L03   .L01     .5
02215  02215  11  01030  15735   700.   .      . TP   .ZERO  .57      .5TH TERM EQ.0
02216  02216  15  00030  02225   701.   .      . XD   .      .PASS7   .5
02217  02217  55  15710  01054   702.   .      . FM   .T1    .T*3     .5
02220  02220  55  01030  15713   703.   .      . FM   .3     .T3      .5

02221  02221  57  01030  15712   704.   .      . FD   .3     .DPM1    .5
02222  02222  55  01030  15714   705.   .      . FM   .3     .SI.CAP  .5
02223  02223  55  01030  15715   706.   .      . FM   .3     .496     .5
02224  02224  55  01030  15737   707.   .      . FM   .4     .55      .5
02225  02225  11  01030  15735   708.   .      . TP   .3     .57      .5TH TERM E (NOT)=0
02226  02226  55  01032  15774   709.   . PASS7 . FM   .3     .C*51    .5
02227  02227  55  01030  01035   710.   .      . FM   .3     .49      .5
02230  02230  01  01030  15735   711.   .      . FD   .41    .57      .5
02231  02231  54  01030  15731   712.   .      . FA   .3     .53      .5
02232  02232  54  01030  15732   713.   .      . FA   .3     .55      .5
02233  02233  54  01030  15735   714.   .      . FA   .3     .55      .5
02234  02234  54  01030  15731   715.   .      . FA   .3     .55      .5

02235  02235  55  01030  15730   716.   .      . FM   .3     .LSIN2   .5
02236  02236  55  01030  15732   717.   .      . FM   .3     .5       .5
02237  02237  11  01030  15731   718.   .      . TP   .3     .53      .3HD TERM OF A*25
02240  02240  55  01033  00011   719.   .      . FM   .C1    .TPTA1   .5
02241  02241  32  01132  00014   720.   .      . FI   .41    .PHI1    .5
02242  02242  54  01030  01013   721.   .      . FA   .3     .44.     .5
02243  02243  13  01030  15722   722.   .      . TM   .3     .56      .4TH TERM OF A*25
02244  02244  55  01130  00015   723.   .      . FM   .42    .PH.2    .5
02245  02245  32  01131  00012   724.   .      . FI   .C2    .TETA2   .5
02246  02246  55  01030  01015   725.   .      . FM   .3     .7       .5
02247  02247  57  01030  01053   726.   .      . FD   .3     .T*3     .SIN(SAMA2)*.12*
02250  02250  54  01030  01014   727.   .      . FA   .3     .442     .5
```

FIG. D-3 COMPUTER PROGRAM (Continued)

```
02251  02251  11  01030  15726   720.   .   . TP   .0   .55   .5
02252  02252  66  01030  06013   727.   .   . FM   .LTP  .SIXHA .5
02253  02253  13  01030  15731   730.   .   . TN   .0   .56   .5
02254  02254  67  15731  01053   731.   .   . FM   .LCOS2 .TPO  .5
02255  02255  13  01030  15735   732.   .   . TN   .0   .57   .5
02256  02256  66  15730  06054   733.   .   . FM   .LSIN2 .533  .5
02257  02257  67  01030  06053   734.   .   . FD   .0   .TPO  .5
02260  02260  54  01030  15735   735.   .   . FA   .0   .57   .5
02261  02261  54  01030  15731   736.   .   . FA   .0   .56   .5
02262  02262  11  15735  15732   737.   .   . FM   .55   .58   .5TH TERM OF A025
02263  02263  54  01030  15665   738.   .   . FA   .0   .51   .5
02264  02264  54  01030  15667   739.   .   . FA   .0   .52   .5

02265  02265  66  01030  15731   740.   .   . FA   .0   .53   .5
02266  02266  11  01030  15737   741.   .   . TM   .0   .582  .A2= END SECOND EQUATION
02267  02267  66  01030  06016   742.   .   . FM   .XW   .U   .5
02270  02270  11  00016  01037   743.   .   . FM   .U   .TC   .5
02271  02271  66  01030  01010   744.   .   . FA   .0   .10   .5
02272  02272  11  01030  15665   745.   .   . TM   .0   .51   .5
02273  02273  66  01016  06016   746.   .   . FM   .d1   .91   .5
02274  02274  11  01030  15665   747.   .   . FM   .W   .51   .5
02275  02275  11  01030  15733   748.   .   . TM   .0   .582  .A328
02276  02276  66  01030  06016   749.   .   . FM   .XW   .U   .5
02277  02277  72  01030  01015   750.   .   . FI   .MC   .91   .5
02300  02300  66  01030  15731   751.   .   . FM   .0   .LCOS2 .5

02301  02301  66  01030  15740   752.   .   . FA   .0   .582  .5
02302  02302  11  01030  15741   753.   .   . TM   .0   .591  .A315
02303  02303  11  01030  15742   754.   .   . TM   .ZERO .593  .A335
02304  02304  66  00511  06011   755.   .   . FM   .TETA1 .TETA1 .5
02305  02305  66  01030  15739   756.   .   . FM   .0   .LSIN2 .5
02306  02306  11  01030  15665   757.   .   . TM   .0   .51   .5
02307  02307  66  01030  06015   758.   .   . FM   .W   .U   .5
02310  02310  72  01030  01015   759.   .   . FI   .MC   .91   .5
02311  02311  66  01030  15665   760.   .   . FM   .0   .51   .5
02312  02312  11  01030  15666   761.   .   . TM   .0   .51   .1ST TERM OF A035
02313  02313  66  15670  01031   762.   .   . FM   .PHF  .595  .5
02314  02314  11  01030  15667   763.   .   . TM   .0   .52   .2ND TERM OF A035

02315  02315  66  15729  06013   764.   .   . FM   .TM   .5   .5
02316  02316  66  01030  01035   765.   .   . FM   .0   .XW   .5
02317  02317  66  01030  06053   766.   .   . FM   .0   .TPO  .5
02320  02320  66  01030  00015   767.   .   . FM   .0   .U   .5
02321  02321  13  01030  15721   768.   .   . TN   .0   .59   .3RD TERM OF A035
02322  02322  66  01030  06016   769.   .   . FM   .XW   .U   .5
02323  02323  72  01030  01016   770.   .   . FI   .MC   .91   .5
02324  02324  66  01030  01032   771.   .   . FM   .0   .5   .5
02325  02325  66  01030  15674   772.   .   . FM   .0   .COS1 .5
02326  02326  13  01030  15732   773.   .   . TN   .0   .59   .4TH TERM OF A035
02327  02327  66  01130  06015   774.   .   . FM   .C2   .W12  .5
02330  02330  72  01131  06012   775.   .   . FI   .C2   .TETA2 .5
```

FIG. D-3 COMPUTER PROGRAM (Continued)

02331	02331	56	51030	01015	770.	.	. FM	.0	.9	.5
02332	02332	57	51030	01053	771.	.	. FD	.0	.TW0	.5
02333	02333	56	51030	01014	770.	.	. FA	.0	.552	.5
02334	02334	56	51030	01015	771.	.	. FM	.0	.9	.5
02335	02335	57	51030	01053	780.	.	. FD	.4	.TW0	.5
02336	02336	13	51030	15735	791.	.	. TN	.0	.59	.5
02337	02337	56	15725	15732	792.	.	. FA	.59	.59	.5
02340	02340	56	51030	15731	793.	.	. FA	.6	.53	.5
02341	02341	56	51030	15747	794.	.	. FA	.0	.52	.5
02342	02342	56	51030	15746	795.	.	. FA	.0	.51	.5
02343	02343	11	51030	15743	796.	.	. TP	.0	.AA3	.5
02344	02344	57	15735	15735	797.	.	. FD	.A12	.811	.5
02345	02345	11	51030	15745	798.	.	. TP	.0	.51	.5
02346	02346	57	15735	15733	799.	.	. FD	.A72	.471	.5
02347	02347	56	51030	15745	790.	.	. FS	.0	.51	.5
02350	02350	13	51030	15714	791.	.	. TN	.0	.911	.9115
02351	02351	57	15737	15735	792.	.	. FD	.A13	.811	.5
02352	02352	11	51030	15745	793.	.	. TP	.0	.51	.5
02353	02353	57	15735	15733	794.	.	. FD	.A73	.471	.5
02354	02354	56	51030	15745	795.	.	. FS	.0	.51	.5
02355	02355	13	51030	15715	796.	.	. TN	.0	.912	.9125
02356	02356	57	15732	15735	797.	.	. FD	.A81	.811	.5
02357	02357	11	51030	15745	798.	.	. TP	.0	.51	.5
02360	02360	57	15737	15733	800.	.	. FD	.A82	.421	.5
02361	02361	56	51030	15745	801.	.	. FS	.0	.51	.5
02362	02362	13	51030	15715	802.	.	. TN	.0	.991	.9115
02363	02363	57	15735	15735	803.	.	. FD	.A12	.811	.5
02364	02364	11	51030	15745	804.	.	. TP	.0	.51	.5
02365	02365	57	15737	15741	805.	.	. FD	.A72	.431	.5
02366	02366	56	51030	15745	806.	.	. FS	.0	.51	.5
02367	02367	13	51030	15717	807.	.	. TN	.0	.921	.9215
02370	02370	57	15737	15735	808.	.	. FD	.A13	.811	.5
02371	02371	11	51030	15745	809.	.	. TP	.0	.51	.5
02372	02372	57	15737	15741	810.	.	. FD	.A73	.471	.5
02373	02373	56	51030	15745	811.	.	. FS	.0	.51	.5
02374	02374	13	51030	15757	812.	.	. TN	.0	.922	.9225
02375	02375	57	15732	15735	813.	.	. FD	.A81	.811	.5
02376	02376	11	51030	15745	814.	.	. TP	.0	.51	.5
02377	02377	57	15743	15741	815.	.	. FD	.AA3	.431	.5
02400	02400	56	51030	15745	816.	.	. FS	.0	.51	.5
02401	02401	13	51030	15751	817.	.	. TN	.0	.992	.9025
02402	02402	56	15744	15750	818.	.	. FM	.911	.922	.5
02403	02403	11	51030	15746	819.	.	. TP	.0	.51	.5
02404	02404	56	15745	15717	820.	.	. FM	.812	.921	.5
02405	02405	56	51030	15746	821.	.	. FS	.0	.51	.5
02406	02406	13	51030	15752	822.	.	. TN	.0	.9CT	.5
02407	02407	11	51030	32030	823.	.	. TP	.0	.A	.5
02410	02410	57	02412	02411	824.	.	. ZJ	.L-2	.L-1	.5

FIG. D-3 COMPUTER PROGRAM (Continued)

```
02411  02411  15 01000 02070   420.   .        . 4J    .        .FILL    .$
02412  02412  46 15720 15716   420.   .        . FM    .372     .441     .$
02413  02413  11 01000 15755   427.   .        . TP    .0       .S1      .$
02414  02414  46 15749 15751   420.   .        . FM    .312     .442     .$
02415  02415  46 01000 15755   427.   .        . FM    .0       .S1      .$
02416  02416  47 01000 15752   430.   .        . FD    .0       .DET     .$
02417  02417  15 01000 02074   431.   .        . FN    .0       .DTETA2  .DTETA2$
02420  02420  46 15749 15751   432.   .        . FM    .311     .442     .$
02421  02421  11 01000 15756   433.   .        . TP    .0       .S1      .$
02422  02422  46 15747 15715   434.   .        . FM    .421     .441     .$
02423  02423  46 01000 15756   435.   .        . FS    .0       .S1      .$
02424  02424  47 01000 15752   436.   .        . FD    .0       .DET     .$

02425  02425  15 01000 02075   437.   .        . FN    .0       .DS      .DS$
02426  02426  46 00778 15710   438.   .        . FM    .DTETA2  .442     .$
02427  02427  46 01000 15743   439.   .        . FS    .0       .443     .$
02430  02430  47 01000 15741   440.   .        . FD    .0       .441     .$
02431  02431  15 01000 02073   441.   .        . FN    .0       .DTETA1  .DTETA1$
02432  02432  11 00311 02076   442.   .        . TM    .TETA1   .PHI1    .$
02433  02433  11 00312 02077   443.   .        . TP    .TETA2   .PHI2    .$
02434  02434  11 00313 02100   444.   .        . TM    .S       .PHI     .$
02435  02435  11 15471 02010   445.   .        . TP    .T1      .T       .$
02436  02436  46 00000 02077   446.   .        . 4J    .        .T       .$
02437  02437  11 01000 02035   447.   . .UOM   . IJ    .1       .PASS3   .UOM TOS (PASS3) FOR PROG. STORES
02440  02440  11 01000 01035   450.   .        . TP    .11      .1       .$

02441  02441  11 15725 02000   460.   .        . TP    .F       .A       .$
02442  02442  47 02147 02443   450.   .        . ZJ    .L+5     .L+1     .$
02443  02443  11 01000 15753   451.   .        . TP    .ZF30    .AYCAM   .$
02444  02444  11 01000 15754   452.   .        . TM    .ZF30    .TAYCAM  .$
02445  02445  11 01000 15755   453.   .        . TP    .ZF30    .XXCAM   .$
02446  02446  46 00000 02471   454.   .        . 4J    .        .PASS4   .$
02447  02447  46 15719 01047   455.   .        . FM    .SIXCAM  .PT      .$
02450  02450  46 01000 01053   456.   .        . FM    .0       .T10     .$
02451  02451  47 01000 15712   457.   .        . FD    .0       .DXXII   .$
02452  02452  46 01000 15715   458.   .        . FM    .0       .R9      .$
02453  02453  46 01000 15727   459.   .        . FM    .0       .SSC     .$
02454  02454  02 15717 02075   460.   .        . FI    .T9      .DS      .$

02455  02455  46 01000 15713   461.   .        . FM    .0       .T2      .$
02456  02456  46 01000 15710   462.   .        . FM    .0       .T1      .$
02457  02457  11 01000 15753   463.   .        . TP    .0       .AYCAM   .$
02460  02460  46 01759 01017   464.   .        . FM    .T20     .PT      .$
02461  02461  46 01000 15714   465.   .        . FM    .0       .SIXCAM  .$
02462  02462  47 01000 15712   466.   .        . FD    .0       .DXXII   .$
02463  02463  46 01000 15737   467.   .        . FM    .0       .SSC     .$
02464  02464  02 15715 02075   468.   .        . FI    .AM5     .DS      .$
02465  02465  46 01000 01021   469.   .        . FM    .0       .4       .$
02466  02466  47 01000 15712   470.   .        . FD    .0       .DXXII   .$
02467  02467  46 01000 15710   471.   .        . FM    .0       .T1      .$
02470  02470  11 01000 15754   472.   .        . TM    .0       .TAYCAM  .$
```

FIG. D-3 COMPUTER PROGRAM (Continued)

```
02471  02471  44 00073 00074   872.   .  PASS4  . FA   .DTETA1  .DTETA2  .$
02472  02472  66 51030 01010   873.   .        . FM   .Q      .IR      .$
02473  02473  11 51030 15545   874.   .        . TP   .Q      .S1      .$
02474  02474  66 15470 01071   875.   .        . FM   .PGF    .EPS     .$
02475  02475  55 51030 15545   876.   .        . FS   .Q      .S1      .$
02476  02476  13 51030 15756   877.   .        . TM   .Q      .TORQ    .TORQUES
02477  02477  55 00073 15731   878.   .        . FM   .DTETA1  .LCOS2   .$
02500  02500  11 51030 15755   879.   .        . TP   .Q      .S1      .$
02501  02501  55 00011 00011   881.   .        . FM   .TETA1  .TETA1   .$
02502  02502  55 51030 15730   882.   .        . FM   .Q      .LSIN2   .$
02503  02503  13 51030 15757   883.   .        . TM   .Q      .S2      .$
02504  02504  44 00011 00012   884.   .        . FA   .TETA1  .TETA2   .$

02505  02505  66 51030 00013   885.   .        . FM   .Q      .S       .$
02506  02506  55 51030 01053   886.   .        . FM   .Q      .TPO     .$
02507  02507  11 51030 15721   887.   .        . TP   .Q      .S3      .$
02510  02510  44 00073 00074   888.   .        . FA   .DTETA1  .DTETA2  .$
02511  02511  55 51030 00016   889.   .        . FM   .Q      .U       .$
02512  02512  11 51030 15732   890.   .        . TP   .Q      .S4      .$
02513  02513  55 01727 15774   891.   .        . FM   .U      .COS1    .$
02514  02514  44 51030 15732   892.   .        . FA   .Q      .S4      .$
02515  02515  44 51030 15721   893.   .        . FA   .U      .S3      .$
02516  02516  44 51030 15757   894.   .        . FA   .Q      .S2      .$
02517  02517  44 51030 15756   895.   .        . FA   .Q      .S1      .$
02520  02520  66 51030 01035   896.   .        . FM   .Q      .WB      .$

02521  02521  11 51030 15757   897.   .        . TP   .Q      .NORM    .NORMS
02522  02522  55 01130 01015   898.   .        . FM   .C2     .S       .$
02523  02523  55 51030 00015   899.   .        . FM   .Q      .PHI2    .$
02524  02524  57 51030 01053   900.   .        . FD   .Q      .TPO     .$
02525  02525  11 51030 15750   901.   .        . TP   .Q      .SPRING  .$
02526  02526  55 01130 01015   902.   .        . FM   .C2     .S       .$
02527  02527  66 51030 00012   903.   .        . FM   .Q      .TETA2   .$
02530  02530  57 51030 01053   904.   .        . FD   .Q      .TPO     .$
02531  02531  11 51030 15751   905.   .        . TP   .Q      .DAMP    .$
02532  02532  44 00015 00015   906.   .        . FA   .PHI1   .PHI2    .$
02533  02533  11 51030 15752   907.   .        . TP   .Q      .ROT     .$
02534  02534  66 15750 01027   908.   .        . FM   .WB     .DELTA   .$

02535  02535  72 15702 01176   909.   .        . FI   .E      .H1      .$
02536  02536  11 51030 15753   910.   .        . TP   .Q      .PRIC    .$
02537  02537  11 02542 16070   911.   .        . 4*FO31 .Z7   .        .$
02540  02540  57 15777 15775
02541  02541  15 00030 02565   912.   .        . SW   .       .NEXT7   .$
02542  02542  00 01751 02513   913.   . Z7     . 00   .1001   .L+1     .$
02543  02543  00 00010 02426   914.   .        . 00   .T      .1302    .$
02544  02544  00 00030 16943   915.   .        . 00   .       .FL      .$
02545  02545  00 00014 02426   916.   .        . 00   .PHI1   .1302    .$
02546  02546  00 00030 16943   917.   .        . 00   .       .FL      .$
02547  02547  00 00015 02426   918.   .        . 00   .PHI2   .1302    .$
02550  02550  00 00030 16943   919.   .        . 00   .       .FL      .$
```

FIG. D-3 COMTPUTER PROGRAM (Continued)

```
02551  02551  30 00719 02426      920.  .        . 30    .U        .1302    .$
02552  02552  30 00730 10543      921.  .        . 30    .         .FL      .$
02553  02553  30 00711 02425      922.  .        . 30    .TETA1    .1302    .$
02554  02554  30 00730 10543      923.  .        . 30    .         .FL      .$
02555  02555  30 00712 02425      924.  .        . 30    .TETA2    .1302    .$
02556  02556  30 00730 10543      925.  .        . 30    .         .FL      .$
02557  02557  30 00713 02425      926.  .        . 30    .S        .1302    .$
02558  02558  30 00730 10543      927.  .        . 30    .         .FL      .$
02559  02559  30 15730 02425      928.  .        . 30    .NB       .1302    .$
02560  02560  30 00730 10543      929.  .        . 30    .         .FL      .$
02561  02561  30 00730 00000      930.  .        . 30    .         .        .$
02562  02562  30 00730 00000      931.  .        . 30    .         .        .$

02563  02563  11 02570 10000      932.  . WCST7  . ANFD31 .CM       .        .$
02564  02564  37 15777 13775
02565  02565  45 00730 02013      933.  .        . EJ    .         .WEAT10  .$
02566  02566  30 01731 02971      934.  . CM     . 30    .1031     .L+1     .$
02567  02567  30 01731 02425      935.  .        . 30    .UPLTA1   .1302    .$
02568  02568  30 00730 10543      936.  .        . 30    .         .FL      .$
02569  02569  30 15731 02425      937.  .        . 30    .ATCA1    .1302    .$
02570  02570  30 00730 10543      938.  .        . 30    .         .FL      .$
02571  02571  30 15730 02425      939.  .        . 30    .TATCA1   .1302    .$
02572  02572  30 00730 10543      940.  .        . 30    .         .FL      .$
02573  02573  30 15724 02425      941.  .        . 30    .TP10     .1302    .$
02574  02574  30 00730 10543      942.  .        . 30    .         .FL      .$

02575  02575  30 15727 02425      943.  .        . 30    .NPWR     .1302    .$
02576  02576  30 00730 10543      944.  .        . 30    .         .FL      .$
02577  02577  30 15730 02426      945.  .        . 30    .SPRINW   .1302    .$
02600  02600  30 00730 10543      946.  .        . 30    .         .FL      .$
02601  02601  30 15731 02425      947.  .        . 30    .UPWR     .1302    .$
02602  02602  30 00730 10543      948.  .        . 30    .         .FL      .$
02603  02603  30 15670 02425      949.  .        . 30    .PWF      .1302    .$
02604  02604  30 00730 10543      950.  .        . 30    .         .FL      .$
02605  02605  30 00730 00000      951.  .        . 30    .         .        .$
02606  02606  30 00730 00000      952.  .        . 30    .         .        .$
02607  02607  11 02415 10000      953.  . WCST10 . ANFD31 .Z10      .        .$
02610  02610  37 15777 13775

02611  02611  45 00730 02035      954.  .        . EJ    .         .PASS3   .$
02612  02612  30 01731 02917      955.  . Z10    . 30    .1031     .L+1     .$
02613  02613  30 01417 01141      956.  .        . 30    .Z13      .409     .$
02614  02614  30 00730 10513      957.  .        . 30    .         .AL      .$
02615  02615  30 01375 02426      958.  .        . 30    .I2       .1302    .$
02616  02616  30 00730 10543      959.  .        . 30    .         .FL      .$
02617  02617  30 15724 02426      960.  .        . 30    .UPWU     .1302    .$
02620  02620  30 00730 10543      961.  .        . 30    .         .FL      .$
02621  02621  30 15762 02426      962.  .        . 30    .RPT      .1302    .$
02622  02622  30 00730 10543      963.  .        . 30    .         .FL      .$
02623  02623  30 15769 02425      964.  .        . 30    .FWIC     .1302    .$
02624  02624  30 00730 10543      965.  .        . 30    .         .FL      .$
```

FIG. D-3 COMPUTER PROGRAM (Continued)

```
02431  02431  30 01731 02426    969.  .        . JN    .ZPS    .1302   .$
02432  02432  30 00300 15943    967.  .        . JN    .       .FL     .$
02433  02433  30 00300 00000    968.  .        . JN    .       .       .$
02434  02434  31 00300 00000    969.  .        . JI    .       .       .$
02435  02435  11 00310 34000    970.  .PASSB   . TP    .T      .A      .$
02436  02436  12 01111 01590    971.  .        . TJ    .TN     .CZB    .$
02437  02437  15 00300 01112    972.  .        . TJ    .       .STANT  .$
02438  02438  11 02513 15000    973.  . JUMP   . INFDJI .TIE    .       .$
02441  02441  17 15777 15775
02442  02442  15 00300 34000    974.  .RETURN. TJ      .       .FILL   .$
02443  02443  30 01731 02444    975.  .TIE     . JN    .1031   .L+1    .$
02444  02444  30 15759 02571    976.  .        . JN    .ISTA   .1801   .$

02445  02445  30 00300 17473    977.  .        . JN    .       .MC     .$
02446  02446  30 15759 02426    978.  .        . JN    .ABSOLT .1302   .$
02447  02447  30 00300 15943    979.  .        . JN    .       .FL     .$
02450  02450  30 00300 00000    980.  .        . JN    .       .       .$
02451  02451  30 00300 00000    981.  .        . JN    .       .       .$
02452  02452  15 00300 02553    982.  .        . INFDJZ .      .MC     .$
02553  02553  11 00300 17435
02554  02554  17 17435 17473
                                983.  .        . JUB   .MOFVER .80     .ACTUALLY ***
                                984.  .        . TPMS  .5      .9      .$
                                985.  .        . INOUT .1      .1      .$
                                986.  .        . TJ    .       .FINST  .$

                                987.  . ERROR  . ALARM .       .       .$
                                988.  . EPIT   . TJ    .       .FILL   .$
                                989.  . ANS    . JN    .FILL   .FILL   .$
                                990.  . FU     . JN    .FILL   .FILL   .$
                                991.  . I      . EQUALS .9     .9      .$
                                992.  . DELT   . EQUALS .309   .309    .$
                                993.  . IML1   . EQUALS .310   .310    .$
                                994.  . IML2   . EQUALS .810   .810    .$
                                995.  . FIRST  . TP    .FO     .A      .$
                                996.  .        . EJ    .961    .L+3    .<1 IS ALWAYS 15
                                997.  .        . TU    .TMLB   .WPB    .$
                                998.  .        . TJ    .       .L+2    .$

                                999.  .        . TU    .TMLA   .WPB    .$
                                1000. .        . FD    .T      .DFL1   .$
                                1001. .        . TP    .Q      .J      .$
                                1002. .        . MZ    .INDOJP .       .$
                                1003. .        . FA    .Q      .<2     .<2 IS 0.7+927*
                                1004. .        . TV    .Q      .INTHR  .$
                                1005. .        . FS    .Q      .<2     .$
                                1006. .        . MZ    .Q      .       .$
                                1007. .        . FS    .Q      .J      .$
                                1008. .        . TN    .Q      .FRACT  .$
                                1009. .        . LQ    .INTGR  .A+1    .$
                                1010. .        . AT    .L+2    .L+2    .$
```

FIG. D-3 COMPUTER PROGRAM (Continued)

FIG. D-3 COMPUTER PROGRAM (CONTINUED)

FIG. D-3 COMPUTER PROGRAM (CONTINUED)

```
17304  17305  00 00000 00033  A  314.  .        .        .        .<31     .$
17306  17306  00 00000 00155  A  315.  .        .        .        .V01     .$
17307  17307  00 00000 00011  A  316.  .        .        .        .V1      .$
17310  17310  00 00000 00033  A  317.  .        .        .        .F1      .$
17311  17311  00 00000 00033  A  318.  .        .        .        .<2      .$
17312  17312  00 00000 00237  A  319.  .        .        .        .<11     .$
17313  17313  00 00000 00321  A  320.  .        .        .        .<21     .$
17314  17314  00 00000 00155  A  321.  .        .        .        .V01     .$
17315  17315  00 00000 00011  A  322.  .        .        .        .V1      .$
17316  17316  00 00000 00033  A  323.  .1       .        .        .        .$
17317  17317  00 00000 00033  A  324.  .        .        .        .        .$
17320  17320  00 00000 00033  A  325.  .        .        .        .        .$

17321  17321  00 00000 00033  A  326.  .        .        .        .        .$
17322  17322  00 00000 00033  A  327.  .        .F       .        .        .$
17323  17323  00 00000 00031  A  328.  .        .        .        .        .$
17324  17324  17 75333 36335  A  329.  .        .F       .        .33333   .$
17325  17325  00 05333 36335  A  330.  .        .F       .        .44447   .$
17326  17326  17 55333 36335  A  331.  .        .F       .        .44447   .$
                               A  332.  .        .INDSUB  .        .        .$
                               A  333.  .        .SUB     .        .80      .$CTUALLY ***
                               A  334.  .        .        .5       .0       .$
                               A  335.  .        .INCUT   .1       .1       .$
17335  17335  15 00000 17340    A  336.  .        .WJ      .        .FINST   .$
17336  17336  07 17330 17353    A  337.  .        .BLANK   .        .        .$

17337  17337  15 00000 36033    A  338.  .        .WJ      .        .FI--    .$
17338  17338  00 00000 36033    A  339.  .        .WD      .FILL    .FI--    .$
17339  17339  00 00000 36033    A  340.  .        .WD      .FILL    .FI--    .$
                               A  341.  .        .EQUALS  .5       .0       .$
                               A  342.  .        .EQUALS  .309     .309     .$
                               A  343.  .        .EQUALS  .313     .313     .$
                               A  344.  .        .EQUALS  .313     .313     .$
17340  17340  11 17337 36033    A  345.  .        .TP      .F0      .1       .$
17341  17341  15 17337 17344    A  346.  .        .SU      .X1      .L-3     .<1 IS ALWAYS 1
17342  17342  15 17374 17351    A  347.  .        .TU      .T-L3    .XP3     .$
17343  17343  15 00000 17345    A  348.  .        .WJ      .        .L-2     .$
17344  17344  15 17372 17351    A  349.  .        .TU      .T-L4    .XP3     .$

17345  17345  67 00010 00455    A  350.  .        .FU      .T       .DEL1    .$
17346  17346  11 51000 15435    A  351.  .        .TP      .0       .J       .$
17347  17347  35 10000 00033    A  352.  .        .WF      .10000000.        .$
17350  17350  44 51000 17370    A  353.  .        .FA      .0       .<2      .<2 IS 0.7***
17351  17351  15 51000 17371    A  354.  .        .TV      .0       .INTGR   .$
17352  17352  55 51000 17370    A  355.  .        .FS      .0       .<2      .$
17353  17353  35 00000 00033    A  356.  .        .WF      .0       .        .$
17354  17354  55 51000 15436    A  357.  .        .FS      .0       .J       .$
17355  17355  13 51000 15437    A  358.  .        .TN      .0       .FRACT   .$
17356  17356  35 17371 36017    A  359.  .        .LO      .INTGR   .8+15    .$
17357  17357  15 17351 17351    A  360.  .        .AT      .L-2     .L-2     .$
17360  17360  75 00000 17362    A  361.  .        .RPB     .2       .L-2     .$
```

FIG. D-3 COMPUTER PROGRAM (CONTINUED)

```
17361  17361  11 30000 17374  X  362.  . AMB  . TP    .FILL   .FA     .$
17362  17362  36 31000 17361  X  363.  .       . ST    .Q      .L-1    .$
17363  17363  65 17375 17374  X  364.  .       . FS    .FB     .FA     .$
17364  17364  01 15437 17374  X  365.  .       . FP    .FRACT  .FA     .$
17365  17365  11 31000 17336  X  366.  .       . TP    .Q      .ANS    .$
17366  17366  45 00000 17335  X  367.  .       . AJ    .       .EXIT   .$
17367  17367  00 00000 00001  X  368.  . K1    . X     .1      .       .$
17370  17370  23 36000 00000  X  369.  . K2    . 323   .36000  .00000  .$
17371  17371  00 00000 00000  X  370.  . INTGR . 300   .       .       .$
17372  17372  00 00436 00000  X  371.  . TBLA  .       .TBL1   .       .$
17373  17373  00 00632 00000  X  372.  . TBLB  .       .TBL2   .       .$
17374  17374  00 00000 00000  X  373.  . FA    . 00    .       .       .$


17375  17375  00 00000 00000  X  374.  . FB    . 00    .       .       .$
                              X  375.  .       . ENDSUB .      .       .$
                              X  376.          SUB     ARF074          74 WORDS
                              X  377.          SUB     ARF051         334 WORDS
                              X  378.          SUB     ARF052          51 WORDS
                              X  379.          SUB     ARF054         200 WORDS
                              X  380.          SUB     ARF055          24 WORDS
```

FIG. D-3 COMPUTER PROGRAM (CONTINUED)

RECOIL MASS - -CARRIAGE INERTIA, RATE, DAMPING COEFF. - -ELEVATING SYSTEM PRELOAD, RATE, DAMPING COEFF.
CAM:BEGINNING :CAM: END- -CONST. RECOIL FRICTION- -ELEVATION- -SEAL FRICT.- -BRG. FRICT. COEFF.- -REC. PRELOAD- -TRIGGER

3.2749000	1.1500000 02	3.5000000 07	0.	0.	1.0000000 06	1.0000000 02	
1.0900000 01	1.0400000 01	5.0000000 02	6.0000000 01	3.0000000-02	3.0000000-02	1.3750000 03	2.1900000 01

TIME DELTA T	PHI-1 AXIAL CAM ROLNO NUMBER	PHI-2 TANGENT. CAM RECOIL DIST.	U MOMENT REACT CRADLE ROT.	PHI-1-DOT NORMAL REACT RECOIL FRICT	PHI-2-DOT SPRING FORCE PADR CPL ARM	U-DOT DAMP. FORCE	RECOIL FORCE POWDER FORCE
1.0000000-03 1.0000000-03	3.3608951-06 0. 1.0000000	-4.2535176-06 0. -4.1484833-05	2.9899941 01 -3.7732409 04 -8.9261948-07	1.1379850-02 1.3451141 03 3.0000033 02	-1.4833679-02 -8.0816833 01 6.3300000-01	4.0109433-02 -2.7424370 01	6.7076888-04 2.9509000 04
1.1000000-02 1.0000000-03	9.3377762-04 0. 1.0000000	-4.8116867-04 0. 1.4718320	2.8428111 01 -1.7768294 04 4.5260913-04	4.8903319-01 3.4067706 03 9.1994973 02	-1.7653939-01 -9.1422010 03 6.3300000-01	-3.3698588 02 -3.3541728 02	8.2599147 03 9.2756001 04
2.1000000-02 1.0000000-03	5.1597353-03 0. 1.0000000	-8.2101478-04 0. 9.4300531	2.4462983 01 9.2367794 04 4.2387210-03	3.4903055-01 3.4520415 03 1.2491818 03	1.3187259-01 -1.7499241 04 6.3300000-01	-4.1172440 02 2.8855793 02	1.5382839 04 9.1799984 03
3.1000002-02 1.0000000-03	1.3381546-02 0. 1.0000000	-4.2098960-04 0. 9.2445675	2.0657629 01 8.3802216 04 1.2954977-02	9.1396476-01 3.1469436 02 1.2293096 03	1.0675183-01 -8.1052025 03 6.3300000-01	-3.5193110 02 3.1682047 02	1.4587394 04 0.
4.1000004-02 1.0000000-03	2.3337765-02 0. 1.0000000	4.5135206-04 0. 1.2480541 01	1.7419455 01 -2.6223031 04 2.3789117-02	9.8972490-01 -4.1760146 03 1.1074955 03	4.5349411-02 8.5756492 03 6.3300000-01	-2.9917397 02 9.6163881 01	1.3957110 04 0.
5.1000005-02 1.0000000-03	3.1[illegible]-02 0. 1.0000000	1.2397262-03 0. 1.5281229 01	1.4618789 01 -1.6552844 05 3.2413079-02	9.9619498-01 -9.2675810 03 1.2264262 03	-1.4345615-02 2.3554797 04 6.3300000-01	-2.6031170 02 -2.3457049 01	1.4689164 04 0.
6.1000007-02 1.0000000-03	3.3752299-02 0. 1.0000000	1.3000103-03 0. 1.7742877 01	1.2177108 01 -2.0240789 05 3.5118306-02	-7.2214451-02 -5.4215166 03 1.2994466 03	-5.7805299-03 2.5954196 04 6.3300000-01	-2.2675348 02 -1.0983067 01	1.5996933 04 0.
7.1000008-02 1.0000000-03	3.0020994-02 0. 1.0000000	8.5709606-04 0. 1.9790382 01	1.0109600 01 -1.2468126 05 3.0878084-02	-9.7462122-01 -2.8199955 03 1.3572229 03	-3.3675175-02 1.0284825 04 6.3300000-01	-1.8595813 02 -4.3982833 01	1.7144459 04 0.

FIG. D-4 COMPUTER OUPUT FORMAT

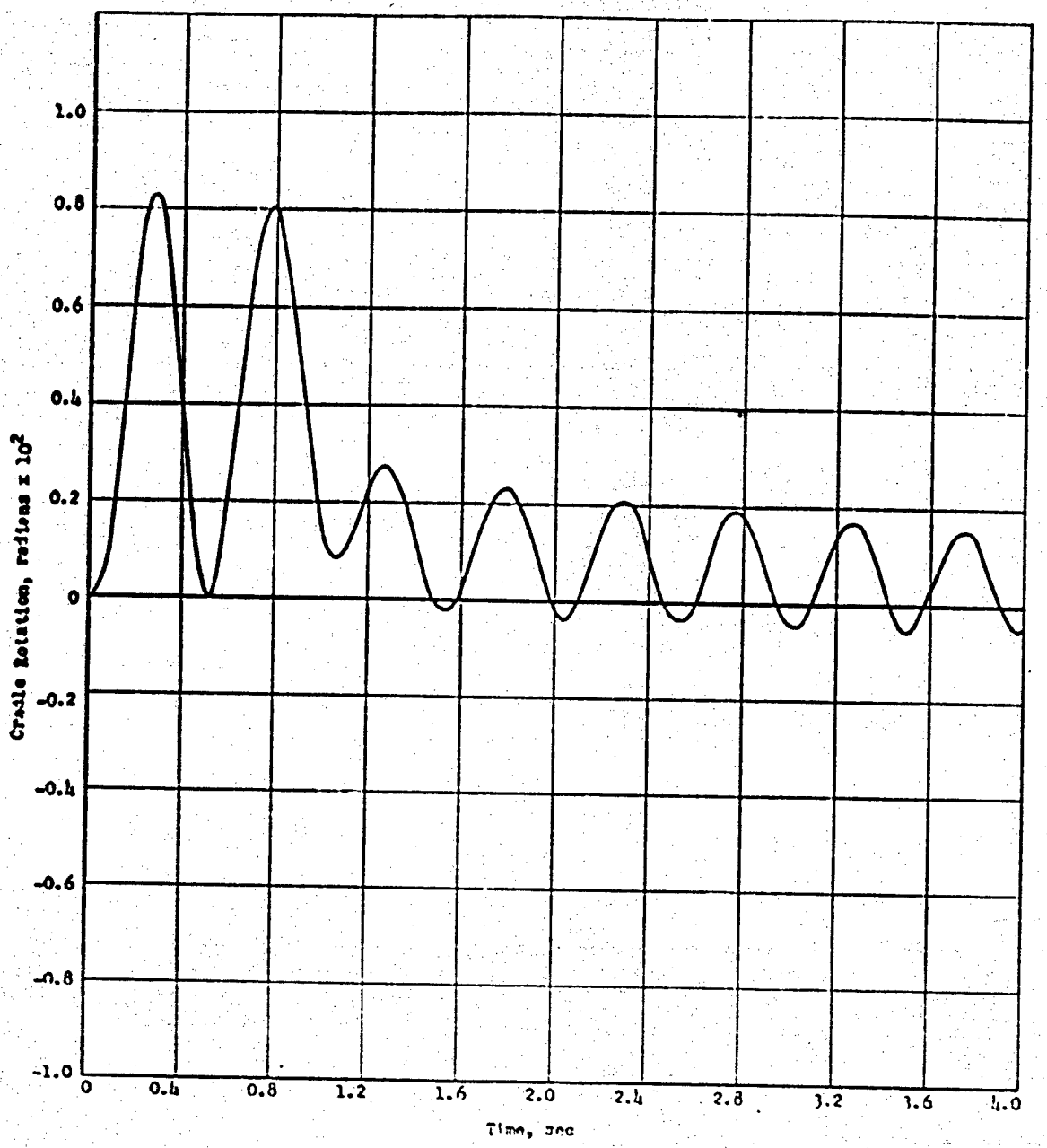

Fig. D-5 LAUNCHER RESPONSE FROM EARLY COMPUTER PROGRAM

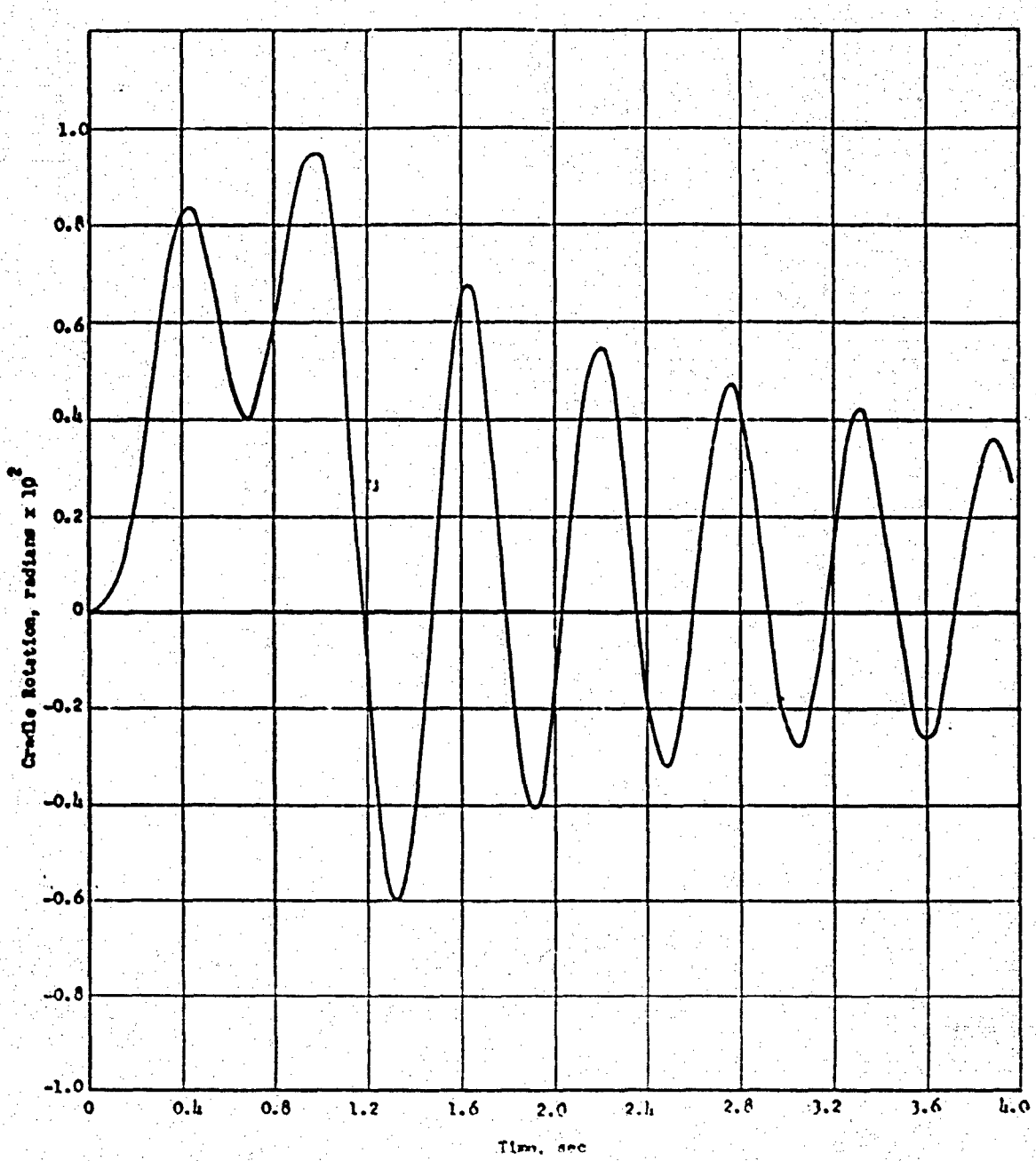

Fig. D-6 LAUNCHER RESPONSE FROM PRESENT COMPUTER PROGRAM

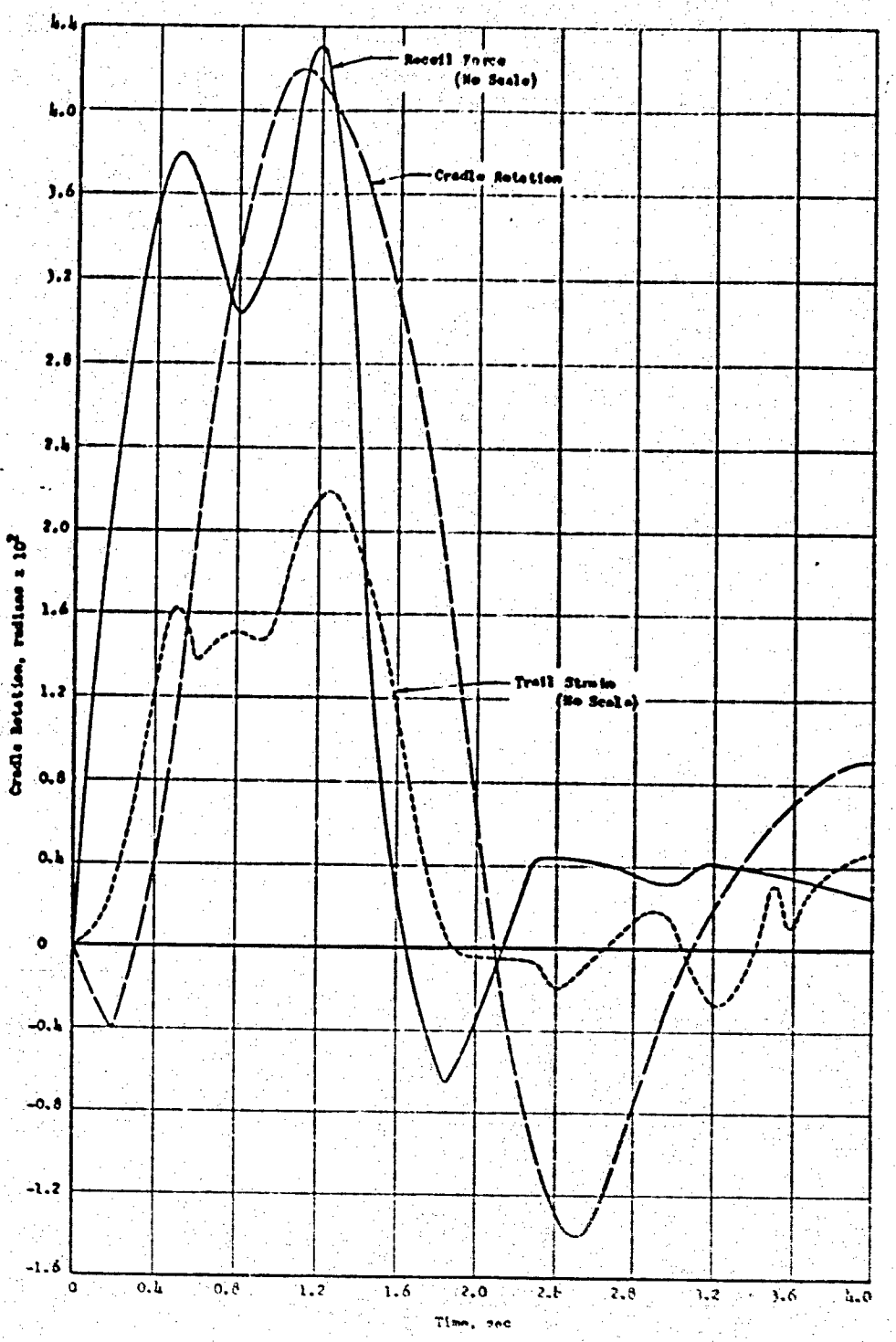

Fig. D-7 EXPERIMENTAL LAUNCHER RESPONSE

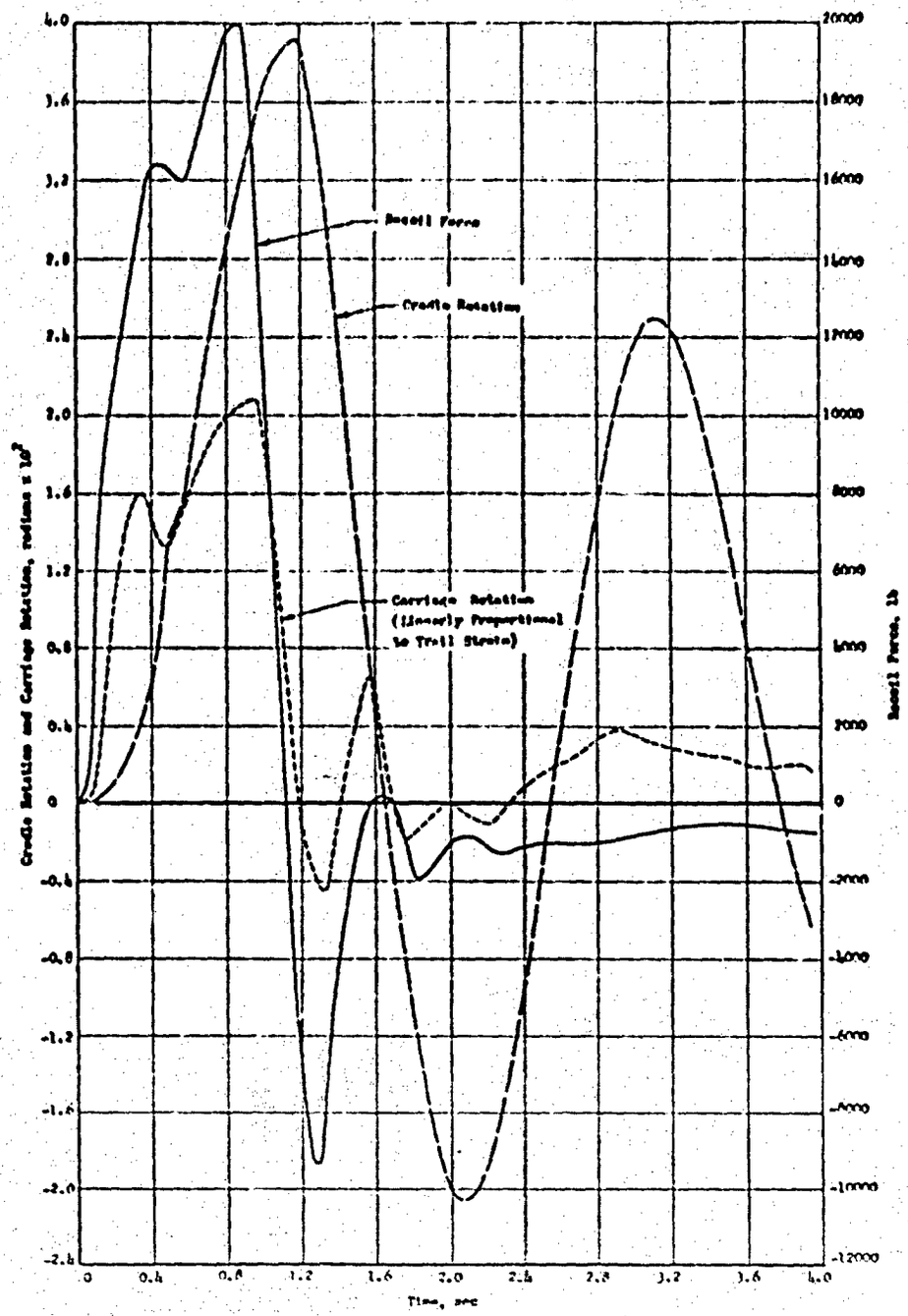

Fig. D-8 LAUNCHER RESPONSE FROM PRESENT COMPUTER PROGRAM CORRESPONDING TO EXPERIMENTAL RESPONSE

APPENDIX E

OPTIMUM ELEVATING SYSTEM PARAMETERS

Coleen Murray

I. INTRODUCTION

The purpose of this study was to determine the effects of various combinations of elevating system stiffness and damping upon gross launcher motion and to find the optimum combination of such stiffness and damping. The optimum combination was defined as that combination which yields a consistently low value of cradle displacement prior to the firing of each of the successive rounds of a burst and which concurrently yields a minimum corresponding cradle velocity. The work was based on the assumption that cradle oscillations sustained during a burst firing contribute directly to launching errors that cause dispersion of the shots of a burst. This study is concerned primarily with cradle motion, although barrel motion relative to the cradle is also a major cause of launching errors.

This study utilizes the work of Philip Meyfarth [1/] in order to define the general area of optimum damping for a given stiffness. Optimization of Meyfarth's third-order system yielded an optimum damping coefficient for any given elevating system stiffness. The damping determined by Meyfarth's work was used to indicate a value about which the damping should be varied in the Model V solutions in order to obtain the actual optimum. The ranges of optimum damping thus obtained for the several values of stiffness were then compared to each other, and a range of optimum stiffness, with corresponding optimum damping, was chosen. The third-order system was used because of the availability of the response data in the reference and the resulting simplification of the optimization procedure for the three-degree-of-freedom computer solution.

A few variations of equivalent carriage stiffness for the optimum elevating system were also investigated to determine the effect of this stiffness

---

1/ Meyfarth, P., Dynamic Response Plots and Design Charts for Third-Order Linear Systems, Research Memo No. R. M. 7401-3, Massachusetts Institute of Technology, 1958.

on cradle motion and trail hop, which is the upward deflection of the trails observed during firing of the XM70E1 launcher when the recoiling assembly is in its extreme recoil position. The values of launcher parameters maintained constant in the study are those of the XM70E1 Prototype No. 3 launcher at 0° traverse and 45° elevation.

II. DISCUSSION

A. Third-Order Analysis

The angular motion of the launcher was approximated by the motion of the following linear system with the proper conversion of units:

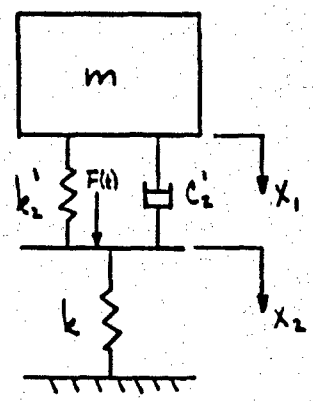

Fig. E-1 MODEL OF THIRD-ORDER SYSTEM

where

m	is an equivalent mass moment of inertia of the tipping parts about the trunnion, 7500 in.-lb-sec^2
k'_2	is the equivalent angular stiffness of the elevating system
c'_2	is the equivalent angular damping coefficient of the elevating system
k	is the combined angular stiffness of the carriages and trails, 3.5×10^7 in.-lb/radian
F(t)	is a forcing function applied to the trunnion.

The equation of motion for m is:

$$m\ddot{x}_1 = -k'_2(x_1 - x_2) - c'_2(x_1 - x_2) \qquad \text{E-1}$$

From the statics at x_2, we have:

$$kx_2 = k'_2(x_1 - x_2) + c'_2(x_1 - x_2) + F(t) \qquad \text{E-2}$$

By eliminating x_2 from E-1 and rewriting in terms of differential operators, one obtains:

$$D^3 x_1 (c'_2) + D^2 x_1 (k + k'_2) + D x_1 (c'_2 k/m) + x_1 (k \cdot k'_2/m)$$
$$= (c'_2/m)\ D\ \left[F(t)\right] + (k'_2/m)\ \left[F(t)\right] \qquad \text{E-3}$$

The left-hand side of Eq. E-3 may be factored into three factors, each representing a root of the system*. When two of these roots are complex conjugates, the parameters τ, ω, and ξ may be defined by the following equations:

$$\frac{c'_2 m}{k k'_2} = \frac{\tau}{\omega^2} \qquad \text{E-4a}$$

$$\frac{(k + k'_2)m}{k k'_2} = \frac{(2\xi\tau\omega + 1)}{\omega^2} \qquad \text{E-4b}$$

$$\frac{c'_2}{k'_2} = \frac{(\tau\omega + 2\xi)}{\omega}, \qquad \text{E-4c}$$

where

τ is the constant of the factor representing the real root

ξ is the damping ratio associated with the complex-conjugate pair

ω is the undamped natural frequency associated with the complex-conjugate pair.

Let the right-hand side of Eq. E-3 be an impulse function of strength I; then, the solution of Eq. E-3 is:

---

* For a complete discussion of the following technique consult Meyfarth, Reference 1.

$$\frac{k\,k'_2}{m\omega^I}\; y(\omega t) = \frac{1}{\frac{1}{\tau\omega} - 2\xi + \tau\omega}\left\{ e^{-t/\tau} + e^{-\xi\omega t} \cdot \left[\frac{\left[\frac{1}{\tau\omega} - 2\xi\right] + \xi}{\sqrt{1-\xi^2}} \sin\sqrt{1-\xi^2}\;\omega t - \cos\sqrt{1-\xi^2}\,\omega t \right] \right\} \qquad \text{E-5}$$

The first of the two terms in the right-hand side of Eq. E-5 is an inverse exponential which decreases with increasing time; the second is the product of an inverse exponential and a sinusoidal function. The sinusoidal function will decay in the shortest time when the values of the coefficients of t in the exponents are minima. The values of τ, ω, and ξ which appeared to yield the best damping were chosen from the graphs in Reference 1 and the corresponding value of damping was then evaluated.

Figure E-2 shows the response for several values of k'_2 with the corresponding optimum damping. The angular stiffness and angular damping coefficient, k'_2 and c'_2, were converted to values corresponding to linear restraints by multiplying by 10^{-3} (the inverse of the square of the distance from the trunnion to the elevating screw bracket).

The following comments are made on the statement preceeding Equation E-4a, concerning the pair of complex roots. Large values of stiffness always result in two of the roots being complex conjugates. However, below a certain stiffness it is possible to get three real roots for some ranges of damping. Furthermore, as the stiffness decreases, there is an increase in the range of damping which causes this. When these damping values were used as input to the computer solutions, they resulted in a continuously increasing (non-oscillatory) displacement, as shown in Figure E-3.

B. Computer Solutions

Initially, the computer solutions were investigated for the combined carriage and trail stiffness of 45×10^6 in.-lb/radian, which is about 30% higher than the measured stiffness. A range of very good response was found for stiffness of 1.0×10^4 lb/in. and damping of 360 to

540 lb-sec/in. Several graphs of cradle rotations resulting from paired values of stiffness and damping in this range are shown in Fig. E-4. The choice of an optimum combination here would be arbitrary because, at the time of each succeeding firing, the cradle displacement is uniform (Fig. E-5) and the velocity is small for all of the responses.

To illustrate that this optimum system is an improvement, its response is compared in Fig. E-6 with a response similar to that of the present weapon (with little damping). Also shown is an over-damped response, to demonstrate that an optimum damping does exist.

It was realized that there were limits on the obtainable values of stiffness and damping in the elevating system. Very high stiffness was shown to be difficult to achieve in previously built launchers, and extremely low stiffness presents a problem of stability during sighting and also is subject to excessive preload deflections. Comparison of experimental and analytical results indicates that damping corresponding to at least 90 lb-sec/in. is inherent in the launcher system; thus, no smaller damping is feasible.

Next, a much lower stiffness with increased damping was investigated to discover if cradle rotation would thus be decreased. Fig. E-3 shows that for damping between the non-oscillating range up to the maximum damping used, increased damping gives better response. Nevertheless, these responses are not as good as those with the higher spring rate (see Fig. E-7 for comparison). Also, the study of a 4-rd burst (Fig. E-8) showed that cradle rotation increased with each round.

Finally, the computer solutions were investigated for the combined carriage and trail stiffness of 35×10^6 in.-lb/radian; this is very close to the experimental value for Prototype No. 3. Although the initial maximum cradle rotation was somewhat greater than for the stiffer structure, the range of good response was similar. The optimum response still occurred for a stiffness of 1.0×10^4 to 1.4×10^4 lb/in. and damping of 360 to 540 lb-sec/in.

Trail hop was significantly affected by the carriage stiffness, k_1, as shown in Fig. E-9, which is a plot of the cradle rotation for three systems with otherwise identical parameters. The maximum negative

rotation at about 0.2 sec of the supporting structure is an indication of the relative magnitude of the hop, illustrating that trail hop greatly decreases with increasing carriage stiffness.

During the course of the study, it was noted that the optimum damping determined from the computer solutions agreed with the optimum predicted by the third-order analysis, where linear stiffnesses from 1.0×10^4 to 1.4×10^4 lb/in. corresponded to optimum damping from 460 to 510 lb-sec/in. Such close agreement was interesting and unexpected, in that the Model V equations include the actual input force, cam path, and many nonlinear launcher effects not considered in the third-order system.

III. CONCLUSIONS

On the basis of the investigations described above, it is concluded that improved firing accuracy can be achieved for the system studied by adding damping to the elevating system. Specifically, the stiffness of the elevating system should be about 1.0×10^4 to 1.4×10^4 lb/in. and the damping of the elevating system should be about 360 to 540 lb-sec/in., for the maximum improvement.

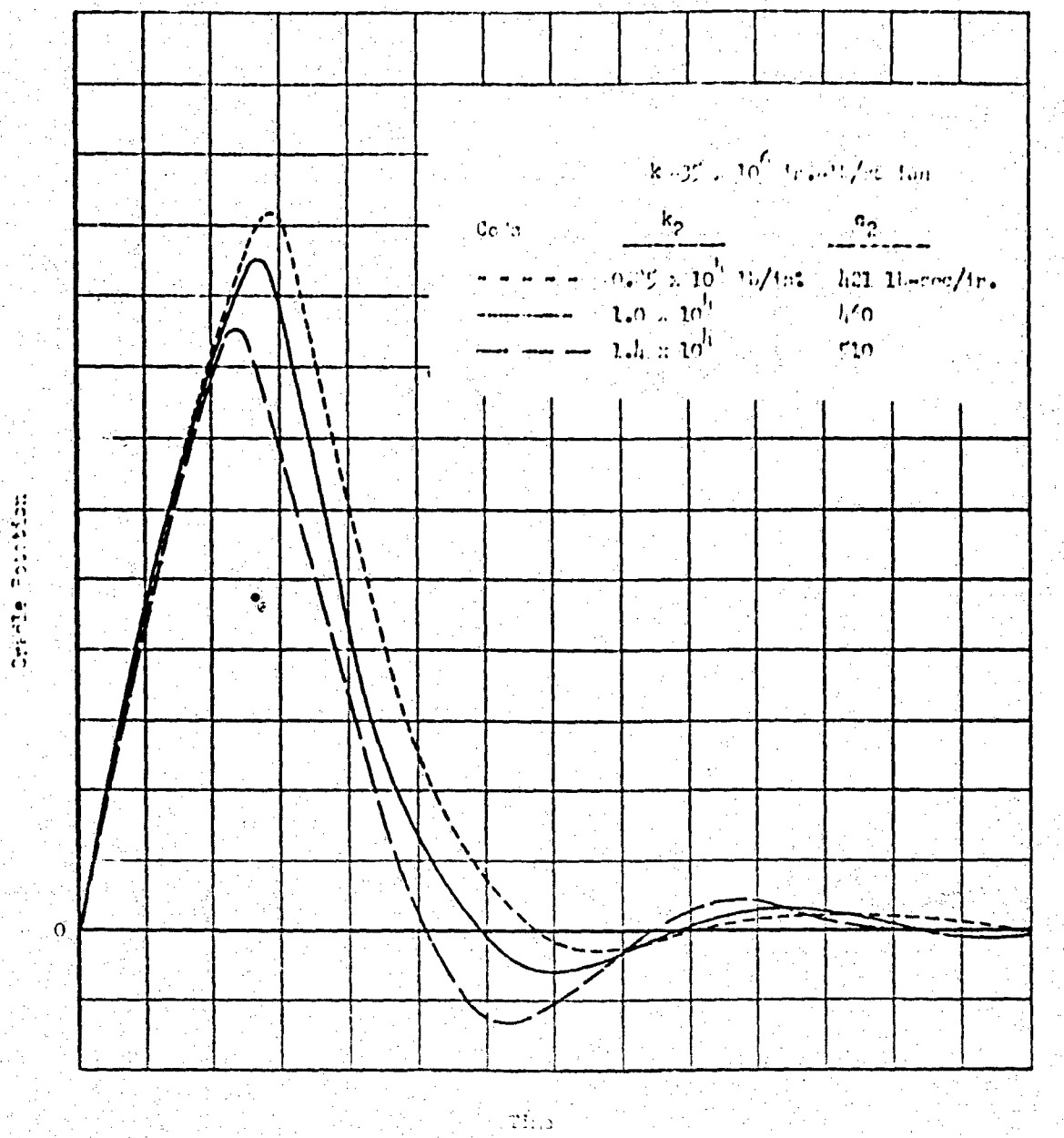

Fig. E-2 CRADLE ROTATION FROM THIRD-ORDER SYSTEM ANALYSIS

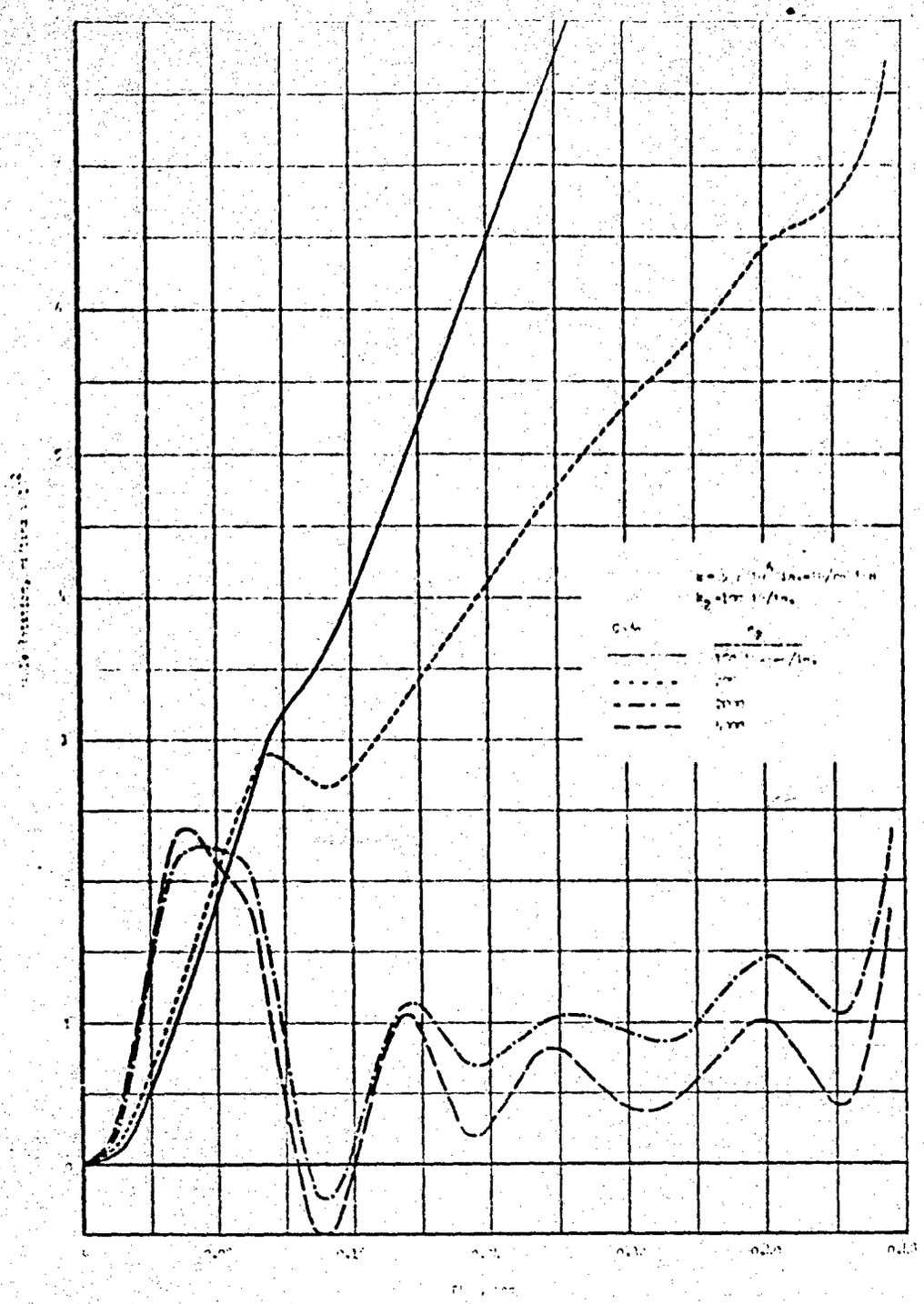

Fig. E-3 EFFECTS OF DAMPING ON CRADLE ROTATION WITH LOW ELEVATING SYSTEM STIFFNESS

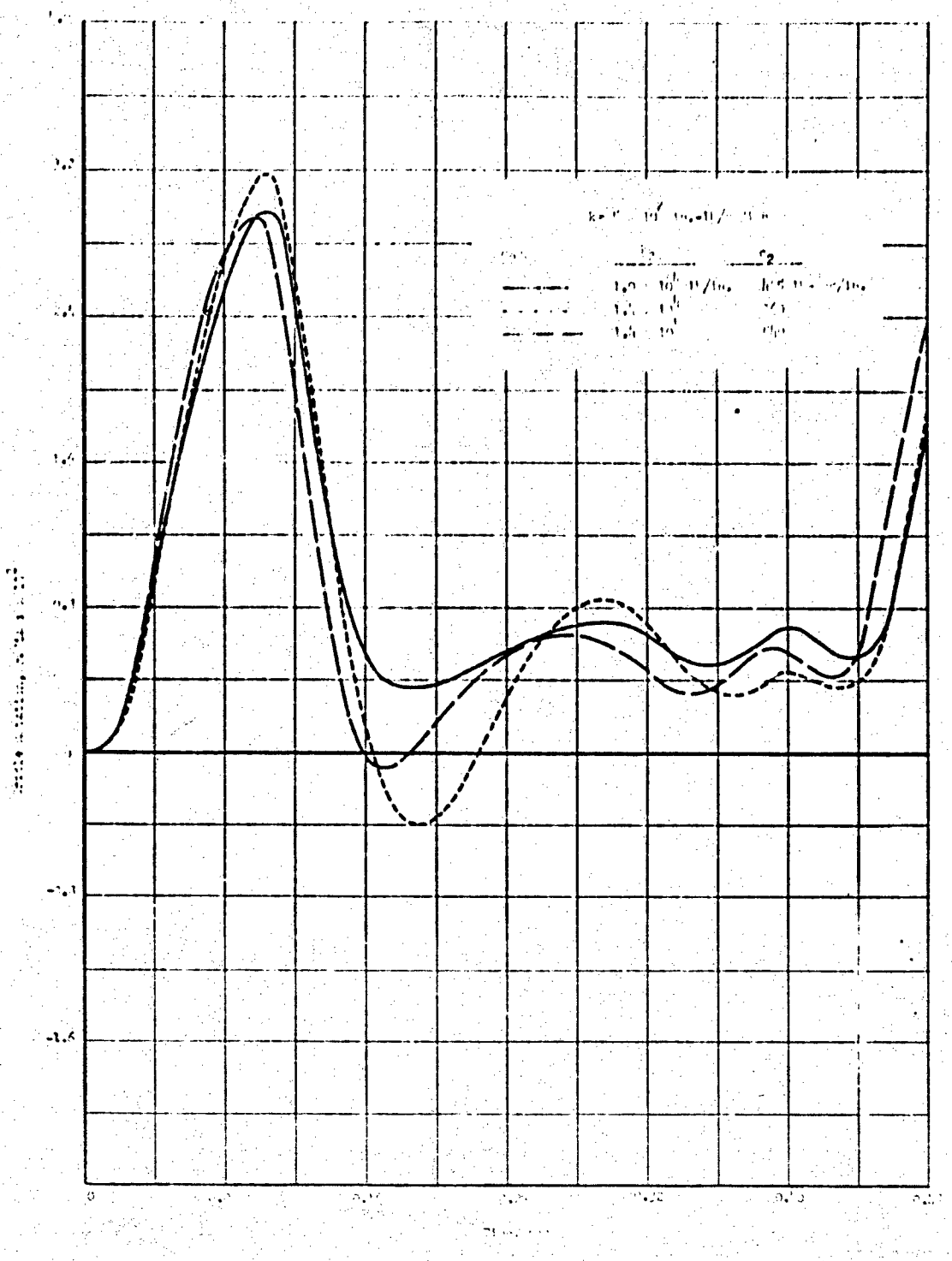

Fig. E-4 OPTIMUM RESPONSES

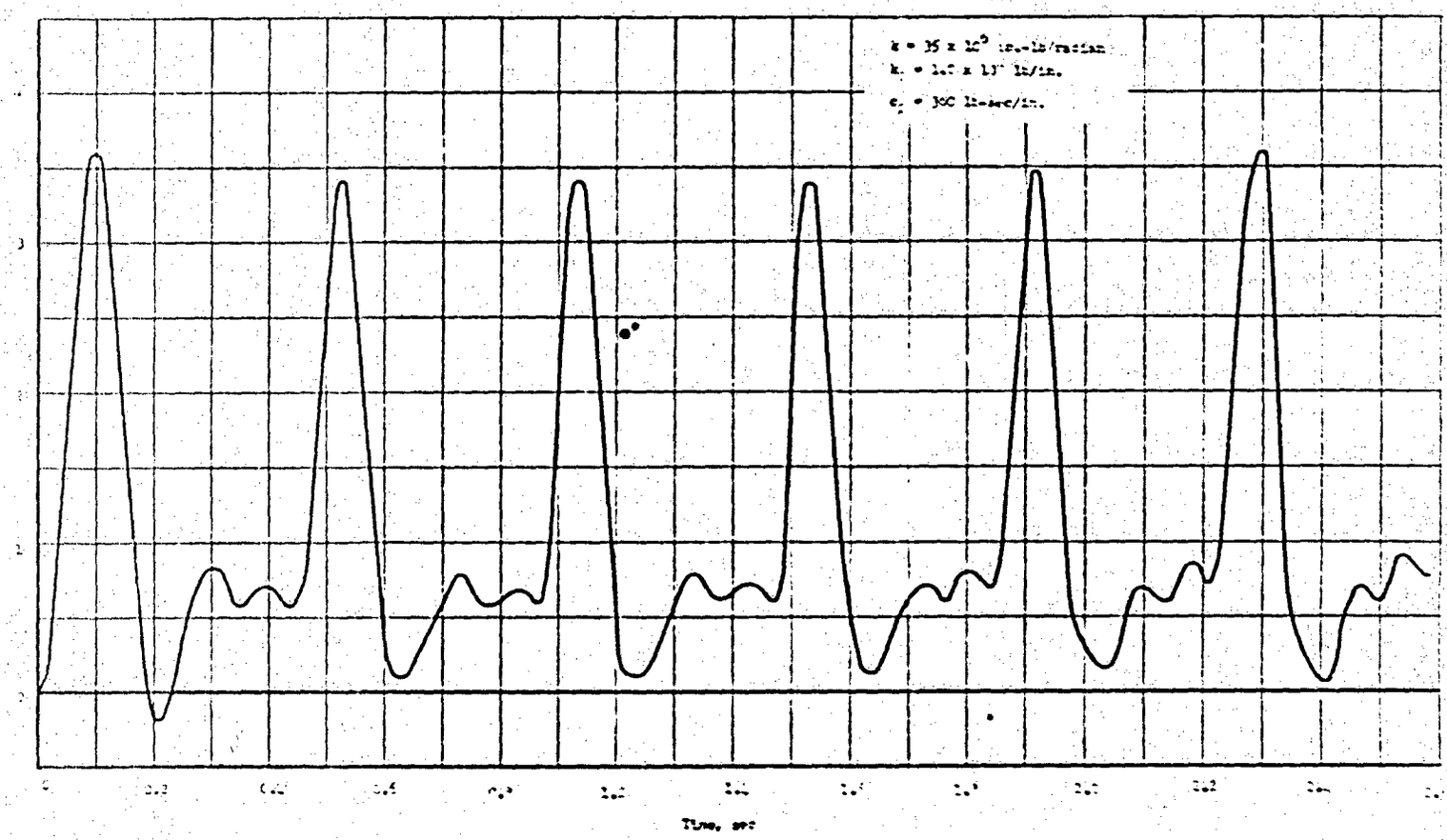

Fig. E-5 CRADLE ROTATION FOR A 6-RD BURST WITH OPTIMUM ELEVATING SYSTEM

ARMOUR RESEARCH FOUNDATION OF ILLINOIS INSTITUTE OF TECHNOLOGY

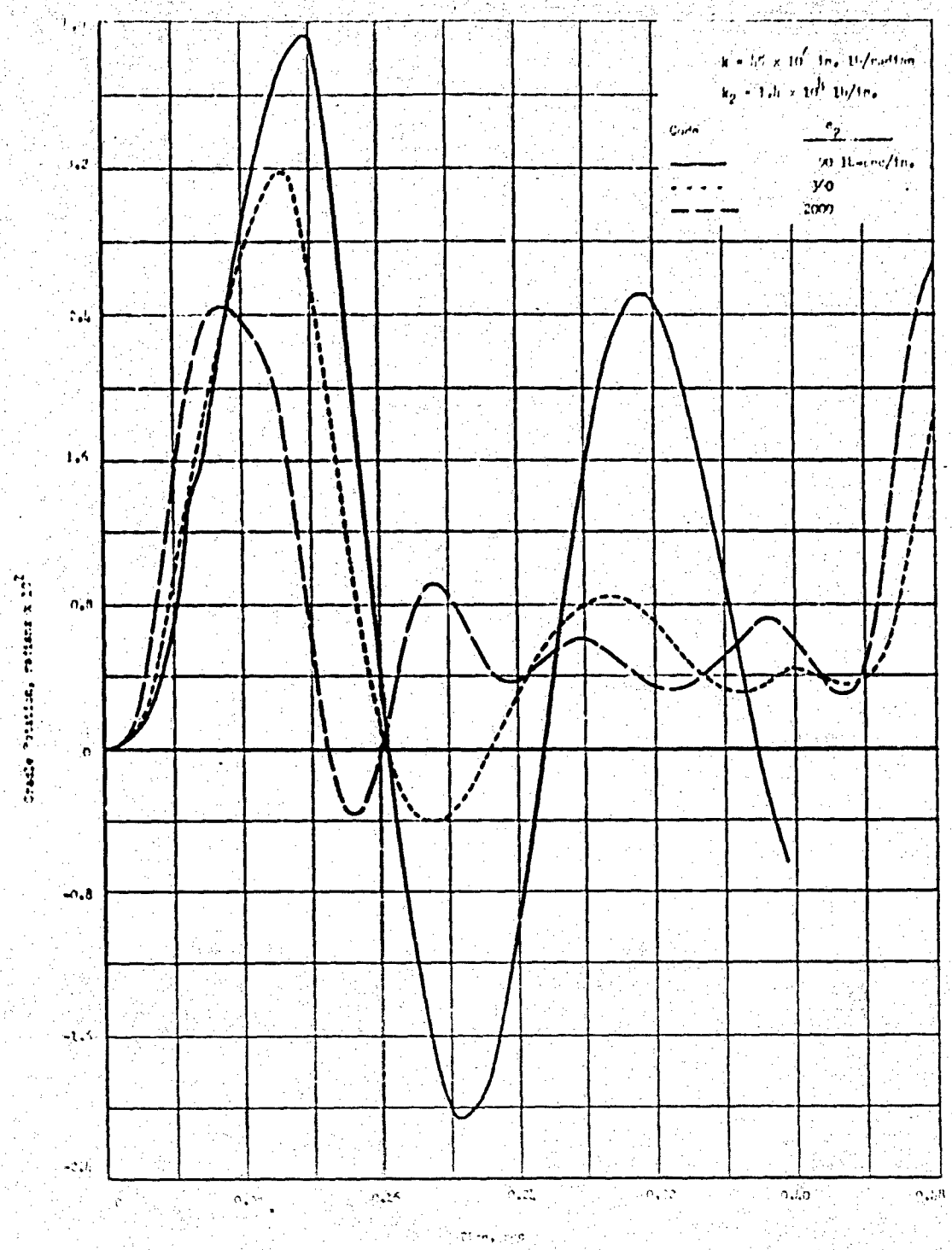

Fig. E-6 RESPONSES FOR VARIOUS ELEVATING SYSTEM DAMPING COEFFICIENTS

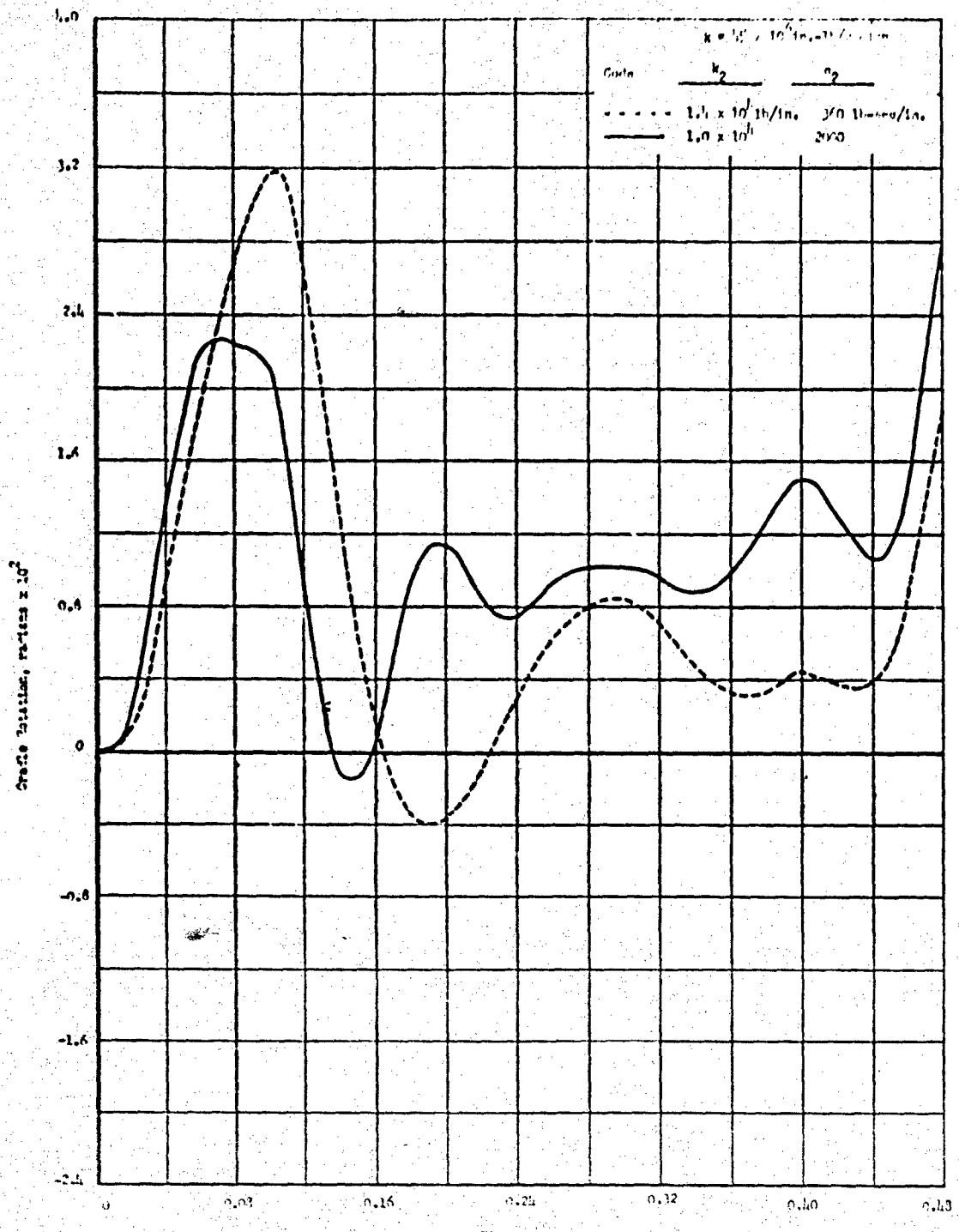

Fig. E-7 COMPARISON OF CRADLE ROTATION FOR A LOW ELEVATING STIFFNESS TO AN OPTIMUM SYSTEM

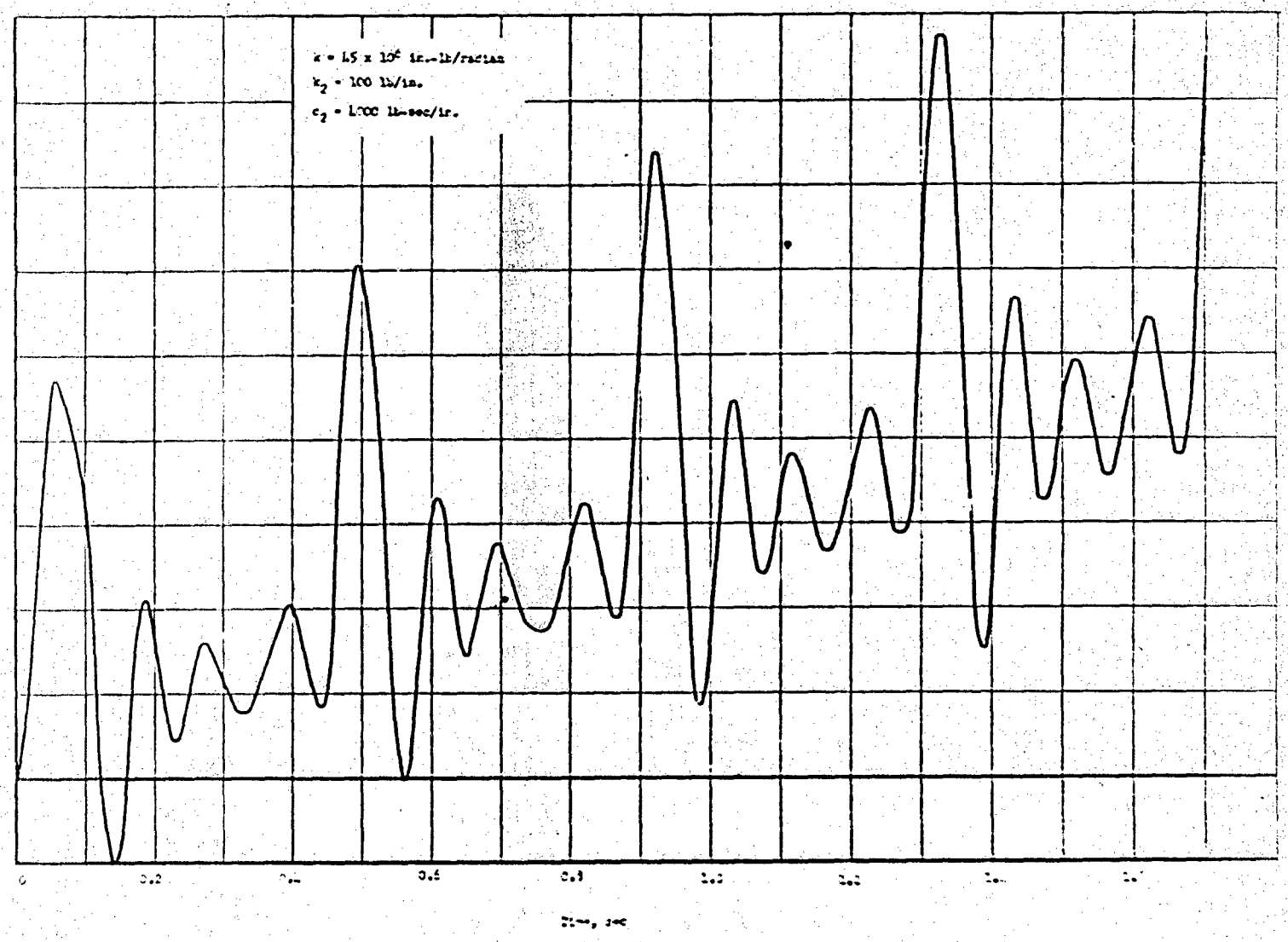

Fig. E-8 **CRADLE ROTATION FOR A 4-RD BURST WITH LOW ELEVATING SYSTEM STIFFNESS**

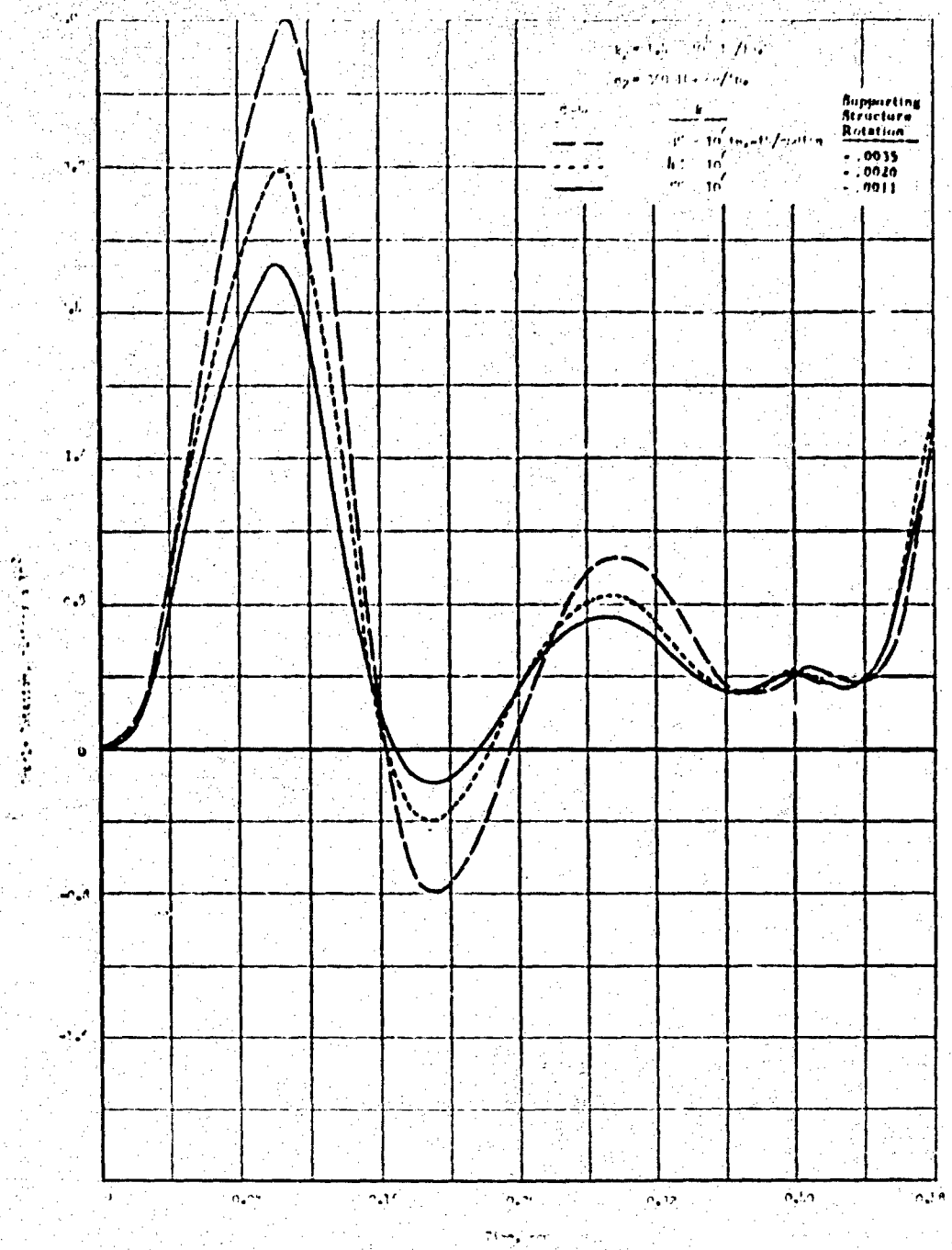

Fig. E-9 EFFECT OF CARRIAGE STIFFNESS ON CRADLE ROTATION

APPENDIX F

GENERAL EQUATIONS OF MOTION OF LAUNCHER DYNAMICS

I. INTRODUCTION

The 3-degree-of-freedom model, presented in Appendix C, was programmed for a digital computer and has been used extensively. As a 3-degree-of-freedom model, it has the advantage of relative simplicity and also reproduces much of the primary behavior of the XM70-type launcher. On the other hand, the very simplicity precludes its application to many of the presumedly secondary features of the launcher. In order to study these features, a more complete model with up to n-degrees of freedom was constructed.

The following are some of the salient features of this more complete model that are present in addition to the features of the 3-degree-of-freedom model:

1. The base of the launcher is not assumed to be fixed to a rigid foundation; instead, the trail pads and base plate are placed on visco-elastic supports which can be assigned parameter values corresponding to various terrain compositions (clay, sand, concrete, etc.). The model takes cognizance of the fact that this may be a one-way support condition so that trail hop and base hop are directly reproduced. Should the need arise, the model can be easily altered to reproduce progressive trail dig-in and base settlement.
2. It is recognized that the launcher does not recoil straight back, maintaining its position in its initial vertical plane. The tendency for three-dimensional rotation about the ball joint is allowed for. Reaction forces and moments at the ball joint, the trunnion supports, the cradle, and the recoiling parts are admitted as three-dimensional quantities.
3. The flexibility of the recoiling assembly is provided for, as are the lateral and vertical variations of center of gravity and inertial force location from shot to shot. The additional features allow the reproduction and study of the "left-right sequencing" phenomenon observed in tests of the XM70 prototype launchers.
4. The transmission of rifling torque to the launcher structure is included, as are the force parameters and geometrical freedoms necessary for interpretation of its effect.

5. The rifled firing tube is represented as a flexible piece with many degrees of freedom in both the vertical and horizontal planes. This permits the investigation of tube whip and vibrations and their effect on both the supporting structure and the projectile.

6. The projectile itself is a part of the model. The resultant effects include the variation of mass during firing and the influence of traveling forces on launcher tube motion.

7. A result of the inclusion of the increased geometrical freedom and applied forces is the introduction of Coriolis forces (in three dimensions) and gyroscopic moments not previously considered. An additional result is the inclusion of more of the coupled effects of the motion of the various launcher components.

This appendix presents a summary of the derivation of the basic equations of this model, as well as graphical and verbal definitions of the known and unknown parameters involved with the basic equations that govern the model. The motion of the launcher can be best expressed in terms of a set of interdependent right-hand three-dimensional coordinate systems, as shown in Fig. F-1. Coordinate system 1 ($[S_1]$) is fixed in the earth at the trail pads with y_1 vertical. Then, x_1 is defined by a plane through y_1 and the initial tube centerline. Systems $[S_2]$ and $[S_3]$ have origins at the ball joint and arise from a translation and a rotation through angle $(\theta_1 + \theta_2)$ and the x_1, y_1 plane. Angle θ_1 is a measure of trail flexibility, while angle θ_2 os a ball-joint rotation. System $[S_4]$ arises through a rotation through angle θ_3 about y_3. Thus, y_4 coincides with y_3. System $[S_5]$ arises through a rotation through angle θ_4 about x_4; x_5 coincides with x_4. It is apparent that θ_3, θ_4, θ_5, represent freedoms at the ball joint. We arrive at $[S_6]$ by means of a translation through distance ℓ_2 and a rotation through angle $\alpha + \theta_5$; the origin of $[S_6]$ is at the trunnions. The angle α is the angle of elevation and θ_5 is the freedom in elevation permitted by the flex system. The tube base is located a distance ℓ_7 along the x_6 axis. Left-right sequencing forces the tube to swing through an angle θ_6 about an axis parallel to y_6. In addition to coordinate systems, Fig. F-1 illustrates many of the quantities which are defined on the following pages and which appear in the equations.

II. SPECIFIED QUANTITIES

ℓ_1	trail length
ℓ_2	carriage side length
ℓ_3	trunnion-to-cradle center of gravity
ℓ_4	ball joint to flex attachment
ℓ_5	y_6-position of breech center of gravity
ℓ_6	z_6-position of breech center of gravity
ℓ_7	distance from breech center of gravity to tube base
L	tube length
u_o	initial x_6-position of breech center of gravity
α	elevation angle
ξ_0	initial projectile position with reference to tube base
ℓ_8	distance from trunnion to flex attachment point
ℓ_9	horizontal (z_6) distance of cluster axle from tube centerline
β_1	carriage side orientation
β_2	flex system orientation
I	tube moment of inertia $= \frac{\pi}{4}(r_2^4 - r_1^4)$
ρ	tube mass density per unit length
m_p	projectile mass
J_x, $J_y = J_z$	mass polar inertial moments of projectile
$\varphi(t)$, $\varphi = \varphi^*$, $\varphi = \xi_9$	prescribed projectile spin history
m_B	breech mass

J_{Bx}, J_{By}, J_{Bz}	mass polar inertial moments of breech
m_A	cradle mass
I_{Ax}, I_{Ay}, I_{Az}	mass polar inertial moments of cradle
m_1	concentrated mass at rear of trails (one-half trail mass)
I_{xc}, I_{yc}, I_{zc}	mass polar inertial moments of carriage about ball joint
m_B	one-half mass of trails plus mass of carriage and trunnion sides concentrated at ball joint
m_r	mass of right ($+ z_o$) cluster and projectiles
m_l	mass of left ($- z_6$) cluster and projectiles
k_1, γ_1	spring and damping constants at trail rear
k_2, γ_2	spring and damping constants at trail front
k_3	angular trail and carriage stiffness (z-axis)
k_4	carriage stiffness for torque about y-axis
k_5	carriage stiffness for torque about x-axis
k_6, γ_6	spring and damping constants for flex system
E	Young's modulus (3×10^7)
μ	coefficient of friction between breech and cradle
F(t)	resultant "powder-gas force"
k_8	breech "stiffness" for right-left sequencing
V_n	eigen values

b_n	wave numbers $b_n^4 = \frac{\rho}{EI} V_n^2$
	$L\, b_1 = 1.875$
	$L\, b_2 = 4.694$
	$L\, b_3 = 7.855$
	$L\, b_4 = 10.996$
	$L\, b_5 = 14.137$
	$L\, b_6 = 17.279$
K	recuperator preload
k_7	recuperator spring rate
H_1	constant recuperator friction force
γ	oil density
A_p	piston area
C_o	orifice coefficient
$\alpha_o(u)$	orifice area
g	acceleration of gravity
δ	proportionality constant; seal friction to recoil force
I_B	cluster inertia moment
R_p	cam pitch radius
h	height of cam path development
u_1	initial cam engagement point $\Big\}$ $u_1 \leq u \leq u_2$
u_2	final cam engagement point

III. LOGICAL SYMBOLS

$$H(\xi) = \begin{cases} 0 \text{ for } \xi \leq 0 \\ 1 \text{ for } \xi > 0 \end{cases} \quad (\xi \text{ generic})$$

$$\epsilon = \begin{cases} 1 \text{ for } \dot{u} < 0 \\ -1 \text{ for } \dot{u} > 0 \\ 0 \text{ for } \dot{u} = 0 \end{cases}$$

$|A|$ = absolute value of A (A generic)

IV. PHYSICAL VARIABLES (Unknowns)

y_T	trail end deflection
y_B	ball joint deflection
u	breech displacement along cradle measured from trunnion
x_f	displacement of tube base: $x_f = u + \ell_7$
ξ	position of projectile measured from tube base; positive in x_6 direction
v	y_6-displacement of tube at point x
w	z_6-displacement of tube at point x
θ_1	angle due to "rigid" base movement $\theta_1 = \arcsin \dfrac{y_B - y_T}{\ell_1}$
θ_2	flexural rotation of combined carriage flexibility
θ_3	transverse angle of rotation about y_3
θ_4	angle of rotation about x_4
θ_5	elevating system flexibility
θ_6	right-left sequencing flexibility of breech
$q_n(t)$	time history for nth vibrational mode of tube in y_6-direction
$h_n(t)$	time history for nth vibrational mode of tube in z_5-direction
$\theta_7 = \psi_y$	rotation about z_8 . . . $\psi_y = -\dfrac{\partial w}{\partial x}$
$\theta_8 = \psi_z$	rotation about y_8 . . . $\psi_z = \dfrac{\partial v}{\partial x}$
R_{6x}, R_{6y}, R_{6z}	ball joint force reactions at trunnion; positive acting on carriage; components in system 6
E_{6x}, E_{6y}	flex system force components; positive acting on carriage; components in system 5

T_{6x}, T_{6y}	trunnion moment reactions; components in system 6; positive acting on carriage
P_{cx}, P_{cy}, P_{cz}	force reaction between cradle and breech; components in system 6; positive acting on cradle
N_{cx}, N_{cy}, N_{cz}	moment reaction between cradle and breech; components in system 6; positive acting on cradle
$S_x(0,t)$, $S_y(0,t)$	shear force between breech and tube
$M_y(0,t)$, $M_z(0,t)$	moments between breech and tube
N_{py}, N_{pz}	force reaction between projectile and tube; components in system 6; positive when acting on projectile
M_{px}, M_{py}, M_{pz}	moment reaction between projectile and breech, when projectile is in breech; components in system 6; positive when acting on projectile
C_{px}	moment reaction between projectile and tube when projectile is in tube -- transferred rigidly to tube-breech connection; component in system 6; positive when acting on projectile
C_5 =	$\cos(\alpha + \theta_5)$
S_5 =	$\sin(\alpha + \theta_5)$
C_9 =	$\cos \varphi$
S_9 =	$\sin \varphi$
R_1	ground reaction and gravity force at y_T
R_2	ground reaction and gravity force at y_B

$$z_x = \ell_2 \cos \beta_1 - \ell_4 \cos \beta_2 + \ell_8 C_5$$

$$z_y = \ell_2 \sin \beta_1 - \ell_4 \sin \beta_2 + \ell_8 S_5$$

$$z = \sqrt{z_x^2 + z_y^2}$$

$$= \Big[\ell_2^2 + \ell_4^2 + \ell_8^2 - 2 \ell_2 \ell_4 \cos (\beta_1 - \beta_2) + 2 \ell_2 \ell_8 \cos (\alpha + \theta_5 - \beta_1) - 2 \ell_4 \ell_8 \cos (\alpha + \theta_5 - \beta_2) \Big]^{1/2}$$

V. DERIVATION OF EQUATIONS OF MOTION

The equations of motion were derived with the use of standard matrix techniques. These procedures are fully covered in "Elementary Matrices and Some Applications to Dynamics and Differential Equations" by R. A. Frazer, W. J. Duncan, and A. R. Collar, Cambridge University Press, 1957.

It is well known that the motion of a body can be represented by equations which characterize the motion of the center of gravity of the body together with those which characterize the rotation of the body about its center of gravity. Figure F-2 illustrates the general case. The coordinates X, Y, Z are fixed in space, while x, y, z are fixed in the body. The motion of point P is defined through the rate of change of $\bar{R}$ or, equivalently, the rates of change of $\bar{\rho}$ and $\bar{r}$. If the point P is fixed in the body, G, the rate of change of $\bar{r}$ is completely defined by the rotation of the body.

$\bar{R}$ is normally referred to X, Y, Z, as is $\bar{\rho}$. On the other hand, $\bar{r}$ is normally expressed in terms of x, y, z. If $\bar{\bar{A}}$ is the matrix for transformation from X, Y, Z to x, y, z we then have

$$\bar{r} = \bar{\bar{A}}\,(\bar{R} - \bar{\rho})$$

with respect to the moving coordinates the velocity of P is

$$\bar{\bar{A}}\,\dot{\bar{R}} = \bar{\bar{A}}\,\dot{\bar{\rho}} + \dot{\bar{r}} + \bar{\bar{w}}\,\bar{r}.$$

where $\bar{\bar{w}}$ is the rotational velocity matrix, defined through

$$\bar{\bar{w}} = -\dot{\bar{\bar{A}}}\,\bar{\bar{A}}^{-1}$$

where $\bar{\bar{A}}^{-1}$ is the inverse of $\bar{\bar{A}}$.

It should be noted that

$$\dot{\bar{R}} = \frac{d\bar{R}}{dt}$$

is the velocity of P with respect to the fixed coordinates and that $\bar{\bar{A}}\,\dot{\bar{R}}$ merely is the result of changing the component bases.

Differentiation leads to the following expression for the acceleration referred to the moving axes

$$\bar{A}\ddot{\bar{R}} = \bar{A}\ddot{\bar{\rho}} + 2\,\bar{\bar{w}}\dot{\bar{r}} + \dot{\bar{\bar{w}}}\bar{r} + \bar{\bar{w}}^2\bar{r} + \ddot{\bar{r}}$$

The kinematic relations can be used directly to obtain the equations of motion for a point mass or the center of gravity of a rigid body. In the moving coordinate system

$$M\bar{A}\ddot{\bar{R}} = \bar{F}$$

where M is the mass and $\bar{F}$ is the force vector. For the rotational equations of motion we observe that the angular velocity can be represented as the matrix, $\bar{\bar{w}}$ or alternatively as the vector $\bar{\rho}$.

$$\bar{\bar{w}} = \begin{Vmatrix} 0 & -w_z & w_y \\ w_z & 0 & -w_x \\ -w_y & w_x & 0 \end{Vmatrix}$$

$$\bar{\rho} = (w_x, w_y, w_z)$$

Let $\bar{J}$ be the polar moment of inertia matrix of the body represented by the body axes. Then the angular momentum vector in the moving system is

$$\bar{H} = \bar{J}\,\bar{\rho}$$

and the time rate of change of angular momentum is

$$\frac{d}{dt}\bar{H} = \bar{M} = \dot{\bar{\bar{J}}}\bar{\rho} + \bar{J}\dot{\bar{\rho}} + \bar{\bar{w}}\bar{\bar{J}}\bar{\rho}$$

where $\bar{M}$ is the vector of applied moments.

Coordinate Transformations

The applicable coordinate systems are shown in Fig. F-1. These systems are related through the following transformations.

$$\bar{R}_2 = \bar{R}_1 - \bar{T}_{21}$$

$$T_{21} = (\ell_1, y_B, 0)$$

$$\bar{R}_3 = \bar{A}_{32}\,\bar{R}_2$$

$$\bar{A}_{32} = \begin{Vmatrix} \cos(\theta_1 + \theta_2) & \sin(\theta_1 + \theta_2) & 0 \\ -\sin(\theta_1 + \theta_2) & \cos(\theta_1 + \theta_2) & 0 \\ 0 & 0 & 1 \end{Vmatrix}$$

$$\bar{R}_4 = \bar{A}_{43}\,\bar{R}_3$$

$$\bar{A}_{43} = \begin{Vmatrix} \cos\theta_3 & 0 & -\sin\theta_3 \\ 0 & 1 & 0 \\ \sin\theta_3 & 0 & \cos\theta_3 \end{Vmatrix}$$

$$\bar{R}_5 = \bar{A}_{54}\,\bar{R}_4$$

$$\bar{A}_{54} = \begin{Vmatrix} 1 & 0 & 0 \\ 0 & \cos\theta_4 & \sin\theta_4 \\ 0 & -\sin\theta_4 & \cos\theta_4 \end{Vmatrix}$$

$$\bar{R}_6 = \bar{A}_{65}\,(\bar{R}_5 - \bar{T}_{65})$$

$$\bar{T}_{65} = [\,\ell_2 \cos\beta_1,\ \ell_2 \sin\beta_1,\ 0]$$

$$\bar{A}_{65} = \begin{Vmatrix} \cos(\alpha+\theta_5) & \sin(\alpha+\theta_5) & 0 \\ -\sin(\alpha+\theta_5) & \cos(\alpha+\theta_5) & 0 \\ 0 & 0 & 1 \end{Vmatrix}$$

$$\bar{R}_7 = \bar{R}_6 - \bar{T}_{76}$$

$$\bar{T}_{76} = (x_f,\ 0,\ 0)$$

$$\bar{R}_8 = \bar{R}_7 - \bar{T}_{87}$$

$$\bar{T}_{87} = (x,\ 0,\ 0)$$

$$\bar{R}_9 = \bar{A}_{98}\,\bar{R}_8$$

$$\bar{A}_{98} = \begin{bmatrix} \cos\psi_Z & \sin\psi_Z & 0 \\ -\sin\psi_Z & \cos\psi_Z & 0 \\ 0 & 0 & 1 \end{bmatrix}.$$

$$\cdot \begin{bmatrix} 1 & 0 & 0 \\ 0 & \cos\varphi^* & \sin\varphi^* \\ 0 & -\sin\varphi^* & \cos\varphi^* \end{bmatrix} \cdot$$

$$\cdot \begin{bmatrix} \cos\psi_y & 0 & -\sin\psi_y \\ 0 & 1 & 0 \\ \sin\psi_y & 0 & \cos\psi_y \end{bmatrix}$$

$$\bar{A}_{98} = \begin{bmatrix} \sin\varphi^* \sin\psi_y \sin\psi_z + \cos\psi_y \cos\psi_z & \cos\varphi^* \sin\psi_z & \sin\varphi^* \cos\psi_y \sin\psi_z - \sin\psi_y \cos\psi_z \\ \sin\varphi^* \sin\psi_y \cos\psi_z - \cos\psi_y \sin\psi_z & \cos\varphi^* \cos\psi_z & \sin\varphi^* \cos\psi_y \cos\psi_z + \sin\psi_y \sin\psi_z \\ \cos\varphi^* \sin\psi_y & -\sin\varphi^* & \cos\varphi^* \cos\psi_y \end{bmatrix}$$

Utilization of these transformations leads to the following equations of motion.

VI. AUXILIARY QUANTITIES AND EXPRESSIONS

$$A_n = V_n''(0) \equiv 2\, b_n^2 / \sqrt{\rho L}$$

$$B_n = V_n'''(0) = -\frac{2\, b_n^3}{\sqrt{\rho L}}\left(\frac{\cosh b_n L + \cos b_n L}{\sin b_n L + \sinh b_n L}\right)$$

$$V_n(\xi) = \frac{1}{\sqrt{\rho L}}\left[\cosh b_n \xi - \cos b_n \xi + \left(\frac{\cosh b_n L + \cos b_n L}{\sin b_n L + \sinh b_n L}\right)(\sin b_n \xi - \sinh b_n \xi)\right]$$

$$V_n'(\xi) = \frac{b_n}{\sqrt{\rho L}}\left[\sinh b_n \xi + \sin b_n \xi + \left(\frac{\cosh b_n L + \cos b_n L}{\sin b_n L + \sinh b_n L}\right)(\cos b_n \xi - \cosh b_n \xi)\right]$$

$$v_0(\xi) = -\frac{\rho g \cos\alpha}{24 EI}\left(\xi^4 - 4\xi^3 L + 6\xi^2 L^2\right)$$

$$v_0'(\xi) = -\frac{\rho g \cos\alpha}{6 EI}\left(\xi^3 - 3\xi^2 L + 3\xi L^2\right)$$

$$v(\xi,t) = v_0(\xi) + \sum_{n=1}^{\infty} V_n(\xi)\, q_n(t)$$

$$v'(\xi,t) = \sum_{n=1}^{\infty} V_n'(\xi)\, h_n(t)$$

$$\dot{v}(\xi,t) = \sum_{n=1}^{\infty} V_n(\xi)\, \dot{q}_n(t) + \dot{\xi} v_0' + \dot{\xi} \sum_{n=1}^{\infty} V_n'(\xi)\, q_n(t)$$

$$\dot{v}'(\xi,t) = \sum_{n=1}^{\infty} V_n'(\xi)\, \dot{h}_n(t) + \dot{\xi} \sum_{n=1}^{\infty} V_n''(\xi)\, h_n(t)$$

$$\theta_7(\xi,t) \equiv \psi_y(\xi,t) = -\sum_{n=1}^{\infty} V_n'(\xi) h_n(t)$$

$$\theta_8(\xi,t) \equiv \psi_z(\xi,t) = v_0'(\xi) + \sum_{n=1}^{\infty} V_n'(\xi) q_n(t)$$

$$\ddot{v}(\xi,t) = \ddot{\xi} v_0' + \dot{\xi}^2 v_0'' + \sum_{n=1}^{\infty} V_n(\xi)\, \ddot{q}_n + 2\dot{\xi} \sum_{n=1}^{\infty} V_n' \dot{q}_n +$$

$$+ \ddot{\xi} \sum_{n=1}^{\infty} V_n' q_n(t) + \dot{\xi}^2 \sum_{n=1}^{\infty} V_n'' q_n(t)$$

$$\ddot{w}(\xi,t) = \sum_{n=1}^{\infty} V_n(\xi) \ddot{h}_n + 2\dot{\xi} \sum_{n=1}^{\infty} V_n' \dot{h}_n + \ddot{\xi} \sum_{n=1}^{\infty} V_n' h_n +$$

$$+ \dot{\xi}^2 \sum_{n=1}^{\infty} V_n'' h_n$$

$$V_n''(\xi) = \frac{b_n^2}{\sqrt{\rho L}} \Big[\cosh b_n \xi + \cos b_n \xi +$$

$$+ \left(\frac{\cosh b_n L + \cos b_n L}{\sin b_n L + \sinh b_n L} \right) \left(-\sin b_n \xi - \sinh b_n \xi \right) \Big]$$

$$V_n'''(\xi) = \frac{b_n^3}{\sqrt{\rho L}} \Big[\sinh b_n \xi - \sin b_n \xi +$$

$$+ \left(\frac{\cosh b_n L + \cos b_n L}{\sin b_n L + \sinh b_n L} \right) \left(-\cos b_n \xi - \cosh b_n \xi \right) \Big]$$

$$\dot{\theta}_7 = -\sum_{n=1}^{\infty} V_n' \dot{h}_n - \xi \sum_{n=1}^{\infty} V_n'' h_n$$

$$\dot{\theta}_8 = \dot{\xi}\, v_0''(\xi) + \sum_{n=1}^{\infty} V_n' \dot{q}_n + \dot{\xi} \sum_{n=1}^{\infty} V_n'' q_n(t)$$

$$\ddot{\theta}_1 = -\sum_1^{\infty} V_n' \ddot{h}_n - 2\dot{\xi}\sum_1^{\infty} V_n'' \dot{h}_n - \dot{\xi}^2 \sum_1^{\infty} V_n''' h_n - \ddot{\xi}\sum_1^{\infty} V_n'' h_n$$

$$\ddot{\theta}_8 - \ddot{\xi} v_0''(\xi) + \dot{\xi}^2 v_0'''(\xi) + \sum_1^{\infty} V_n' \ddot{q}_n + 2\dot{\xi}\sum_1^{\infty} V_n'' \dot{q}_n +$$

$$+ \dot{\xi}^2 \sum_1^{\infty} V_n''' q_n(t) + \ddot{\xi}\sum_1^{\infty} V_n'' q_n(t)$$

$$v_0''(\xi) = -\frac{\rho g \cos\alpha}{2EI}\left(\xi^2 - 2\xi L + L^2\right)$$

$$v_0'''(\xi) = -\frac{\rho g \cos\alpha}{EI}\left(\xi - L\right)$$

$\therefore$ LET $\theta_9 = \varphi(\xi(t))$

$\varphi(\xi)$ IS THE RIFLING EQUATION

$$\varphi'(\xi) = \frac{d}{d\xi}\varphi(\xi)$$

$$\varphi''(\xi) = \frac{d^2}{d\xi^2}\varphi(\xi)$$

THEN $\dot{\theta}_9 = \dot{\xi}\,\varphi'(\xi)$

$$\ddot{\theta}_9 = \ddot{\xi}\,\varphi'(\xi) + (\dot{\xi})^2\,\varphi''(\xi)$$

$$\Delta_1 = (\dot\theta_1 + \dot\theta_2 + \dot\theta_5)^2 + (\dot\theta_3 S_5 + \dot\theta_4 C_5)^2$$

$$\Delta_2 = 2\left[(\dot\theta_1 + \dot\theta_2)(\theta_4 S_5 - \theta_3 C_5) + \dot\theta_3 S_5 + \dot\theta_4 C_5\right]$$

$$\Delta_3 = (\ddot\theta_1 + \ddot\theta_2)(\theta_4 S_5 - \theta_3 C_5) - (\dot\theta_1 + \dot\theta_2 - \dot\theta_5)(\theta_3 C_5 - \theta_4 S_5) + \\ + \ddot\theta_3 S_5 + \ddot\theta_4 C_5$$

$$\Delta_4 = (\dot\theta_3 S_5 + \dot\theta_4 C_5)(\dot\theta_3 C_5 - \dot\theta_4 S_5)$$

$$\Delta_5 = 2(\dot\theta_1 + \dot\theta_2 - \dot\theta_3 \theta_4 + \dot\theta_5)$$

$$\Delta_6 = C_5 - (\theta_1 + \theta_2) S_5$$

$$\Delta_7 = \left\{\left[\dot\theta_3^2 + (\dot\theta_1 + \dot\theta_2)^2\right] S_5 + (\ddot\theta_1 + \ddot\theta_2 - \theta_4 \ddot\theta_3) C_5\right\} l_2 \cos\beta_1 + \\ + \left\{(\ddot\theta_1 + \ddot\theta_2 - \theta_4 \ddot\theta_3 - 2\dot\theta_4 \dot\theta_3) S_5 - \left[(\dot\theta_1 + \dot\theta_2)^2 + \dot\theta_4^2\right] C_5\right\} l_2 \sin\beta_1$$

$$\Delta_8 = \dot\theta_3^2 + \dot\theta_4^2$$

$$\Delta_9 = (\dot\theta_1 + \dot\theta_2 + \dot\theta_5)(\dot\theta_3 C_5 - \dot\theta_4 S_5)$$

$$\Delta_{10} = (\ddot\theta_1 + \ddot\theta_2)(\theta_4 C_5 + \theta_3 S_5) + \ddot\theta_3 C_5 - \ddot\theta_4 S_5 + (\dot\theta_1 + \dot\theta_2 - \dot\theta_5)(\dot\theta_3 S_5 + \dot\theta_4 C_5)$$

$$\Delta_{11} = 2\left[(\dot\theta_1 + \dot\theta_2)(\theta_4 C_5 + \theta_3 S_5) + \dot\theta_3 C_5 - \dot\theta_4 S_5\right]$$

$$\Delta_{12} = \left[\ddot\theta_4 - (\ddot\theta_1 + \ddot\theta_2)\theta_3\right] l_2 \sin\beta_1 - \left[\ddot\theta_3 + (\ddot\theta_1 + \ddot\theta_2)\theta_4\right] l_2 \cos\beta_1$$

$$\Delta_{13} = (\theta_1 + \theta_2) C_5 + S_5$$

$$\Delta_{14} = (\dot\theta_1 + \dot\theta_2 + \dot\theta_5)^2 + (\dot\theta_3 C_5 - \dot\theta_4 S_5)^2$$

$$\Delta_{15} = \ddot{\theta}_1 + \ddot{\theta}_2 - \ddot{\theta}_3\theta_4 + \ddot{\theta}_5 - \dot{\theta}_3\dot{\theta}_4$$

$$\Delta_{16} = (\dot{\theta}_1 + \dot{\theta}_2 + \dot{\theta}_5)(\dot{\theta}_3 S_5 + \dot{\theta}_4 C_5)$$

$$\Delta_{17} = \left\{(\ddot{\theta}_1 + \ddot{\theta}_2 - \ddot{\theta}_3\theta_4)S_5 - [\dot{\theta}_3^2 + (\dot{\theta}_1 + \dot{\theta}_2)^2]C_5\right\} l_2 \cos\beta_1 +$$
$$- \left\{(\ddot{\theta}_1 + \ddot{\theta}_2 - \ddot{\theta}_3\theta_4 - 2\dot{\theta}_3\dot{\theta}_4)C_5 + [\dot{\theta}_4^2 + (\dot{\theta}_1 + \dot{\theta}_2)^2]S_5\right\} l_2 \sin\beta_1$$

A. PROJECTILE EQUATIONS

$$\begin{aligned} F(t) = m_p\Big\{ & \ddot{\xi} + \ddot{u} + \Delta_{13}\ddot{y}_B - (\Delta_5 + \theta_6\Delta_2)\dot{v} + (\Delta_{11} + 2\dot{\theta}_6)\dot{w} + \\ & -(\Delta_{14} + 2\theta_6\Delta_{16} + \dot{\theta}_6\Delta_{11})(\xi + u + x + l_1) + \\ & +[\Delta_4 - \Delta_{15} - \theta_6(\Delta_9 + \Delta_3)]v + \Delta_{17} - \theta_6\Delta_{12} + \\ & +[\Delta_{10} + \Delta_{16} + \theta_6(\Delta_8 - \Delta_{14}) + \ddot{\theta}_6]w\Big\} \end{aligned} \qquad \text{(F-1)}$$

$$\begin{aligned} N_{py} = m_p\Big\{ & \ddot{v} + \Delta_6(\ddot{y}_B + g) + (\Delta_5 + \theta_6\Delta_2)(\ddot{\xi} + \ddot{u}) - (\Delta_2 - \theta_6\Delta_5)\dot{w} + \\ & -\Delta_1 v + [\Delta_4 + \Delta_{15} - \theta_6(\Delta_9 - \Delta_3) + \dot{\theta}_6\Delta_2](\xi + u + x + l_1) + \\ & +[\Delta_9 - \Delta_3 + \theta_6(\Delta_4 + \Delta_{15}) + \dot{\theta}_6\Delta_5]w + \Delta_7\Big\} \end{aligned} \qquad \text{(F-2)}$$

$$N_{pz} = m_p\Big\{\ddot{w} + (\theta_6\Delta_{13} - \theta_4)(\ddot{y}_B + q) - (\Delta_{11} + 2\dot{\theta}_6)(\dot{\xi} + \dot{u}) +$$

$$+ (\Delta_2 - \theta_6\Delta_5)\dot{v} - [\Delta_8 - 2\theta_6\Delta_{16} + \dot{\theta}_6\Delta_{11}]w +$$

$$+ [\Delta_{16} - \Delta_{10} + \theta_6(\Delta_8 - \Delta_{14}) - \ddot{\theta}_6](\xi + u + x + \ell_7) + \qquad (F\text{-}3)$$

$$+ [\Delta_9 + \Delta_3 + \theta_6(\Delta_4 - \Delta_{15})]v + \Delta_{12} + \theta_6\Delta_{17}\Big\}$$

$$C_{px} = J_x\Big\{\ddot{\theta}_9 + \Delta_3 + \theta_8 C_9\Delta_{10} + \tfrac{1}{2}[(\dot{\theta}_8 S_9 - \dot{\theta}_6 - \dot{\theta}_7)\Delta_5 + \dot{\theta}_8 C_9\Delta_{11} +$$

$$+ (\theta_8 S_9 - \theta_7 - \theta_6)\Delta_{15}]\Big\} \qquad (F\text{-}4)$$

$$C_y = -J_y\Big\{C_9(\ddot{\theta}_6 + \ddot{\theta}_7) - \ddot{\theta}_9\theta_8 - \dot{\theta}_9\dot{\theta}_8 - \dot{\theta}_9\dot{\theta}_6 S_9 - \dot{\theta}_9\dot{\theta}_7 S_9 +$$

$$+ (\theta_6 S_9 + \theta_7 S_9 - \theta_8)\Delta_3 + C_9\Delta_{10} + S_9\Delta_{15} + \qquad (F\text{-}5)$$

$$+ \tfrac{1}{2}[(\dot{\theta}_6 S_9 + \dot{\theta}_7 S_9 - \dot{\theta}_8)\Delta_2 - \dot{\theta}_8 S_9\Delta_{11} + \dot{\theta}_9 C_9\Delta_5]\Big\} +$$

$$- (J_x - J_y)[\dot{\theta}_8\dot{\theta}_9 - S_9\dot{\theta}_9(\dot{\theta}_7 + \dot{\theta}_6) + C_9\Delta_{16} - S_9\Delta_4]$$

$$C_z = -J_y\Big\{\ddot{\theta}_8 - (\ddot{\theta}_6 + \ddot{\theta}_7)S_9 - (\dot{\theta}_6 + \dot{\theta}_7)\dot{\theta}_9 C_9 - S_9\Delta_{10} +$$

$$+ (\theta_6 + \theta_7)C_9\Delta_3 + C_9\Delta_{15} + \tfrac{1}{2}[(\dot{\theta}_6 + \dot{\theta}_7)C_9\Delta_2 - (S_9 + C_9)\dot{\theta}_9\Delta_5]\Big\} +$$

$$+ (J_x - J_y)[C_9\dot{\theta}_9(\dot{\theta}_7 + \dot{\theta}_6) + C_9\Delta_4 + S_9\Delta_{16}] \qquad (F\text{-}6)$$

B. **DETERMINATION OF** $_6$

$$k_8\theta_6 = (m_\ell - m_p)(\ddot{u} + \Delta_{13}\ddot{y}_B - \Delta_{14}u + \Delta_{17}) + - (m_\ell + m_p)\, l_8(\Delta_{10} + \Delta_{16}) \qquad \text{(F-7)}$$

C. **TUBE EQUATIONS**

$$\begin{aligned}
\ddot{q}_n + [V_n^2 - \Delta_1]q_n = & -[N_{pY}V_n(\xi) + C_Y V_n'(\xi)]H(\xi)H(L-\xi) + \\
& - \frac{B_n E I_q}{V_n^4}\cos\alpha(\Delta_1 - V_n^2) - (\Delta_2 - \theta_6\Delta_5)\dot{h}_n + \\
& + [\Delta_9 - \Delta_3 + \theta_6(\Delta_4 + \Delta_{16}) + \dot{\theta}_6\Delta_5]h_n + \\
& + [\Delta_{15} + \Delta_4 - \theta_6(\Delta_9 - \Delta_3) + \dot{\theta}_6\Delta_2]\frac{\rho A_n}{b_n^4} + \\
& - \frac{\rho B_n}{b_n^4}\Big\{[\Delta_{15} + \Delta_4 - \theta_6(\Delta_9 - \Delta_3) + \dot{\theta}_6\Delta_2](u + l_7) + \\
& + (\Delta_5 + \theta_6\Delta_2)\dot{u} + \Delta_6(\ddot{y}_B + g) + \Delta_7\Big\}
\end{aligned} \qquad \text{(F-8)}$$

$$\ddot{h}_n + [V_n^2 - (\Delta_8 - 2\theta_6\Delta_{16} + \dot{\theta}_6\Delta_{11})]h_n =$$

$$\begin{aligned}
& -[N_{pz}V_n(\xi) - C_Y V_n'(\xi)]H(\xi)H(L-\xi) + \\
& + (\Delta_2 - \theta_6\Delta_5)\Big[\dot{q}_n - \frac{B_n E I_q}{V_n^4}\cos\alpha\Big] + \\
& + [\Delta_{16} - \Delta_{10} + \theta_6(\Delta_8 - \Delta_{14}) - \ddot{\theta}_6]\Big[\frac{\rho A_n}{b_n^4} - \frac{\rho B_n}{b_n^4}(u + l_7)\Big] + \\
& - \frac{\rho B_n}{b_n^4}[\Delta_{12} + \theta_6\Delta_{17} + (\theta_6\Delta_{13} - \theta_4)(\ddot{y}_B + g) + \\
& \quad - (\Delta_{11} + 2\theta_6)\dot{u}]
\end{aligned} \qquad \text{(F-9)}$$

D. END SHEARS AND MOMENTS

$$\left.\begin{aligned}
S_y(0,t) &= \rho g L \cos\alpha + EI \sum_1^\infty B_n q_n \\
M_z(0,t) &= -\tfrac{1}{2}\rho g L^2 \cos\alpha + EI \sum_1^\infty A_n q_n \\
S_z(0,t) &= EI \sum_1^\infty B_n h_n \\
M_y(0,t) &= -EI \sum_1^\infty A_n q_n
\end{aligned}\right\} \qquad \text{(F-10)}$$

E. BREECH EQUATIONS

$$\begin{aligned}
&(\rho L + m_B)\big[\ddot{u} + \Delta_{13}(\ddot{y}_B + g) - \Delta_{14} u + (\Delta_4 - \Delta_{12})\ell_5 + \\
&\qquad + (\Delta_{10} + \Delta_{16})\ell_6 + \Delta_{17}\big] = \\
&\qquad = \rho L(\ell_1 + \tfrac{1}{2}L)\Delta_{14} - P_{cx} - F(t)
\end{aligned} \qquad \text{(F-11)}$$

$$\begin{aligned}
&m_B\big[\Delta_6(\ddot{y}_B + g) + \Delta_5 \ddot{u} - \Delta_1 \ell_5 + (\Delta_4 + \Delta_{12}) u + \\
&\qquad + (\Delta_9 - \Delta_3)\ell_6 + \Delta_7\big] = \\
&\qquad = -P_{cy} - S_y(0,t) - [1 - H(\xi)] N_{Py}
\end{aligned} \qquad \text{(F-12)}$$

$$\begin{aligned}
&m_B\big[-\Theta_4(\ddot{y}_B + g) - \Delta_{11}\ddot{u} - \Delta_8 \ell_6 + \Delta_{12} + (\Delta_{16} - \Delta_{10}) u + \\
&\qquad + (\Delta_9 + \Delta_3)\ell_5\big] = \\
&\qquad = -P_{cz} - S_z(0,t) - [1 - H(\xi)] N_{Pz}
\end{aligned} \qquad \text{(F-13)}$$

$$(J_{Ex} + 2\rho L I)\Delta_3 + (J_{Ex} - J_{BY})\Delta_9 =$$

$$= -N_{cx} - P_{cy}\ell_6 + P_{cz}\ell_5 - C_{px}H(\xi)H(L-\xi) + \qquad \text{(F-14)}$$

$$+ [H(\xi) - 1] J_x (\ddot{\theta}_9 + \Delta_3)$$

$$J_{BY}\Delta_{10} + (J_{Bx} - J_{Bz})\Delta_{16} =$$

$$= -N_{cy} + M_y(0,t) + \ell_7 S_z(0,t) +$$

$$+ [1 - H(\xi)][(\ell_7 + \xi) N_{pz} - J_y(C_9\Delta_{10} + S_9\Delta_{15}) + \qquad \text{(F-15)}$$

$$- (J_x - J_y)(C_9\Delta_{16} - S_9\Delta_4)]$$

$$J_{Bz}\Delta_{15} + (J_{BY} - J_{Ex})\Delta_4 =$$

$$= -N_{cz} - \ell_7 S_y(0,t) + M_z(0,t) - F(t)\ell_5 +$$

$$+ [H(\xi) - 1][(\ell_7 + \xi) N_{py} + J_y(C_9\Delta_{15} - S_9\Delta_{10}) + \qquad \text{(F-16)}$$

$$- (J_x - J_y)(C_9\Delta_4 + S_9\Delta_{16})] +$$

$$- \rho L \ell_5 [\ddot{u} + \Delta_{13}\ddot{y}_B - \Delta_{14}(u + \ell_7 + \tfrac{1}{2}L) + \Delta_{17}]$$

F. COUNTERRECOIL MECHANISM

$$F_{cx} = -K - \epsilon H_1 - k_7(u_0 - u) - \frac{\epsilon \gamma A_p^3 (1+\delta)\dot{u}^2}{2g C_0^2 \alpha_0^2} + \qquad \text{(F-17)}$$

$$- H(u - u_1) H(u_2 - u) \frac{I_B h^2}{R_p^2 (u_2 - u_1)^2} \left[2\pi \sin 2\pi \frac{u - u_1}{u_2 - u_1} \left(1 - \cos 2\pi \frac{u - u_1}{u_2 - u_1}\right) \dot{u}^2 \right.$$

$$\left. + \left(1 - \cos 2\pi \frac{u - u_1}{u_2 - u_1}\right)^2 \right] \frac{1 - \epsilon}{2}$$

G. TRAILS AND GROUND REACTIONS

DEFINITION:

$$R_1 = \begin{cases} -k_1 y_T - \gamma_1 \dot{y}_T & \text{FOR } y_T \le 0 \\ -m_1(\ddot{y}_T + g) & \text{FOR } y_T > 0 \end{cases} \qquad \text{(F-18)}$$

$$R_2 = \begin{cases} -m_3 \ddot{y}_B - k_2 y_B - \gamma_2 \dot{y}_B & \text{FOR } \dot{y}_B \le 0 \\ -m_3(\ddot{y}_B + g) & \text{FOR } y_B > 0 \end{cases} \qquad \text{(F-19)}$$

$$\theta_1 = \frac{y_B - y_T}{l_1} \qquad \text{(F-20)}$$

$$l_1 R_1 = k_3 \theta_2 \qquad \text{(F-21)}$$

H. VERTICAL EQUILIBRIUM AT BALL JOINT

$$R_1 + R_2 + \Delta_{13} R_{Gx} + \Delta_G R_{Gy} - \theta_4 R_{Gz} + (\theta_1 + \theta_2) E_{Gx} + E_{Gy} = 0 \qquad \text{(F-22)}$$

I. ANGULAR MOTION OF THE BALL JOINT

$$l_1 R_1 \theta_3 - k_5 \theta_4 + R_{Gz} l_2 \sin\beta_1 + T_{Gx} C_5 - T_{Gy} S_5 + -I_{cz}(\dot{\theta}_1 + \dot{\theta}_2)\dot{\theta}_3 - I_{xc}[\ddot{\theta}_4 - (\ddot{\theta}_1 + \ddot{\theta}_2)\theta_3 - (\dot{\theta}_1 + \dot{\theta}_2)\dot{\theta}_3] = 0 \qquad \text{(F-23)}$$

$$-l_1 R_1 \theta_4 - k_4 \theta_3 - R_{Gz} l_2 \cos\beta_1 + T_{Gx} S_5 - T_{Gy} C_5 + -(I_{xc} - I_{zc})(\dot{\theta}_1 + \dot{\theta}_2)\dot{\theta}_4 = 0 \qquad \text{(F-24)}$$

$$-l_1 R_1 + k_4 \theta_3 \theta_4 - E_{Gx} l_4 \sin\beta_2 + R_{Gx} \sin(\alpha - \beta_1 + \theta_5) +$$

$$+ E_{Gy} l_4 \cos\beta_2 + R_{Gy} \cos(\alpha - \beta_1 + \theta_5) + I_{xc} \dot{\theta}_3 \dot{\theta}_4 + \qquad \text{(F-25)}$$

$$- I_{zc}(\ddot{\theta}_1 + \ddot{\theta}_2 - \ddot{\theta}_3 \theta_4 \cdot \dot{\theta}_3 \dot{\theta}_4) = 0$$

J. ANGULAR MOTION OF CRADLE

$$\Delta_3 I_{xA} + (I_{zA} - I_{yA}) \Delta_9 = N_{cy} - l_6 P_{cy} - T_{Gx} \qquad \text{(F-26)}$$

$$\Delta_{10} I_{yA} + (I_{yA} - I_{zA}) \Delta_{16} = N_{cy} + l_6 P_{cx} - (u - l_3) P_{cz} +$$

$$- T_{Gy} - l_3 R_{Gz} \qquad \text{(F-27)}$$

$$\Delta_{15} I_{zA} + (I_{yA} - I_{xA}) \Delta_4 = N_{cz} + (u - l_3) P_{cy} + l_3 R_{Gy} +$$

$$+ (l_5 - l_3) S_B E_{Gx} - (l_5 - l_3) C_5 E_{Gy} \qquad \text{(F-28)}$$

K. LINEAR MOTION OF CRADLE CENTER OF GRAVITY

$$m_A[\Delta_{13}(\ddot{y}_B + g) - \Delta_{14} l_3 + \Delta_{17}] =$$

$$= P_{cx} - R_{Gx} - E_{Gx} C_5 - E_{Gy} S_5 \qquad \text{(F-29)}$$

$$m_A[\Delta_6(\ddot{y}_B + g) + (\Delta_4 + \Delta_{15}) l_3 + \Delta_7] =$$

$$= P_{cy} - R_{Gy} + E_{Gx} S_5 - E_{Gy} C_5 \qquad \text{(F-30)}$$

$$m_A\left[-\theta_4(\ddot{y}_B+g)-(\Delta_{10}-\Delta_{16})\ell_3+\Delta_{12}\right]=P_{cz}-R_{6z} \qquad \text{(F-31)}$$

L. FLEXIBLE SYSTEM FORCE

$$E_{6x}=k_6\frac{z_x}{z}\ell_8(C_5-\cos\alpha)+ \qquad \text{(F-32)}$$
$$+b_6\frac{z_x}{z^2}\ell_8\dot{\theta}_5\left[\ell_4\sin(\alpha+\theta_5-\beta_2)-\ell_2\sin(\alpha+\theta_5-\beta_1)\right]$$

$$E_{6y}=k_6\frac{z_y}{z}\ell_8(C_5-\cos\alpha)+ \qquad \text{(F-33)}$$
$$+b_6\frac{z_y}{z^2}\ell_8\dot{\theta}_5\left[\ell_4\sin(\alpha+\theta_5-\beta_2)-\ell_2\sin(\alpha+\theta_5-\beta_1)\right]$$

VII. COMPILATION OF UNKNOWNS

Unknown	Equation	Unknown	Equation	Unknown	Equation
E_{6x}	631	y_T	619	y_B	621
3	623	5	627	T_{6y}	626
R_{6x}	628	R_{6z}	630	E_{6y}	632
P_{cy}	611	N_{cx}	613	N_{cz}	615
q_n	607	6	606	C_y	604
	600	N_{pz}	602	2	620
1	624	4	622	T_{6x}	625
P_{cx}	616	R_{6y}	629	u	610
P_{cz}	612	N_{cy}	614	S_y, S_z	609
				M_z, M_y	
h_n	608	C_{px}	603	C_z	605
N_{py}	601				

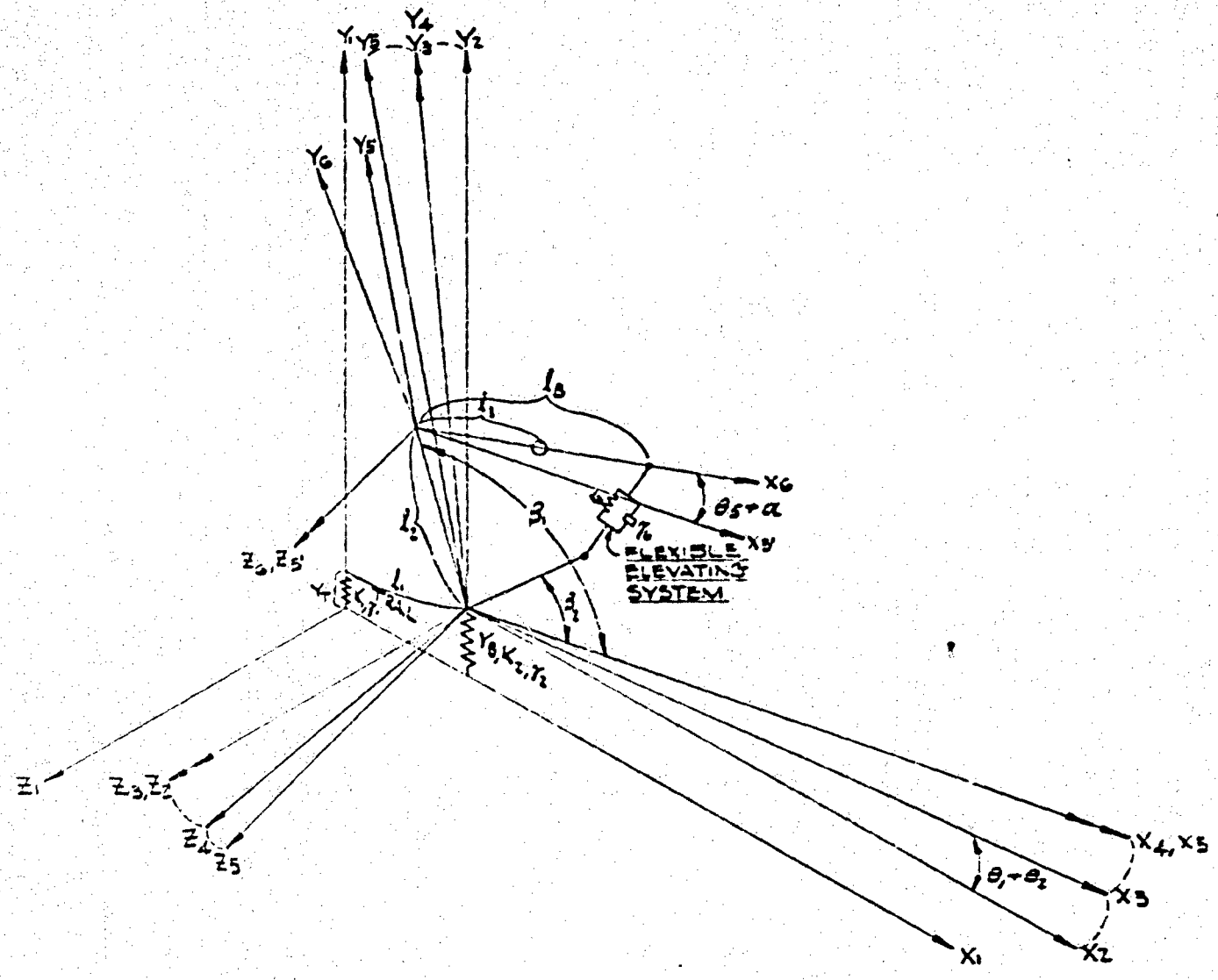

Fig. F-1 DIAGRAM OF COORDINATE SYSTEMS DESCRIBING LAUNCHER MOTION FOR MATHEMATICAL MODEL VI

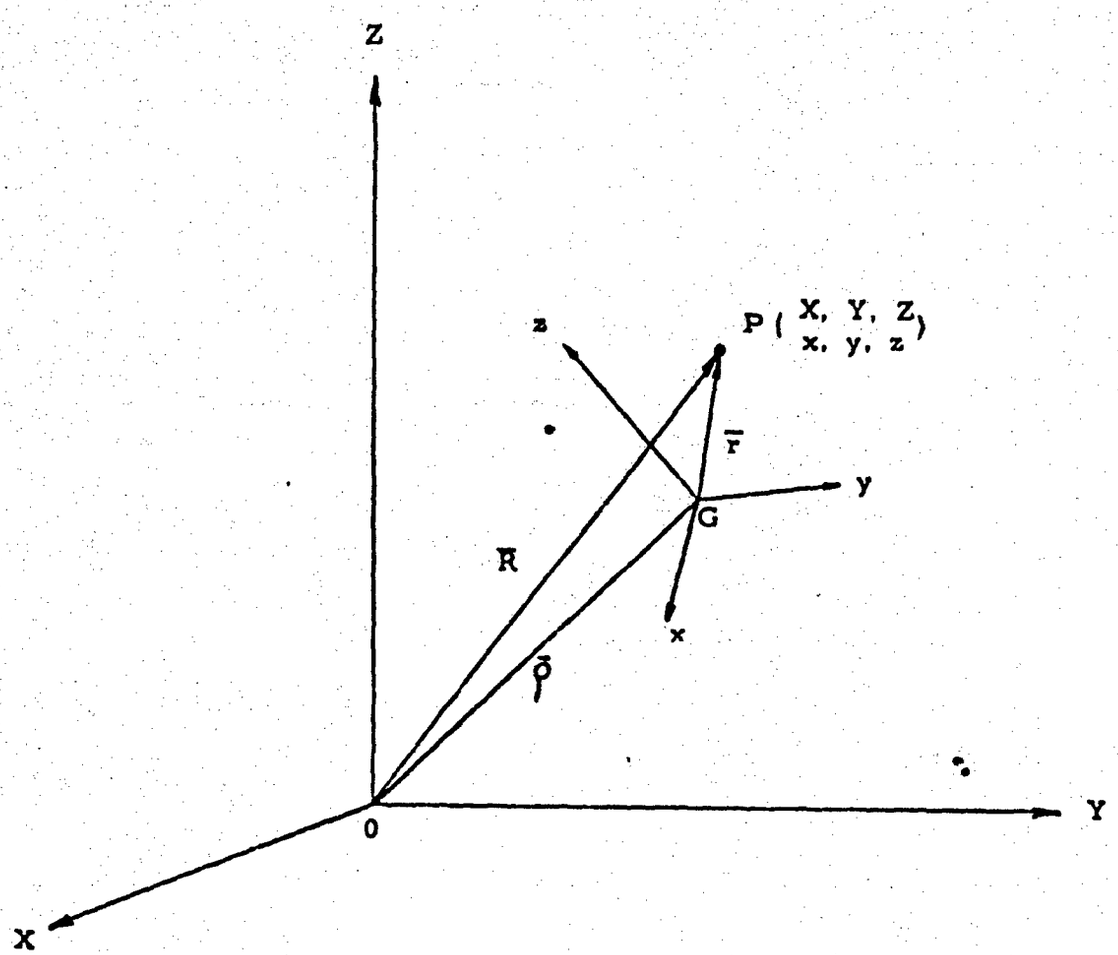

Fig. F-2 COORDINATE SYSTEM

APPENDIX G

FIXTURE DESIGNS

I. INTRODUCTION

The purpose and some of the operations of the experimental structure modifications are described in the body of the report. This appendix shows the details of the construction of the more important fixtures, the dampers, and the elevating system flexibilities. Not only the springs and dampers used on the program are shown, but also a design showing a combination spring and damper which could be used in the actual launcher. (The fixture used in the experimental program prohibited changes in elevation.)

II. FIXTURE DESCRIPTION

Figure G-1 shows the assembly of the auxiliary dampers used for the firing program. It is simply a piston submerged in a fluid inside a cylinder; the piston has orifices so that its motion gives a force approximately proportional to the square of the velocity. A detail drawing of the piston is shown in Figure G-2.

Figure G-3 shows the assembly of the flexibility added to the elevating rod; Figure G-4 gives the spring characteristics. This assembly was inserted into the present elevating system simply by moving the existing elevating screw up, and placing the spring assembly between the support in the upper carriage side and the screw. The flexibility could be removed, if desired, by replacing the spring by a rigid spacer. An alternate method was used, however, that of replacing the entire elevating screw by more rigid rods.

Figure G-5 shows a possible configuration of a spring-damper combination. The entire spring is submerged in hydraulic fluid; in this case the spring end retainers have orifice holes and act as the damper pistons. The lower, smaller spring and piston assembly is a device which acts as a fluid reserve which compensates for changes in ambient temperature. The entire assembly would be keyed so that it could transmit the torques for elevating the launcher.

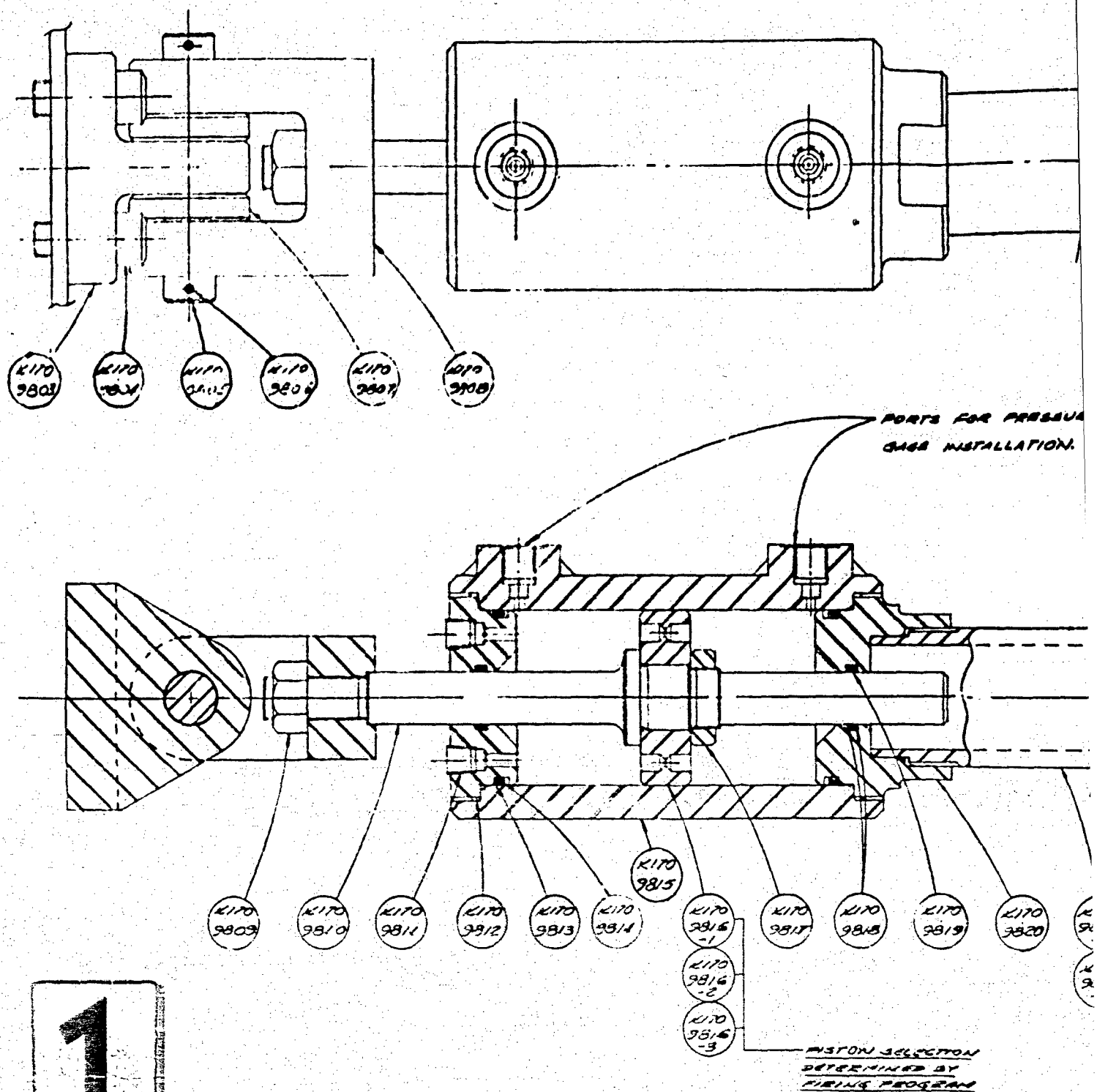

Fig. G-1 Viscous Damper As

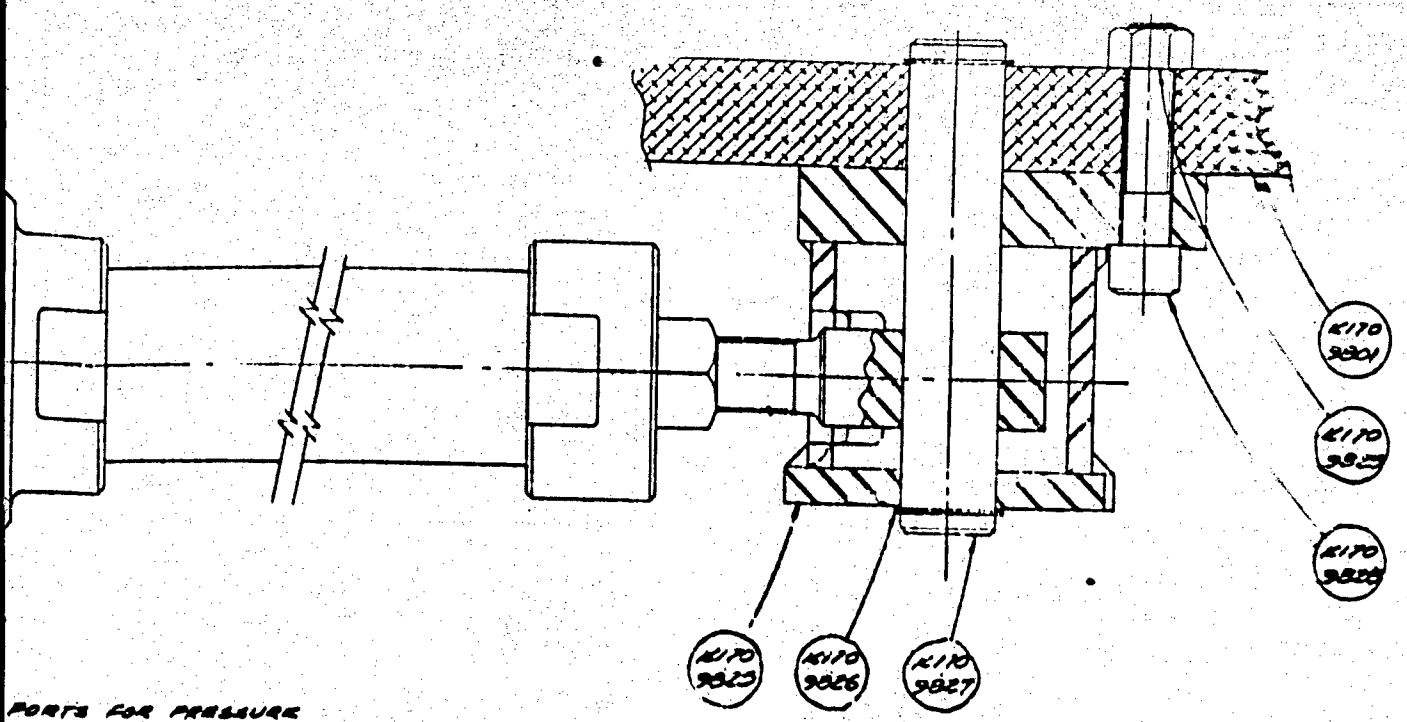

PORTS FOR PRESSURE GAGE INSTALLATION.

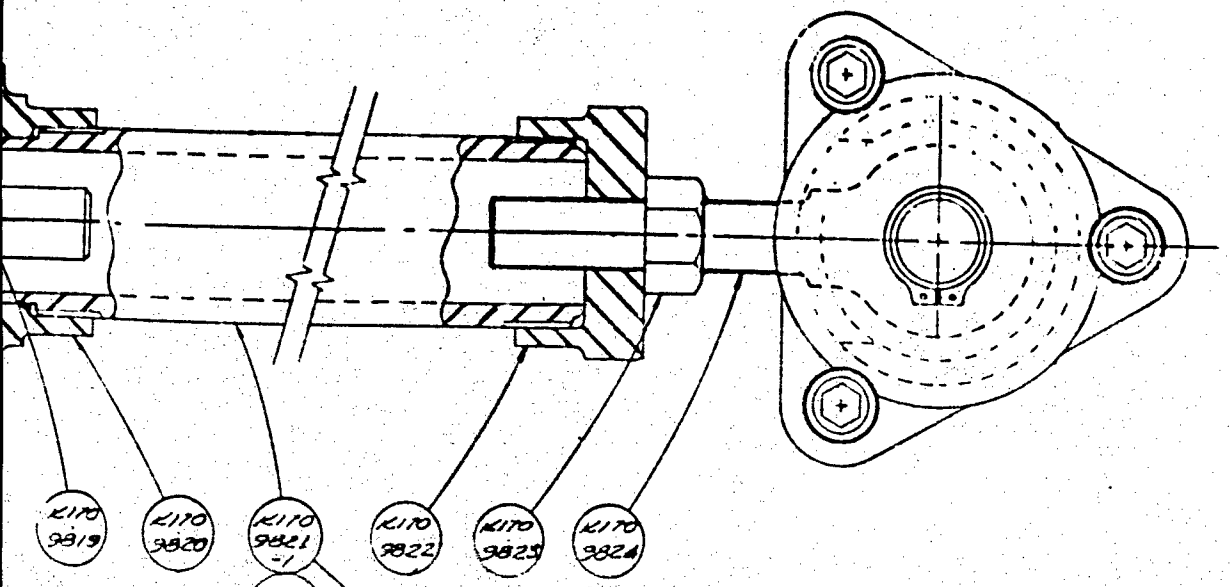

ELECTION
USED BY
ROGRAM

2

iscous Damper Assembly

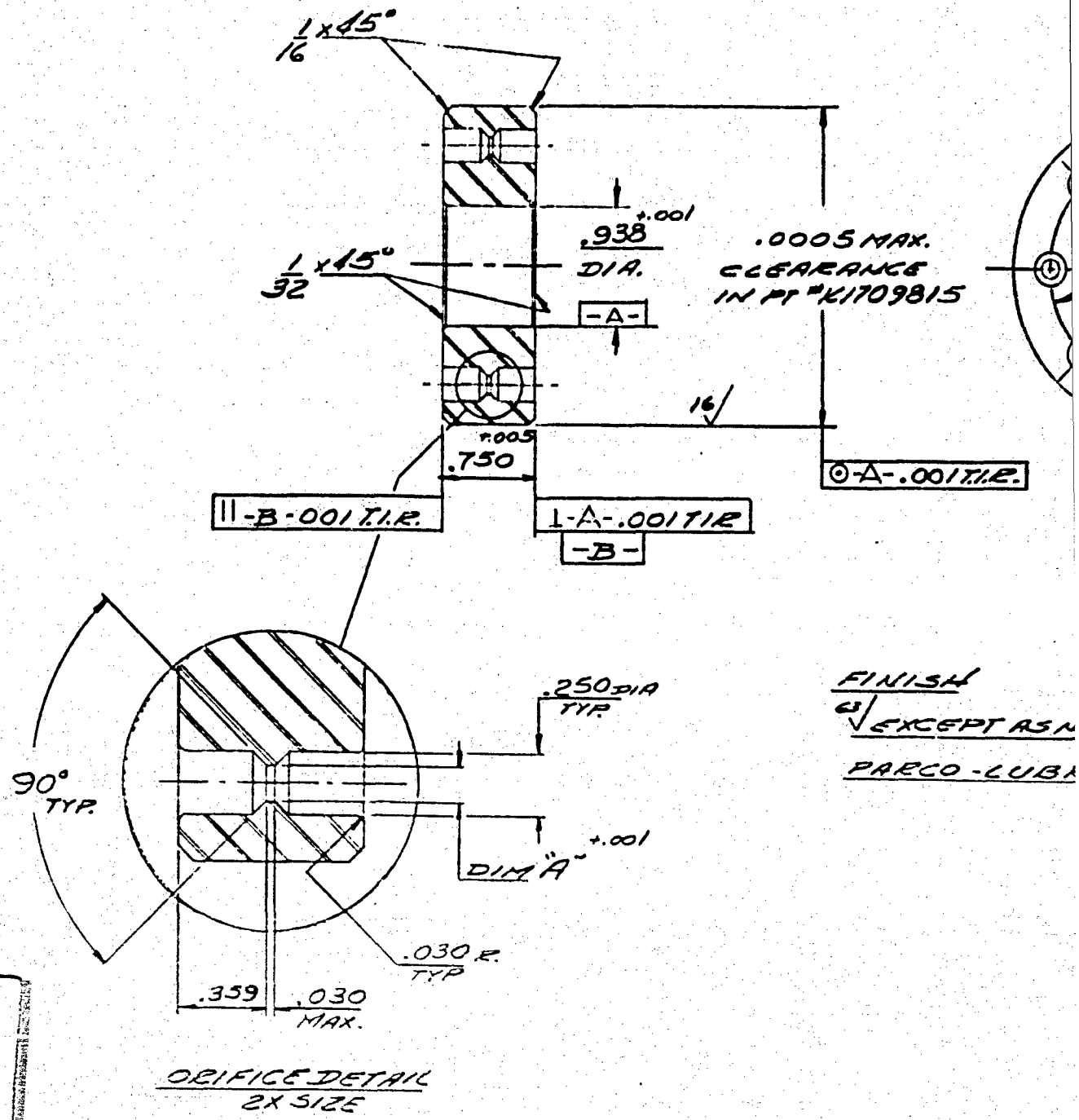

Fig. G-2 Damper-Pisto

PART No.	DIM "A"	No REQ.
K1709816-1	.045	2
K1709816-2	.089	2
K1709816-3		

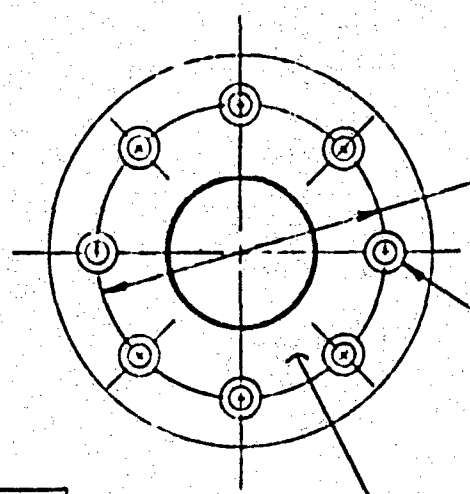

MAX.
ICE
09815

-.001 T.I.R.

NISH
EXCEPT AS NOTED
ARCO-LUBRIZE

2

-2 Damper-Piston

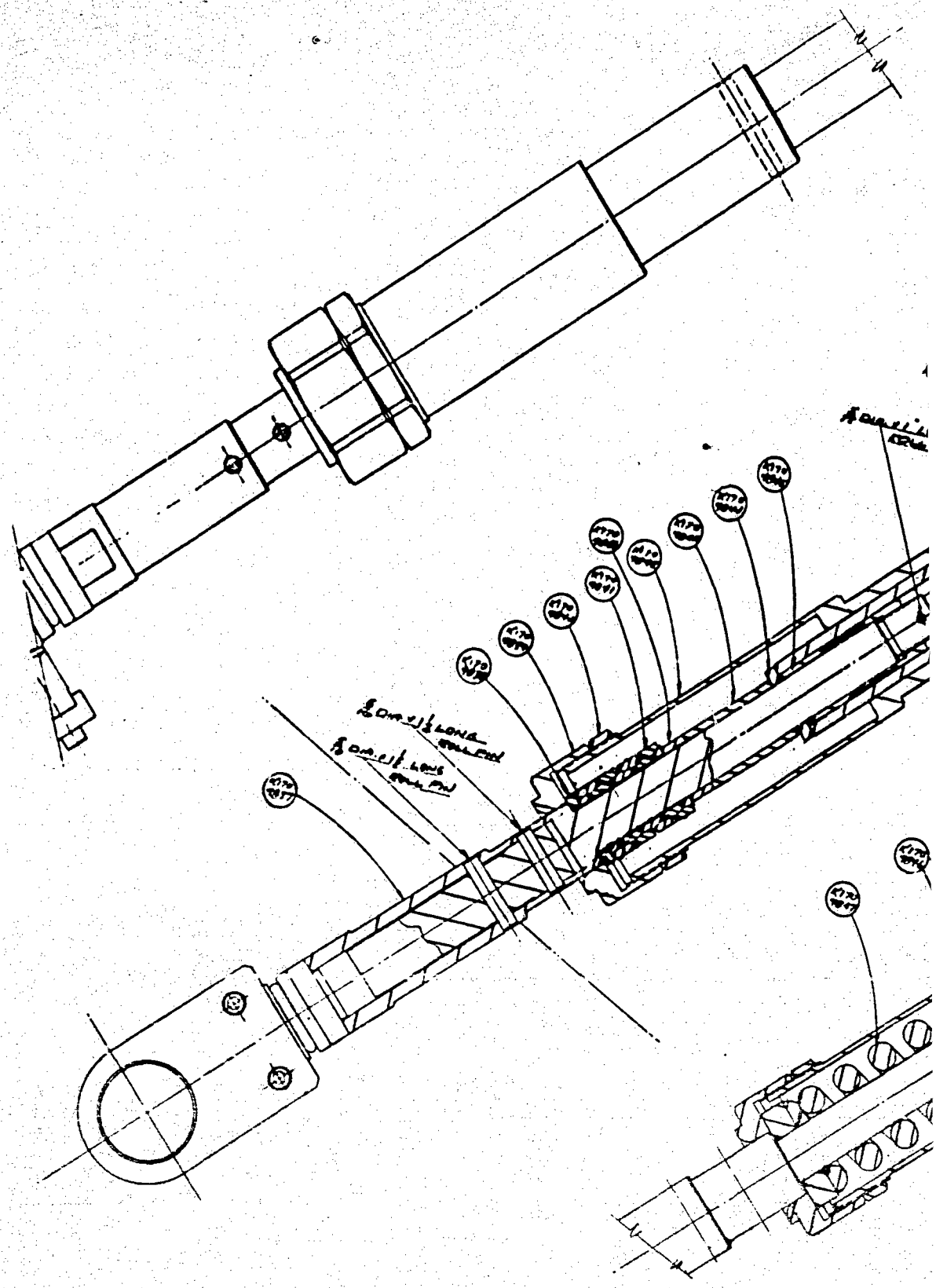

Fig. G-3 Spring Damper Combinati

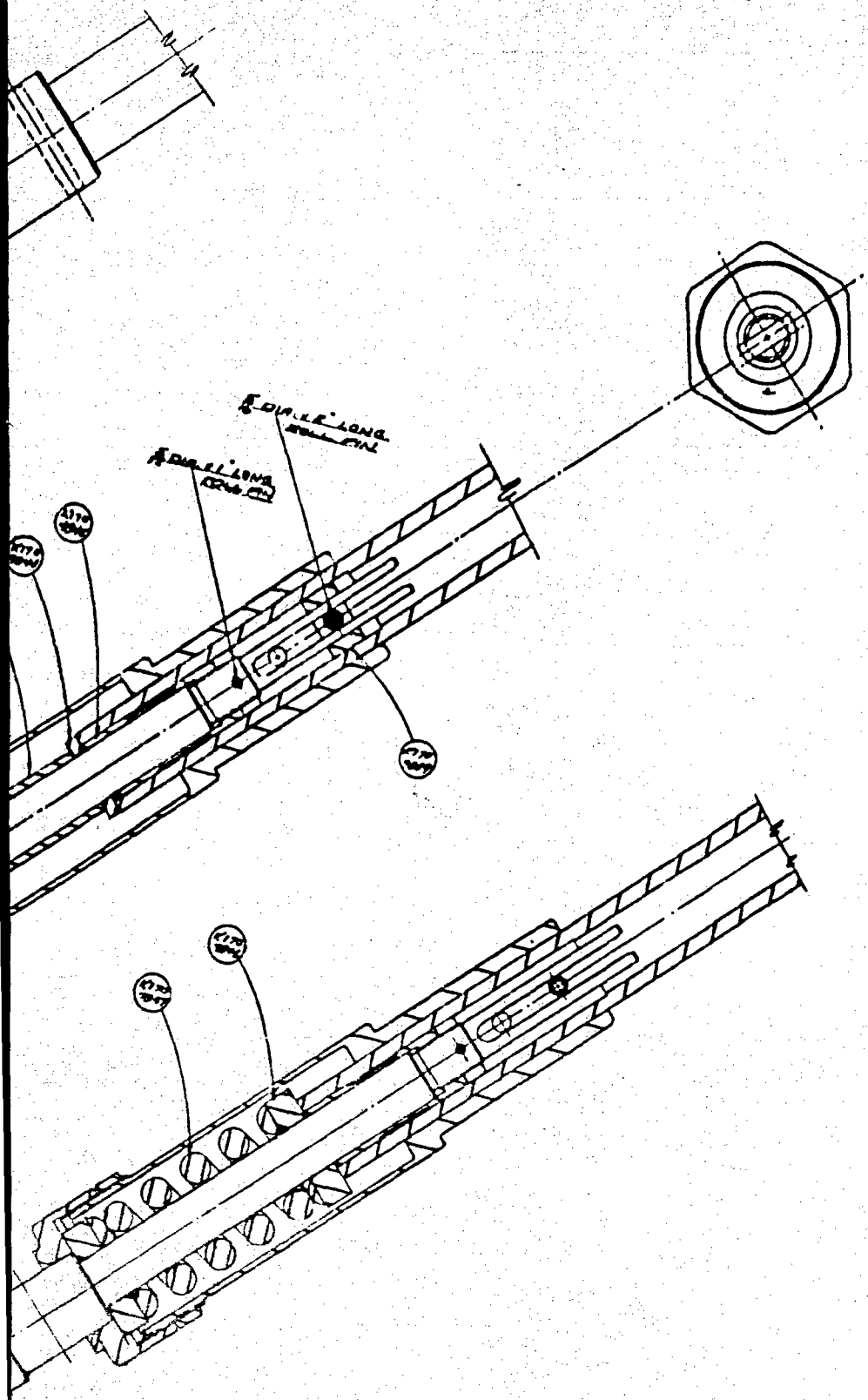

2

Damper Combination Assembly

SPRING DATA

MATL.	AISI 1095 SPRING STL.
WIRE DIA.	1/2 "
MEAN DIA.	1-7/16"
ACTIVE COILS	4-1/3
TOTAL COILS	6-1/3
RATE	7000 lb/in.
FREE HEIGHT	3-13/16
SOLID HEIGHT	3-3/16
INSTALLED HEIGHT	3-5/8
PRE-LOAD	1200 lb
DEFLECTION	.572"
MAX. LOAD	4000 lb
STRESS	115,000 p.s.i.
WOUND	R.H. - L.H.
ENDS	SQUARED & GROUND

Fig. G-4 SPRING DATA

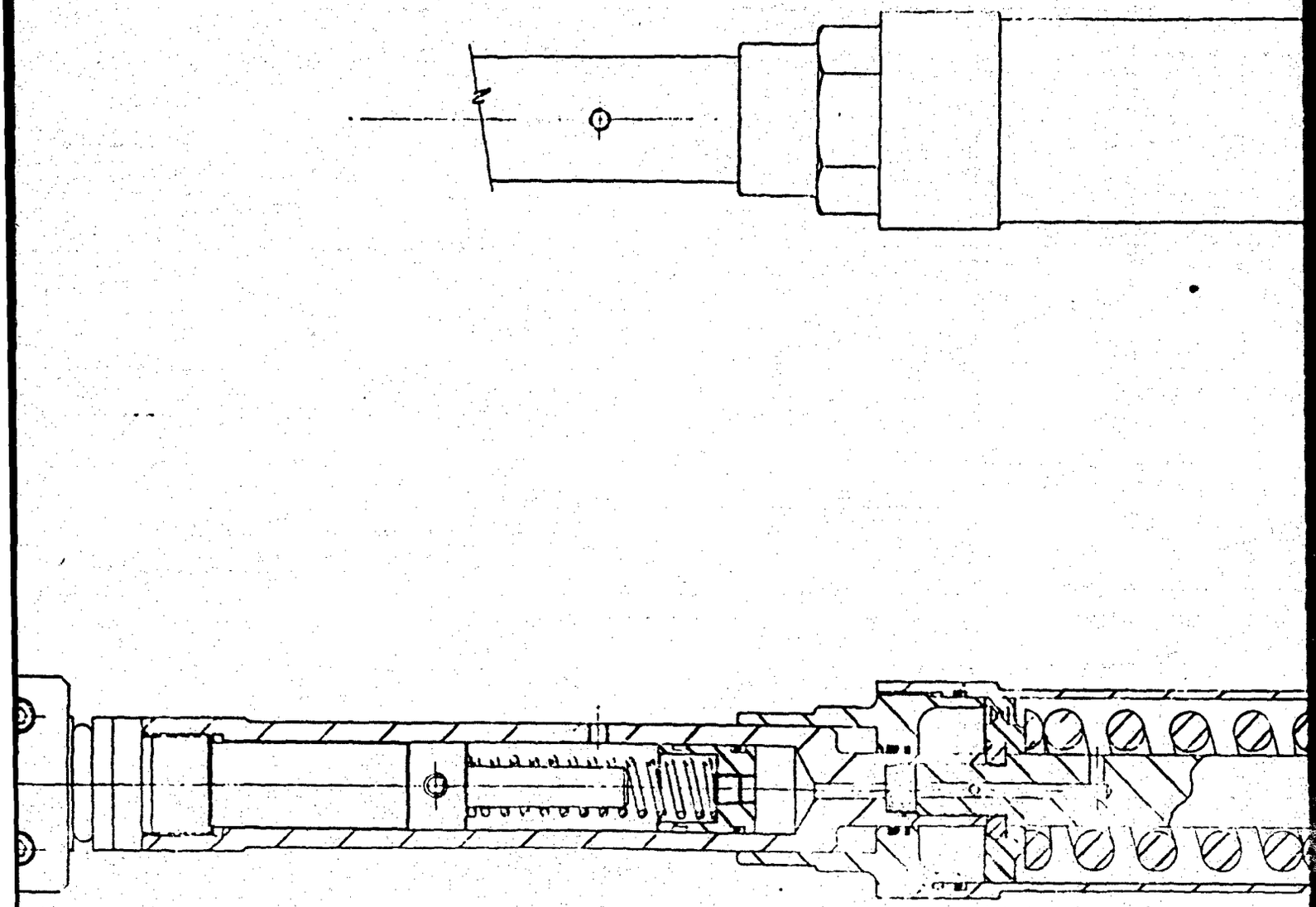

Fig. G-5 Spring Damper Combi

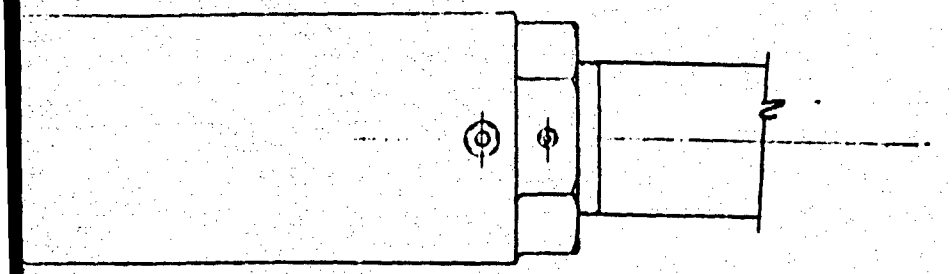

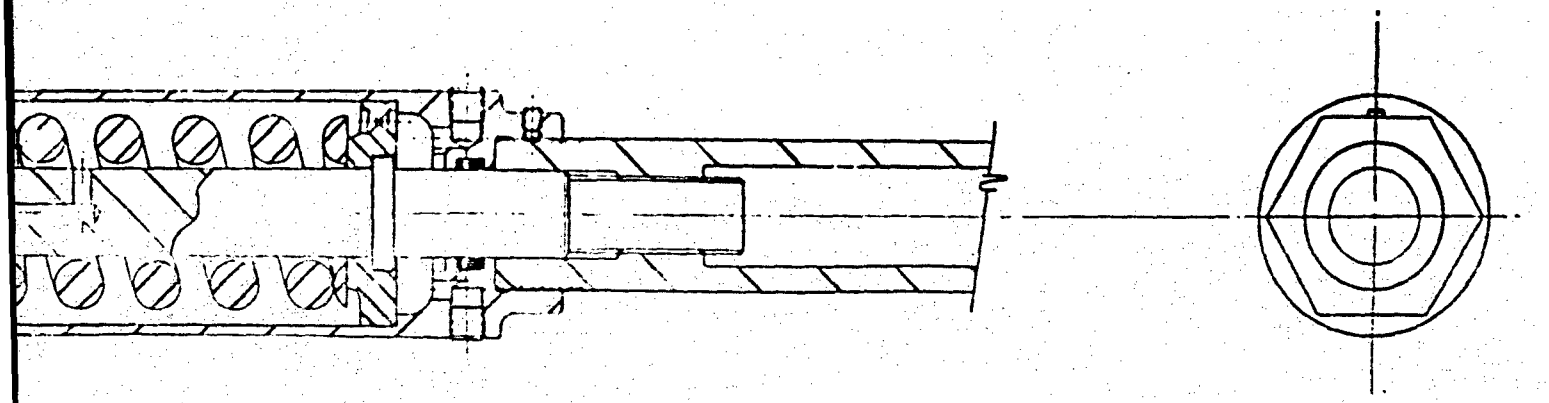

2

Spring Damper Combination

APPENDIX H

STRUCTURAL STIFFNESS MEASUREMENTS

R. M. Brach and R. H. Van Beek

I. INTRODUCTION

In order to improve launcher accuracy by choosing optimum launcher parameters, the individual effect of each significant parameter must be determined. Studies with mathematical models are being used to determine these effects, followed by firing programs to substantiate the theoretical conclusions. The success of using mathematical models for this purpose depends upon at least two major points: (1) the degree to which the models qualitatively represent the dynamics of the launcher and (2) the quantitative agreement between the mathematical model output values and actual measurements of launcher motion. In order to optimize the quantitative agreement, the numerical input values to the mathematical models should correspond closely to measured values for the actual launcher. For this reason, static stiffness measurements were made of a number of launcher structural components using Prototype No. 3 as well as the trails of Prototype No. 1. Another equally important reason for making these measurements is to enable comparison of the actual stiffness values of the manufactured parts with the intended design stiffness.

The overall, or combined, stiffness of the launcher structure below the trunnions is desired. It would also be very useful to determine which components, such as the carriage box-sections, trail hinge-pins, etc., contribute the most to the total flexibility. As it would have been time consuming and costly to disassemble the entire structure and measure the stiffness of each part, the stiffness of the entire structure was first measured, and then, wherever disassembly was simple, as for example, the removal of the trails, separate measurements were taken. An attempt was made to determine the stiffness of certain components by eliminating their contributions to flexibility by means of auxiliary stiffeners. In general, no special consideration was given to the measurement procedures to develop

extreme accuracy since stiffness values accurate within 5% to 10% were regarded as sufficient with respect to the mathematical models. Standard laboratory test machines were used wherever possible.

II. MEASUREMENTS

Static stiffness measurements were made for the following components and assemblies:

1. The entire structure below the trunnions(supporting structure).
2. The entire structure below the trunnions with the upper and lower carriage box-sections clamped together.
3. The entire structure below the trunnions with the carriage box-sections clamped together and struts inserted between the trunnions and trails. (Trails were parallel to the firing tube.)
4. The entire structure without stiffeners but traversed:
   a. 20° right
   b. 20° left
5. Elevating screw support
6. Trails:
   a. Prototype No. 3
   b. Prototype No. 1

The stiffness of the entire supporting structure was measured by applying a known load perpendicular to a bar supported through the trunnions, and measuring the deflection of the trunnions with dial gages. A side elevation of this system is shown in Fig. H-1. The load was measured with calibrated strain gages on the loading bar.

The trail stiffness was measured with the two trails clamped together by a relatively stiff fixture at their hinge-pin ends. This enabled the measurement and loading of the system to be performed as a simply supported beam (see Fig. H-2b). Again, the deflections were measured with dial gages.

The load-deflection characteristics of the jack screw supports in the upper carriage sides were measured by the procedure shown in Fig. H-2a. The compressive load applied to the screw was determined, as was the displacement of the screw relative to the upper carriage.

One parameter required by the mathematical models is a dynamic equivalent for the mass moment of inertia of the supporting structure, about a line through the ball joint perpendicular to the plane of elevation. This equivalent inertia, which permits the elastic carriage to be represented by a single flexibility and single inertia, can be measured indirectly by measuring the first mode natural frequency of the elastic carriage. In order to do this, an electro-dynamic shaker was attached to the bar through the trunnions for the purpose of applying to the launcher a harmonic force of variable frequency. The dynamic stiffness was measured as

$$k_D = \frac{Fw^2}{a},$$

where F is the applied force, w is the frequency, and a is the acceleration. Zero or very small values of the dynamic stiffness indicate resonance, and the smallest of the resonant frequencies is the first normal mode frequency.

III. DISCUSSION OF RESULTS AND CONCLUSIONS

Figure H-3 shows the load-deflection characteristics for the carriage. When converted to angular rotation about the base pivot, the average of the two sides yields a stiffness for the carriage of 32×10^6 lb-in./radian. Figure H-4 shows the stiffness of the same assembly, but with wedges between the upper and lower carriages and links of ties bolting the two together. The stiffness is 38.5×10^6 lb-in./radian. Figure H-5 shows the stiffness of the same assembly as Figure H-4, but with additional links connecting the trunnions to the trails. The stiffness is 55.5×10^6 lb-in./radian.

Figures H-6 and H-7 show the load-deflection characteristics of the carriage in full traverse, right and left, respectively. Traverse to the right stiffens the right trunnion and adds flexibility to the left trunnion, and vice versa; but there is a net decrease in the average stiffness. For both right and left traverse, the average stiffness is 25×10^6 lb-in./radian.

Figure H-8 shows the load-deflection characteristics of the lower elevating screw supports loaded in compression. This deflection occurs in the complicated structure consisting of the elevating screw gear box and its mounting.

Figure H-9 shows the load-deflection characteristics of the Prototype No. 3 trails joined at the hinge-pins and loaded as a single, simply supported beam. Converted to angular rotation, which would be produced about the base pivot, the combined stiffness of the two trails is 145×10^6 lb-in./radian. Figure H-10 gives the same data for the Prototype No. 1 trails, for which the combined stiffness is 109×10^6. The trails on the two prototypes are of different lengths, and the stiffness varies as the length squared. For purposes of comparison, the stiffness of the Prototype No. 3 trails was extrapolated to the value they would have if their length were the same as that of the Prototype No. 1 trails. This value is 223×10^6 lb-in./radian. The weight of the Prototype No. 3 trails is 385 lb; of the Prototype No. 1 trails, 351 lb. On the basis of these stiffnesses and weights, the stiffness-to-weight ratio of the Prototype No. 3 trails is computed to be 87% greater than that of the Prototype No. 1 trails.

Figure H-11 shows the results of the dynamic stiffness measurements on the carriage. The data are not conclusive, but it is probable that resonance in the first normal mode is indicated at 70 cps. The inertia of a torsional system having a stiffness of 32×10^6 lb-in./radian and a natural frequency of 70 cps agrees reasonably well with the calculated equivalent inertia of the carriage.

Each elevating screw and upper bracket assembly was loaded in compression in a universal testing machine. Fig. H-12 shows the resulting load-deflection curve for each screw-bracket assembly. The nonlinearities are due primarily to nonlinear local deflections under the balls in the ball nuts and also to clearances between the balls and the nut.

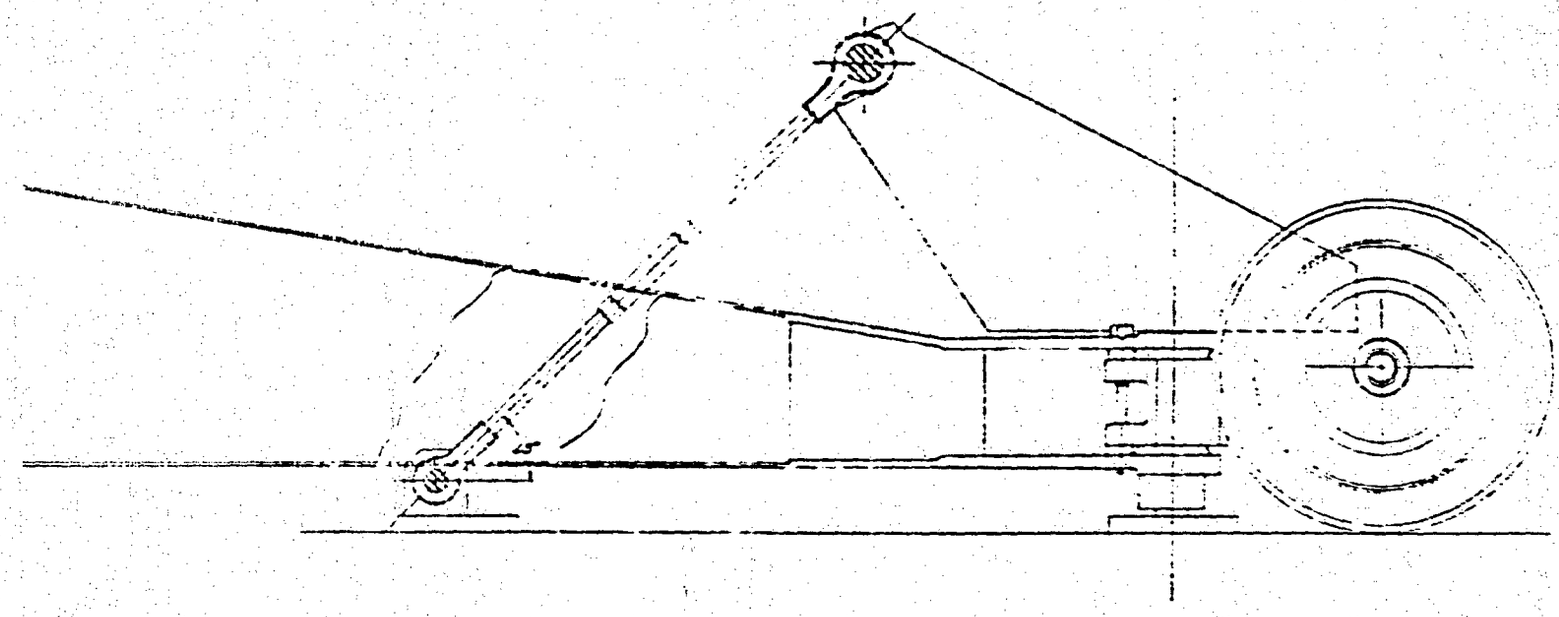

Fig. H-1 **TEST SETUP FOR MEASURING CARRIAGE STIFFNESS AT TRUNNIONS**

Fig. H-2a Stiffness of Elevating Screw Support

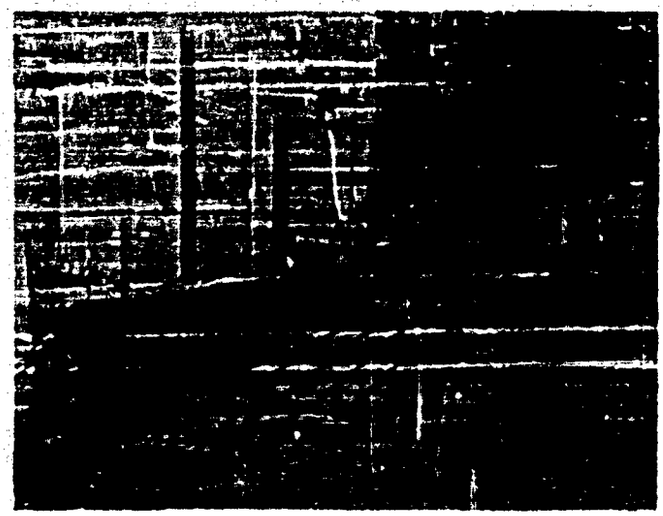

Fig. H-2b Stiffness of Trails

Fig. H-2c Natural Frequency of Carriage

Fig. H-2 LAUNCHER COMPONENTS UNDERGOING TESTS

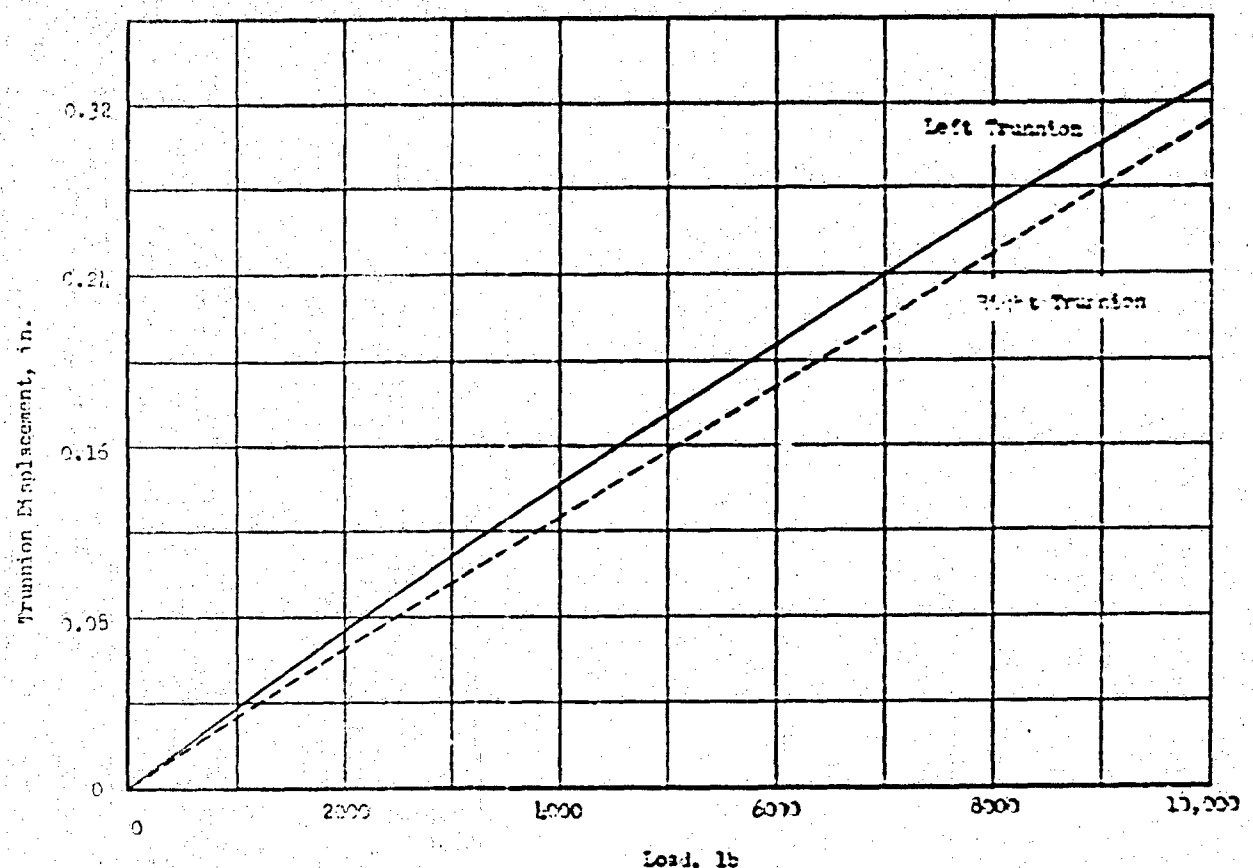

Fig. H-3 STIFFNESS OF CARRIAGE AT TRUNNIONS WITHOUT STIFFENERS

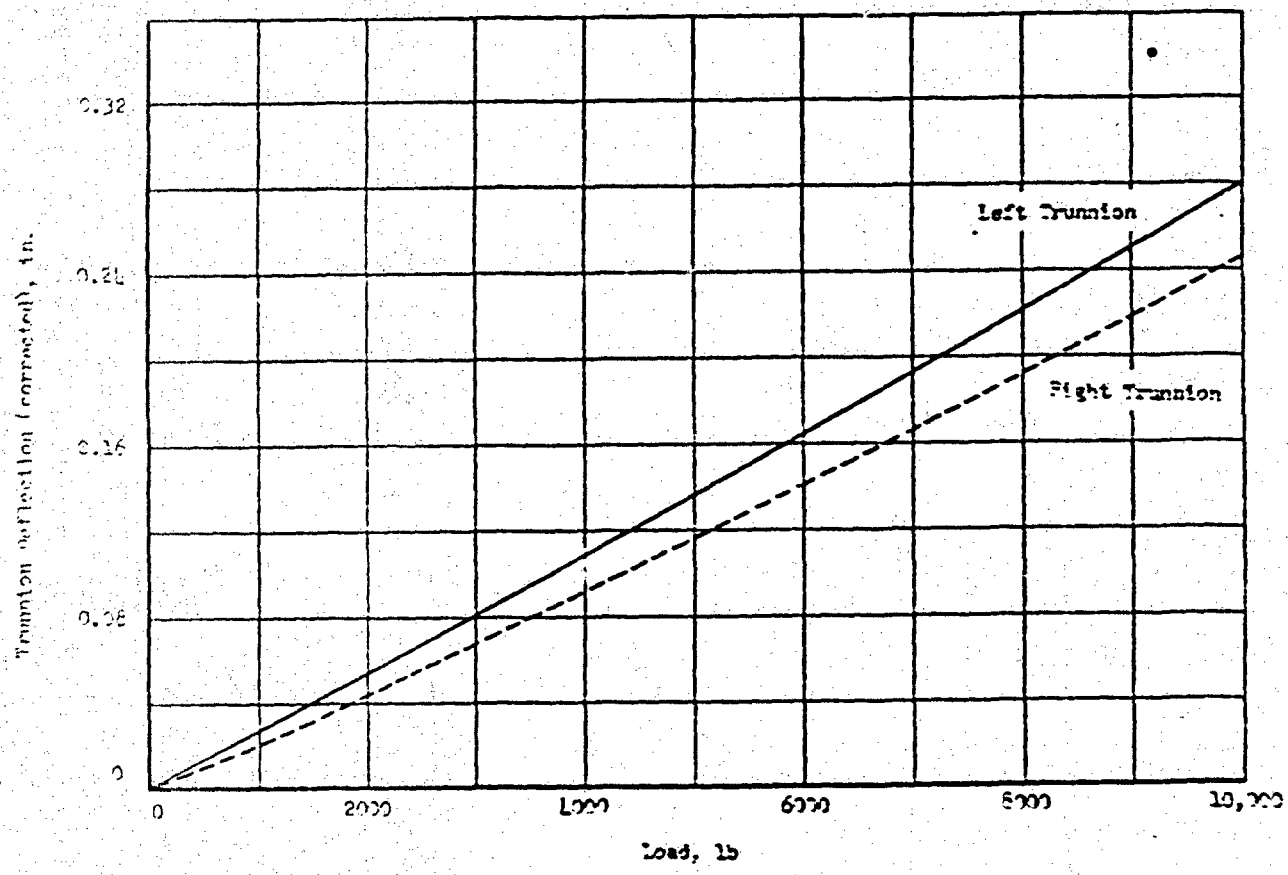

Fig. H-4 STIFFNESS OF CARRIAGE AT TRUNNIONS WITH WEDGES AND TIES

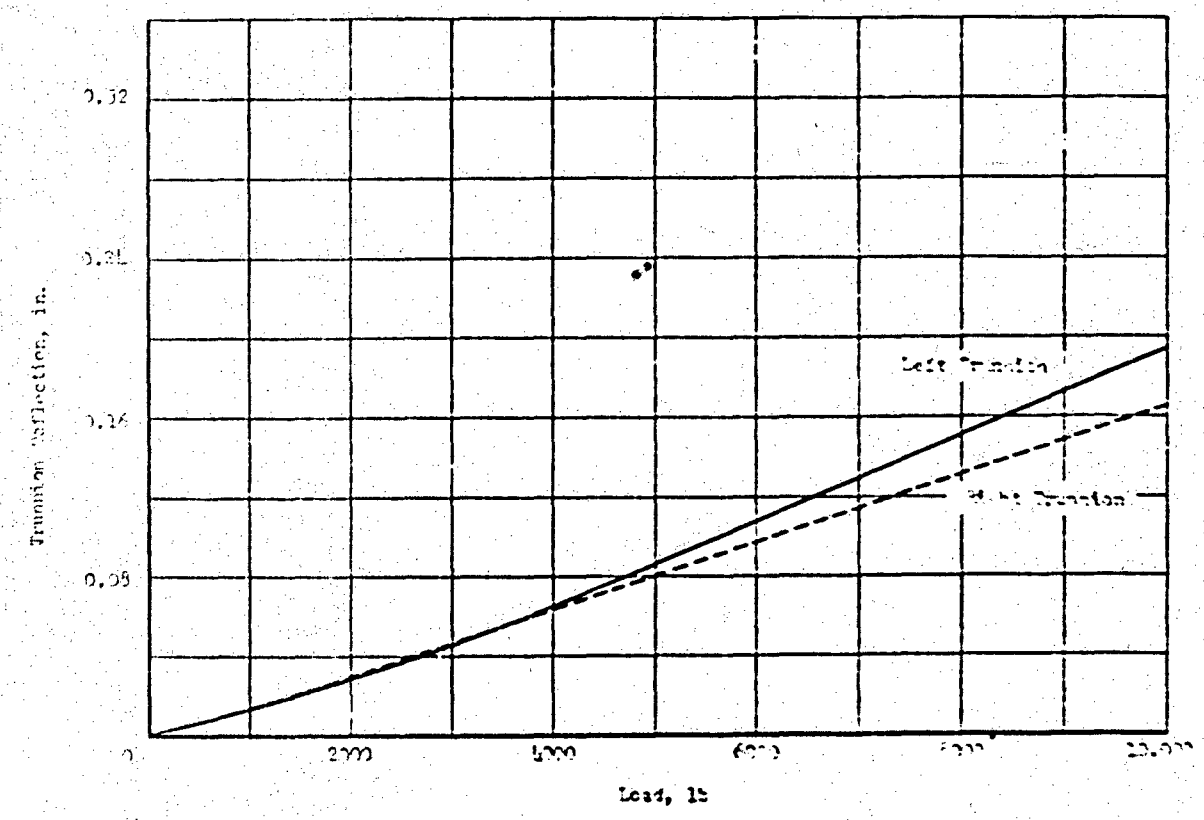

Fig. H-5 **STIFFNESS OF CARRIAGE AT TRUNNIONS WITH WEDGES, TIES, AND LINKS BETWEEN TRUNNIONS AND TRAILS**

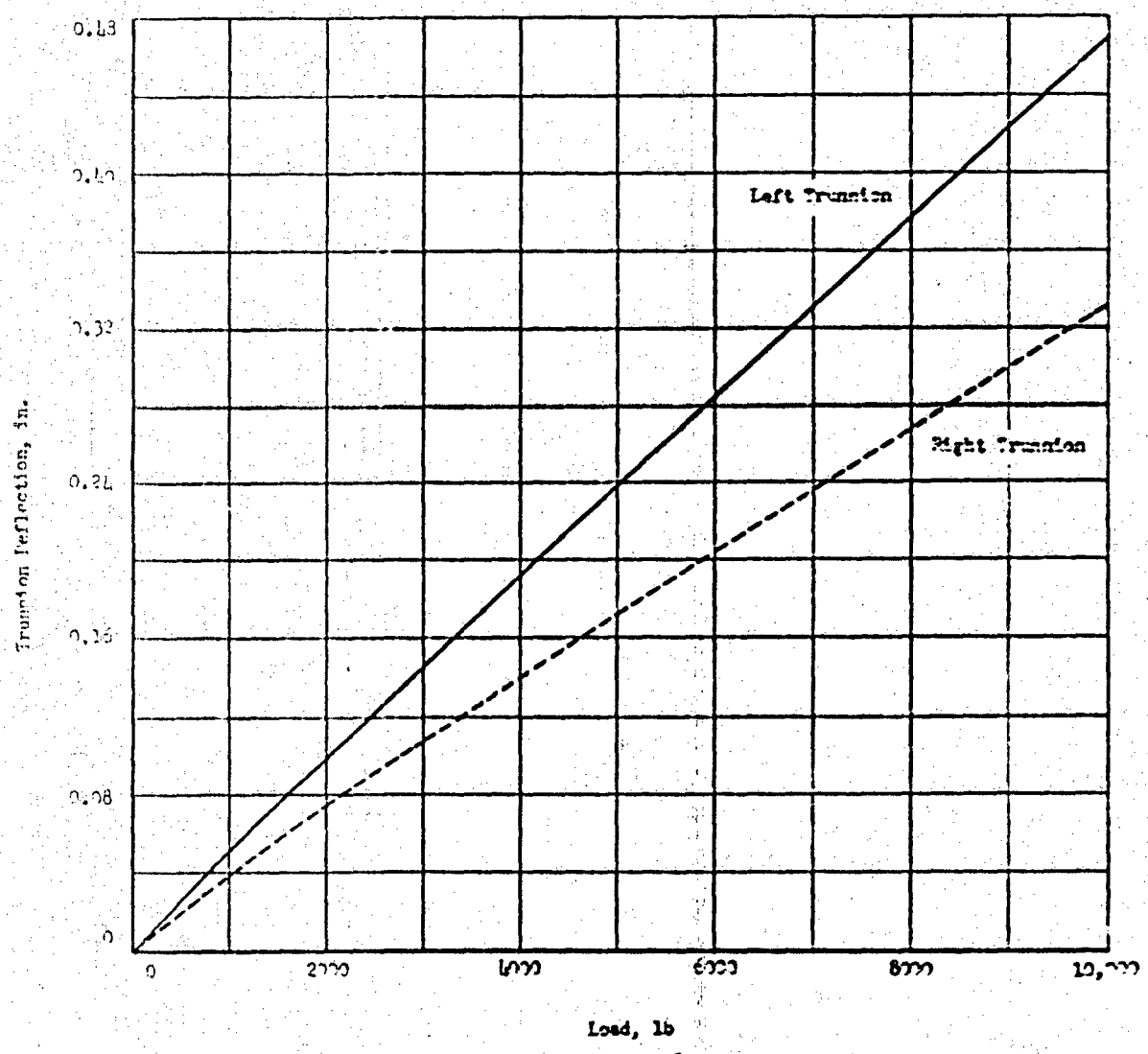

Fig. H-6 **STIFFNESS OF CARRIAGE AT FULL TRAVERSE, 20° RIGHT**

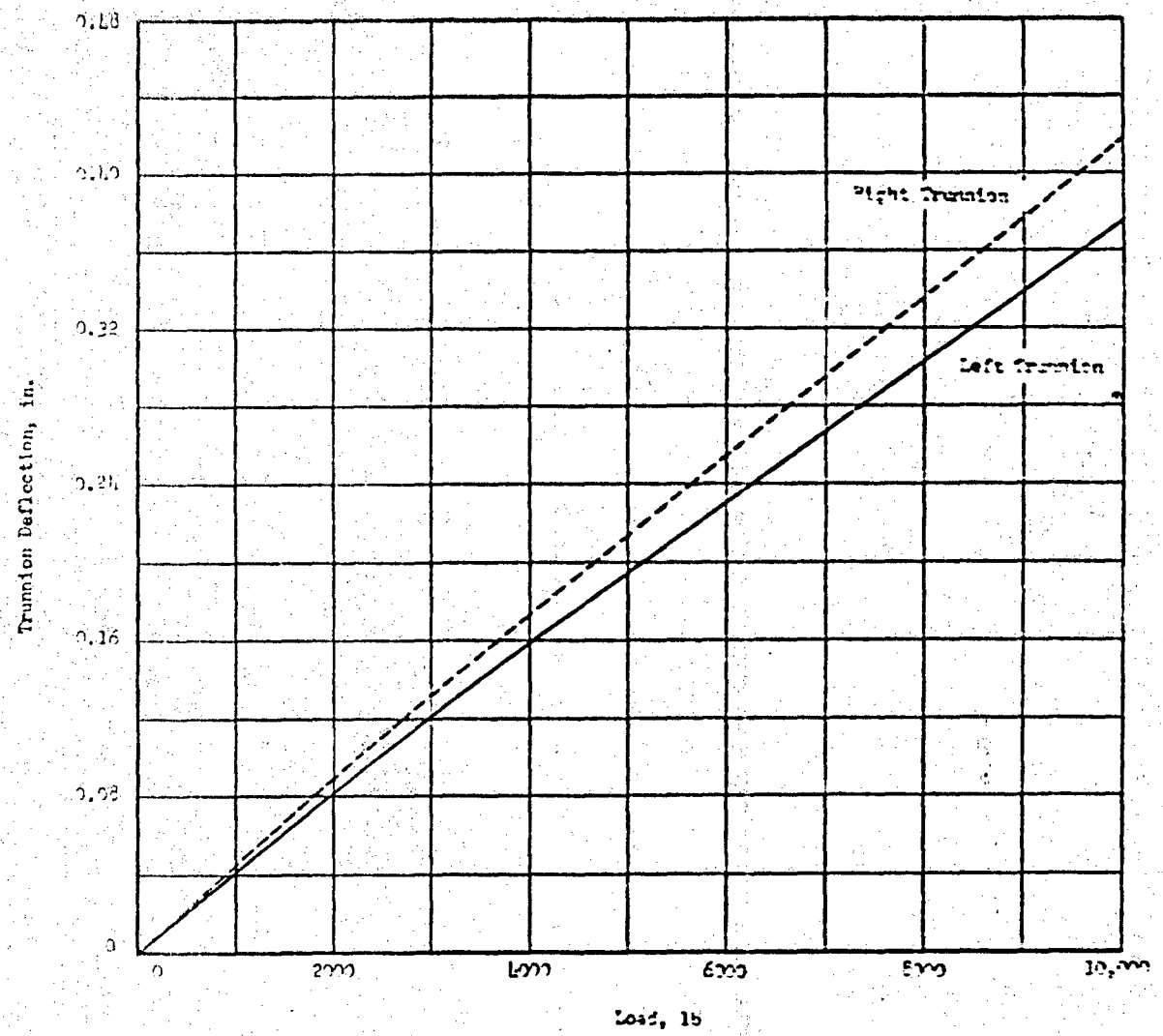

Fig. H-7 **STIFFNESS OF CARRIAGE AT FULL TRAVERSE, 20° LEFT**

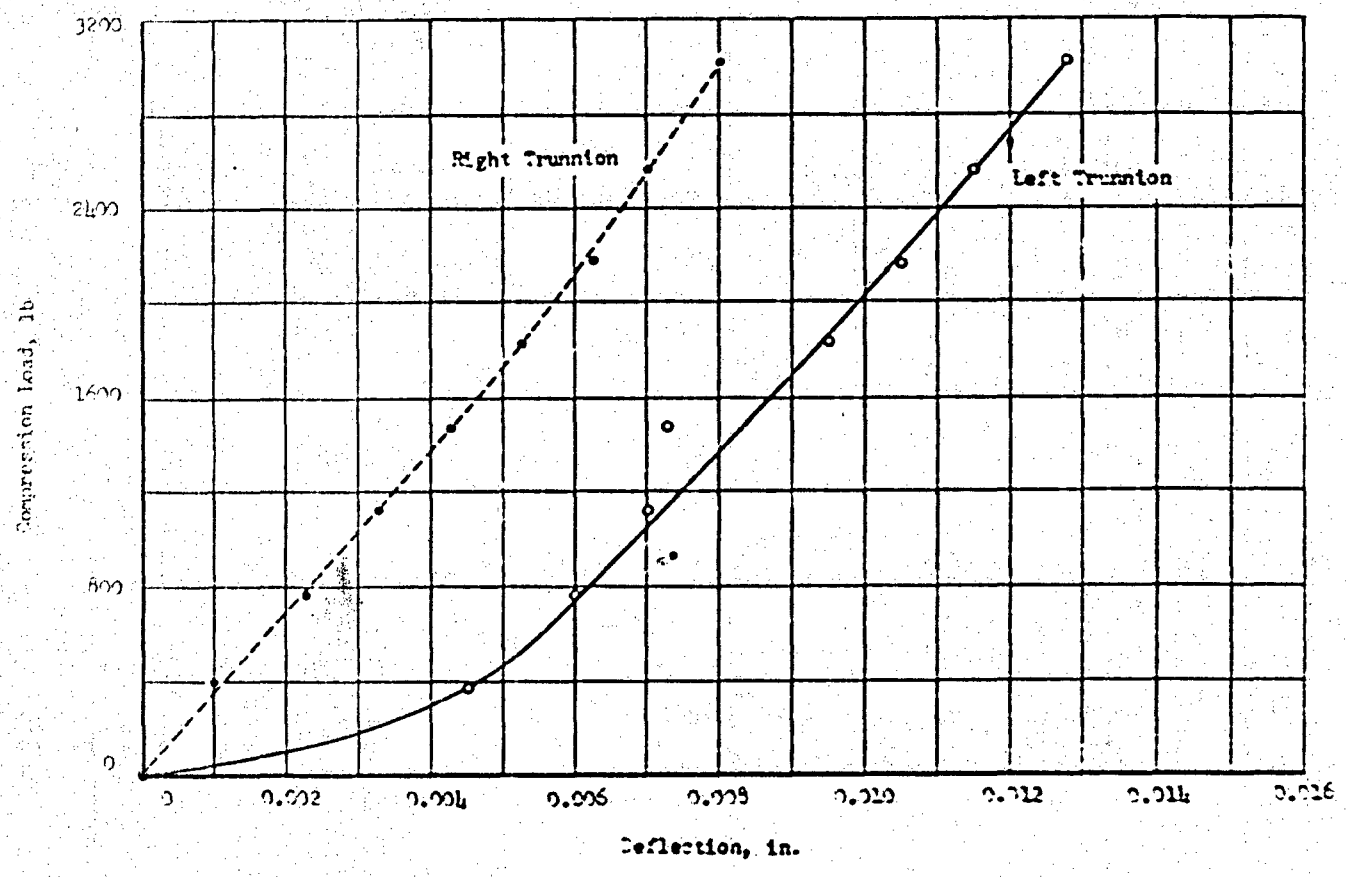

Fig. H-8 **STIFFNESS OF ELEVATING SCREW SUPPORTS**

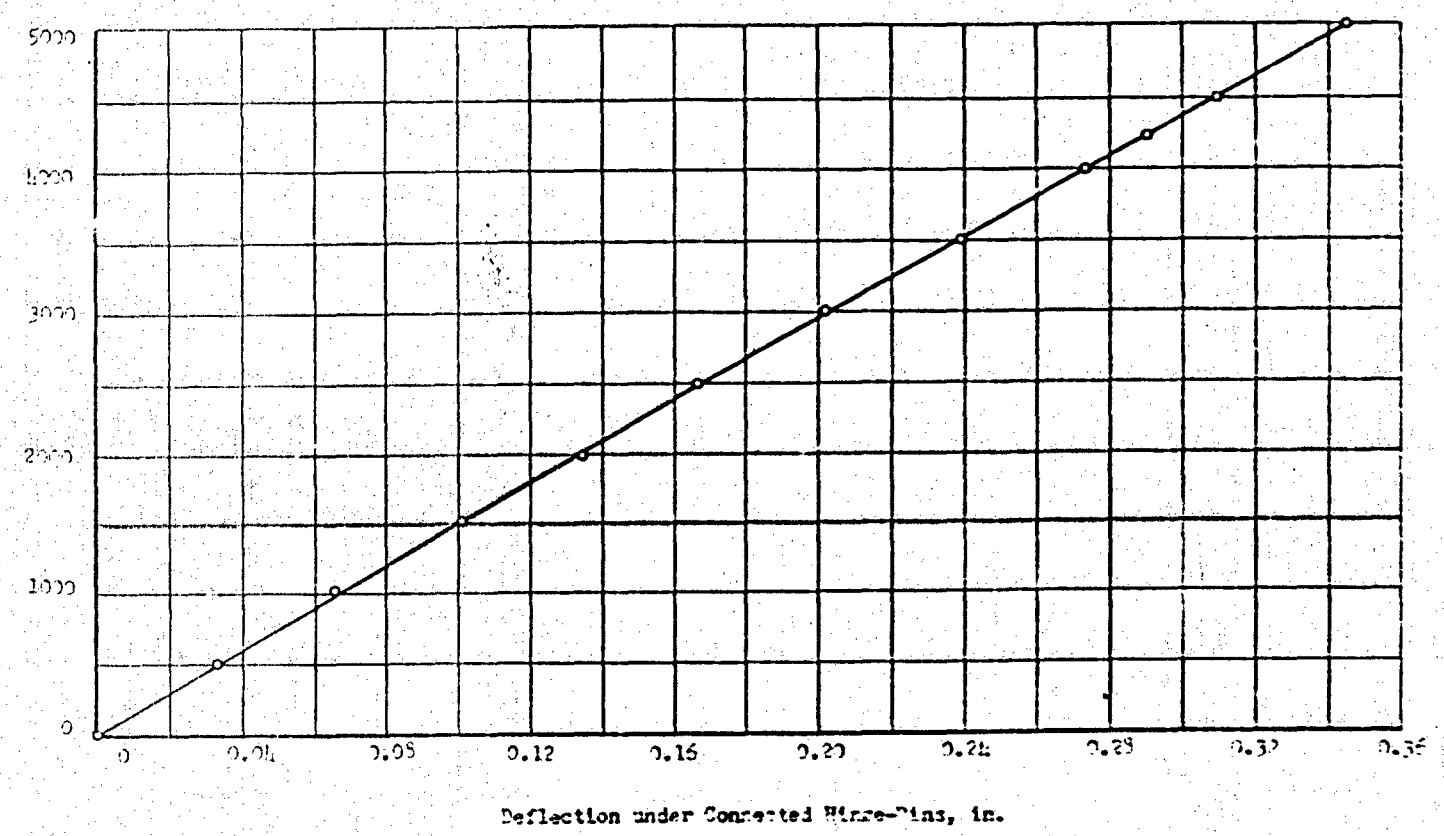

Fig. H-9 STIFFNESS OF PROTOTYPE NO. 3 TRAILS

ARMOUR RESEARCH FOUNDATION OF ILLINOIS INSTITUTE OF TECHNOLOGY

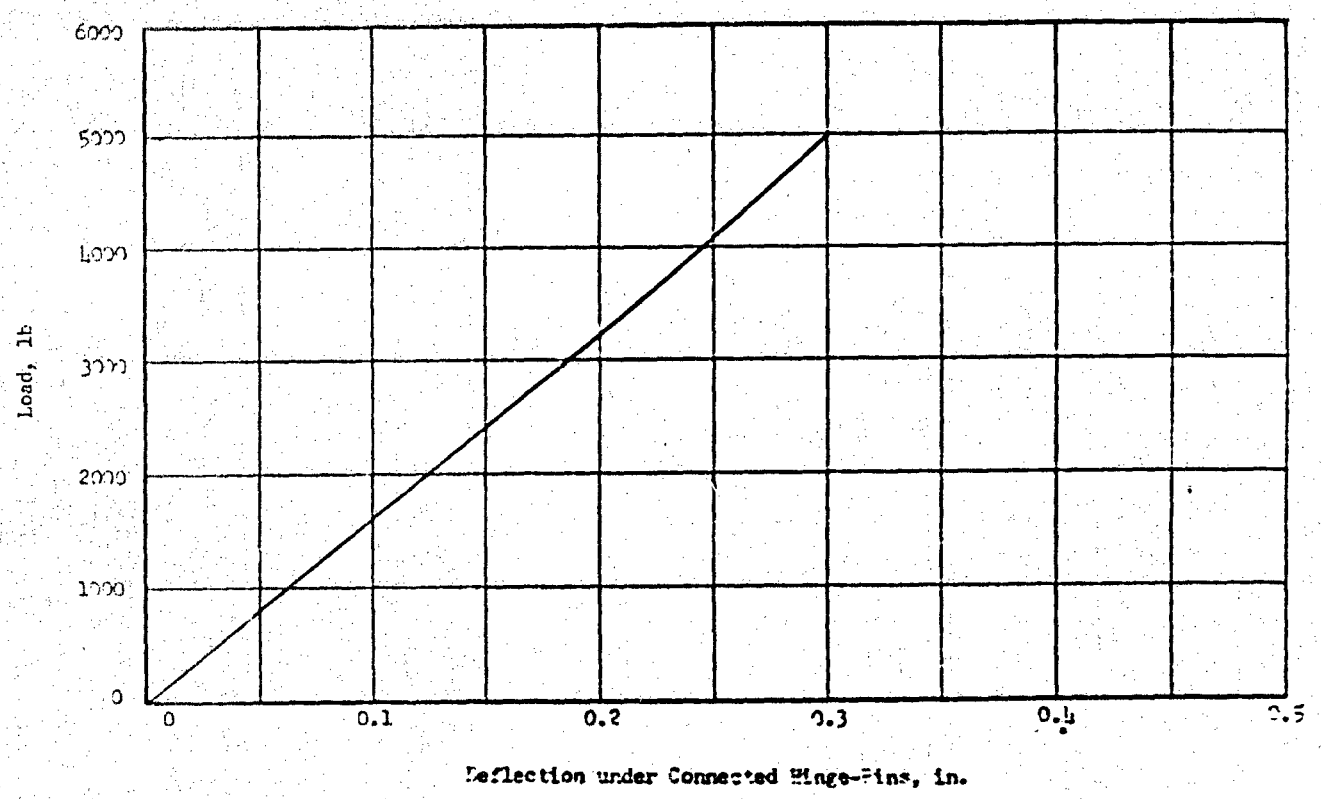

Fig. H-10 **STIFFNESS OF PROTOTYPE NO. 1 TRAILS**

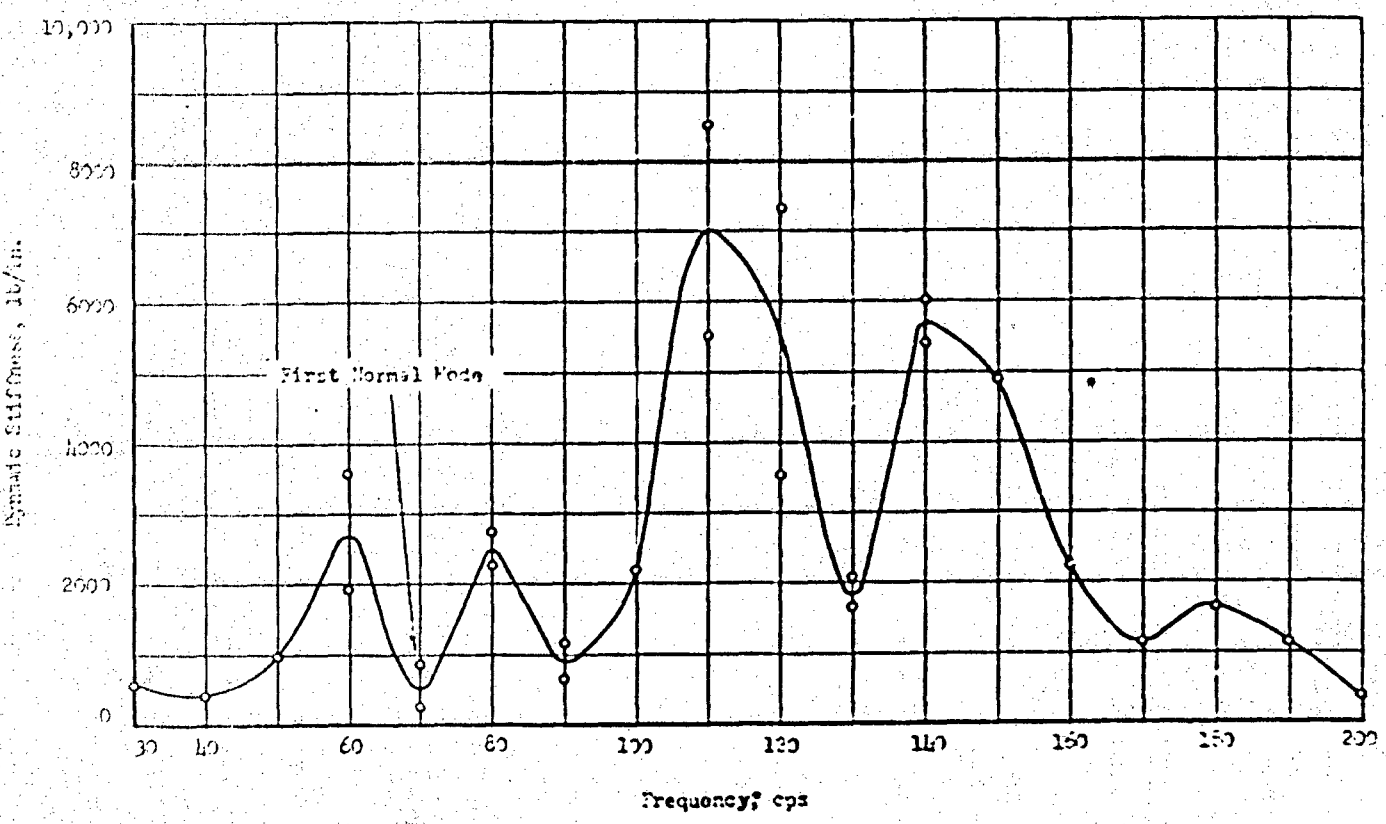

Fig. H-11 **NATURAL FREQUENCY OF LAUNCHER CARRIAGE**

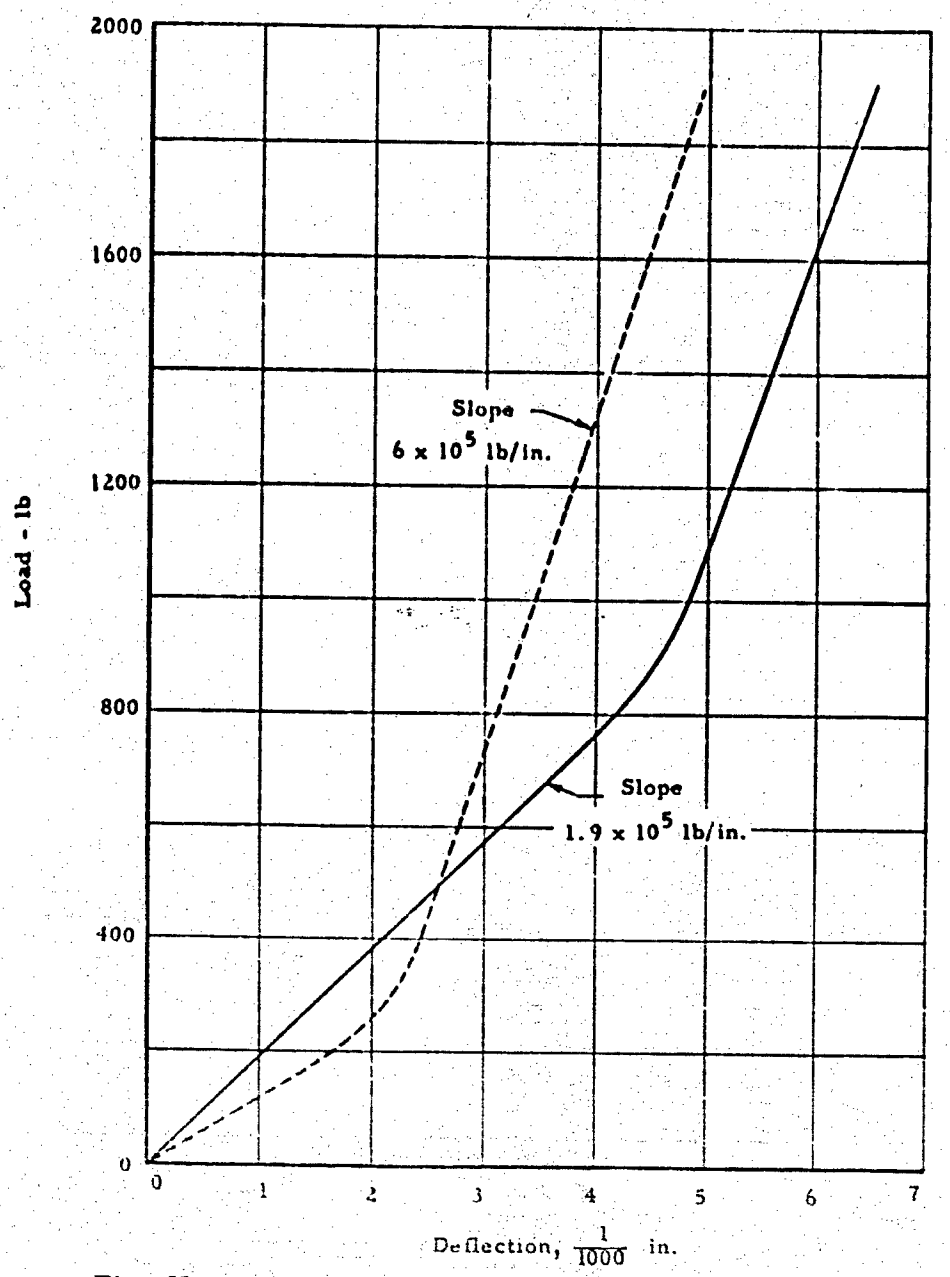

Fig. H-12 STIFFNESS OF ELEVATING SCREWS AND UPPER BRACKETS

APPENDIX I

FIRING PROGRAM

This Appendix presents a list of the firings conducted in order to obtain the launcher response in the vertical plane (see Appendix J). The instrumentation for each firing is listed as well as the structural configuration. The bursts are coded with B followed with a number; each round is individually marked by R with a corresponding number.

Because of instrumentation difficulties, some bursts were repeated. These are not listed because they were under identical conditions. Also some additional firings were made such as those to study the horizontal dispersion problem; these are described in the report body and not listed here.

TABLE I-1
FIRING SCHEDULE

Burst No.	Round No.	Zone Elevation / Traverse	Target	Instrumentation	Fixtures	Movies	Comments
S. S.	R-1	8/60°/0°	No	4, 5, 6, 8, 10	None	None	To seat firing base and stakes
S. S.	R-2	8/60°/0°	No	4, 5, 6, 8, 10	None	None	and also to adjust C' recoil buf-
S. S.	R-3	8/60°/0°	No	4, 5, 6, 8, 10	None	None	fer. Checkout instrumentation.
B-1	R-4	8/45°/0°	Yes	3, 4, 5, 6, 8, 10	None	On	This will be a burst to be used
	R-5	8/45°/0°	Yes	3, 4, 5, 6, 8, 10	None	Target	for comparison purposes but
	R-6	8/45°/0°	Yes	3, 4, 5, 6, 8, 10	None	(See	also to check out the left-right
	R-7	8/45°/0°	Yes	3, 4, 5, 6, 8, 10	None	Comments)	sequencing. Have a movie cam-
	R-8	8/45°/0°	Yes	3, 4, 5, 6, 8, 10	None	Black &	era on the target to record se-
	R-9	8/45°/0°	Yes	3, 4, 5, 6, 8, 10	None	White	quence. Regular 16MM camera
							at high speed.
B-2	R-10	9/45°/0°	Yes	3, 4, 5, 6, 8, 10	None	On target	Same as previous burst
	R-11	9/45°/0°	Yes	3, 4, 5, 6, 8, 10	None	On target	
	R-12	9/45°/0°	Yes	3, 4, 5, 6, 8, 10	None	On target	
	R-13	9/45°/0°	Yes	3, 4, 5, 6, 8, 10	None	On target	
	R-14	9/45°/0°	Yes	3, 4, 5, 6, 8, 10	None	On target	
	R-15	9/45°/0°	Yes	3, 4, 5, 6, 8, 10	None	On target	
B-3	R-16	9/45°/0°	Yes	3, 4, 5, 6, 8, 10	None	On target	Repeat of previous burst to
	R-17	9/45°/0°	Yes	3, 4, 5, 6, 8, 10	None	On target	check similarity of results.
	R-18	9/45°/0°	Yes	3, 4, 5, 6, 8, 10	None	On target	(Mainly to check the similarity
	R-19	9/45°/0°	Yes	3, 4, 5, 6, 8, 10	None	On target	of target patterns.)
	R-20	9/45°/0°	Yes	3, 4, 5, 6, 8, 10	None	On target	
	R-21	9/45°/0°	Yes	3, 4, 5, 6, 8, 10	None	On target	

Burst No.	Round No.	Zone Elevation / Traverse	Target	Instrumentation	Fixtures	Movies	Comments
B-4	R-22	9/45°/0°	Yes	3, 4, 5, 6, 8, 10	None	None	To complete a set of three records
	R-23	9/45°/0°	Yes	3, 4, 5, 6, 8, 10	None	None	at this condition for comparison.
							Record round sequence through
							target.
B-5	R-24	9/45°/0°	Yes	3, 4, 5, 6, 8, 10	1a, 3	None	Large damper holes. Record
	R-25	9/45°/0°	Yes	3, 4, 5, 6, 8, 10	1a, 3	None	round sequence through target.
S. S.	R-26	9/45°/0°	No	3, 4, 5, 6, 8, 10	1a, 3	None	Single shot repeat of preceding
							burst.
S. S.	R-27	9/45°/0°	No	3, 4, 5, 6, 8, 10	1a, 3	None	Repeat of preceding test.
B-6	R-28	9/45°/0°	Yes	3, 4, 5, 6, 8, 10	1a, 3	None	Change to small diameter holes
	R-29	9/45°/0°	Yes	3, 4, 5, 6, 8, 10	1a, 3	None	in hydraulic damper. Record
							round sequence through target.
S. S.	R-30	9/45°/0°	No	3, 4, 5, 6, 8, 10	1a, 3	None	Single shot repeat of preceding
							test.
S. S.	R-31	9/45°/0°	No	3, 4, 5, 6, 8, 10	1a, 3	None	Repeat of preceding test.
B-7	R-32	9/45°/0°	Yes	3, 4, 5, 6, 7	1a, 3, 4, 5, 6	None	Small dia. holes in damper coil
	R-33	9/45°/0°	Yes	3, 4, 5, 6, 7	1a, 3, 4, 5, 6	None	spring in elevating system.
S. S.	R-34	9/45°/0°	No	3, 4, 5, 6, 7	1a, 3, 4, 5, 6	None	Single shot repeat of preceding
							test.
S. S.	R-35	9/45°/0°	No	3, 4, 5, 6, 7	1a, 3, 4, 5, 6	None	Repeat of preceding test.

Burst No.	Round No.	Zone Elevation / Traverse	Target	Instrumentation	Fixtures	Movies	Comments
B-8	R-36	9/45°/0°	Yes	3, 4, 5, 6, 7, 8	2,3,4,5,6	None	Small dia. damper holes.
	R-37	9/45°/0°	Yes	3, 4, 5, 6, 7, 8	2,3,4,5,6	None	record target sequence.
S. S.	R-38	9/45°/0°	No	3, 4, 5, 6, 7, 8	2,3,4,5,6	None	Single shot repeat of preceding test.
S. S.	R-39	9/45°/0°	No	3, 4, 5, 6, 7, 8	2,3,4,5,6	None	Repeat of preceding test.
B-9	R-40	9/45°/0°	No	3, 4, 5, 6	1b	None	Install ring springs into
	R-41	9/45°/0°	No	3, 4, 5, 6	1b	None	elevating system.
S. S.	R-42	9/45°/0°	No	3, 4, 5, 6	1b	None	Single-shot repeat of preceding test.
B-10	R-43	9/45°/0°	No	3, 4, 5, 6, 7	1b, 3	None	Repeat of previous test with
	R-44	9/45°/0°	No	3, 4, 5, 6, 7	1b, 3	None	damper added. Small dia. holes.
B-11	R-45	7/45°/0°	No	3	1a	None	No recoil pressure
	R-46	7/45°/0°	No	3	1a	None	

ARMOUR RESEARCH FOUNDATION OF ILLINOIS INSTITUTE OF TECHNOLOGY

The following fixtures were required for the experimental firings of Pilot No. 3 at Ft. Sheridan. The corresponding numbers in the following list will be used in the firing schedule.

1. Variable flexibility elevating rods with: a.) coil springs and b.) friction damped ring springs,
2. Rigid elevating rods,
3. Hydraulic dampers between carriage sides and cradle with interchangeable pistons,
4. Shorter pad placement on the trails,
5. Trunnion-to-trail stiffening struts,
6. Brackets and wedges for stiffening the carriage box-sections.

The following instrumentation was required for the experimental firings of Pilot No. 3 at Ft. Sheridan. The combination of instruments to use for each particular firing will be found on the firing schedule. Each of the following list will be referred to by number.

1. One strain gage on the rear plate of the recoiling parts for a firing signal.
2. One strain gage on each trail.
3. Two linear pots between cradle and ground, one on each side of the cradle, perpendicular to it at 45° elevation, a few inches behind the cradle front. Maximum expected motion, ± 3 in.
4. One strain gage on each elevating rod including the fixtures. Maximum expected strain, 300×10^{-6} in./in.
5. Two linear pots, one on each side of the launcher, trunnion to ground, parallel to the cradle at 45° elevation. Expected maximum motion, ± 3/4 in.
6. Two linear pots, one on each side, trunnion to ground, perpendicular to the cradle at 45° elevation. Maximum expected motion, ± 1/2 in.
7. Two strain gages, one on each damper rod, to measure tension and compression. Maximum expected strain, 200×10^{-6} in./in.
8. One linear pot on each trail end, perpendicular to the ground. Maximum expected vertical displacement (+6, -1/4) in.

   (The firing base will be staked to prevent rearward displacements.)
9. Strain gages on the indexing system shafts.
10. Recoil system pressure (one gage, right or left side)

INSTRUMENTATION NOTE: Gages 1, 2 and II (rear plate, trail, & recoil pressure) will be used for all firings unless otherwise noted.

APPENDIX J

EXPERIMENTAL LAUNCHER RESPONSE CURVES

I. INTRODUCTION

The list of the firings and the instrumentation for each burst in Appendix I shows that a very large amount of data was recorded. The most significant portion of this data is that which actually illustrates the response of the launcher. In order to limit the amount of data to a reasonable level, only the cradle response and trail strain are shown. (Exceptions to this are Fig. 22 and 23 in the body of the report.) These curves are presented for each of the structural configurations.

II. DISCUSSION

The cradle response is shown in inches of displacement. This is the motion of the cradle front perpendicular to the plane containing the trunnions and firing tube. If the trunnions remain motionless, this cradle motion, by dividing by the proper distance, gives cradle rotation. For this purpose, the trunnion motion in the vertical plane was found experimentally to be negligible; dividing the cradle displacement by 60 in. is a good approximation of cradle rotation.

If the trails respond primarily in their first mode shape, the trail strain is approximately proportional to the angular deflection of the trail at its connection with the lower box member. Again, experiments show that the use of the trail strain to indicate rotation is a good assumption. This strain and the cradle displacement serve to show the launcher response.

The following figures show the cradle response and trail strains for the birst conditions described in Appendix I.

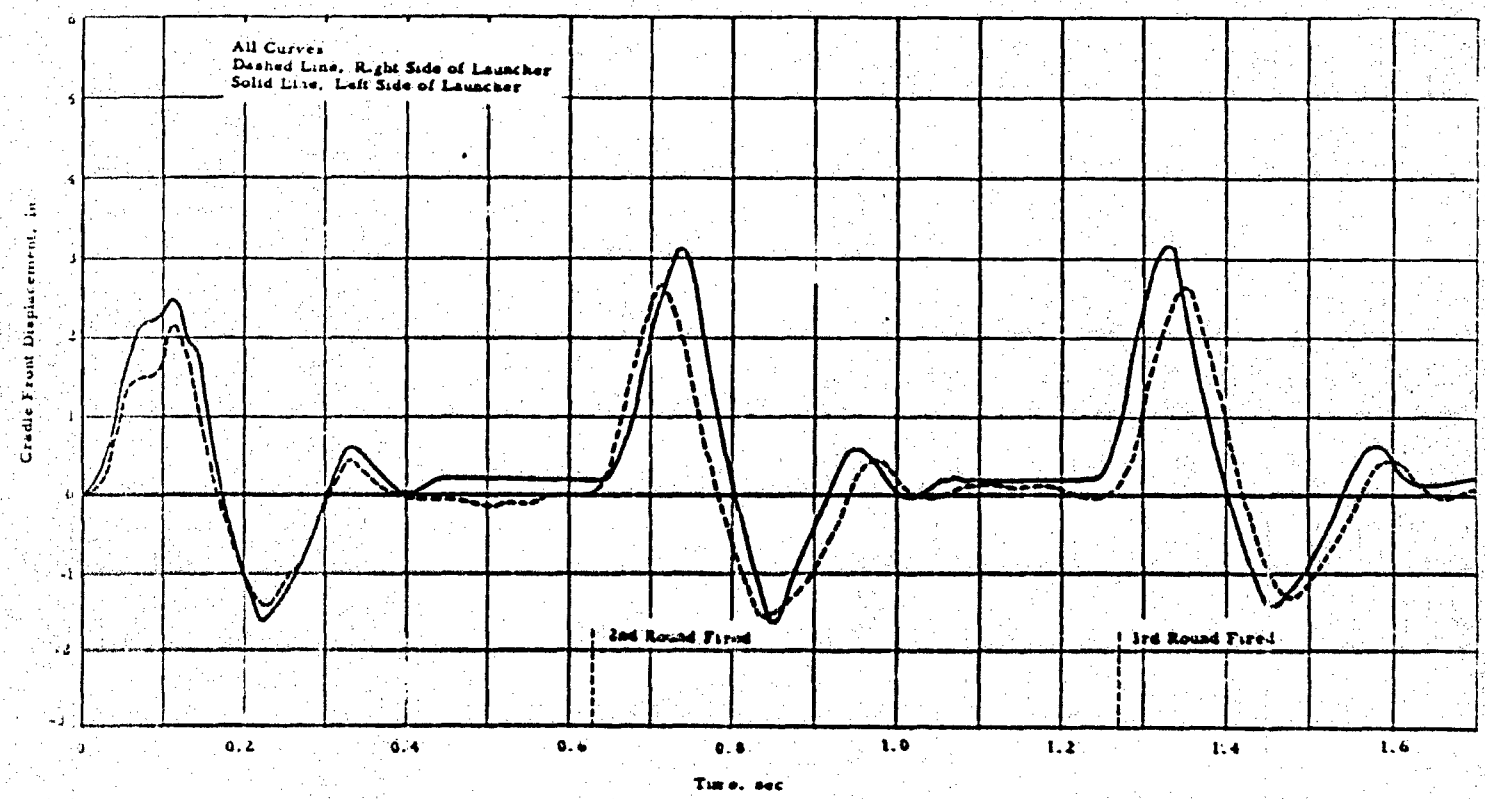

Fig. J-1 CRADLE MOTION, BURST B-2

ARMOUR RESEARCH FOUNDATION OF ILLINOIS INSTITUTE OF TECHNOLOGY

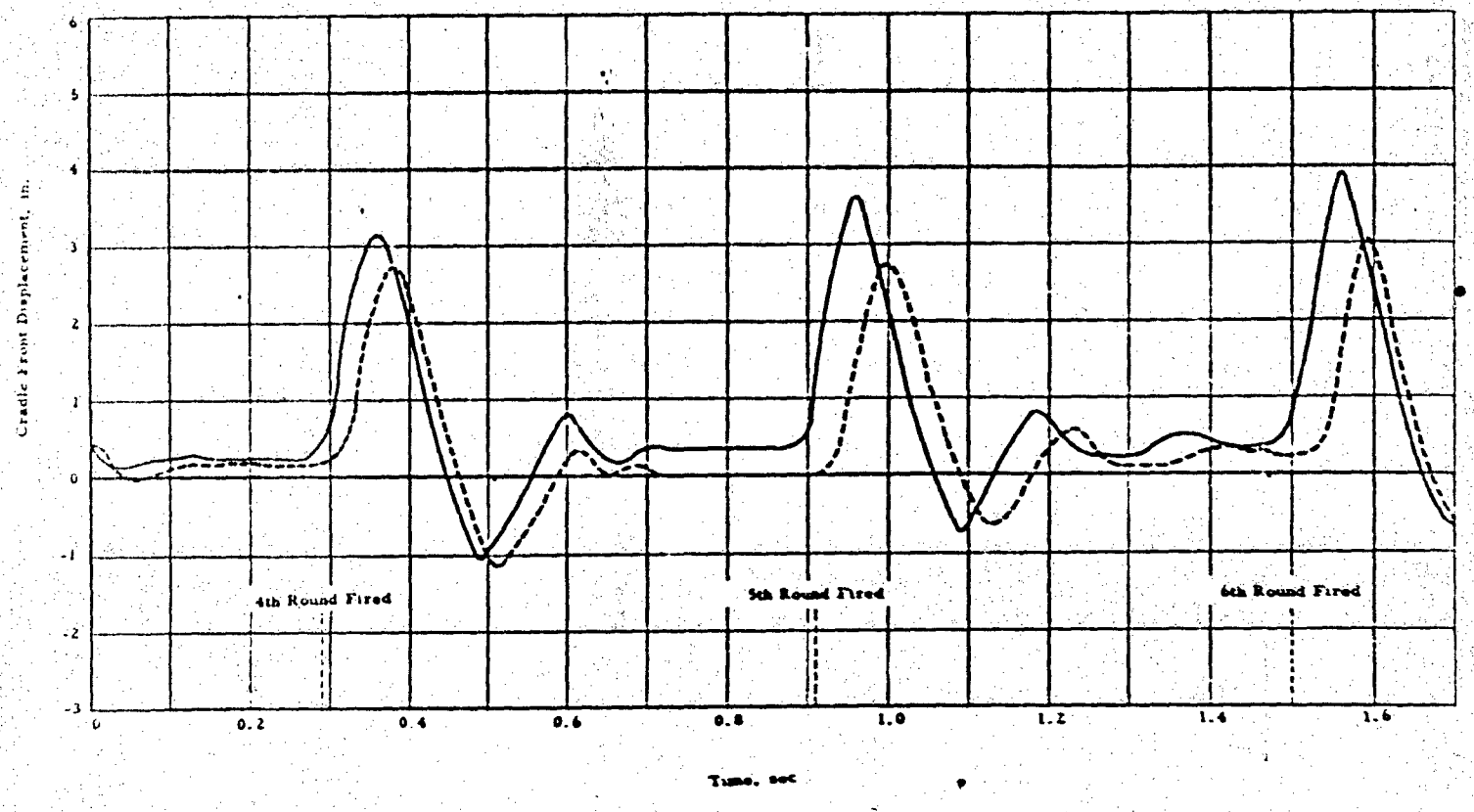

Fig. J-2 CRADLE MOTION, BURST B-2

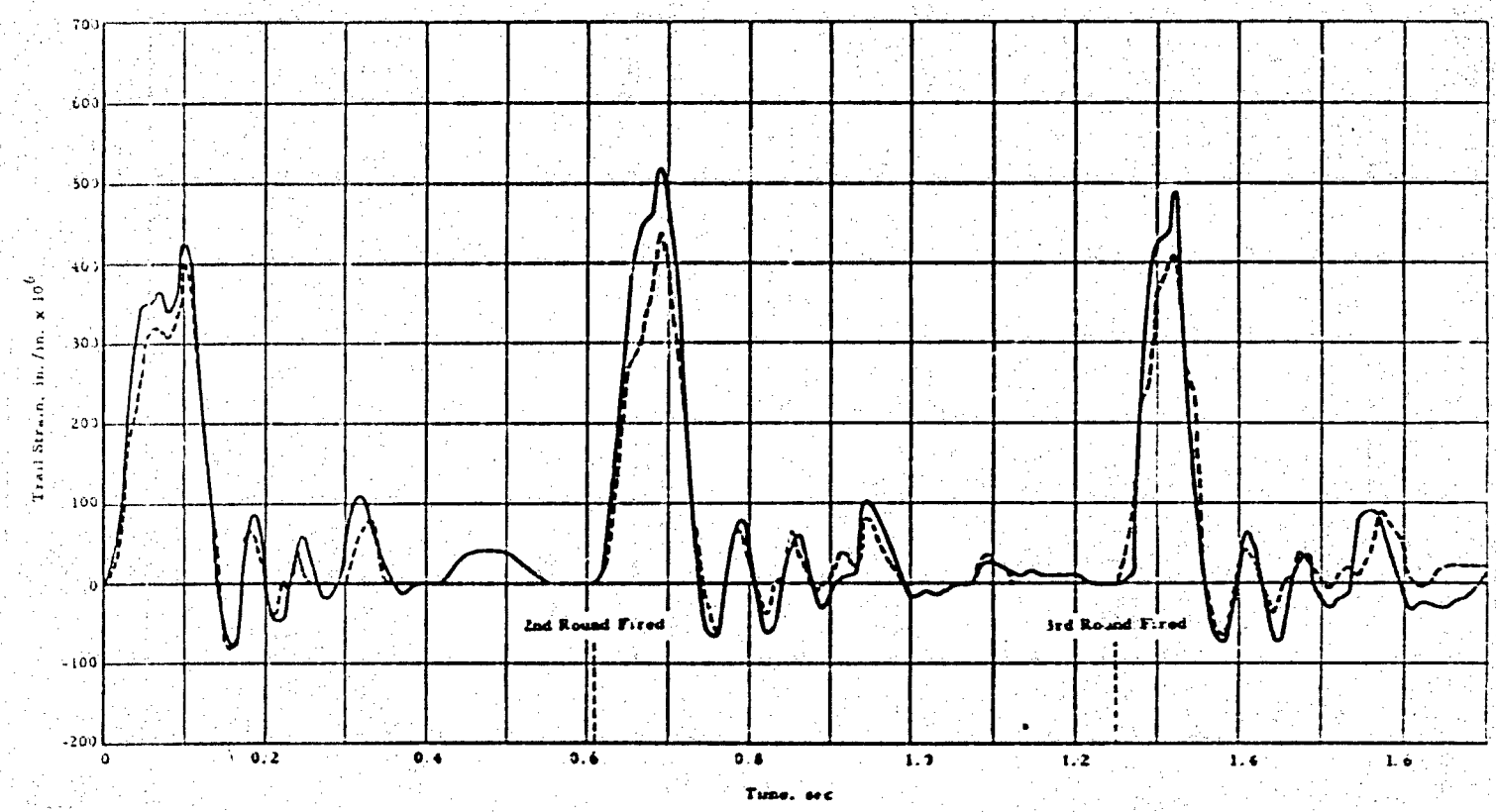

Fig. J-3 **TRAIL STRAIN, BURST B-2**

ARMOUR RESEARCH FOUNDATION OF ILLINOIS INSTITUTE OF TECHNOLOGY

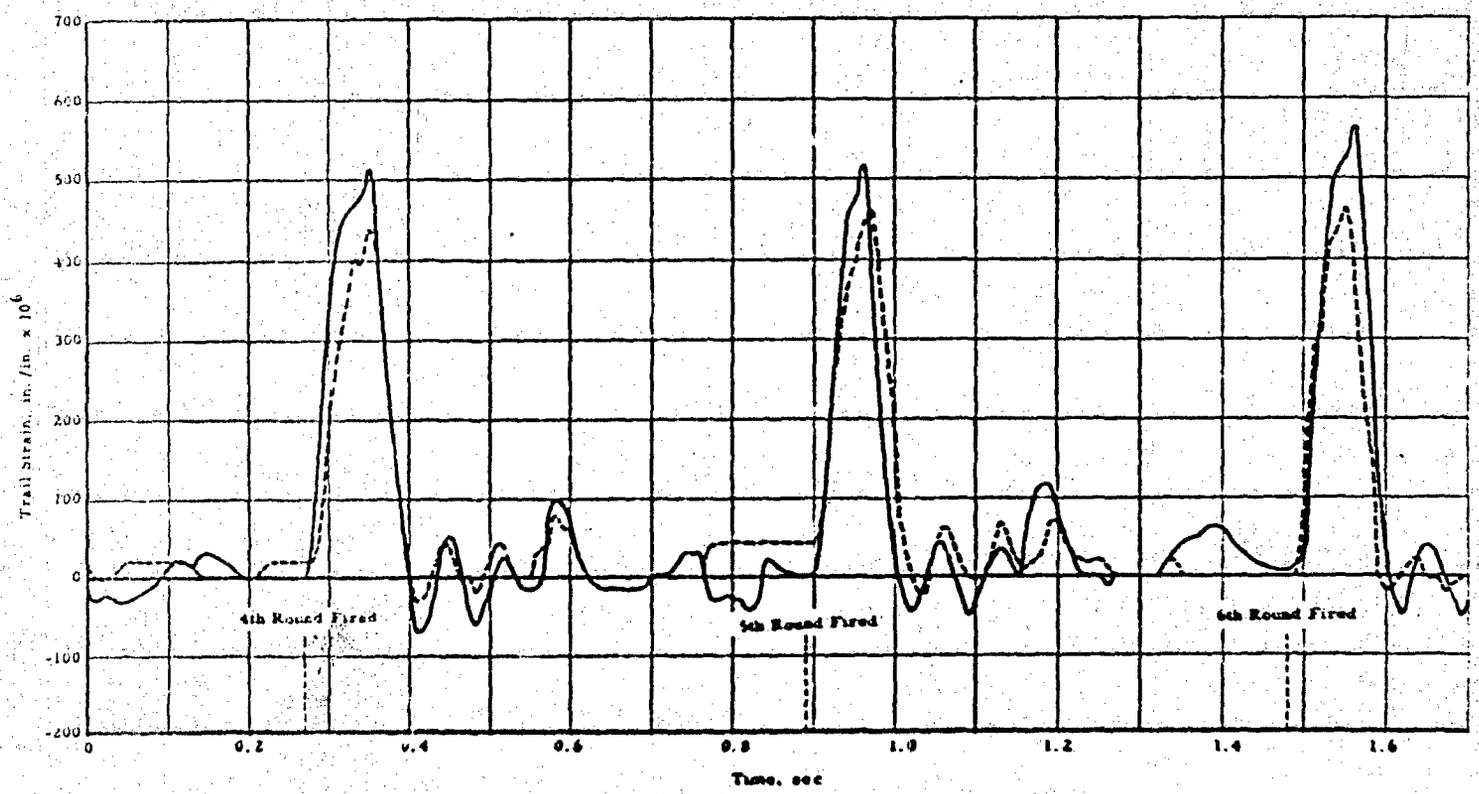

Fig. J-4 TRAIL STRAIN, BURST B-2

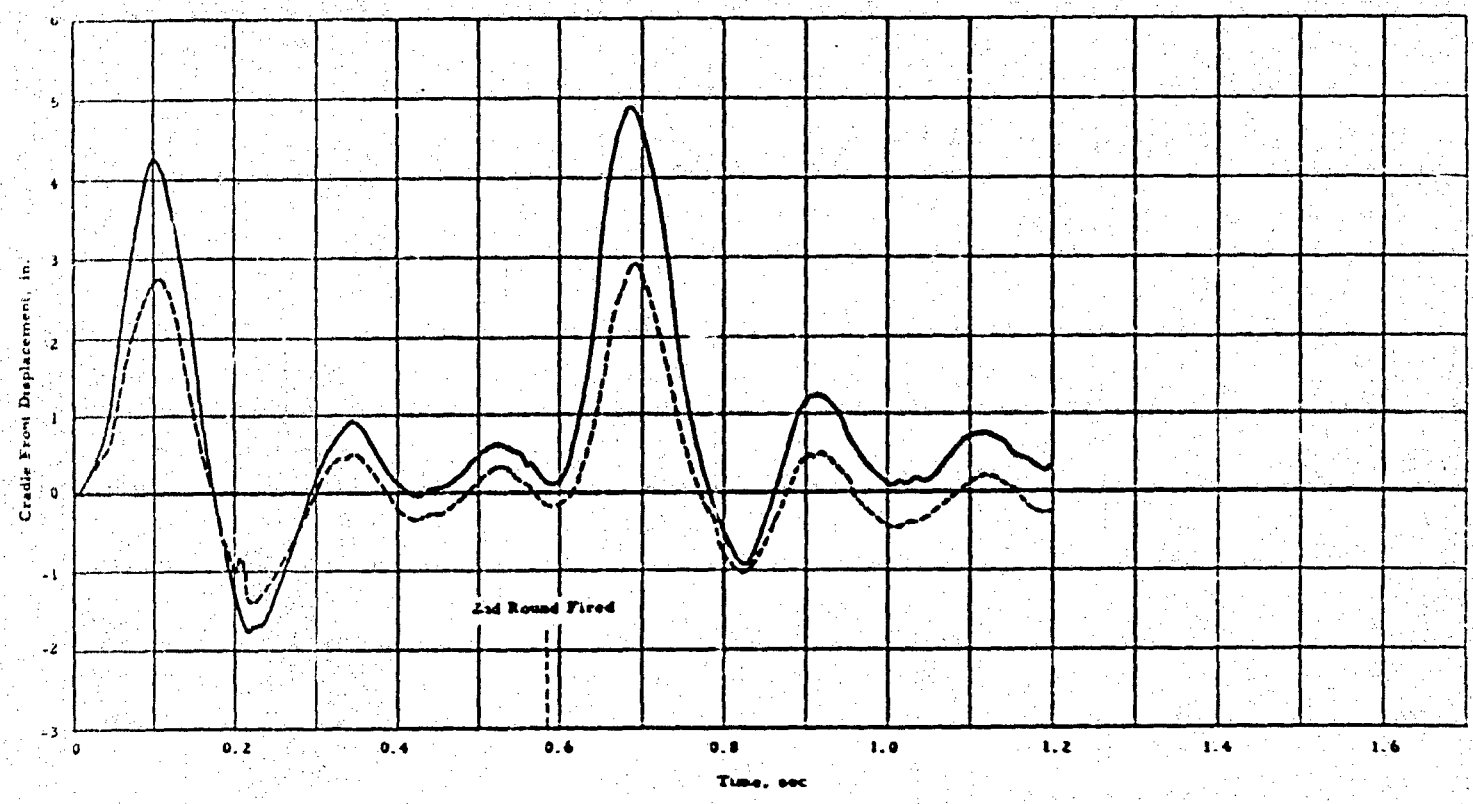

Fig. J-5 CRADLE MOTION, BURST B-5

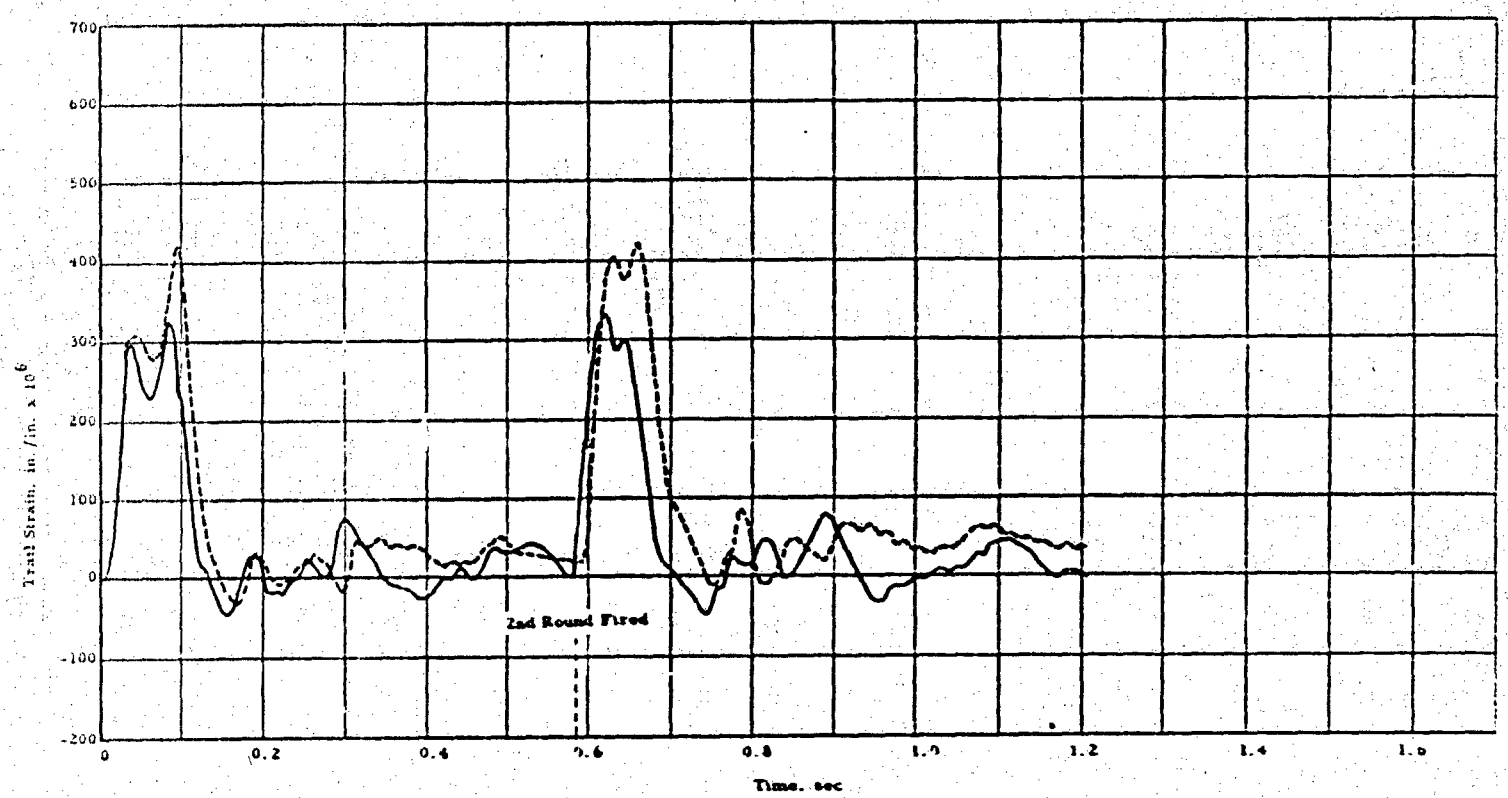

Fig. J-6 TRAIL STRAIN, BURST B-5

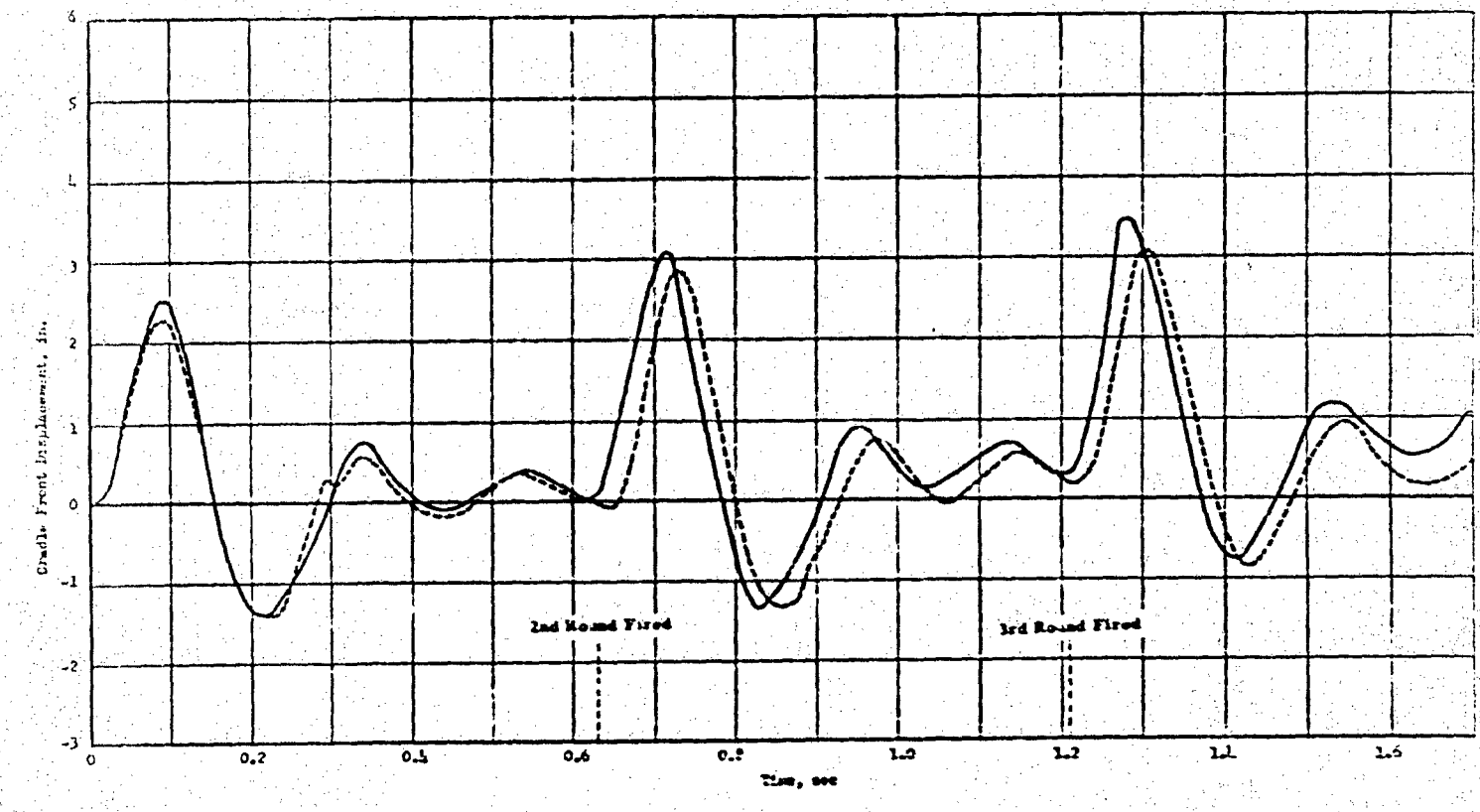

Fig J-7 **CRADLE MOTION, BURST B-6**

ARMOUR RESEARCH FOUNDATION OF ILLINOIS INSTITUTE OF TECHNOLOGY

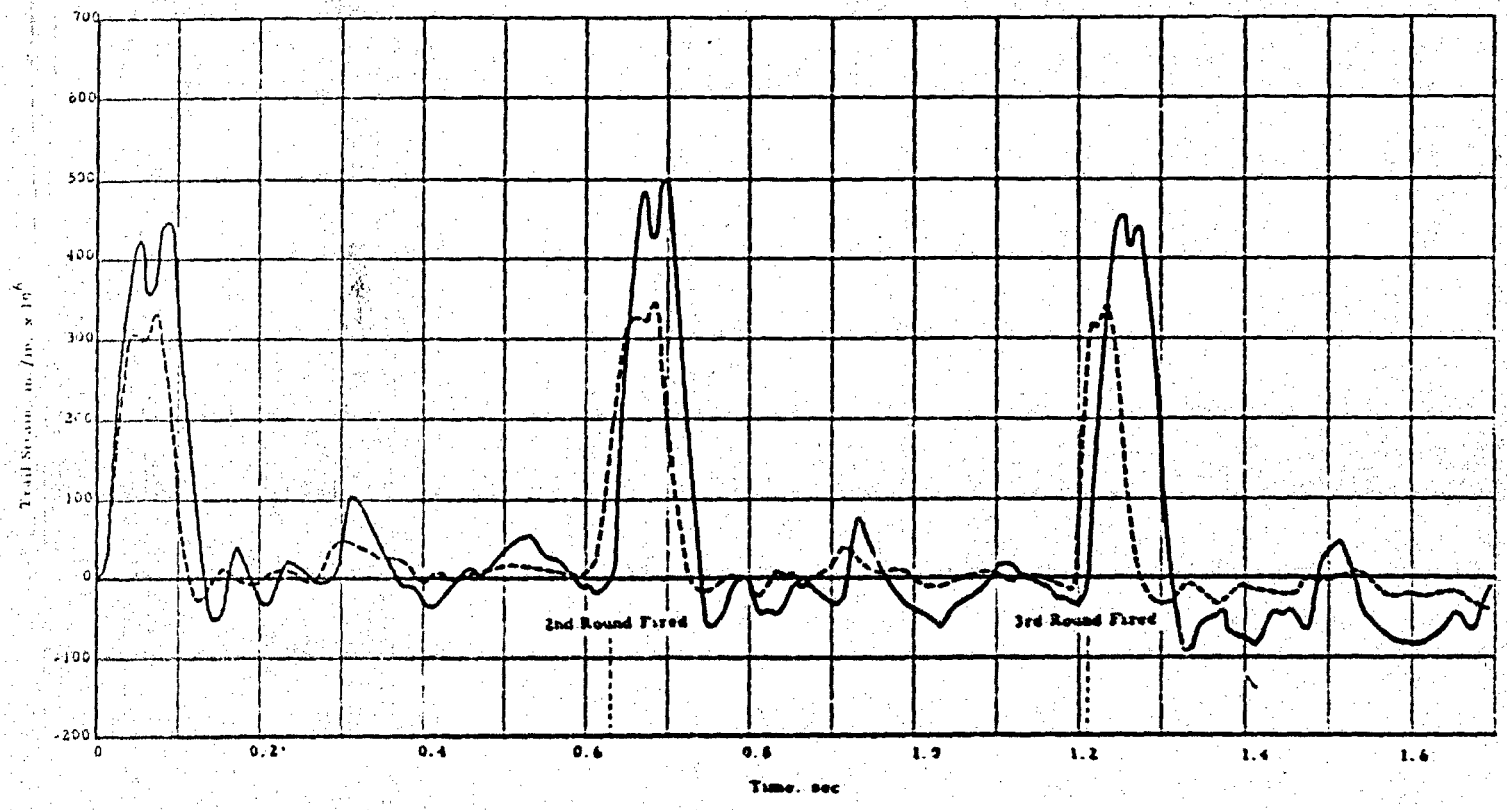

Fig. J-8 TRAIL STRAIN, BURST B-6

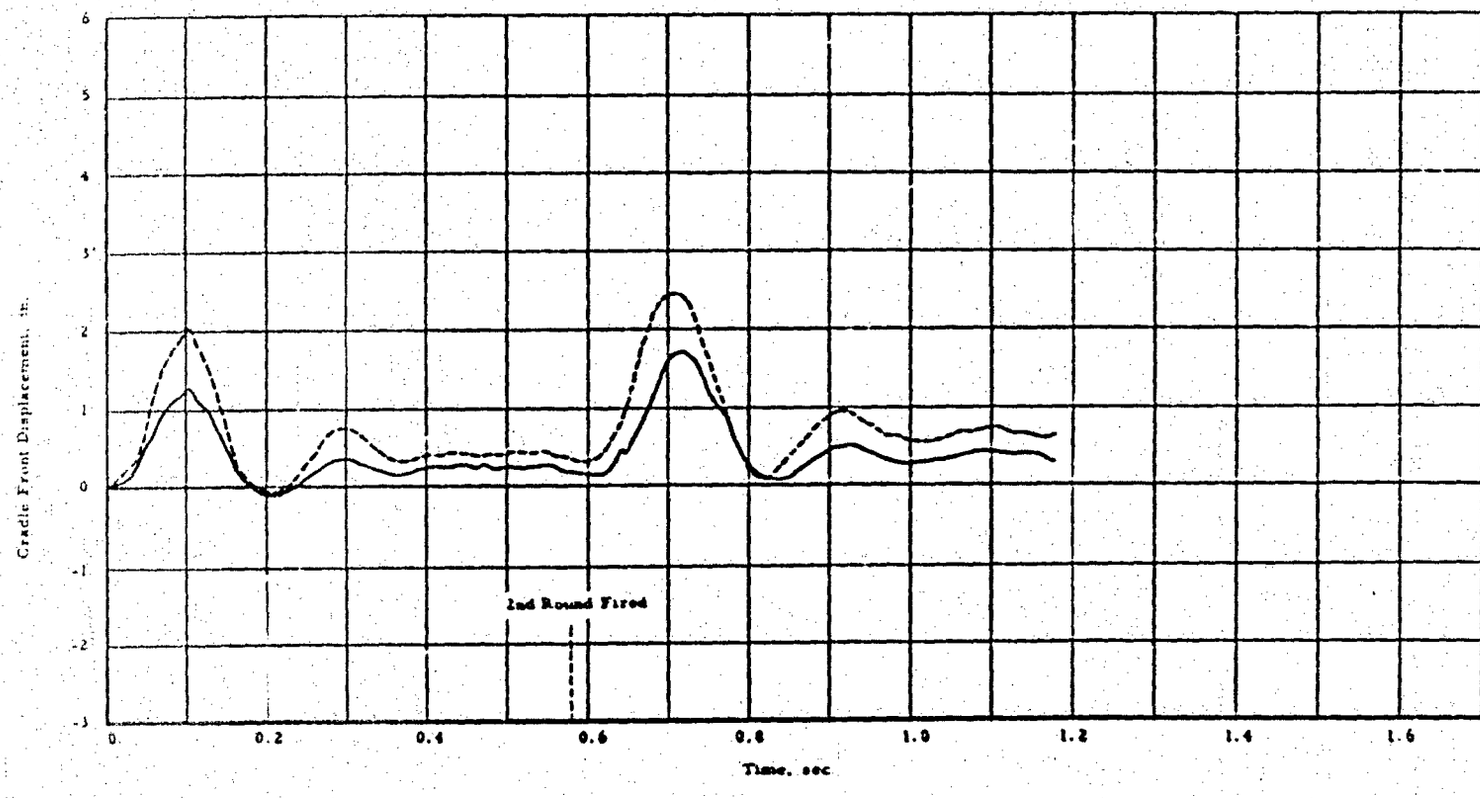

Fig. J-9 CRADLE MOTION, BURST B-7

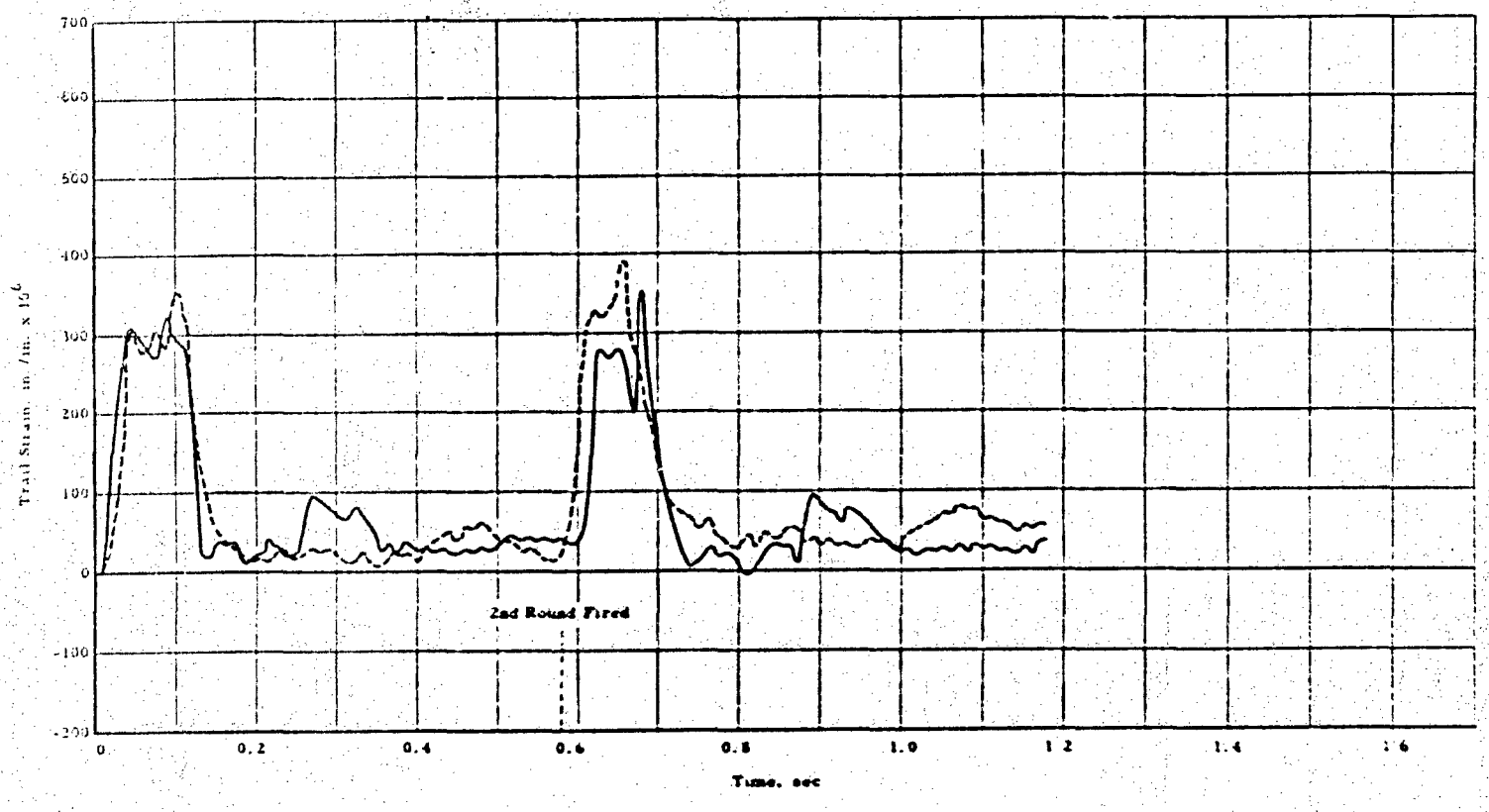

Fig. J-10 TRAIL STRAIN, BURST B-7

ARMOUR RESEARCH FOUNDATION OF ILLINOIS INSTITUTE OF TECHNOLOGY

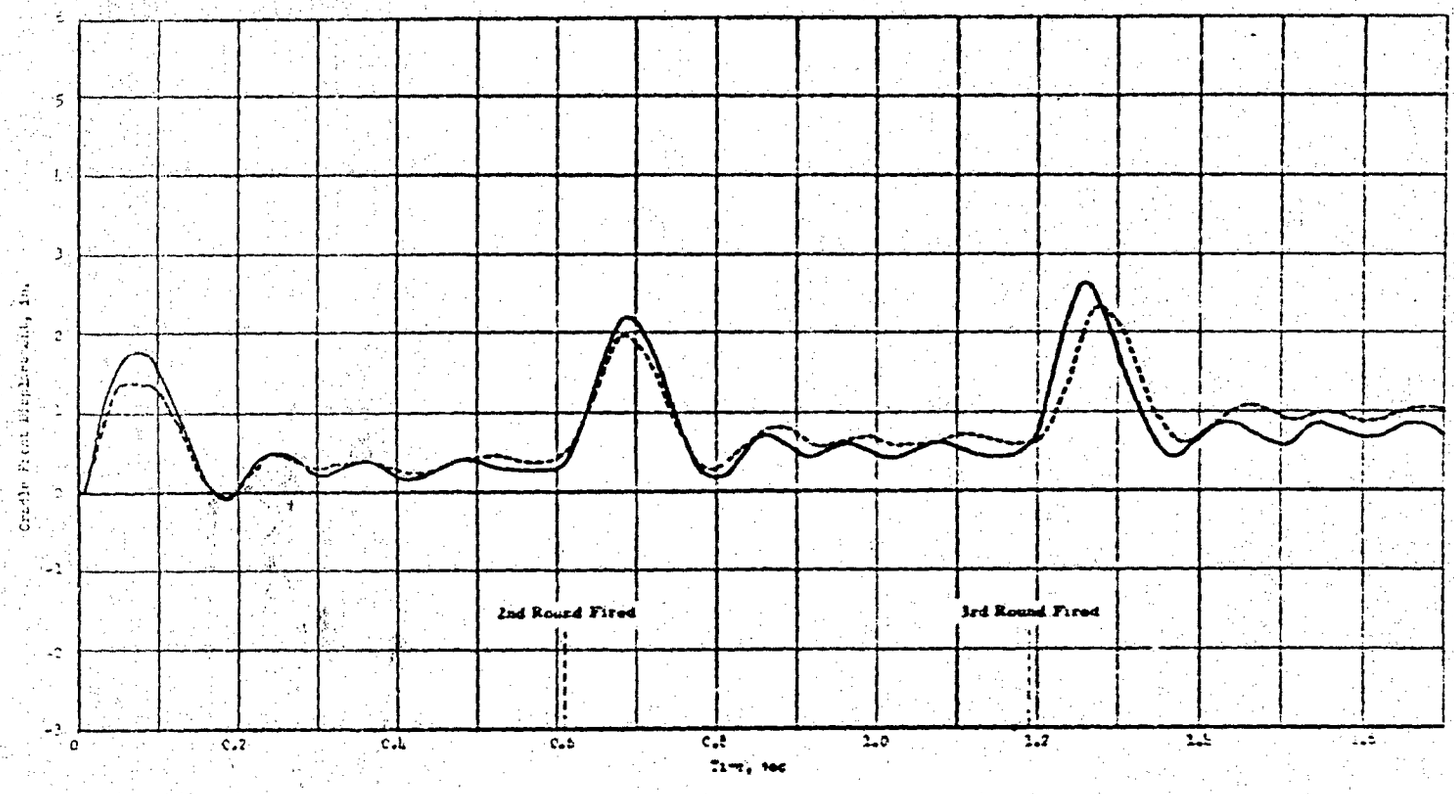

Fig. J-11 CRADLE MOTION, BURST B-8

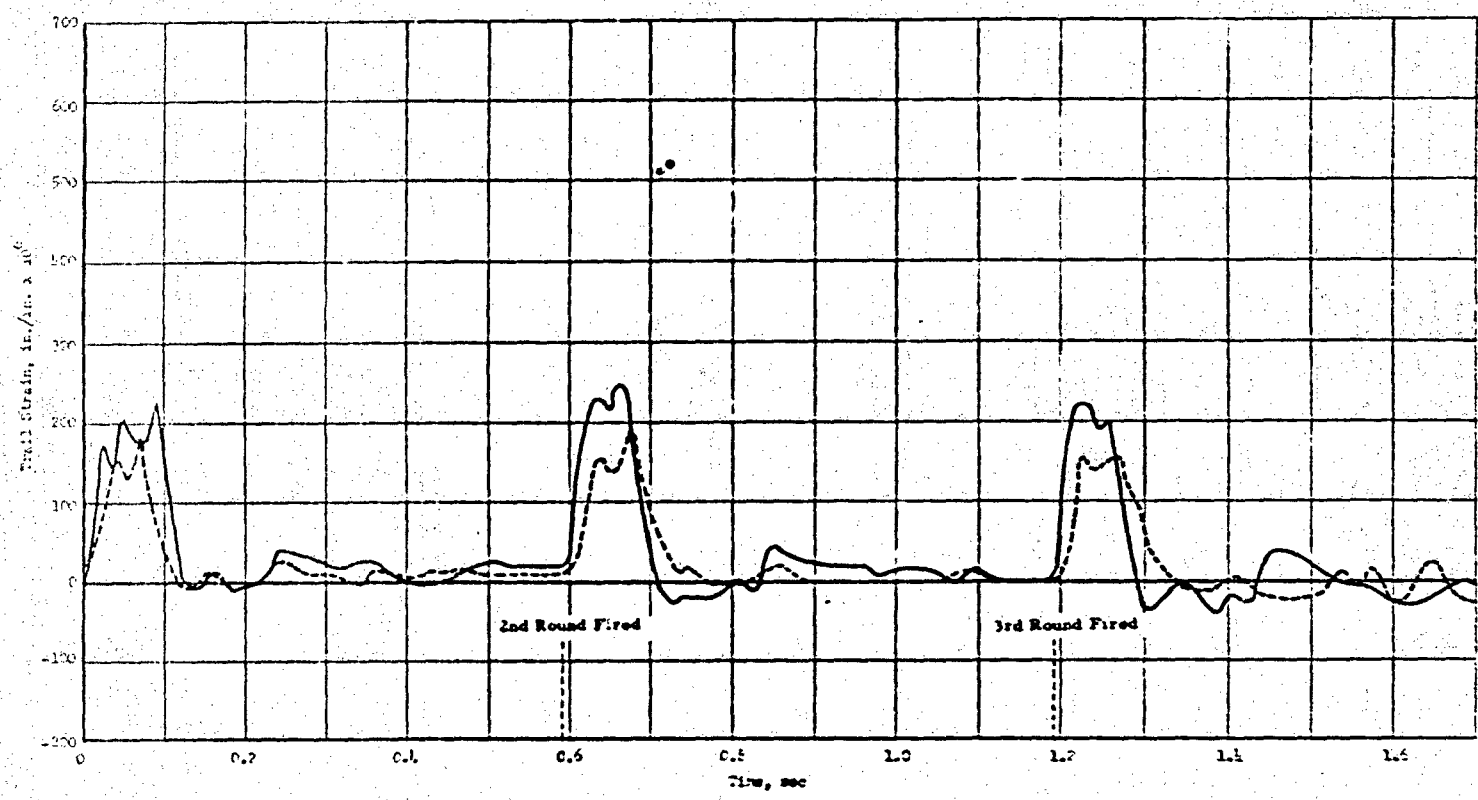

Fig. J-12 **TRAIL STRAIN, BURST B-8**

ARMOUR RESEARCH FOUNDATION OF ILLINOIS INSTITUTE OF TECHNOLOGY

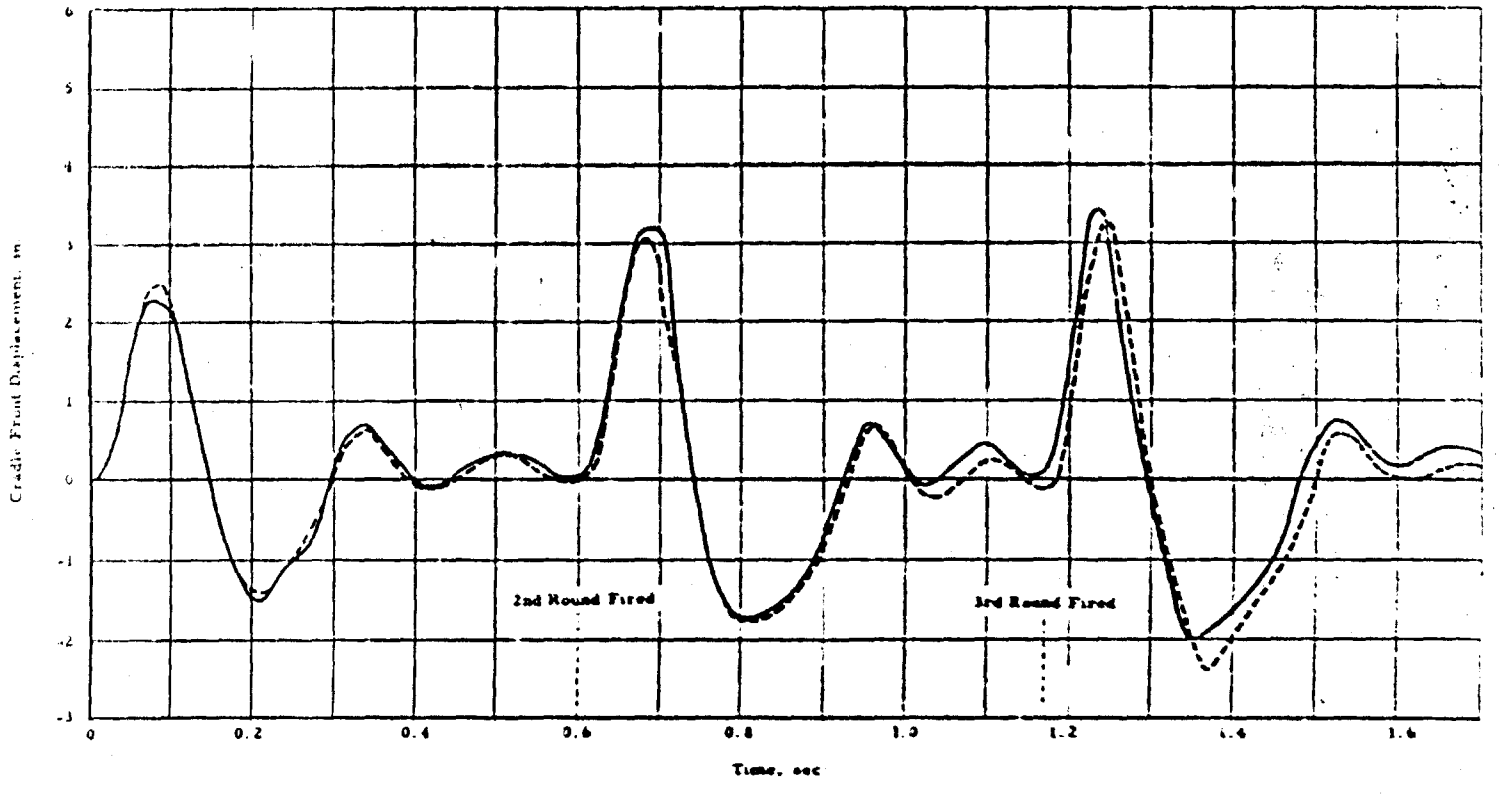

Fig. J-13 CRADLE ROTATION, BURST B-9

ARMOUR RESEARCH FOUNDATION OF ILLINOIS INSTITUTE OF TECHNOLOGY

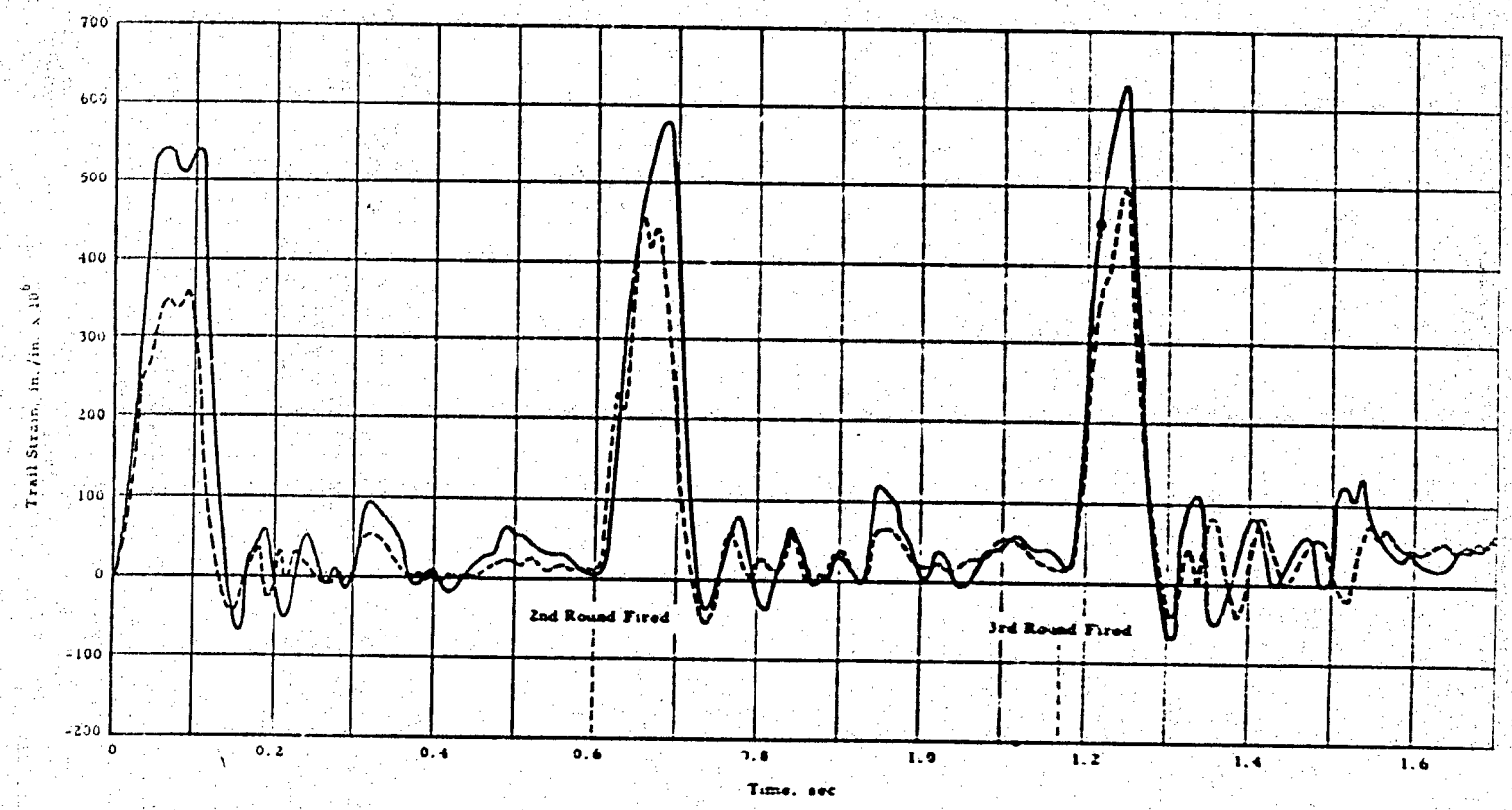

Fig. J-14 **TRAIL STRAIN, BURST B-9**

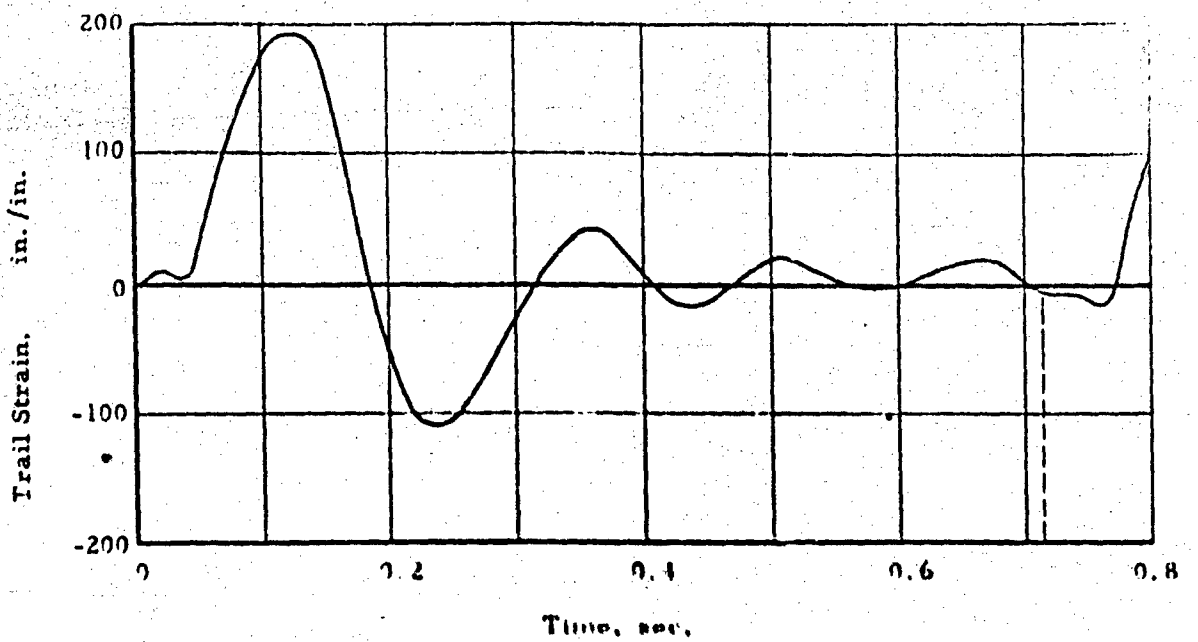

Fig. J-15 TRAIL STRAIN, BURST B-10

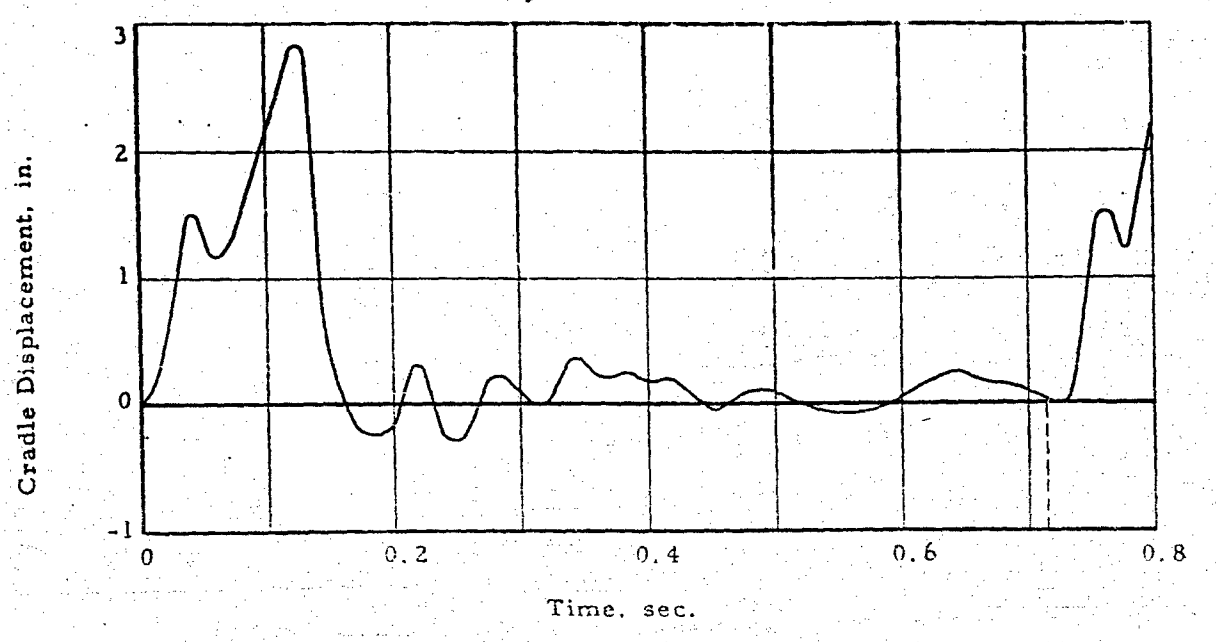

Fig. J-16 CRADLE MOTION, BURST B-10